NWC TP 7110

15th Annual Electronics Manufacturing Seminar Proceedings

Sponsored by
Soldering Technology Branch
Engineering Department

20-22 FEBRUARY 1991

NAVAL WEAPONS CENTER
CHINA LAKE, CA 93555-6001

Naval Weapons Center

FOREWORD

The proceedings contained herein are compiled and published by the Engineering Department, Naval Weapons Center, as supporting documentation for the 15th Annual Electronics Manufacturing Seminar to be held 20 through 22 February 1991 and sponsored by NWC, China Lake, Calif. This document is a compilation of information that was provided by both nongovernment and government sources.

This document, which was prepared for timely presentation, contains information developed primarily by sources outside the Naval Weapons Center. The Center assumes no responsibility for technical or editorial accuracy.

Approved by
R. E. RIGGS, *Acting Head*
Engineering Department
January 1991

Under authority of
D. W. COOK
Capt., U.S. Navy
Commander

Released for publication by
W. B. PORTER
Technical Director

Off-Center requests for additional copies of these proceedings should be addressed to the Defense Technical Information Center, Cameron Station, Alexandria, VA 22314-6145. Publications pertinent to the collection of DTIC are, with few exceptions, available to authorized requesters.

Copies of specific articles should be requested from the individual authors.

NWC Technical Publication 7110

Published by ..... Technical Information Department
Collation ..... Cover, 150 leaves
First printing ..... 600 copies

REPORT DOCUMENTATION PAGE

Form Approved
OMB No. 0704-0188

1. AGENCY USE ONLY (*Leave blank*)	2. REPORT DATE	3. REPORT TYPE AND DATES COVERED
	February 1991	Proceedings

4. TITLE AND SUBTITLE
15th Annual Electronics Manufacturing Seminar Proceedings

5. FUNDING NUMBERS

6. AUTHOR(S)

7. PERFORMING ORGANIZATION NAME(S) AND ADDRESS(ES)
Naval Weapons Center
China Lake, CA 93555-6001

8. PERFORMING ORGANIZATION REPORT NUMBER
NWC TP 7110

9. SPONSORING/MONITORING AGENCY NAME(S) AND ADDRESS(ES)
Naval Weapons Center
China Lake, CA 93555-6001

10. SPONSORING/MONITORING AGENCY REPORT NUMBER

11. SUPPLEMENTARY NOTES

12a. DISTRIBUTION/AVAILABILITY STATEMENT
A Statement; approved for public release; distribution is unlimited.

12b. DISTRIBUTION CODE

13. ABSTRACT (*Maximum 200 words*)

Presented are the proceedings of the 15th Annual Electronics Manufacturing Seminar, held on 20-22 February 1991, in Ridgecrest, California. The proceedings include the papers presented at the Seminar and cover all aspects of soldering technology and electronics manufacturing. The proceedings are a compilation of information provided by both nongovernment and government sources. The proceedings are published in the interest of furthering communication and broadening awareness of current activities among soldering technology and electronics manufacturing specialists.

14. SUBJECT TERMS
See reverse.

15. NUMBER OF PAGES
299

16. PRICE CODE

17. SECURITY CLASSIFICATION OF REPORT	18. SECURITY CLASSIFICATION OF THIS PAGE	19. SECURITY CLASSIFICATION OF ABSTRACT	20. LIMITATION OF ABSTRACT
UNCLASSIFIED	UNCLASSIFIED	UNCLASSIFIED	SAR

14. (Contd.)

Aqueous cleaning
Automated inspection
Capillary action measurement
CFC reduction
Cleaning agents
Design of experiments (DoE)
Electrical impedance measurement
Electronics manufacturing
Environmental stress screening
Fine-pitch lead spacing
HCFC solvents
Machine-vision inspection
Military PWAs
Plated-through-hole reliability
Printed-wiring-board/PWA cleaning
Quality improvement
Semi-aqueous cleaning
Solderability
Solderability inspection
Solder connection
Solder joint quality measurement
Solder paste flux
Surface-mount assemblies
Temperature cycling
Toxic waste reduction
Ultrasonic cleaning
Wave soldering process
X-ray inspection

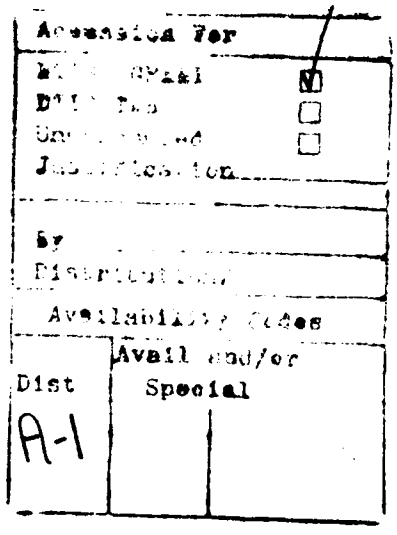

CONTENTS

ACKNOWLEDGMENT

We gratefully acknowledge the assistance and support of the Electronics Manufacturing Productivity Facility (EMPF) in the production of these, the proceedings of the 15th Annual Electronics Manufacturing Seminar. During the last half of 1990, the EMPF was relocated to the Naval Avionics Center (D/460), 6000 E. 21st Street, Indianapolis, IN 46219-2189.

INTRODUCTION

The ever-changing, fast-paced technological advances being made today in electronics manufacturing present a challenge to us all. To help meet this challenge, we must work together. This Seminar—the 15th Annual Electronics Manufacturing Seminar—gives us an excellent opportunity to do just that. This Seminar promotes an open exchange of information on all issues of electronics manufacturing. It provides a forum for all persons involved in this technology, whether from government, industry, or academia. Here we can openly discuss these issues and share our ideas. Here we can work together toward our common goal: to improve the U.S. electronics industrial base.

To help make this improvement we must continue to work toward the goals of productivity, producibility, and quality. We must maintain a concerted effort to resolve production-line problems. Then, we must develop process controls and methods to solve them. Because productivity, producibility, and quality are inseparable, it is critical that our designers learn from past problems and that they design for ease of manufacturing. The Navy is continuing to work with industry through the efforts of the Naval Avionics Center Electronics Manufacturing Productivity Facility (EMPF) and the Naval Weapons Center Soldering Technology Branch.

The continuing goal of the Soldering Technology Branch is to ensure producibility and quality in electronics manufacturing. We evaluate requirements and provide solutions for concerns on specific NWC programs, as well as for government and industry in general. We are continuing to support standardization of specification requirements as evidenced through the evolution of requirements from WS-6536E, DOD-STD-2000, MIL-STD-2000, and currently Revision A to MIL-STD-2000. Developing technologies, processes, and manufacturing philosophies are providing unique challenges to us all. We are determined to remain in the forefront of this fast-paced world.

We are indeed looking forward to working with you to improve our electronics industrial base.

We appreciate your interest in electronics manufacturing and thank you for joining us at this Seminar.

Dr. John W. Fischer, *Head*
Soldering Technology Branch
Product Assurance Division
Engineering Department

THE USE OF CAPILLARY ACTION MEASUREMENTS FOR SOLDERABILITY IMPROVEMENT

by

Mike Wolverton, Member, Group Technical Staff
Billy Ables, Member, Technical Staff

Texas Instruments Incorporated
Defense Systems & Electronics Group
Advanced Technology Manufacturing Operations
P.O. Box 655474
Dallas, Texas 75265

ABSTRACT

This paper describes the tests performed to evaluate the solder capillary action which occurs within a gap between two solderable surfaces during soldering. The goal was to determine the optimal gap distance for maximum capillary flow in the attainment of hermetic solder joints capable of withstanding extreme temperature cycles and various mechanical shocks.

One of the test conditions was arranged so that the gap thicknesses would vary while the width of the gaps remained constant. In a second condition, the gap thicknesses remained constant while the gap widths varied.

Three plating designs were evaluated. They were nickel plating; nickel overplated with gold; and nickel, copper intermediate, with tin overplate.

The capillary action of all three plating combinations deposited onto aluminum specimens, with the gap configurations previously described, was evaluated. The capillary results were measured with x-ray and microstructural data.

End use solder joint designs were determined from the capillary results. These designs are shown and they include the best plating design for the application. In addition, an unexpected result was obtained that is useful for testing the solderability of all finishes—the Configured Capillary Solderability Test.

INTRODUCTION

This effort was begun with the intent of establishing a quantitative method for determining a solder joint design. The study was to take into account the following factors:

1. Solder gap volume
2. Plating finishes
3. Solder alloy selection
4. Soldering procedure
5. Evaluation
6. Practical application.

The major concern was proper selection of methods to quantify the factors mentioned.

Because the formation of all joints depends on at least some capillary action, it was decided that making use of this capillary action in some defined, controlled measurement would lead to the desired quantifiable joint design.

One method used previously to evaluate capillary action (primarily climb) was the "open book" approach. Figure 1 is a depiction of the "open book" design (Reference 1).

In general, we felt that this approach, although it had merit, was not designed to offer the numerical answers we were seeking. Therefore, it was necessary to define an approach that did produce results that could be quantified. This led to our method, described in detail later, which we call configured capillary.

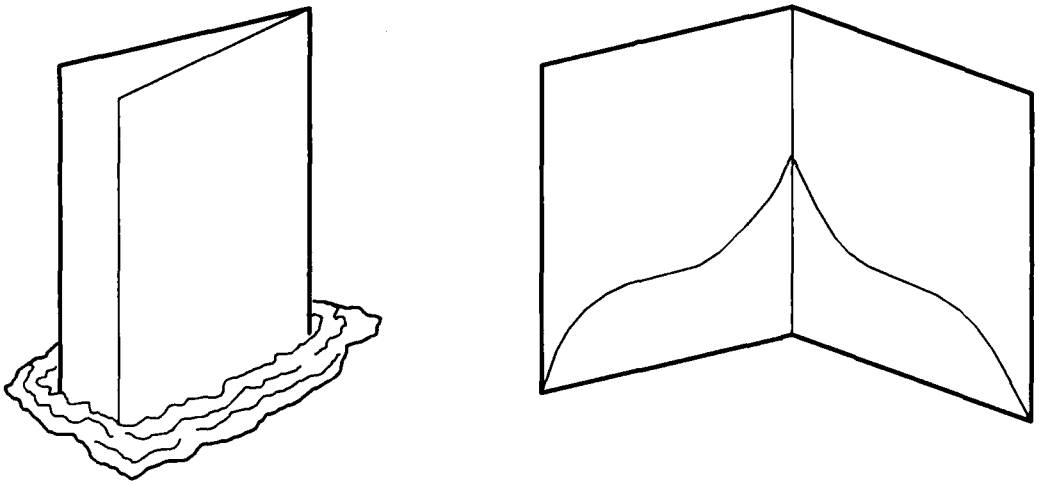

(A) V-SHAPED PIECE IN SOLDER

(B) SOLDER PATTERN

F01592001

FIGURE 1. "Open Book" Technique.

During the testing, and specifically after assessing the results, we found that we had come upon a methodology by which improved solderability testing for the electronics industry in general is possible.

STATEMENT OF PROBLEM

The problem facing all microwave module suppliers is that at least 85 percent of all module housings use one or more soldered feedthroughs that must be mechanically sound and hermetic.

The feedthroughs can have many configurations, from a small cylindrical feedthrough in the 0.060-inch diameter range up to rectangular shapes as large as 1.0 inch in length and 0.250 inch in width. For all soldered joints, the results must be the same—hermetic and strong.

Thus, it is necessary to provide the processing and manufacturing areas with joint designs and procedures that are robust. A multiplicity of joint designs is required, given the variance in size and shape of the feedthroughs. All designs must produce results that meet the physical specifications of the module.

Therefore, the problem is not to design a single configured solder joint, but rather to understand and define *how* to design all solder joints.

SOLUTION TO PROBLEM

FABRICATING TEST BLOCKS

The capillary test pieces were configured in general as two simply made test blocks that, when screwed together, formed a series of varying size rectangular flues.

The test blocks were cut from 2219 aluminum. Two configurations were selected. One set of blocks had all gap widths set at 320 mils, while the thicknesses of the gaps varied logarithmically from 1.0 to 17.8 mils. The second group had set gap thicknesses of 3.2 mils, but the widths of the gaps were set at 320, 560, and 1,000 mils. Figure 2 is a picture of two blocks before assembly.

As can be seen from Figure 2, the top portion shows the milled gaps, while the bottom of the photograph shows the cover. The upper portion of the picture depicts gaps from left to right that have depths and resulting solder joint thicknesses as follows: 1.0 1.8, 3.2, 5.6, 10.0, and 17.8 mils.

Initially, the blocks were made at a height of 0.70 inch. Because some of the gaps were relatively deep, it was thought that the results of the upward flow could be quantified, thus producing a graph depicting the climb of the solder versus the size of the gap. To our surprise, on the 0.70-inch blocks, the solder reached the top of each flue. Thus, creating the desirable graph was not possible.

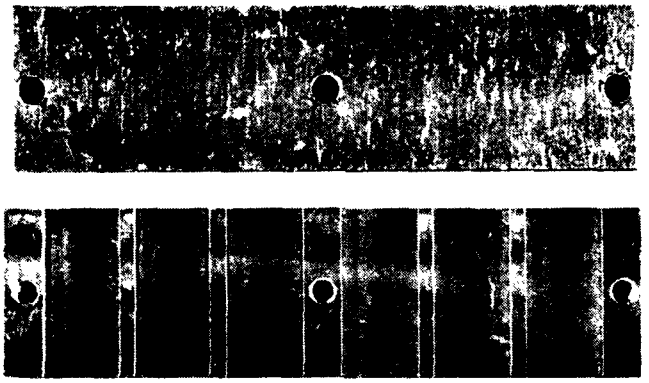

FIGURE 2. Configured Capillary Test Block (0.7-In. Height).

More blocks then were constructed having heights of 2.5 inches. These blocks had the same physical dimensions as the first group, with the exception of the height, which provided the desired sensitivity to capillary climb.

SELECTION OF PLATING

After fabricating the blocks, the next step was to plate the blocks for the solderability tests. The plating on these blocks was selected so that several plating constituents and thicknesses could be observed as to their influence on the capillary action. These blocks were plated according to the chart shown in Table 1.

The baths used in the plating were of concern to us since the constituents of the baths were expected to have marked effects on the results of the tests that would follow. We used a phosphorus (ite) electroless nickel bath. The nominal phosphorus content was 7 percent. All the copper baths were cyanide. A new ARC gold bath was used containing no brighteners. This bath produced Type III, Grade A gold, per MIL–G–45204C.

In plating, we took particular precautions when monitoring and maintaining the gold bath. Of particular interest is the control of the contaminants iron, nickel, and cobalt per the military standard, plus additional controls on thallium, nickel, copper, and lead (Reference 2). The additional controls are necessary for post-solder assembly when wire bonding is required. Furthermore, an experience base dictates that the total of all thallium, cobalt, iron, arsenic, and nickel impurity levels should be maintained below 50 ppm for wire bonding.

TABLE 1. Plating Finishes.

Group	Plating Design
A	200 μin minimum; electroless nickel
B	200 μin minimum; electroless nickel 30 to 70 μin; Type III Grade A Gold
C	200 μin minimum; electroless nickel 200 μin minimum; copper 200 to 500 μin; tin
D	200 μin minimum; electroless nickel 200 μin minimum; copper 100 to 200 μin; tin

The design of the metallization layers, which were plated onto the aluminum housing, was first evaluated by measurements of solderability using plated wire specimens. Four designs were selected. These were: nickel, nickel-gold, nickel-copper-tin (thick), and nickel-copper-tin (thin). Details of the platings and their thicknesses are shown in Table 2.

The 30-mil-diameter aluminum wire was plated with only a partial compliance to the thickness design. It is evident from Table 2 that nickel and copper thicknesses were within specified tolerances, while tin and gold were both excessively thick.

The solderability data is shown in Table 3. The two solderability tests used were the dip-and-look test per MIL–STD–202, Method 208, and the wetting balance test per MIL–STD–883, Method 2022. There was one significant exception to these tests, namely, the use of Sn96 solder instead of Sn63 and the increase of molten solder temperature from 245 to 283°C. The solder temperature was selected to maintain the 62°C delta between melting point and dip temperature. For reference, the eutectic melting point of Sn63 is 183°C, and that of Sn96 is 221°C. Test temperatures are typically 15°C below process temperatures to enhance test sensitivity to any solderability problems.

Looking first at the dip-and-look solderability results in Table 3, it is important to note the standard test requires 8 hours of steam aging. All five of the nickel wire specimens subjected to the military standard test failed. The steam aging requirement was deleted for the sake of some additional data, and in this case, only one of five nickel specimens failed.

The steam aging test has not been correlated to any particular storage time; however, some specification writers believe it indicates a 2-year storage life when the solderable metal (e.g., nickel or copper) is properly coated with a dense and adherent layer of a protective material such as tin or gold. Such is not the case for bare nickel. Here, no correlation of the aging to storage has been offered.

TABLE 2. Plating Design of Solderability Tested Wires.

Solderability Sample	Requested Design (μin)	Measured Thickness			
		Element	Quantity	Mean (μin)	Standard Deviation (μin)
A	200 minimum electroless nickel	Ni	16	291	9
B	200 minimum electroless nickel	Ni	16	281	8
	50 nominal Type III Gold	Au	16	254	69
C	200 minimum electroless nickel	Ni	16	334	14
	200 minimum copper	Cu	16	307	29
	200 to 500 tin	Sn	16	941	129
D	200 minimum electroless nickel	Ni	16	335	20
	200 minimum copper	Cu	16	224	66
	100 to 200 minimum tin	Sn	16	434	56

Note: Thicknesses were measured metallographically on 30.0-mil-diameter aluminum wire.

Other dip-and-look results show that nickel-gold and nickel-copper-tin, with the thicknesses shown in Table 2, pass the test.

In the wetting balance test, we have a relative measure of solderability, where the shorter wetting time indicates higher solderability. In Table 3, the wetting time parameter is "Time to Zero," which is the time period starting at the partial submergence of the vertical wire into the molten Sn96 solder when the wire depresses the solder surface and ending at the time when the surface is exactly horizontal.

The aged nickel never reached the zero point. This indicates there was never a positive wetting force for aged nickel (i.e., poor solderability).

All other metallization designs had wetting times less than 2 seconds, with the nickel-gold, both aged and unaged, performing best at 0.68 second. The fact that nickel-gold had no change in wetting time from the aging means that it holds up well to the steam aging environment

TABLE 3. Solderability Test Results.

Solderability Sample	Outer Finish	Dip-and-Look Test				Wetting Balance Time to Zero (seconds)
		Quantity	Pass	Fail	Comments	
A Unaged	nickel	5	4	1	Lot failed	1.18
Aged	nickel	5	0	5	Lot failed	>5.00
B Unaged	gold	5	5	0	Lot passed	0.68
Aged	gold	5	5	0	Lot passed	0.68
C Unaged	tin	5	5	0	Lot passed	1.08
Aged	tin	5	5	0	Lot passed	1.10
D Unaged	tin	5	5	0	Lot passed	1.12
Aged	tin	5	5	0	Lot passed	1.76

Notes:

1. A detailed description of the wires used in this test is shown in Table 2.
2. Each "time to zero" is the average of readings from five specimens. Different specimens were used in the dip-and-look test.
3. The standard dip-and-look solderability test states the specimens shall be aged for 8 hours in steam before being subjected to the solderability test.

There are two observations regarding the nickel-copper-tin metallization: (1) the thick tin is more solderable than the thin tin and (2) a separate evaluation found that excessively thick tin can glob up in the vapor phase reflow process, with about 250°C vapors. This tin coalescence is believed to be caused by the natural surface tension of the tin (232°C melting point) and is not considered a dewet failure per se.

Nevertheless, the tin finish poses a cosmetic problem after soldering, whereas, the gold finish does not.

EXPERIMENTAL PROCEDURE AND RESULTS

The test blocks were plated in accordance with the four groups shown in Table 1 after completion of the preliminary solderability tests on plated wires. The test block plating thicknesses were measured to enable correlation of fabricated finishes to capillary solderability test results.

We had a keen interest in the thicknesses of the nickel and the gold. The nickel was to be greater than 100 μin, and the gold was to be no greater than 70 μin.

The gold was of particular interest, since this outer finish influences to a large extent the formation of the undesired intermetallic compound (IMC) $AuSn_4$.

X-ray fluorescence (XRF) readings showed all test block platings were within the specified thickness limits.

SOLDERING THE BLOCKS

Once the blocks were fabricated and plated, it was time to solder them. Sn96 solder was selected because of its relatively high reflow temperature (221°C), which lends itself to post-feedthrough processing, and because it has good fatigue life characteristics as well (Reference 3).

A solder pot was set so that the temperature of the solder was at 300°C. Each block was preheated to a nominal temperature of 200°C on a hot plate also set at 300°C. Alpha 611 RMA flux was applied, after which the block was lowered into the molten Sn96 to a depth of 0.250 inch and left for 10.0 seconds. The immersion and emersion rates were 1 inch per minute. The block was then removed and left to cool. This operation was done one block at a time.

Both types of blocks, the 0.7- and the 2.5-inch. (heights), were soldered using the same procedure.

It should be noted that the depths to which the blocks were submerged is not a critical aspect of the experiment, since the gaps are all so small that capillary action is required before any solder enters any of the gaps.

RESULTS

X-rays and sections were performed on certain of these blocks so that the capillary action could be assessed. Figure 3(A) shows the results of x-rays on a block plated with nickel-gold. Figure 3(B) shows a nickel-copper-tin block from Group D of Table 1. The important parameter assessed for these 0.7-inch-high blocks is solder joint voids.

As one views these figures, one should keep in mind that the capillary action is from the bottom of the photographs upward with the page. One can see, looking from left to right, that the capillary action diminishes drastically as the gaps get smaller than 3.2 mils. In fact, with the tin plating [Figure 3(B)], this occurs below 5.6 mils.

Another observation is that in the larger gaps, the voids tend to take on more of a circular form rather than an "amoebic" shape. This could indicate that smaller gaps are restricting the work of the flux as well as the flow of the solder. During the examination of many of the sections taken from both groups of blocks, dried flux was observed in what was revealed by x-ray as a void. Thus, voids certainly result if the solder reflow overruns the flux before its evaporation.

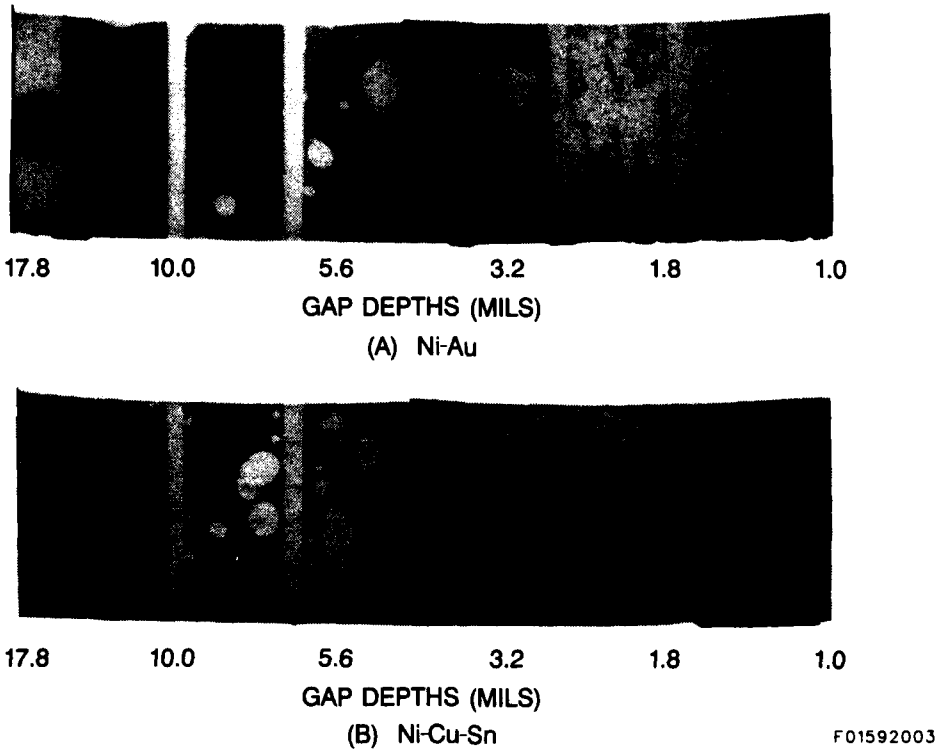

FIGURE 3. X-Ray Photographs of Solder Flow.

Looking at the photographs, it can be seen that the gold plating [Figure 3(A)] tends to promote capillary action more than does the tin plating. This is significant when selecting a finish design. The 10.0-mil gap dramatically illustrates the better quality of the gold, which results in a lower void content than with the tin finish. Furthermore, looking at the 5.6- and 3.2-mil gaps, it becomes obvious that designing a solder gap below 3.2 mils is not acceptable for proper flow. The results of the capillary action in these two gaps, as compared with the tin finish, further demonstrate the better joint quality from the gold finish.

Examinations of the 2.5-inch-high blocks revealed several interesting facts. The first was that we could, indeed, create a graph plotting solder climb as a function of the gap depths. Figure 4 depicts this variance across the gaps.

The second observation was from microstructural analyses of cross sections. These revealed that as the solder flowed up the gaps, the flow was so dramatic that the gold dissolution and compound formation was highest at the top of the joint. That is, the tin at the top experienced a higher level of reaction with the gold. The result of this greater gold concentration in the Sn96 solder was an increase in the formation of $AuSn_4$ the farther up the flue the sections were taken. Figure 5 graphically depicts these white crystalline structures.

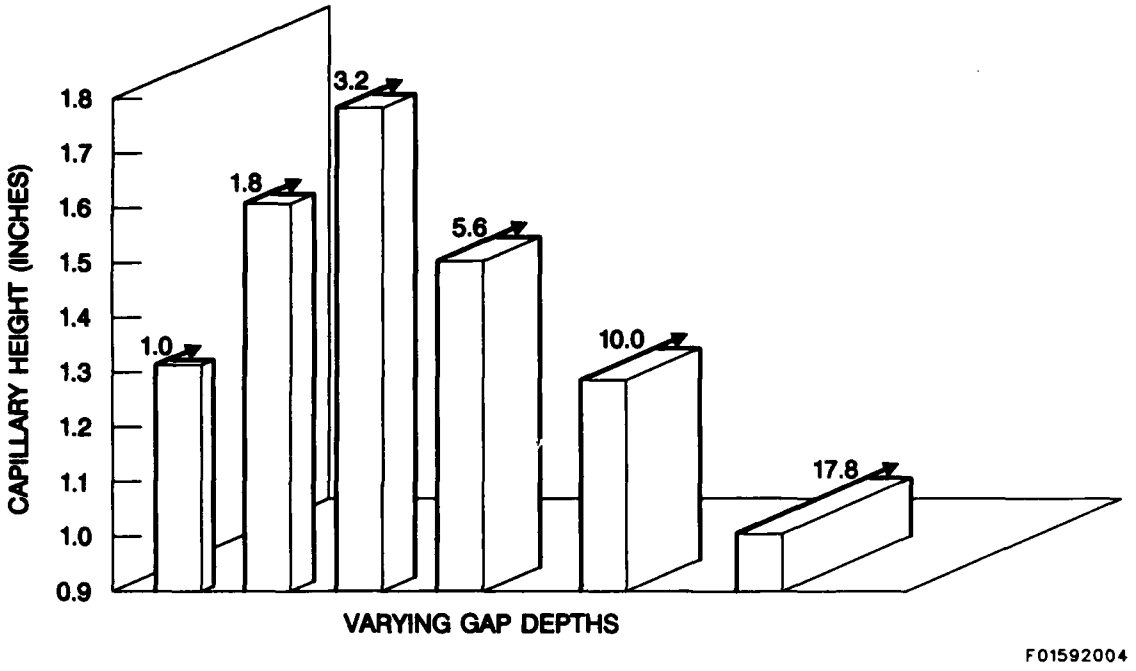

FIGURE 4. Gap Depth Versus Solder Capillary Action (i.e., Joint Thickness).

This $AuSn_4$ was observed in yet another way. As the gap increased from 1.0 to 17.8 mils, the thickness of the gold obviously remained constant, whereas the volume of the solder varied dramatically. As a result, the growth of the $AuSn_4$ decreased at an appreciable rate as the gap sizes increased. Sections of each gap (from a single block) were photographed and are shown in Figure 6. The gaps were photographed in the same relative locations. If these results are compared with those in the previous figure, the phenomena can be explained again as a greater concentration of gold in the Sn96 in the smaller gaps.

The observation of this intermetallic compound $AuSn_4$ substantiates pictorially what has been known for several years—this compound becomes predominant when the gold/tin ratio goes out of balance. The calculations for preventing excessive $AuSn_4$ formation are discussed below.

PRACTICAL APPLICATION

All the information discussed to this point has little or no use unless it can be reduced to some practical application.

We have found that use of the information is vital in the proper design of a solder joint and in calculating solder volumes used in the designed joints.

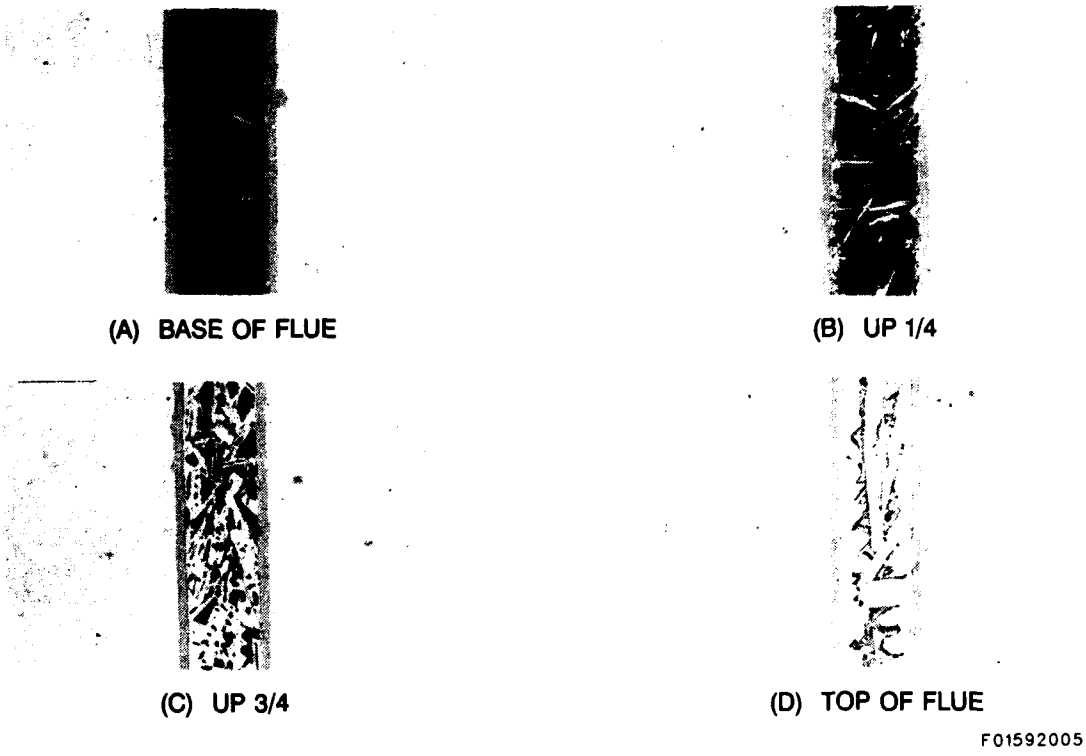

FIGURE 5. $AuSn_4$ (IMC) Concentrations Within a Single 1.0-Mil Capillary.

From the results of the capillary flow up the flues in the blocks, we have concluded that to produce a consistent, high quality solder joint using Sn96, a gap size of greater than 4.0 mils and less than 10.0 mils is desirable. All evidence seems to point to a nominal gap size of 6.0 mils. This design takes into account shear strength data reported by others (Reference 4).

CALCULATING GOLD CONTENT IN A SOLDER JOINT

X-rays discussed earlier revealed that in our specific experiment the nickel-gold design is best for solderability. However, solder joint integrity is a separate question and must be addressed as such.

Specifically, there is a concern regarding gold embrittlement. The key to preventing brittle joints is to maintain a standard gold plating thickness range (e.g., 30 to 70 μin) and to control the solder joint thickness in manufacture.

In a more general sense, the thickness requirements provide a control on the maximum gold content in the joint. This gold content is important because a brittle gold compound forms at 20 atomic percent (At%) gold. This $AuSn_4$ intermetallic compound (IMC) is shown as γ at 80 At% tin in Figure 7 (Reference 5).

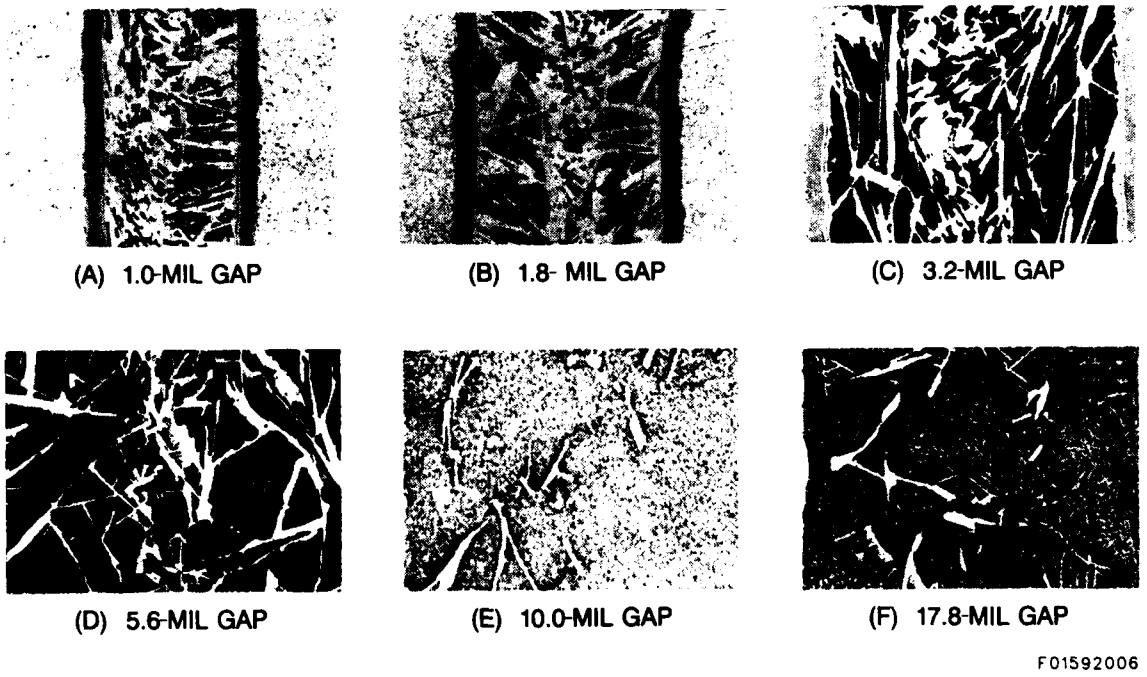

FIGURE 6. $AuSn_4$ (IMC) Concentrations in Varying Gap Depths.

Most discussion of gold content refers to weight percent (Wt%). For example, the $AuSn_4$ is 29.3 Wt% gold. Table 4 shows a calculation of this, using the molecular weights of gold and tin. Considering that Sn96 is 96 Wt% tin and 4 Wt% silver, the conversion of all the tin into the $AuSn_4$ compound would occur with about 29 Wt% gold in the solder joint.

Therefore, just 10 Wt% gold in the joint would cause one-third of the joint to be loaded up with the embrittling compound.

TABLE 4. Conversion of Gold At% in $AuSn_4$ to Gold Wt% in $AuSn_4$.

$AuSn_4$ = 20 At% gold
Molecular weight Au = 197.20 gm
Molecular weight Sn = 118.70 gm
Molecular weight $AuSn_4$ = 672.0 gm
$\frac{197.20}{672.0}$ = 29.34% by weight gold

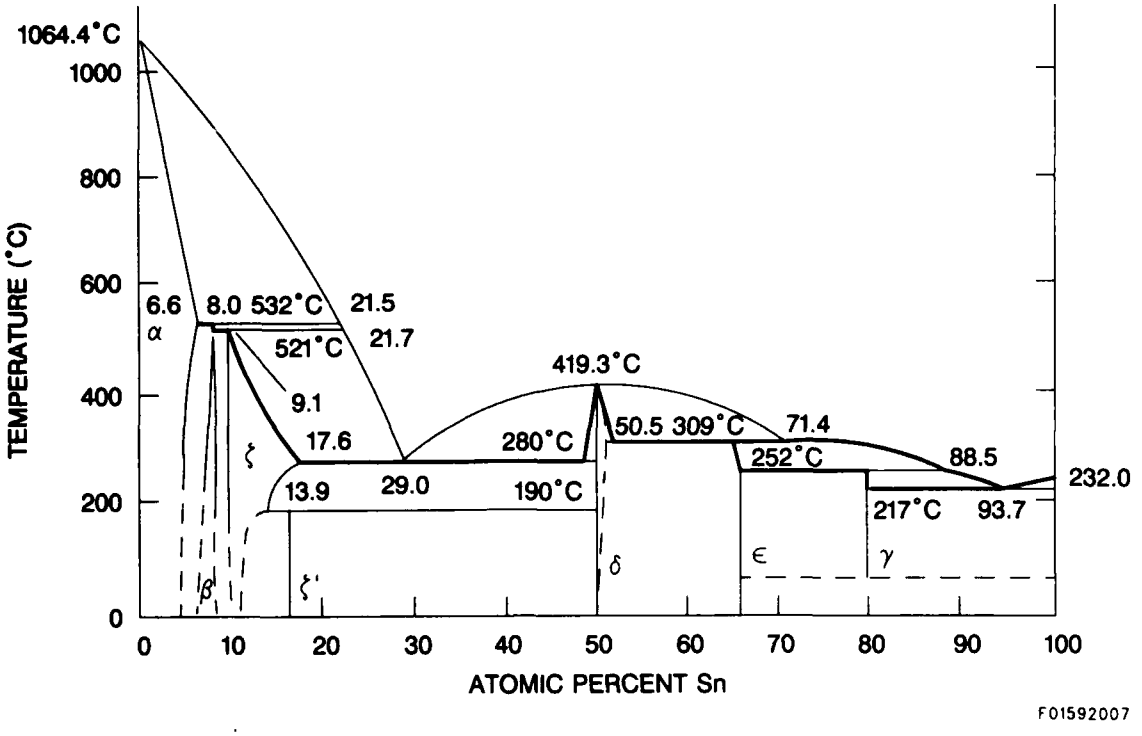

FIGURE 7. Equilibrium Phase Diagram for Gold-Tin Composition.

This simple calculation presumes that the gold finish is completely dissolved into the Sn96 solder during soldering. Such dissolution usually was found in cross-sectional analysis of the housing port test blocks. This calculation assumes the liquid alloy is in an equilibrium state with the 4% Ag* contributing little to the $AuSn_4$ formation.

The Sn96 preform volume and the gold plate volumes are critical to the determination of gold content and embrittling IMC content in solder joints. Minimum and maximum preform volumes must be calculated based on the designed gaps between feedthrough component outside diameter and housing inside diameter. These gaps should be measured from solderable metallization to solderable metallization; for example, from nickel to nickel, in the case of nickel-gold plating.

The preform volumes, gaps, and solderable metallization area all control the solder thickness and gold content of the joint.

Understanding and controlling the tin-gold compound formation is attainable in practice by using the algebraic relationship shown in Table 5. This relationship allows the designer to define a gap thickness per a given gold weight percent represented by the gold plating thickness.

TABLE 5. Calculating Maximum Gold to Solder Thickness Ratio, To Prevent a Gold Embrittlement Problem From Excessive $AuSn_4$ Compound.

For a constant area of solder and plating,

$$Wt\%(Au) = \frac{[Th(Au) \cdot D(Au)] \cdot 100\%}{[Th(Au) \cdot D(Au)] + [Th(Sn96) \cdot D(Sn96)]}$$

or,

$$\frac{Th(Au)}{Th(Sn96)} = \frac{D(Sn96)}{D(Au)} \cdot \frac{Wt\%(Au)}{100\% - Wt\%(Au)}$$

where

Th(Au) = Total thickness of gold on housing plus gold on component

Th(Sn96) = Gap thickness or solder joint thickness

D(Au) = Density of gold

D(Sn96) = Density of Sn96 solder

Wt%(Au) = Weight percent gold in the solder joint.

For a joint having a maximum of 10 Wt% gold in a simple rectangular joint design,

$$\frac{Th(Au)}{Th(Sn96)} = \frac{7.4\ gm/cc}{19.3\ gm/cc} \cdot \frac{10.0\%}{90.0\%} = 0.0426\ maximum$$

For example, a Th(Au) of 0.000170 inch requires a minimum gap thickness of 0.004 inch.

PORT DESIGN

The gap size is of major importance, but there are other factors that influence the design of a hermetic, mechanically sound, solderable joint.

One concern is the location of the plating in a port into which a feedthrough is to be soldered. Care must be taken to have the plating on the receptor walls contiguous with that of the feedthrough. And if there is a danger of shorting a pin, the plating must have a barrier to prevent such shorting. Usually, a simple mechanical removal of some plated area takes care of the problem.

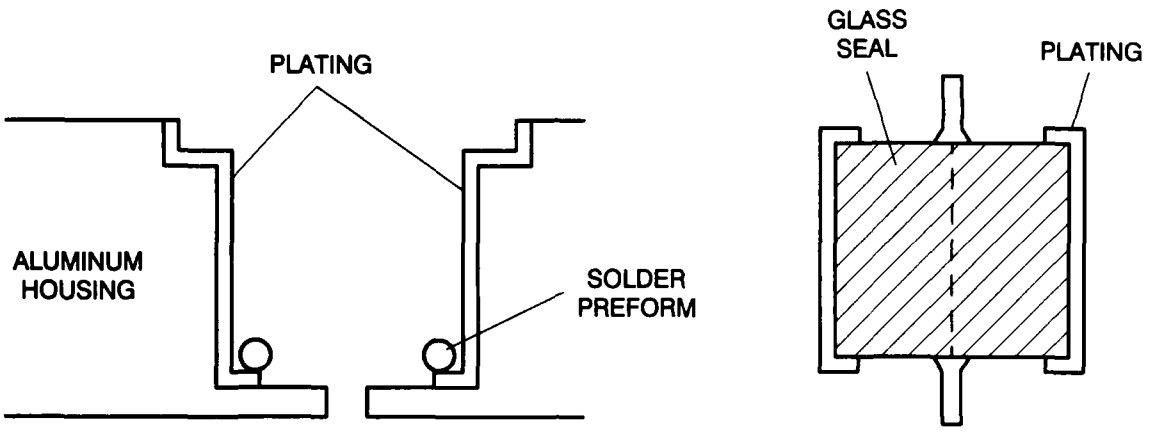

FIGURE 8. Location of Plating in a Properly Designed Port.

Figure 8 is a graphic representation of a solder joint having the plating in its proper location to receive the feedthrough.

In this figure, plating (gold specifically) is found on the port walls and a section of the floor of the port. This section on the floor is determined by the geometry of the metal ring, which is an integral part of the glass-to-metal seal of the feedthrough. This ring is also gold plated.

It is important that the solder preform be located below the feedthrough; that is, a solder ring (of proper volume) must rest on the port floor in the area where two small circles are shown. The feedthrough then would be placed down into the port on top of the solder preform before reflow.

The following data shows the validity of these recommendations. Cross sections were taken of soldered-in feedthroughs on a module involved in a development program. Figure 9(A) and (B) are photographs of two such joints. In Figure 9(A), the feedthrough is not parallel with the housing wall. This port did not have plating on the floor to accommodate solder flow. Therefore, the solder "collected" at the bottom of the plated ring, causing the feedthrough to become nonparallel.

In Figure 9(B), however, the feedthrough is parallel with the port wall. In this port, the plating was on the floor contiguous with that on the feedthrough.

The gap size between the feedthrough and the housing wall was below the recommended nominal of 6.0 mils. These gaps were only 2.0 to 3.0 mils. In addition, gold plating thicknesses

(A) NONPERPENDICULAR FEEDTHROUGH

(B) PERPENDICULAR FEEDTHROUGH PLATING ON PORT FLOOR

F01592009

FIGURE 9. Seating of Feedthroughs in Two Separate Ports.

were excessive for these particular experimental joints. Thus, the growth of $AuSn_4$ is clearly noted as white crystalline spikes.

CONCLUSIONS

After fabricating, plating, and reflowing the configured capillary blocks and finally examining the results, the following conclusions became readily clear:

1. The capillary blocks provide a technique for solderability testing in general. Table 6 shows a comparison of other techniques with the configured capillary block.

2. The method for calculating the gold weight percent of a joint was established, as shown in Table 5. This method provides a means of controlling gold embrittlement to acceptable levels, by evaluation of gold weight percentage in joints that survive product requirements.

3. Analysis of the equilibrium phase diagram for gold-tin (Figure 7) revealed that while the embrittling compound can form at lower temperatures, once formed it does not melt at temperatures below 252°C. Therefore, one should attempt to reach the reflow temperature (we chose 300°C) as quickly as possible. Reflowing above the 252°C temperature is important in helping to reduce the amount of $AuSn_4$ compounds formed before cooldown.

4. For mechanically and hermetically sound solder joints, gap sizes should be nominally 6.0 mils and should not fall below 4.0 mils nor go above 10.0 mils.

TABLE 6. The Conventional Dip-and-Look and Wetting Balance Solderability Tests Have Inherent Problems Compared to the Proposed Configured Capillary Solderability Test.

Test	Geometric Area Tested	Fallacies	Advantages
Dip-and-look	Large	• Forced immersion • Forced emersion • Subjective criteria • Tests only tinnability	• Fast • Easy for end use finishes
Wetting balance	Minuscule	• Statistically inconclusive • Correlation difficulty • Small area	• Quantitative results on end use finishes
Configured capillary	Large	• Requires x-ray and/or sectioning abilities • May require simulation of end use finishes	• Relates to all joint designs • Quantitative results on finishes

5. When configurations call for feedthroughs to be soldered into ports, it is imperative to follow recommended locations of the plating finishes. The solder preform volume must be calculated and the preassembly location of the preform must be specified.

6. Sn96 is the preferred solder for strong hermetic joints. It has an elevated melting temperature, 221°C, and possesses good fatigue life characteristics.

7. Nickel-gold is the preferred solderable finish for use with Sn96 solder.

8. Nickel-copper-tin is a solderable finish, but it is inferior to nickel-gold.

9. The nickel-plated blocks, whether new or aged, did not exhibit wettability; therefore, this finish should be used with caution.

ACKNOWLEDGEMENTS

We would like to acknowledge the contribution of Mr. Al Lee, M.E., for his innovative suggestion in the formulation of the capillary blocks and Mrs. Nela Rice, Sr. Met., for capably performing all the sections. We also want to thank Mr. Paul Diem and Mr. Joe Colangelo for their point source x-ray work and Mr. Pat Barry for solderability test results.

REFERENCES

1. W. Thwaites. *Capillary Joining—Brazing and Soft-Soldering.* John Wiley & Sons Ltd., 1982, p. 49.

2. G.G. Harmon. *Wire Bonding in Microelectronics.* Reston, VA, ISHM, 1989, p. 107.

3. J.A. DeVore. "The Makeup of a Surface-Mount Solder Joint," in *Circuits Manufacturing.* June 1990, p. 42.

4. *Soldering Manual.* Miami, Florida, American Welding Society, 1978, pp. 129, 130, and 143.

5. J. Ciulik and M.R. Notis. "Phase Equilibria and Physical Properties in the Au-Sn System," in *Microelectronic Packaging Technology.* Metals Park, OH, ASM International, 1989, p. 60.

Mike Wolverton is a member of the Group Technical Staff in the Advanced Technology Manufacturing Operations Division of TI. He has 15 years' experience in materials science and engineering. He is responsible for metallurgical joining producibility, with expertise in solder and plating materials, metallization, and bonding processes.

Mike holds a BS degree in Materials Engineering from Brown University and an MSME from Washington University, St. Louis. He is a member of ASM International, ISHM, and past president of his local chapter of SMTA. He has published or presented some 20 technical papers, several of which he presented here at previous Seminars.

Address: Texas Instruments, DSEG
P.O. Box 655474, MS 436
Dallas, TX 75265

CFC AND TOXIC WASTE REDUCTION

by Daniel Z. Gould, P.E.
Supervisor, Process Engineering/Advanced Manufacturing Engineering
GTE Government Systems Corporation
Needham Heights, MA 02194-2892

ABSTRACT

In August of 1989, the State of Massachusetts passed the Massachusetts Toxic Use Reduction Act (TURA). This law became effective in January of 1990. The objective of TURA is to prevent pollution rather than cleanup after the discharge of toxic chemicals into the environment. Similar laws are now being considered by other New England States.

This technical brief will focus on the environmental issues faced by GTE Government Systems Corporation; the steps that are being considered for a 50% reduction of toxic waste by 1997; and controls which need to be put into place in order to maintain the gains achieved.

TOXIC USE REDUCTION ACT (TURA)

In August of 1989, the State of Massachusetts passed the Toxic Use Reduction Act (TURA). This law became effective in January of 1990. The objective of this new law is to prevent pollution rather than cleanup after the discharge of toxic chemicals into the environment. This law has become a model for the nation, and similar laws are now being considered by other New England states. The law requires that companies pay an annual fee to the State of Massachusetts based on the amount of their toxic chemical waste emissions to the environment.

By reducing the in-process sources of toxic chemical waste, GTE hopes to achieve a 50% reduction in toxic chemical waste; reduce the cost of hazardous waste disposal; and exercise its moral and social responsibilities to the community.

OVERALL GOALS AND OBJECTIVES

In order to comply with the new law, GTE first established a Task Force made up of representatives of:

1. Engineering
2. Safety
3. Procurement
4. Human Resources
5. Environmental Compliance
6. Operations

The major objective of this Task Force was to establish an implementation plan for new law.

In July of 1990, the Task Force decided upon the following course of action:

- Identify all toxic chemicals being ordered and the amounts being used.
- Submit the required toxic chemical waste fees to the Massachusetts Department of Environmental Protection (MDEP).
- Develop a facility-wide policy statement on toxic chemical waste reduction.
- Develop and implement a toxic waste reduction plan.
- Monitor and control toxic chemical usage and the amounts of toxic waste being generated..

The major focus of this paper will relate to the development and implementation of the toxic use reduction plan, and the controls established to measure and maintain the gains achieved.

THE TOXIC WASTE REDUCTION PLAN

The Toxic Waste Reduction Plan proposed by the Task Force was designed to focus on three (3) major areas of concern:

- Printed Wire Assembly (PWA)
- Waste Water Treatment Plant (WWTP)
- Machine Shop Operations

PRINTED WIRE ASSEMBLY (PWA)

In the PWA area, the major source of toxic waste generation results from the removal of contaminants, namely the solder flux used in the assembly of printed circuit boards. If assemblies are to be conformally coated, which is usually the case in the production of circuit cards produced for the Military, additional cleaning is also required. These cleaning processes utilize some sort of solvent, or a combination of solvents, to enable the assemblies to meet stringent cleanliness requirements.

The solvent or solvents chosen must have at a minimum, the ability to remove grease, oil, dirt, flux and other debris. They should be selected for their ability to remove both ionic and non-ionic contamination. The solvent must also not damage or degrade the materials or parts being cleaned.

Cleaning of circuit card assemblies for Military applications limits the cleaning processes and cleaning solvents to those specified in the Military specifications. At the present time these solvents are generally limited to the following:

- Ethyl Alcohol
- Isopropyl Alcohol
- Methyl Alcohol*
- Butyl Alcohol*
- Stoddard Solvent*
- Water (Resistivity 1 Megohm-CM, Minimum)
- Detergent, Saponifiers **
- 1, 1, 1 Trichloroethane
- Chlorofluorocarbons (CFC Based Solvents)

In addition to those listed in the Military specifications, there are a variety of new cleaning technologies which include HCFC solvents and "semi-aqueous" cleaning solvents. HCFC solvents are presently being tested for toxicity and cleaning effectivity. "Semi-aqueous" cleaning solvents, such as terpene, necessitate new and fairly expensive cleaning equipment. These solvent cleaning systems are essentially two-part systems which use water rinsing as a final cleaning step. They can be used in both batch and in-line equipment.

Along with being able to meet Military requirements, if applicable, and the ability to properly clean, the ideal solvent or solvents chosen should have little or no toxicity, be nonflammable and be capable of regeneration (distillation). This is a tall order which the solvent and cleaning equipment manufacturers are trying hard to meet.

The major cleaning operations used at GTE include aqueous/detergent cleaning systems.

These conveyorized, in-line cleaning systems are used for post-wave solder flux removal. At bench operations, hand brush/solvent cleaning is used. This is followed by a fine cleaning in an aqueous/detergent solution. Aqueous cleaning is also used for pre-conformal coat cleaning. Several small vapor degreasing units are used where aqueous cleaning is impractical or the assembly is not compatible with aqueous/detergent cleaning solutions. This accounts, however, for a very small throughput. In the degreasing units and at bench cleaning operations, the solvent used is CFC/alcohol based.

With the vapor degreasers, education of personnel in proper methods of equipment operation has minimized usage and thus toxic waste disposal. Retraining personnel and the addition of signs detailing proper immersion and removal techniques has been implemented. Stressing the impact of CFCs and toxic waste disposal on the environment has been found to be a strong motivator of operating personnel.

(*) May be used only if purchased as a constituent of an already blended solvent.

(**)Subject to approval by the Military.

All CFC solvent is reclaimed by distillation in a regeneration unit purchased specifically for this operation. After analysis the distilled solvent is reused. This minimizes not only the amount purchased, but also the amount which becomes toxic waste passed on to the environment.

With the addition of a second in-line aqueous cleaner in early 1991, GTE will rely even less on CFC based solvents. It is expected that the use of solvent degreasers will be cut by 50% or more. Investigations are also underway into the use of HCFC solvents as well as the use of terpenes and other semi-aqueous cleaning systems. Results of these investigations will be reported in mid-1991.

WASTEWATER TREATMENT PLANT (WWTP)

Currently the Machine Shop discharges hexavalent chromium (Cr^{6+}) with several other processes into the Wastewater Treatment Plant. Hexavalent chromium is a known carcinogen and is generally believed to be more toxic than trivalent chromium (Cr^{3+}).

Part of the toxic waste reduction plan is to isolate the hexavalent chromium waste stream and reduce it to the less toxic trivalent state. By installing a transfer station in the process area and isolating this waste stream, the hexavalent chromium can be reduced to trivalent chromium by the addition of an aqueous solution of sodium bisulfite ($NaHSO_3$). Once the hexavalent chromium is reduced to trivalent chromium, it can be separated from solution in conjunction with other metallic salts by alkaline precipitation.

The project was approved and budgeted for 1991. It is estimated that the project will be completed by mid-1991 and that there will be a 50% reduction in the toxicity of the chromate waste being generated.

In addition, water restrictors have been placed in all of the feed lines to the WWTP resulting in significant savings of water which translates into generation of less toxic waste.

CONFORMAL COATING OPERATIONS

In the conformal coating process, a urethane conformal coat material is used. This coating has, in the past, been primarily a dip coating process. This produced a significant quantity of urethane material which later became toxic waste requiring disposal. By shifting to a spray conformal coat process, the quantity of coating used has been reduced by approximately 60%. The thinner required in the formulation of the urethane coating has also been reduced, resulting in more solids being applied and less thinner being exhausted into the atmosphere. Investigations are under way to test 100% solids conformal coat systems with no solvent thinners. This investigation will be completed in 1991.

MACHINE SHOP OPERATIONS

Several areas of the Machine Shop have been affected by the new TURA Law. They are:

1. Painting
2. Machining
3. Packaging

In the Painting Area, several hazardous solvents are used to clean aluminum chromated parts prior to painting. Degreasers using 1, 1, 1 trichorethane and chlorofluorocarbon-based solvents are currently being used.

New aqueous-based cleaning equipment is being investigated; however, heavy oils, grease and smut are not easily cleaned from product which was machined in milling, drilling, and turning equipment.

As a direct result of the new TURA Law, investigations have begun into the possible use of water-soluble oils in some of the machining equipment. These water soluble oils, although they will still necessitate cleaning from the product, can be pre-cleaned with aqueous-based solvents, thus reducing the amount of CFCs and hazardous solvents required for a complete cleaning operation. *Although some CFCs and hazardous* solvents will still be used, the amounts used will be significantly reduced from the current level.

Water-soluble oils are now being used in several lathes and milling machines in the Machine Shop. These oils can be used for long periods of time without changing; and plans are now under way to expand the use of these oils to additional equipment in the Shop. An estimated 50% reduction in disposal costs and toxic waste generation are *expected to be achieved over the next several years.*

In the Packaging Area a new polyurethane packaging foam system that does not use CFCs was introduced in mid 1990. This equipment is used for packaging product using the "foam-in-place" method. The basic blowing agent is water rather than CFCs. The system consists of two 55-gallon drums of material with individual pumps and a dispensing gun. The CFC free foaming agent provides a "foam-in-place" material which meets the requirements of MIL-F-8367.

SUMMARY AND CONCLUSIONS

The new Massachusetts TURA Law has focused on the reduction of CFCs and toxic waste through prevention of pollution rather than cleanup after discharging of toxic wastes.

The areas which are of the greatest concern to GTE are:

1. Cleaning of printed circuit assemblies.
2. Conformal coating of printed circuit assemblies.
3. Chromating and cleaning of aluminum parts.
4. Painting, machining and packaging of product.

In the PWA area, aqueous cleaning has become the major cleaning process. Where solvent cleaning is absolutely necessary, training and education has been provided to employees on the ways to reduce the amounts of solvents being used through proper immersion techniques, solvent reclamation techniques, etc.

Investigations are currently underway into possible usage of HCFCs, terpenes and other semi-aqueous cleaning systems in the PWA area.

In the conformal coating operations, spray conformal coating has replaced dipping techniques, thus reducing the quantity of coating material being used, and the amount of thinner used in the formulation. Investigations are currently underway to test 100% solids conformal coating systems with no solvent thinners required in the formulation.

In the Waste Water Treatment Plant, hexavalent chromium is being reduced to the less toxic trivalent chromium along with very stringent controls on water utilization.

In the Packaging Area, CFC "foam-in-place" equipment has been replaced with a new water-based "foam-in-place" system thus eliminating the use of any CFCs in this area.

GTE Government Systems Corporation has taken a pro-active role in CFC and toxic chemical waste reduction. The gains achieved to this point will be monitored and controlled very carefully. CFC and toxic waste reduction is an on-going process which requires constant monitoring and control so that the gains achieved will not be lost by the substitution of a more toxic material for one that is less toxic or non-toxic.

To that end, one central chemical data base will be established within the new Production Planning and Control MRP II System. This data base will be used to monitor and control the purchasing, use, and disposal of all CFCs and toxic materials.

ACKNOWLEDGEMENTS

The author would like to thank Mr. Barrie Candeas, Process Engineering, GTE for his contributions in reducing CFC usage in the PWA area, and his help in preparing a section of this report.

I would also like to thank Mr. J. Graulich and Mr. J. Goldrick for their work in reducing toxic waste in the Packaging and Machine Shop Areas.

Daniel Gould is Supervisor of Process Engineering at GTE Government Systems Corporation. He has 25 years' experience in chemical engineering operations management and manufacturing engineering. He holds a BS degree in Chemical Engineering and an MBA. He is a Registered Professional Engineer and a member of IPC, EIA, and ACS.

Address: GTE Government Systems Corporation
77 "A" St. Needham Heights, MA 02194

NWC TP 7110

PWA AQUEOUS AND SEMI-AQUEOUS CLEANING:

SYSTEM APPROACHES AND TRADEOFFS

by

James J. Andrus
Electronics Group Cleaning Manager
Hollis Automation, Inc.
Nashua, New Hampshire

ABSTRACT

The initial question of CFC replacement was whether the replacement system or technology cleaned as well as the solvent it was replacing. Developments in the past several years have proven that aqueous and semi-aqueous processes do perform as well or better than CFC solvent systems. Nevertheless, conversion to these aqueous and semi-aqueous systems is complicated by the issue of waste water treatment and economics. Assemblers are justifiably reluctant to trade an air pollution problem for a water pollution problem. Assemblers are equally resistent to adopt a more costly cleaning process. The purpose of this paper is to discuss the issues of aqueous and semi-aqueous PWA cleaning and how they relate to waste water treatment and operating costs.

INTRODUCTION

There is a whirlwind of controversy surrounding the question of whether or not to clean printed circuit assemblies. Numerous confusing technologies are proposed as specific solutions to PWA cleaning needs. Often the confusion is aggravated by simplistic absolutes like "Aqueous and semi-aqueous cleaning create water pollution problems" and "Machine X cleans best." Such simplistic absolutes do not address the important questions of "cleaning at what cost" and "process discharge into what regulatory environment." To focus the scope of this paper and attempt to eliminate some confusion, the following assertions will be assumed to be true:

- Environmental forces are making CFC solvent cleaning processes less attractive.
- Surface mount technology is placing new challenges on the cleaning process.
- Aqueous processes have been used successfully for over fifteen years to clean printed circuit assemblies.

- Aqueous cleaning systems have changed to accommodate the more demanding cleaning and drying requirements of modern PWAs.

- Aqueous processes, both water soluble "OA" and detergent assisted rosin cleaning, have been proven successful in active production environments.

- Recent developments in semi-aqueous chemistry and equipment have shown good PWA cleaning potential.

Many of these assertions were points of controversy as recently as nine months ago. Today, continuing research, field history and common sense are proving their validity. Nevertheless, much controversy exists over the topic of PWA cleaning. In general, the controversial issues of PWA aqueous cleaning can be summarized by two issue questions and answers.

Issue Question #1: Do aqueous and semi-aqueous processes substitute a water pollution problem for an air pollution problem?

Issue Answer #1: In general, aqueous and semi-aqueous PWA cleaning processes are harmonious with natural and man-made treatment processes; therefore, the potential for environmental damage is very small when compared with CFC cleaning systems.

The Issue of Water Treatment

The controversy of water treatment starts with the regulations governing its discharge by PWA assemblers. There is no national set of regulations governing the type and quantity of process effluent chemicals that PWA cleaning systems are permitted to discharge. The Clean Water Act, enforced by the EPA, generally relegates PWA water cleaning system discharges to the local publicly owned treatment works (POTW). It is the POTW that must take all the water drained into its sanitary sewer system and treat it to EPA and state requirements prior to discharge into the local receiving stream. A receiving stream can be a river, lake or ocean.

The term used to define the process of preparing waste process water by an industrial user for discharge into the public treatment system is "pretreatment." The Clean Water Act defines pretreatment as "the reduction of the amount of pollutants, the elimination of pollutants, or the alteration of the nature of pollutant properties in wastewater prior to or in lieu of discharging or otherwise introducing such pollutants into the POTW."

The goal of the POTW is to follow EPA and state regulations by enforcing pretreatment requirements on industrial users. In general, POTW, State and EPA requirements are in place to protect the waste treatment system and its supporting piping networks and to prevent industrial discharges that may pass through or damage the treatment processes at the POTW. General categories of pretreatment requirements fall into the following noninclusive list:

- Temperature
- pH
- Heavy Metals
- BOD (Biological Oxygen Demand)
- COD (Chemical Oxygen Demand)
- Suspended Solids
- Grease, Oil & Fat
- TTO (Total Toxic Organics)

Temperature of discharged process waters are regulated because excessive temperatures can damage the structural treatment facilities and the biological organisms that are vital to the treatment processes. pH or the relative level of acidity or alkalinity is regulated for the same reasons temperature is limited.

Regulated heavy metals are generally defined to include copper, lead, nickel, chromium, silver, cadmium and zinc. These heavy metals are regulated because of their well known deleterious effects on human and animal life. The heavy metals are regulated because POTWs are regulated by the EPA and their respective states on the concentration and volume of heavy metals that they are permitted to discharge into the receiving stream. The POTW meets its heavy metal standards by capturing industrial heavy metal discharges into its sludges through precipitation or other methods. POTWs pay close attention to industrial heavy metal discharges. An unexpected increase in the concentration of heavy metals into its sludges can suddenly make the sludge a hazardous waste, a waste that requires expensive special handling by the POTW.

At this point it is important to note that the definitions of hazardous wastes are specific. A water or sludge may contain a small concentration of, say lead, and not be defined as hazardous. Only after the lead concentration exceeds a specified concentration is the fluid or sludge defined as hazardous.

BODs and CODs are related measures of chemicals that can remove oxygen from a receiving stream or POTW. BODs are chemicals that microorganisms use as a food source. Microorganisms eat the BODs as part of natural digestion, and in so doing, consume oxygen. CODs are an expanded category of BODs in that they are chemicals that

may not be organic food, but may contribute to oxygen depletion through chemical processes. Large concentrations of BODs and CODs in relation to the capacity of the POTW or receiving steam can starve the stream or facility for oxygen, thus "suffocating" plant and animal life. Good examples of high BOD/COD chemicals used in the printed circuit assembly process are detergents, saponifiers and terpenes.

Suspended solids are regulated because they can clog treatment facilities or contribute to excessive sludge build-ups. Grease, oil and fats receive special regulation because these materials require special POTW treatment processes like skimming. And Total Toxic Organics are toxic chemicals regulated by the EPA and thus treated by the POTW. Examples of TTOs are 1,1,1-trichloroethane and toluene. For TTOs, treatment plants usually use an activated carbon absorption process.

In a recent survey of fifteen water treatment authorities, Hollis Automation compiled six regional averages of local pretreatment regulations. In general, the survey indicated that there are a variety of pretreatment regulations. Some treatment requirements are similar across the country. Other requirements vary greatly from one community to the next.

Table A
Pretreatment Regulations Survey

Category	Average Limitations, (mg/liter)						
	North-East	Mid-Atlantic	South-East	Mid-West	South-Central	South-West	North-West
Temperature	160°F	147°F	145°F	127°F	132°F	143°F	147°F
Grease, Oil, Fat	100	84	100	125	133	283	100
pH	5.5 - 9.5	5.3 - 10.0	5.5 - 10.0	5.7 - 9.5	5.8 - 9.8	5.5 - 11.2	5.5 - 10.5
BOD	275	317	383	250	275	300	300
COD	700	450	580	UDL	UDL	UDL	900
Suspended Solids	300	333	250	258	288	300	350
Copper	3.1	3.1	1.4	6.0	2.5	6.9	2.5
Lead	1.9	0.9	0.4	4.8	2.2	2.5	1.4
Nickel	2.3	3.3	1.2	5.3	2.8	8.2	2.7
Chromium	3.3	2.9	1.4	7.7	3.7	4.3	3.7
Silver	2.5	1.8	0.2	0.8	2.1	3.6	0.5
Cadmium	0.3	0.6	0.1	0.4	0.4	5.6	1.4
Zinc	2.9	4.2	1.5	6.4	4.0	11.8	3.4
Fluorides	UDL	UDL	14.0	UDL	UDL	10.0	15.0
TTO (Total toxic org)	5	1.42	2.1	3.1	2.1	1.0	1.4

(UDL stands for Undefined Limit)

It was also observed that many treatment officials, often referred to as Pretreatment Coordinators, are unfamiliar with the specific nature of PWA cleaning. Often the offi-

cials assumed that PWA cleaning was the same as circuit board fabrication which fall under specific EPA pretreatment requirements. Nevertheless, two general rules emerged from the survey: dilution is not the solution to discharge pollution and water cleaners often require a permit from the local water treatment authorities.

Aqueous Versus Semi-Aqueous Process Discharges

At this point it is important to compare and contrast aqueous and semi aqueous systems. An aqueous system can clean both water soluble organic acid "OA" fluxes and rosin fluxes. In "OA" cleaning, typical aqueous cleaners use only water wash and water rinse cycles. For rosin cleaning, an aqueous system complements its wash water with a detergent chemistry. This detergent is typically called a saponifier.

A semi-aqueous system is very similar to an aqueous system designed to clean rosin chemistries. The difference between the aqueous and the semi-aqueous is the wash station chemistry. In semi-aqueous processes, the wash chemistry tends to be a solvent like chemical, like terpene, at a concentration of 100%. Like an aqueous system, a water rinse follows the wash stages. Therefore, in terms of process, semi-aqueous systems are very similar to aqueous systems.

Aqueous systems are also very similar to semi-aqueous systems in terms of process water discharge. A general simple rule for water discharge is as follows:

Water contaminants out = PWA contaminants + incoming water contaminants + assisting cleaning chemicals.

PWA contaminants are dominated by the fluxing process but can also include component, fabrication and material handling chemicals. Incoming water that is not deionized, typically includes some degree of water hardness. And waste contaminants can also be impacted by the assisting wash chemistry. In simple "OA" cleaning, the wash chemistry is typically plain water. But in rosin cleaning, the detergents or semi-aqueous chemicals in the wash stations typically migrate into the process effluents. When all of these water contaminants combine, there are nearly infinite possibilities of waste water chemistries. Nevertheless, the diversity or exact composition of the waste chemistries is not the issue. The issue of water treatment is the relationship of these chemistries to waste water regulations.

In general, the vast majority of PWA cleaning systems discharge chemicals that are well below POTW pretreatment regulations, or if pretreatment is required, then simple treatment solutions are available. For example, lead is often thought to be such a large byproduct of PWA cleaning that all process discharges are defined as hazardous. This is

simply not true. In many water soluble "OA" and rosin cleaning processes, the lead that is introduced into the rinse process effluents is often of such a low concentration that it is undetectable with standard testing methods. In cases where the lead is concentrated in the wash tanks of cleaning systems, the common process of deionization can often be used to reduce its concentration to POTW standards.

Other chemical groups that are often an issue are BODs and CODs. BODs and CODs are primarily generated in rosin cleaning systems, be they aqueous or semi-aqueous processes. Detergents, saponifiers and semi-aqueous chemistries like terpenes are high BOD/COD chemicals. A typical wash tank can have a BOD reading of 40,000 parts per million (ppm) and a COD reading of 55,000 ppm.

Where applicable, the simplest treatment strategy for BOD/COD chemicals is discharge into the POTW. Remember, BOD/COD chemicals are biodegradable materials, organic food, that are commonly treated at POTWs. It is also possible to reduce BOD/COD concentrations through the use of inorganic saponifiers or through decanting systems found in many semi-aqueous systems. It is additionally important to note that discharges into the POTW should always be in accordance with local regulations and fee structures.

Table B summarizes and generalizes an actual noninclusive analysis of a rinse water waste stream from an aqueous cleaner cleaning rosin paste with saponifiers.

Table B

Parameter	Milligrams/liter
pH	10
Lead	BDL
BOD	250
COD	1,000
Cadmium	BDL
Chromium	BDL
Copper	BDL
Mercury	BDL
Tin	.1
Zinc	1.0
T. Sus. Solids	5
Oil & Grease	30

Note: BDL means below detection limit.

Table B illustrates the point that the rinse stream from a specific aqueous system had relatively low levels of contaminants. In the specific example, the manufacturer simply discharged the rinse stream effluent into the POTW sewer system. An inexpensive surcharge was paid for BOD discharge. As can be seen from table B, lead was not an issue in the discharge of this example. It is also interesting to note that the cleaning system of this example did not incorporate recent chemical isolation technologies that are designed to significantly reduce migration of BOD and COD chemicals from the wash stations into the rinse stream.

Again, it is important to note that the characteristic of waste streams is dependent upon the exact manufacturing conditions. Additionally, the permission to discharge into POTW systems is according to local POTW rules and permitting procedures. All PWA assemblers instituting aqueous cleaning processes should work closely with chemical vendors, equipment vendors and the local authorities to match their water use conditions to the regulatory environment.

Issue Question #2: What are the economic considerations and tradeoffs of aqueous and semi-aqueous processes?

Issue Answer #2: Although similar in performance, aqueous and semi-aqueous cleaning systems can have different economic implications.

There is a vast array of variables that impact the economic performances of aqueous and semi-aqueous cleaning systems. To analyze the costs and interaction of many of these variables, the CLEANMACHINE computer simulation program was developed. CLEANMACHINE simulates the cost and operating structure of most aqueous and semi-aqueous cleaning systems.

To understand the difference among aqueous and semi-aqueous cleaning systems, multiple CLEANMACHINE scenarios were run under similar operating assumptions. Table C lists the operating parameters and assumptions. Table D summarizes the results of the CLEANMACHINE analyses.

Table C
Operating Parameters & Assumptions for CLEANMACHINE Simulations

Operating Parameters	Mid-Range Aqueous (OA)	Large Aqueous (OA)	Large Aqueous (Rosin)	Large Semi-Aqueous (Rosin)
Hours of Operation per Day	8	8	8	8
Days of Operation per Year	250	250	250	250
Times per Year Wash Tank Changed	250	250	125	2
Times per Year Rinse Tank Changed	250	250	250	250
Water/Sewage Fees ($/gal)	.005	.005	.005	.005
Cost of Power ($/KW hour)	0.050	0.050	0.050	0.050
Chemical Cost ($/gal)	N/A	N/A	9	32
Wash Tank Chemical Concentration (%)	N/A	N/A	7%	100%
Chemical Drag-out & Evaporation (gal/day)	N/A	N/A	3.75	2
Inerting Atmosphere ($/day)	N/A	N/A	N/A	Not included
Gallon Flow Through Rate (gal/min)	4	5	5	5
Closed-Loop Operation	No	No	No	No

Table D
CLEANMACHINE Analyses
Operating Cost Comparison

Cleaning System	Water Cost	Power Cost	Chemical Cost	Total Cost
Mid-Range Aqueous	$2,838	$10,572	$5,108	$18,517
Large Aqueous, OA	3,550	14,479	6,390	24,419
Large Aqueous, Rosin	3,365	16,106	22,370	41,841
Large Semi-Aqueous, Rosin	3,250	13,156	24,410	40,816

CLEANMACHINE Analyses

The CLEANMACHINE results summarized in Table D give a clear indication that the operating costs of aqueous type cleaning systems can differ greatly. First, the type of cleaning chemistry has a great impact on cleaning cost. Water soluble cleaning systems that do not need saponifiers or semi-aqueous chemicals cost far less than chemical assisted rosin cleaning systems. The issue of chemistry also is apparent when one compares aqueous rosin cleaning with semi-aqueous rosin cleaning. The CLEANMACHINE analysis calculated that the simulated semi-aqueous operating cost structure was very similar to the saponified aqueous cost structure. The similarity of values is interesting in spite of the fact that saponified aqueous systems can consume and use more energy and water than similar semi-aqueous systems. The differentiating factor between semi-aqueous and saponified aqueous systems is the cost and usage of wash chemicals. Although saponified systems are assumed to use more detergents through higher drag-out rates and more frequent tank changes, the unit cost of many semi-aqueous chemicals is far higher than the unit costs of the detergents. For example, semi-aqueous chemicals can cost approximately $32.00 per gallon. Many saponifiers cost $8.00 to $12.00 per gallon.

Second, all four analyzed systems consumed power and water in a "flow-through" type of operation. Water and power were consumed in relation to cleaning power and ion contaminant load. If the analyses had been run using a "closed-loop" type of operation, water and power usage would have been reduced; chemical recirculation costs would have been increased.

Third, the CLEANMACHINE analyses did not include pretreatment costs due to the huge diversity in local pretreatment regulations and their relationship to the huge diversity in cleaning processes and their associated discharge chemistries. Some manufactures can discharge all effluents to drain, while others must use a closed-loop treatment to discharge nothing to drain. The operating cost differential between these two extremes can be considerable!

The four CLEANMACHINE analyses summarized in Table D and detailed in Appendices A through D are theoretical values based on specific operating and cost assumptions. Because there is no "right" answer to cleaning system operation, the theoretical CLEANMACHINE model serves to give a good general view of the operating and cost environment of aqueous and semi-aqueous cleaning systems. Like any good model, CLEANMACHINE attempts to be simple enough for easy use, while being sophisticated enough to accurately approximate actual operating situations.

CONCLUSION

Successful aqueous type PWA cleaning processes consider capital, cost and water treatment requirements. All cleaners discharge some chemicals into the environment, be they aqueous or semi-aqueous systems. The important consideration for cleaner discharge is the relative ease of treatment. Many aqueous and semi-aqueous effluents can be directly discharged into the POTW sewer system, or if pretreatment is required, simple, cost effective treatment technologies are readily available.

Cost of successful operation is, perhaps, the most important cleaning issue. SMT cleaning can be accomplished. Rosin and "OA" residues can be removed. Waste water discharges can be pretreated. But at what cost? Many assemblers will be surprised to learn that many complete water cleaning systems -- including cleaner and supporting sub-systems -- cost far less to operate than traditional solvent systems. It all depends on the integration of PWA type, chemistry, cleaning system and treatment environment. There are no absolute answers, only "better" answers in relation to all the considerations.

REFERENCES

1. K.G. Boynton, "Cleaning of High Density Printed Wiring Boards and Environmental Consequences," 1980.

2. "The Clean Water Act," in *Code of Federal Regulations*.

3. "Resource Conservation and Recovery Act of 1976," in *Code of Federal Regulations*.

4. CLEANMACHINE Analysis run "China 1", December 3, 1990.

5. CLEANMACHINE Analysis run "China 2", December 3, 1990.

6. CLEANMACHINE Analysis run "China 3", December 3, 1990.

7. CLEANMACHINE Analysis run "CLNTERCHINA", December 3, 1990.

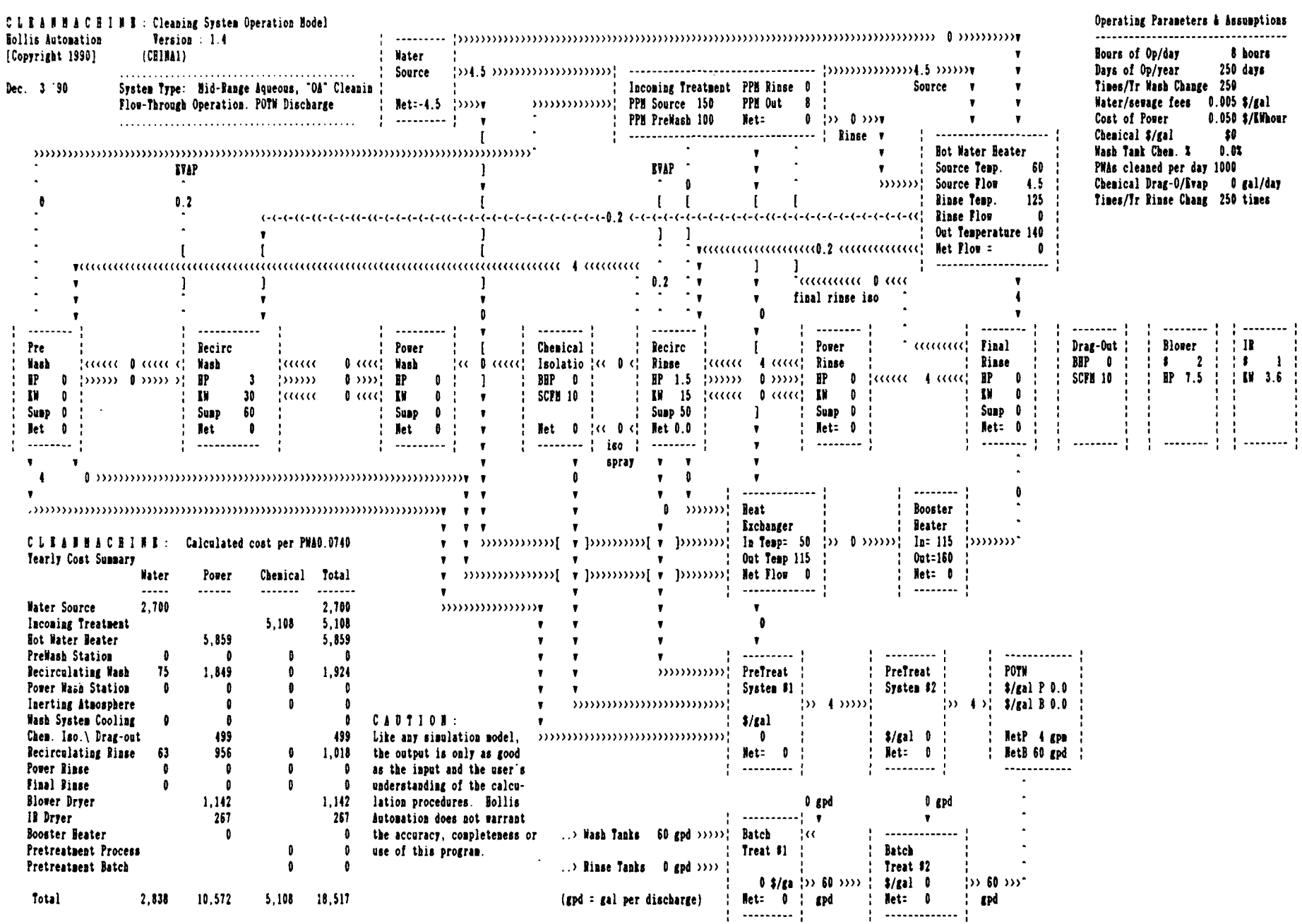
CLEANMACHINE : Cleaning System Operation Model
Hollis Automation Version : 1.4
[Copyright 1990] (CHINA1)
Dec. 3 '90
System Type: Mid-Range Aqueous, "OA" Cleanin
Flow-Through Operation. POTW Discharge
Water Source
Net:-4.5
Incoming Treatment PPM Rinse 0
PPM Source 150 PPM Out 8
PPM PreWash 100 Net: 0
Rinse
Source
Operating Parameters & Assumptions
Hours of Op/day 8 hours
Days of Op/year 250 days
Times/Tr Wash Change 250
Water/sewage fees 0.005 $/gal
Cost of Power 0.050 $/KWhour
Chemical $/gal $0
Wash Tank Chem. % 0.0%
PWAs cleaned per day 1000
Chemical Drag-O/Evap 0 gal/day
Times/Tr Rinse Chang 250 times
Hot Water Heater
Source Temp. 60
Source Flow 4.5
Rinse Temp. 125
Rinse Flow 0
Out Temperature 140
Net Flow = 0
EVAP
Pre Wash
HP 0
KW 0
Sump 0
Net 0
Recirc Wash
HP 3
KW 30
Sump 60
Net 0
Power Wash
HP 0
KW 0
Sump 0
Net 0
Chemical Isolatio
BHP 0
SCFM 10
Net 0
iso spray
Recirc Rinse
HP 1.5
KW 15
Sump 50
Net 0.0
final rinse iso
Power Rinse
HP 0
KW 0
Sump 0
Net= 0
Final Rinse
HP 0
KW 0
Sump 0
Net= 0
Drag-Out
BHP 0
SCFM 10
Blower
2
HP 7.5
IR
1
KW 3.6
Heat Exchanger
In Temp= 50
Out Temp 115
Net Flow 0
Booster Heater
In= 115
Out=160
Net= 0
PreTreat System #1
$/gal
0
Net= 0
PreTreat System #2
$/gal 0
Net= 0
POTW
$/gal P 0.0
$/gal B 0.0
NetP 4 gpm
NetB 60 gpd
0 gpd
0 gpd
Batch Treat #1
0 $/ga
Net= 0
Batch Treat #2
$/gal 0
Net= 0
60 gpd
60 gpd
CLEANMACHINE : Calculated cost per PWA0.0740
Yearly Cost Summary
Water Power Chemical Total
Water Source 2,700 2,700
Incoming Treatment 5,108 5,108
Hot Water Heater 5,859 5,859
PreWash Station 0 0 0 0
Recirculating Wash 75 1,849 0 1,924
Power Wash Station 0 0 0 0
Inerting Atmosphere 0 0 0
Wash System Cooling 0 0 0
Chem. Iso.\ Drag-out 499 499
Recirculating Rinse 63 956 0 1,018
Power Rinse 0 0 0 0
Final Rinse 0 0 0 0
Blower Dryer 1,142 1,142
IR Dryer 267 267
Booster Heater 0 0
Pretreatment Process 0 0
Pretreatment Batch 0 0
Total 2,838 10,572 5,108 18,517
CAUTION :
Like any simulation model, the output is only as good as the input and the user's understanding of the calculation procedures. Hollis Automation does not warrant the accuracy, completeness or use of this program.
..> Wash Tanks 60 gpd
..> Rinse Tanks 0 gpd
(gpd = gal per discharge)

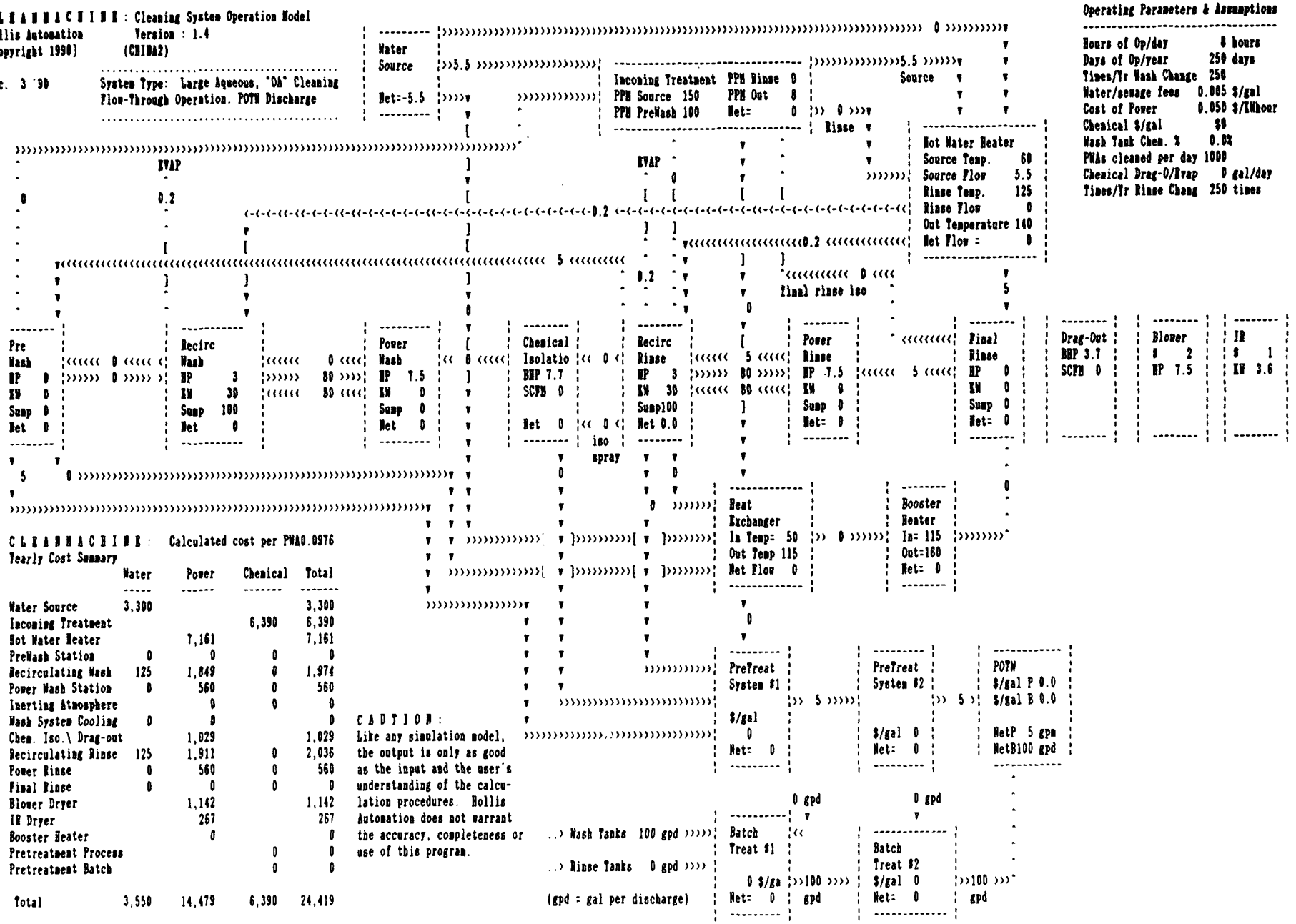

CLEANMACHINE : Calculated cost per PWA0.0976

Yearly Cost Summary

	Water	Power	Chemical	Total
Water Source	3,300			3,300
Incoming Treatment			6,390	6,390
Hot Water Heater		7,161		7,161
PreWash Station	0	0	0	0
Recirculating Wash	125	1,849	0	1,974
Power Wash Station	0	560	0	560
Inerting Atmosphere		0	0	0
Wash System Cooling	0	0		0
Chem. Iso.\ Drag-out		1,029		1,029
Recirculating Rinse	125	1,911	0	2,036
Power Rinse	0	560	0	560
Final Rinse	0	0	0	0
Blower Dryer		1,142		1,142
IR Dryer		267		267
Booster Heater		0		0
Pretreatment Process			0	0
Pretreatment Batch			0	0
Total	3,550	14,479	6,390	24,419

CAUTION:

Like any simulation model, the output is only as good as the input and the user's understanding of the calculation procedures. Hollis Automation does not warrant the accuracy, completeness or use of this program.

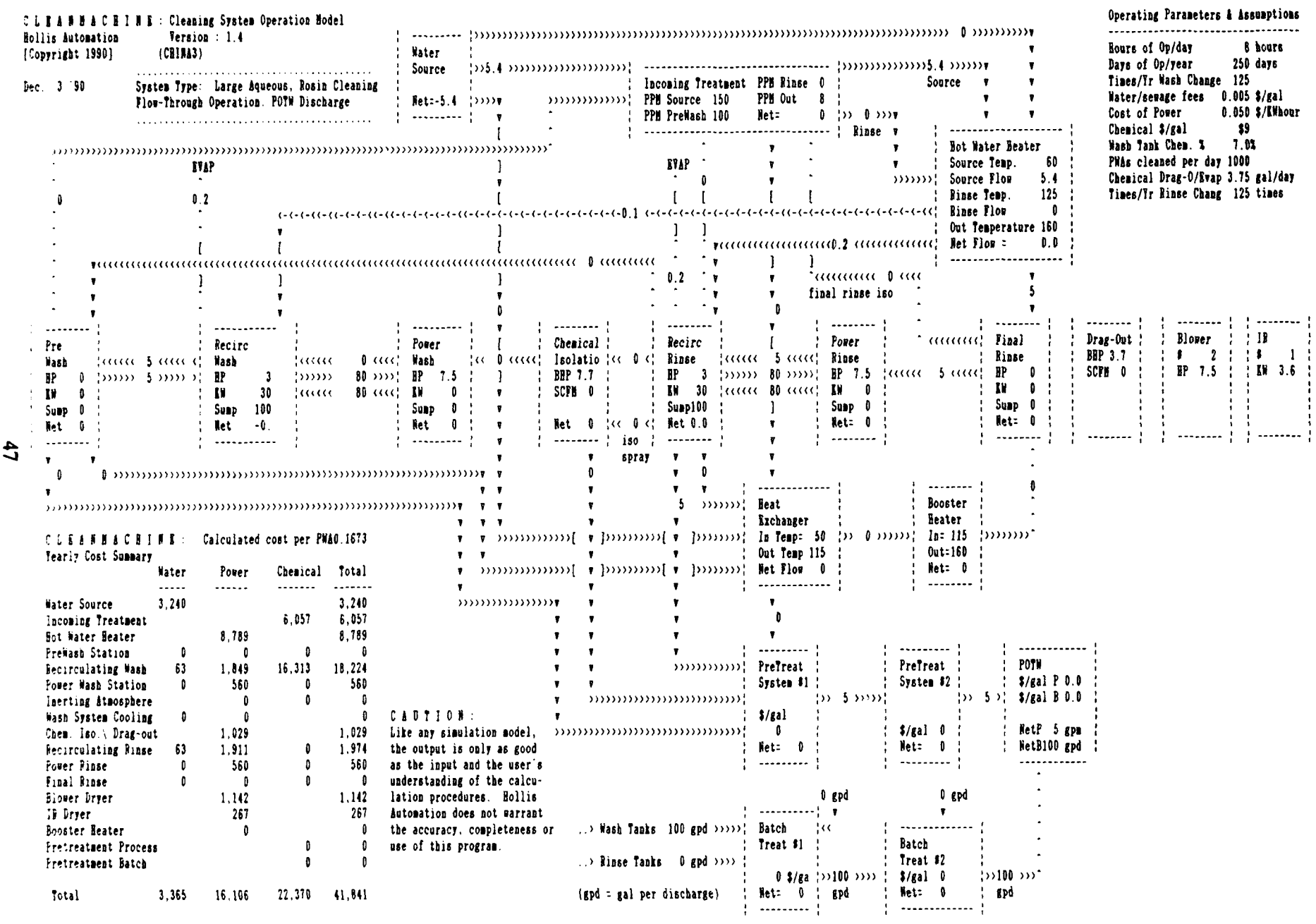
C L E A N M A C H I N E : Cleaning System Operation Model
Hollis Automation Version : 1.4
[Copyright 1990] (CHINA3)
Dec. 3 '90
System Type: Large Aqueous, Rosin Cleaning
Flow-Through Operation. POTW Discharge
Water Source
Net:-5.4
Operating Parameters & Assumptions
Hours of Op/day 8 hours
Days of Op/year 250 days
Times/Yr Wash Change 125
Water/sewage fees 0.005 $/gal
Cost of Power 0.050 $/KWhour
Chemical $/gal $9
Wash Tank Chem. % 7.0%
PWAs cleaned per day 1000
Chemical Drag-O/Evap 3.75 gal/day
Times/Yr Rinse Chang 125 times
Incoming Treatment
PPM Source 150
PPM PreWash 100
PPM Rinse 0
PPM Out 8
Net= 0
Rinse
Source
Hot Water Heater
Source Temp. 60
Source Flow 5.4
Rinse Temp. 125
Rinse Flow 0
Out Temperature 160
Net Flow = 0.0
EVAP
Pre Wash HP 0 KW 0 Sump 0 Net 0
Recirc Wash HP 3 KW 30 Sump 100 Net -0.
Power Wash HP 7.5 KW 0 Sump 0 Net 0
Chemical Isolatio BHP 7.7 SCFM 0 Net 0
iso spray
Recirc Rinse HP 3 KW 30 Sump100 Net 0.0
Power Rinse HP 7.5 KW 0 Sump 0 Net= 0
final rinse iso
Final Rinse HP 0 KW 0 Sump 0 Net= 0
Drag-Out BHP 3.7 SCFM 0
Blower # 2 HP 7.5
IR # 1 KW 3.6
Heat Exchanger In Temp= 50 Out Temp 115 Net Flow 0
Booster Heater In= 115 Out=160 Net= 0
PreTreat System #1 $/gal 0 Net= 0
PreTreat System #2 $/gal 0 Net= 0
POTW $/gal P 0.0 $/gal B 0.0
NetP 5 gpm
NetB100 gpd
Batch Treat #1 0 $/ga Net= 0
Batch Treat #2 $/gal 0 Net= 0
0 gpd
100 gpd
gpd
Wash Tanks 100 gpd
Rinse Tanks 0 gpd
(gpd = gal per discharge)
C L E A N M A C H I N E : Calculated cost per PWA0.1673
Yearly Cost Summary
Water Power Chemical Total
Water Source 3,240 3,240
Incoming Treatment 6,057 6,057
Hot Water Heater 8,789 8,789
PreWash Station 0 0 0 0
Recirculating Wash 63 1,849 16,313 18,224
Power Wash Station 0 560 0 560
Inerting Atmosphere 0 0 0
Wash System Cooling 0 0 0
Chem. Iso.\ Drag-out 1,029 1,029
Recirculating Rinse 63 1,911 0 1,974
Power Rinse 0 560 0 560
Final Rinse 0 0 0 0
Blower Dryer 1,142 1,142
IR Dryer 267 267
Booster Heater 0 0
Pretreatment Process 0 0
Pretreatment Batch 0 0
Total 3,365 16,106 22,370 41,841
C A U T I O N :
Like any simulation model, the output is only as good as the input and the user's understanding of the calculation procedures. Hollis Automation does not warrant the accuracy, completeness or use of this program.

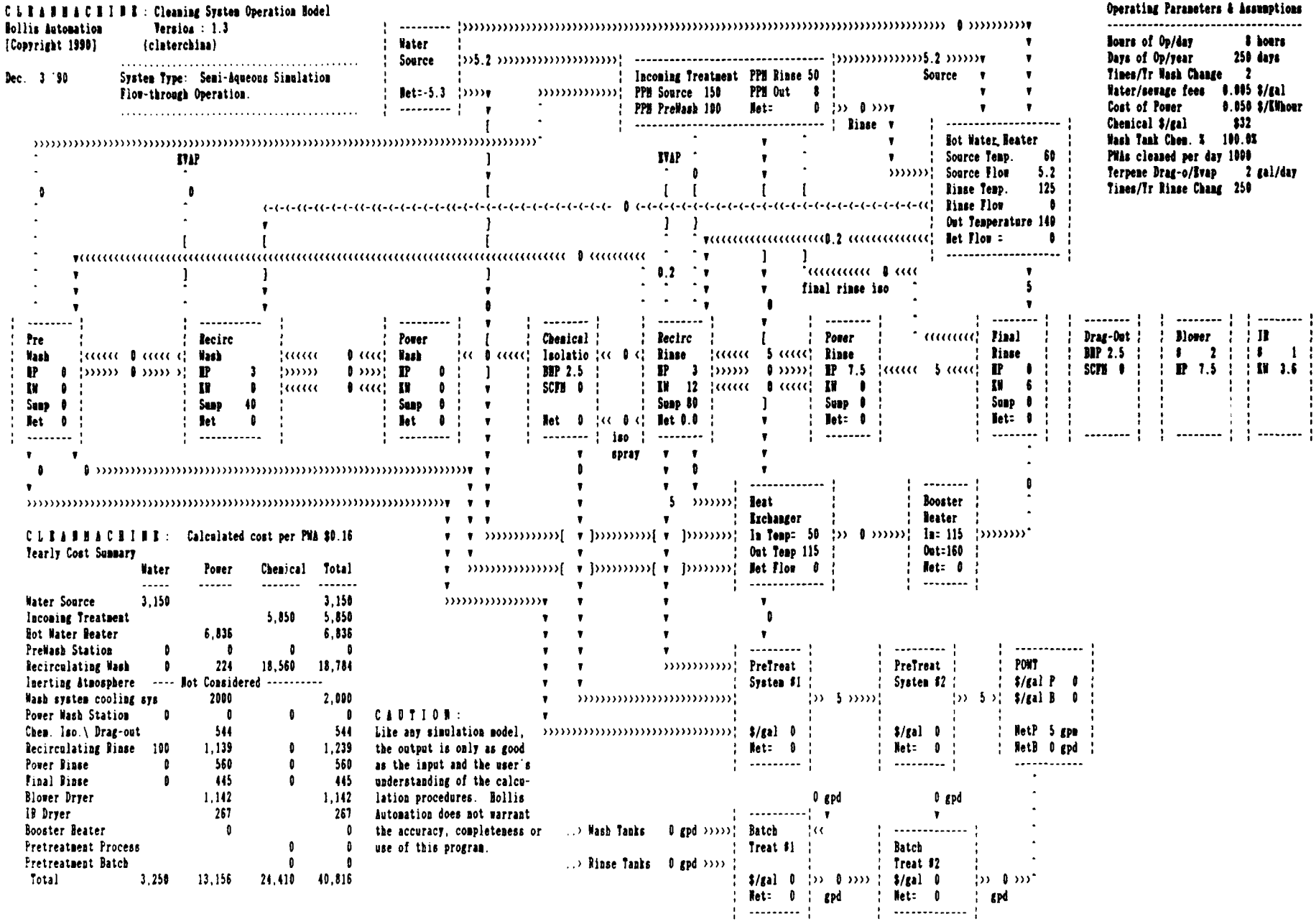

CLEANMACHINE : Calculated cost per PWA $0.16

Yearly Cost Summary

	Water	Power	Chemical	Total
Water Source	3,150			3,150
Incoming Treatment			5,850	5,850
Hot Water Heater		6,836		6,836
PreWash Station	0	0	0	0
Recirculating Wash	0	224	18,560	18,784
Inerting Atmosphere	---- Not Considered ----			
Wash system cooling sys		2000		2,000
Power Wash Station	0	0	0	0
Chem. Iso.\ Drag-out		544		544
Recirculating Rinse	100	1,139	0	1,239
Power Rinse	0	560	0	560
Final Rinse	0	445	0	445
Blower Dryer		1,142		1,142
IR Dryer		267		267
Booster Heater		0		0
Pretreatment Process			0	0
Pretreatment Batch			0	0
Total	3,250	13,156	24,410	40,816

CAUTION :
Like any simulation model, the output is only as good as the input and the user's understanding of the calculation procedures. Hollis Automation does not warrant the accuracy, completeness or use of this program.

James Andrus is the Manager of the Electronics Cleaning Group at Hollis Automation and has 12 years' combined experience in product design, marketing, and process-water use. He is the architect of all new Hollis cleaning systems and the creator of the CLEANMACHINE cleaning system simulation model.

Jim earned a BS degree in Civil/Structural/ Environmental Engineering from the University of Cincinnati and a Master of Management degree from the J. L. Kellog School at Northwestern University.

Address: Hollis Automation, Inc.
15 Charron Avenue
Nashua, NH 03063

MICROSTRUCTURAL MECHANISMS ASSOCIATED WITH THE ELECTRICAL IMPEDANCE CHARACTERISTIC OF SOLDER PASTE FLUX

by

Dr. Mark H. Polczynski
and
Mr. Timothy L. Hoeller
Eaton Corporation
Milwaukee, Wisconsin

Dr. Martin Seitz
and
Mr. Richard Hirthe
College of Engineering
Marquette University
Milwaukee, Wisconsin

ABSTRACT

It has been shown that alternating current electrical impedance measurement techniques can be used to monitor changes in solder paste properties. Impedance measurements are sensitive to changes in solder paste caused by heating and aging, and a correlation between impedance characteristics and solder paste per cent metal content has been demonstrated. To date, studies in this area have not addressed the underlying mechanisms responsible for the impedance characteristics of solder paste. However, an understanding of the microstructural changes responsible for observed impedance changes is essential before practical impedance-based solder paste monitoring instruments can be developed. The purpose of the work reported here is to provide a basic understanding of the microstructural mechanisms responsible for the impedance characteristics of the flux component of solder paste.

INTRODUCTION

It has been shown that physical and chemical changes occurring in solder paste are reflected in the alternating current electrical impedance characteristics of this material (Reference 1,2). Recently, a strong correlation between

solder paste impedance characteristics and per cent metal content has been demonstrated (Reference 3). However, the work to date has dealt only with the correlation between impedance characteristics and macroscopic solder paste properties. Correlations between impedance characteristics and underlying physical and chemical impedance mechanisms must also be established. This is a necessary step before impedance techniques can be applied to the measurement and monitoring of the properties of solder paste during manufacturing processes. To put this another way, the microscopic aspects of solder paste impedance characteristics must be understood before impedance techniques can be used to evaluate macroscopic properties of the paste.

This presentation describes an initial attempt to correlate impedance changes observed in the flux component of solder paste with physical and chemical changes occurring within the flux as temperature is varied. (For the purposes of this presentation, the flux component of solder paste is considered to include all of the constituents of whole paste less the solder metal particles). This association is important for two reasons. First, it aids in the general correlation between microscopic and macroscopic aspects of solder paste behavior. Second, since the impedance characteristics of flux are readily extracted from those of whole paste (Reference 1, 2), an understanding of the microscopic to macroscopic association in flux can be applied directly to establishing an understanding of the behavior of whole solder paste.

AC ELECTRICAL IMPEDANCE TECHNIQUES

Alternating current electrical impedance techniques have been used to monitor changes in the properties of a wide variety of systems (Reference 1,2). The following procedure is used to apply these techniques:

1. A physical model of the microscopic structure of the material is devised. The model should contain all physical elements which might contribute to electrical charge transfer or charge storage;

2. An equivalent electrical circuit is derived from the physical model. In this circuit, the charge transfer elements of the model become resistors, and the charge storage elements in the model become capacitors;

3. The impedance of the material being studied is measured over a wide range of frequencies, and the frequency response of the impedance is characterized;

4. The impedance characteristics of the material are compared to the theoretical response of the equivalent circuit. If discrepancies between the actual and theoretical response are noted, one or more of the preceding steps are repeated until a correlations is achieved.

Once correlation between the physical model and the equivalent circuit is established, changes in the elements of the physical model can be observed by identifying changes in the associated elements in the equivalent circuit, as revealed by changes in the frequency response of the material's impedance. This procedure amounts to what is essentially a spectrographic analysis, and the general technique is sometimes termed impedance spectroscopy.

Previous work (Reference 3) has indicated that the microstructure of solder paste can be represented by the physical model of Figure 1. Here, large solder particles, a, and small rosin particles, b, are suspended in a flux vehicle, c. The electrical resistivity and permittivity differs for the three constituents of this model.

It has also been shown (Reference 3) that the physical model of Figure 1 can be represented by the equivalent electrical circuit of Figure 2a. The conduction and polarization phenomena occurring within the electrically dissimilar constituents of the system give rise to the R_2-C_2 and R_3-C_3 parallel circuit combinations. The R_2-C_2 circuit combination has been associated with the solder paste flux, and the R_3-C_3 combination has been associated with solder paste metal particles.

Figure 2b shows the frequency response typically found for solder paste, when graphed as a complex impedance. Here, the X-axis represents the real (resistive) component of impedance, and the Y-axis represents the imaginary (capacitive) component of impedance. When the same scale is used for both axes, the plot of the series-measured impedance traces semicircular paths with centers that lie on the X-axis. Since it is only the flux portion of the paste that is being studied here, the R_3-C_3 combination will not be present in the equivalent circuit, and only one semicircle will be observed in the impedance plot.

The values of R_2 and C_2 can be obtained from the impedance plot in the following manner. Referring to Figure 2b, the resistance is determined directly from the chord length of the semi-circle along the abscissa. The capacitance are then obtained from the frequency, f_2, at which the imaginary component of the impedance reaches a local maximum value. Circuit theory shows that capacitance is related to these frequencies by:

$$f_2 = \frac{\omega_2}{2\pi} = \frac{1}{2\pi R_2 C_2},$$

where ω is angular frequency.

This relationship leads to the definition of a time constant, τ_2, which is independent of the geometrical factors determining the magnitudes of R_2 and C_2,

$$\tau_2 = R_2 C_2 = \left[\frac{\rho L}{A} \right] \left[\frac{\varepsilon A}{L} \right] = \rho_2 \varepsilon_2$$

where L and A are geometrical lengths and area associated with the charge storage and charge transfer mechanisms occurring within this system. The resistivity, ρ_2, is a material property which reflects the type, concentration, and mobility of the charge carrying species within the material, while the permittivity, ε_2, is a material property functionally related to the operative polarization processes, and the type and concentration of polar molecules in this material.

TEST METHODS

The purpose of this study was to associate the impedance characteristics of solder paste flux with the physical and chemical properties of this material. This was done by varying the temperature of the flux, and then correlating the resulting impedance changes with observed physical and chemical changes.

Several forms of analysis were used to examine the physical and chemical changes occurring in the flux during heating. Scanning electron microscopy (SEM) was used to visually examine structural changes in the flux. Thermogravimetric anaylsis (TGA) was used to measure weight loss in the flux during heating. Differential scanning calorimetry (DSC) was used to examine exothermic reactions

associated with the melting of flux constituents. Changes in the chemical composition of the flux as a result of heating were examined by fourier transform infra-red spectraphotometry (FTIR).

For SEM and FTIR analysis, samples were brought up to temperature, then cooled to room temperature and prepared for analysis. For TGA and DSC analysis, measurements were made continuously as temperature was increased.

AC impedance data was obtained in two ways. One set of data was obtained by heating samples, then cooling to room temperature and measuring impedance. Data was also obtained for samples measured at the elevated temperatures without cooling to room temperature before measurement.

TEST RESULTS

Figures 3 through 6 shows SEM photographs of flux heated from room temperature to 100°C. No obvious changes are noticed from room temperature (Figure 3) to 50°C (Figure 4), although the flux particles appear to be somewhat larger in the photo of flux heated to 50°C.

At 75°C (Figure 5), a major morphological change has taken place. By 100°C (Figure 6), it appears that the flux is completely melted, leaving a homogeneous glassy materials.

Figure 7 and 8 show another view of the structural change occurring around 75°C. Note the difference in magnification between these two figures. Figure 9 and 10 show lower magnification views of the flux at 75°C.

Some insight into the meaning of these photos can be deduced from the DSC scan of Figure 11. The hump in the DSC scan around 80°C indicates an exothermic reaction that is probably related to the melting cyrstalline portion of the of the flux particles. The large humps seen in Figures 5 and 8 may be islands of unmelted flux floating in a melted flux matrix. The low magnification photos of Figures 9 and 10 appear to show pools of completely melted flux separating areas of partially melted material.

Returning to Figure 11, the cooling portion of the DSC scan indicates no re-crystallization of the flux, an interpretation that is corroborated by the lack of structure noted in Figure 6.

The TGA plot of Figure 12 shows that for heating rates on the order of 20°C per minute, virtually no loss of material occurs for flux heated up to the 80°C range, with approximately 4% loss of material at 100°C. However, the isotherms shown in the TGA plots of Figure 13 indicate that more significant weight losses occur for protracted heating times.

Further information on material loss is provided by the FTIR plots of Figures 14a and 14b. The peaks at approximately 3400, 1800, and 1000-1500 wave numbers are greatly reduced after heating the flux for 20 minutes at 75°C. These peaks appear to be associated primarily with alcohol groups within the flux.

A set of impedance plots for solder paste flux are shown in Figure 15. For this set of curves, flux was heated to the temperatures indicated, then cooled to room temperature before impedance was measured. Plots for impedance measurements made at temperature (not cooled before measurement) were similar to those shown in Figure 15.

Plots of R_2, C_2, and τ_2 vs. temperature derived from Figure 15 are shown in Figure 16, 17, and 18. Plots of R_2 and C_2 derived from impedance measurements made at temperature (not cooled) before measurement are shown in Figures 19, and 20.

Figure 17 and 20 indicate a slight decrease in C_2 with increasing temperature. The behavior of C_2 does not change as the flux proceeds through the morphological changes occurring around 80°C.

In contrast, Figure 18 shows a strong temperature dependence for R_2 and a major change in the temperature dependence of R_2 as temperature passes through 80°C. The moderate temperature dependence of C_2 and the strong correlation between R_2 and the τ_2 value shown in Figure 19 indicates that changes in resistivity, ρ_2, are responsible for the observed behaviors.

As in Figure 16, Figure 19 shows a strong temperature dependence, but for this data (measurements made at temperature, not cooled before measurement), resistance falls with increasing temperature, rather than rising with increased temperature.

For this second set of impedance measurements, τ_2 (not shown) tracks R_2 very closely, again indicating that the observed impedance changes are due to changes in ρ_2.

DISCUSSION

Regarding the impedance test results, the similarities of Figures 17 and 20, and the lack of any significant temperature dependence of C_2 indicate that the capacitive element of Figure 2b is probably that of the test fixture used to hold the samples of solder paste flux, a conclusion that will be checked in future studies. This interpretation also explains the lack of any measurable R_2 component; R_1 is just the series resistance of the test fixture wiring and connections.

According to this interpretation, the flux can be modeled by a simple resistive element R_2. Thus, it would seem that the time and trouble of doing AC impedance measurements over a wide range of frequencies is unnecessary. This is not the case, however, since only extrapolation of R_2 using the calculated chord length of the impedance semicircle can eliminate errors induced by test fixture capacitance, for single-frequency AC measurements, and errors induced by electrode voltage off-sets and drift, for DC measurements.

Another advantage of the techniques used here is that measurements of R, C, and τ are derived from a large number of data points. The extremely close tracking of R_2 and τ_2 for both sets of impedance data attest to the accuracies that can be achieved using this technique.

Examining now the data for R_2, Figure 19 (impedance measured at temperature) shows that the resistivity of the flux falls as temperature is increased. This negative temperature coefficient is what would be expected as the mobility of charge carriers within the flux increases with increasing temperature.

On the other hand, Figure 16 (impedance measured after cooling to room temperature) shows a behavior opposite to that of Figure 19. This could be associated with the loss of volatiles, as shown in Figures 12 and 14.

Figure 13 illustrates a source of confusion for the set of tests reported here. Since the rate of loss of volatiles is temperature dependent and can continue for several hours, and since R_2 appears to depend on the amount of volatiles in the flux, the measured value of R_2 will depend on the length of time a sample has been held at the measurement temperature before the impedance data is obtained.

This is an important consideration if one is looking for an accurate quantitative evaluation of R_2. Note that sample geometry (e.g., exposed surface area to volume ratio) and sample holder configuration (e.g., sealed vs. vented) also affect the ability to establish good quantitative relationships.

Given the preceding interpretations, it should be noted that Figure 19 probably shows a combination of two impedance characteristics. As noted, the plot appears to show a negative temperature coefficient for R_2, but the evaporation of solvents upon heating (which increases the value of R_2) probably reduces the rate of decline of R_2 in Figure 19.

The final point of interpretation related here deals with the major change in R_2 noted as the flux is heated beyond to 80°C melting range. Two possible explanations present themselves. First, as the flux becomes liquid it is possible for the volatile elements to leave the flux at a much higher rate. If loss of solvent causes an increase in resistance, then a large increase in resistance could be caused by a significant loss of solvent with melting.

The DSC curve of Figure 11 suggests another possible mechanism. While the heating portion of this curve shows a relatively small but distinct endothemric reaction characteristic of melting, the cooling portion shows no distinct exothermic reaction, indicating that nothing equivalent to re-crystallization occurs upon cooling. This implies that some type of non-reversible molecular re-organization is occurring within the flux. This change may be responsible for the sudden increase in R_2 upon melting.

ACKNOWLEDGMENTS

The authors would like to thank Brian Bauer and John McMaster of Heraeus Cermalloy for providing flux samples for this study, and for assisting in the interpretation of our results.

1. M. Polczynski, M. Seitz, and R. Hirthe. "A New Technique for Monitoring Solder Paste Characteristics", in Proceedings of the 14th Annual Electronics Manufacturing Seminar, Naval Weapons Center, China Lake, CA, February 1990.

2. M. Polczynski, M. Seitz, and R. Hirthe, "A New Technique for Monitoring Solder Paste Characteristics for Statistical Process Control," Surface Mount Technology, Vol. 4, No. 10, October 1990. Pp. 54-60.

3. M. Polczynski, M. Seitz, and R. Hirthe, "Measuring Solder Paste Metal Content Using Alternating Current Electrical Impedance Techniques", in Proceedings of the 1990 International Symposium on Microelectronics, Chicago, IL, October 1990. Pp. 174-182.

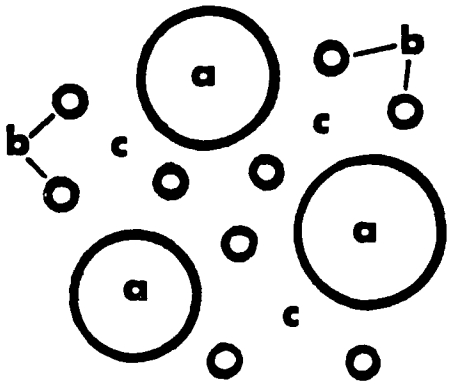

Figure 1. Physical Model for a Solder Paste.

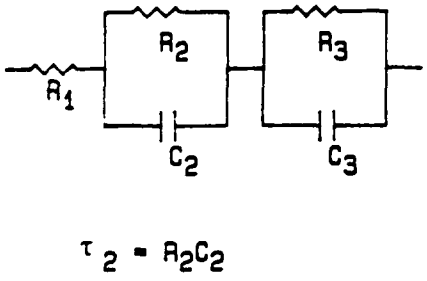

a) Equivalent Circuit

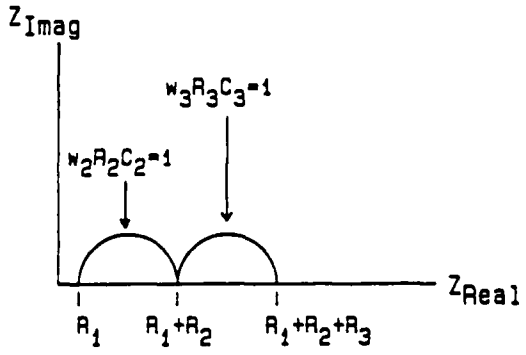

b) Complex Impedance Plot

Figure 2. Equivalent Circuit and Impedance Plot for the system shown in Figure 1.

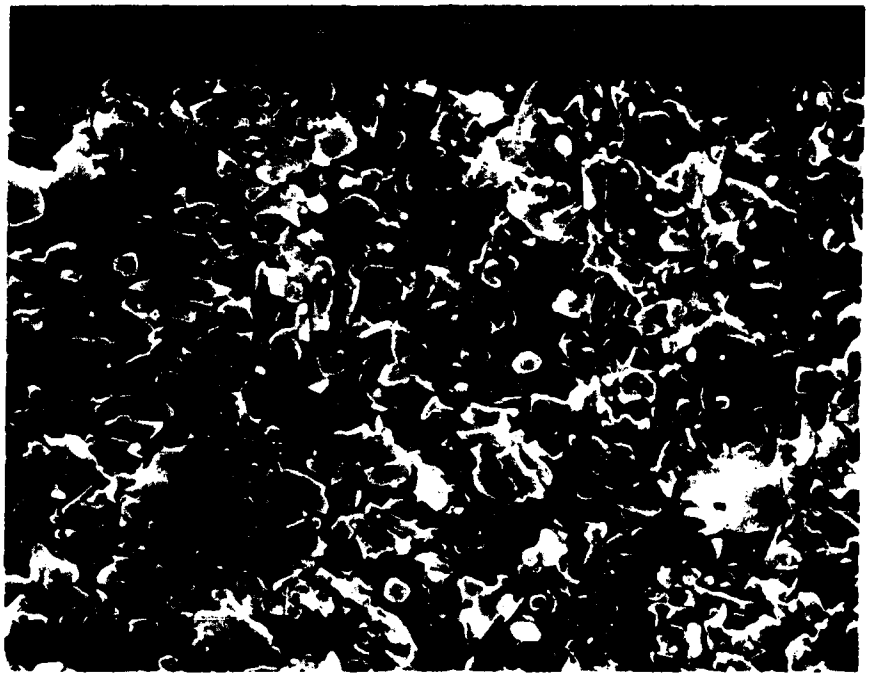

Figure 3: SEM Photograph of Flux at 1000x, Held at Room Temperature.

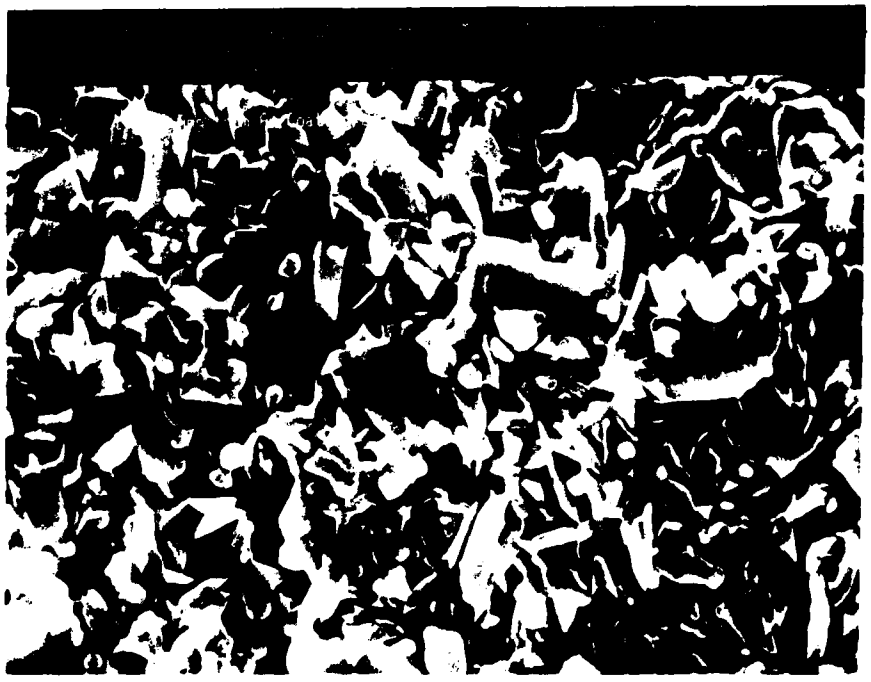

Figure 4: SEM Photograph of Flux at 1000x, Heated at 50°C.

Figure 5: SEM Photograph of Flux at 1000x, Heated at 75°C.

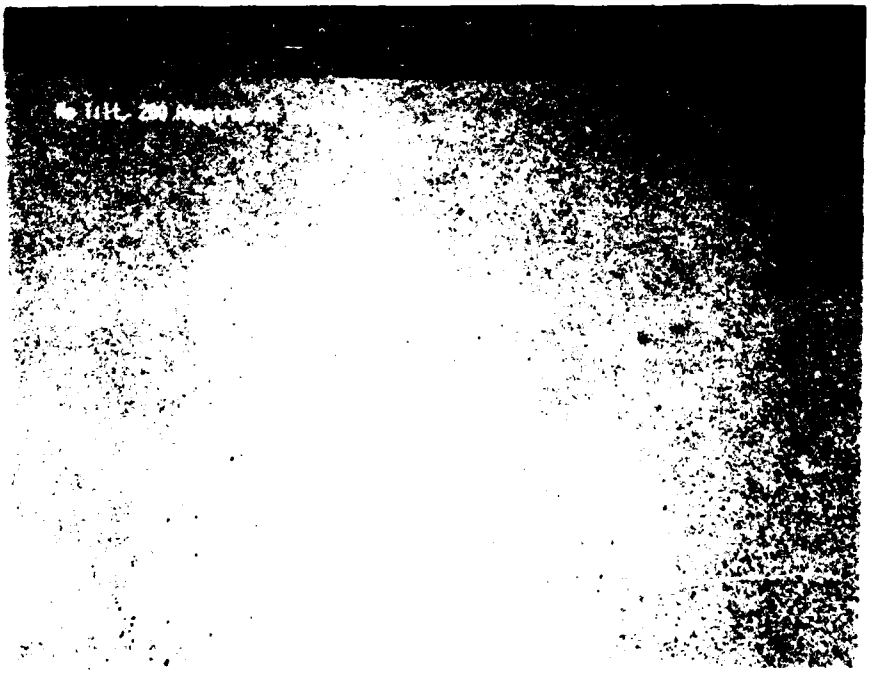

Figure 6: SEM Photograph of Flux at 1000x, Heated at 100°C.

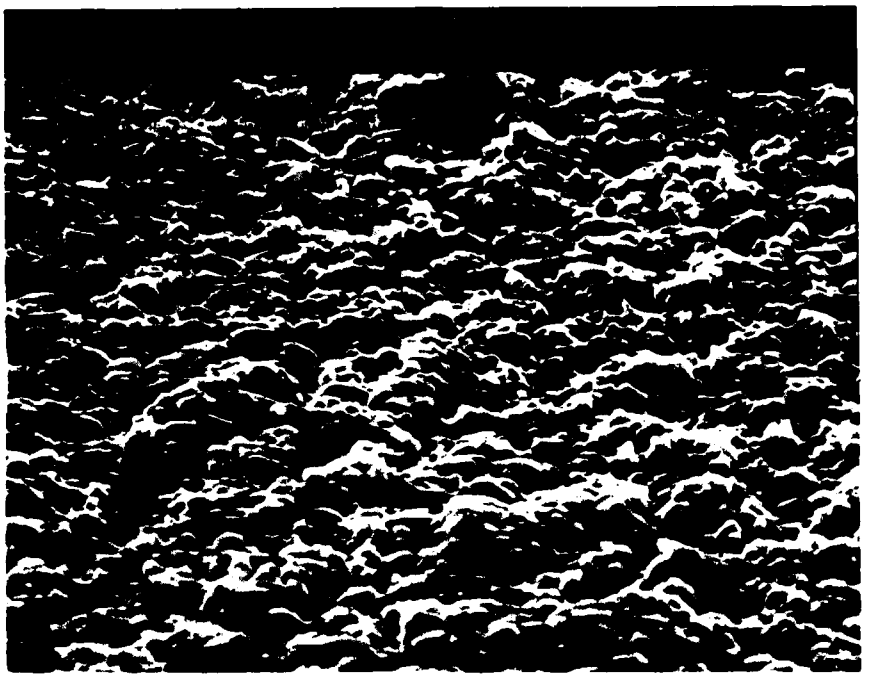

Figure 7: SEM Photograph of Flux at 1000x, Held at Room Temperature.

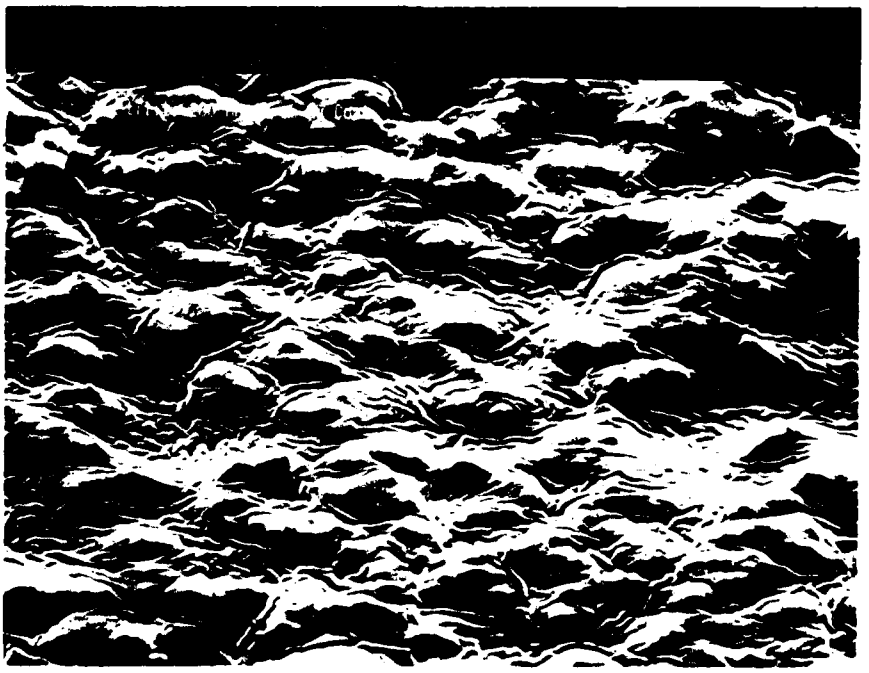

Figure 8: SEM Photograph of Flux at 500x, Heated at 75°C.

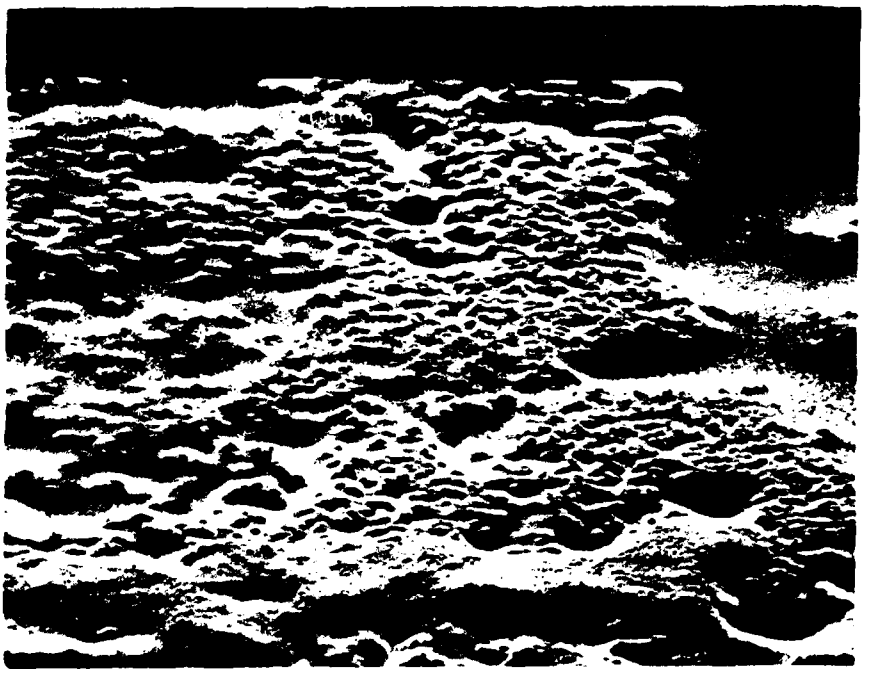

Figure 9: SEM Photograph of Flux at 100x, Heated at 75°C.

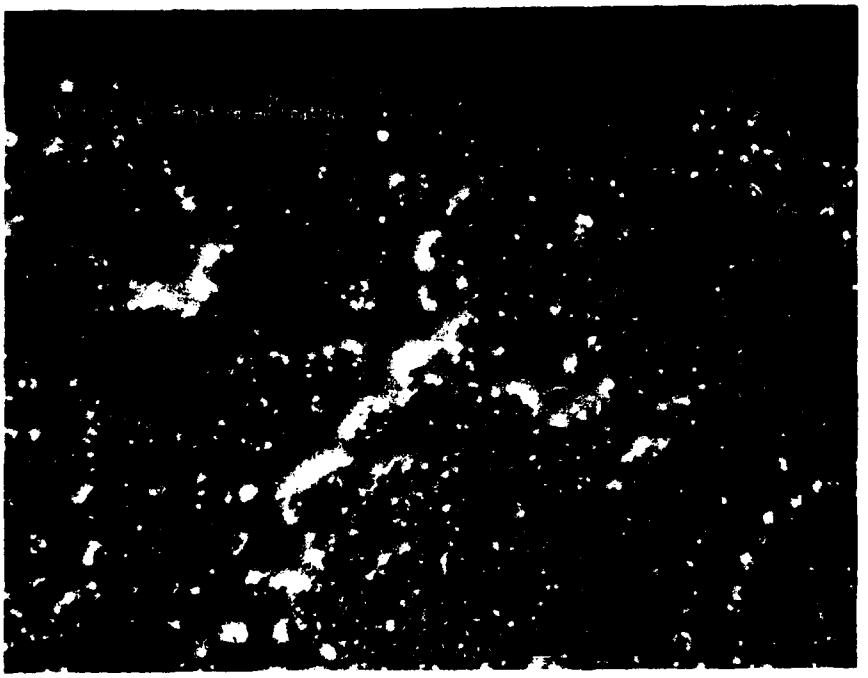

Figure 10: SEM Photograph of Flux at 100x, Heated at 75°C.

Figure 11
DIFFERENTIAL SCANNING CALORIMETRY OF SOLDER FLUX PASTE

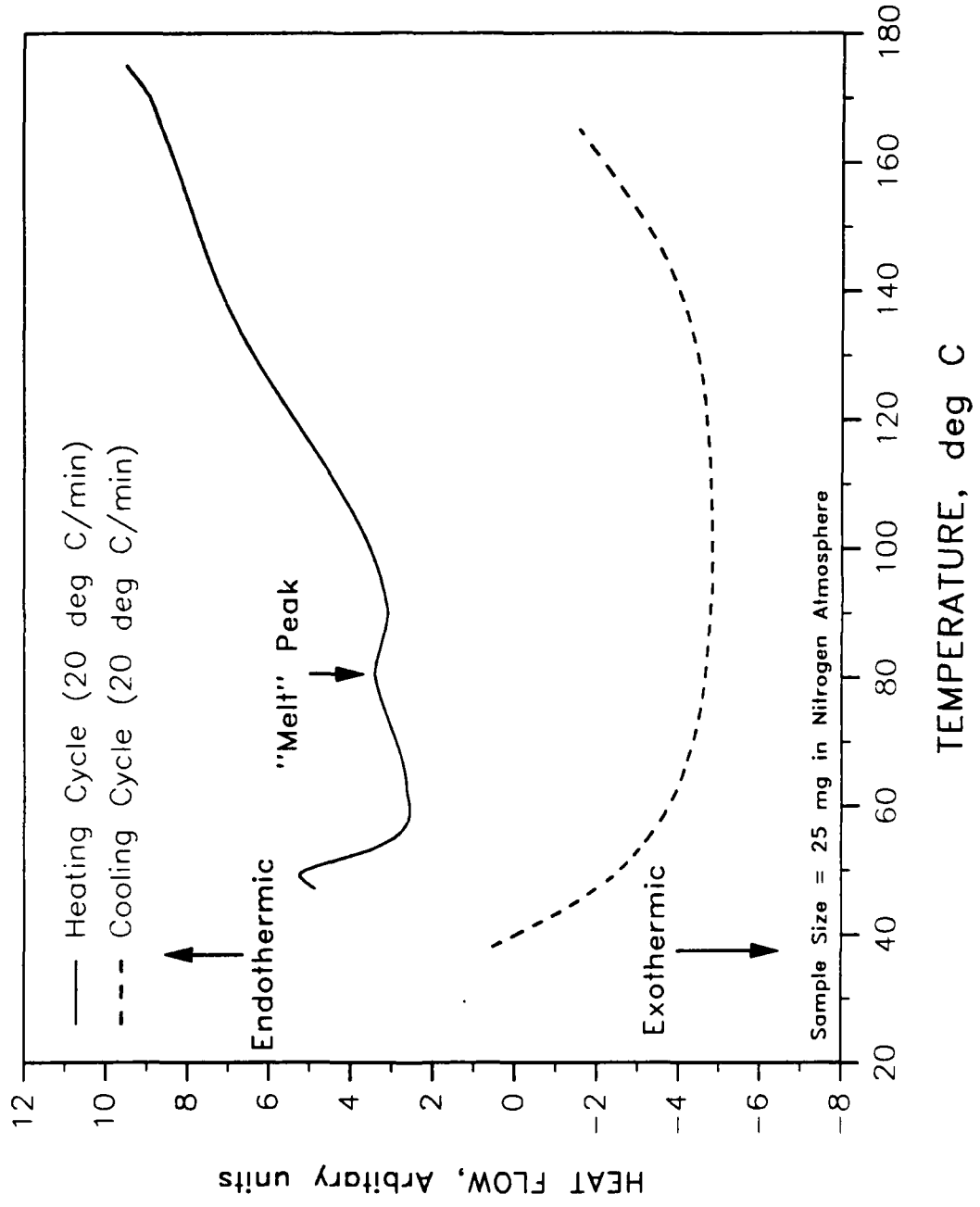

Figure 12 Thermogravimetric Analysis Of Solder Flux Paste

Sample: SOLDER FLUX PASTE
Size: 9.6970 mg
Method: TGA-CAOX
File: SOLDPASTE.01
Operator: HOELLER

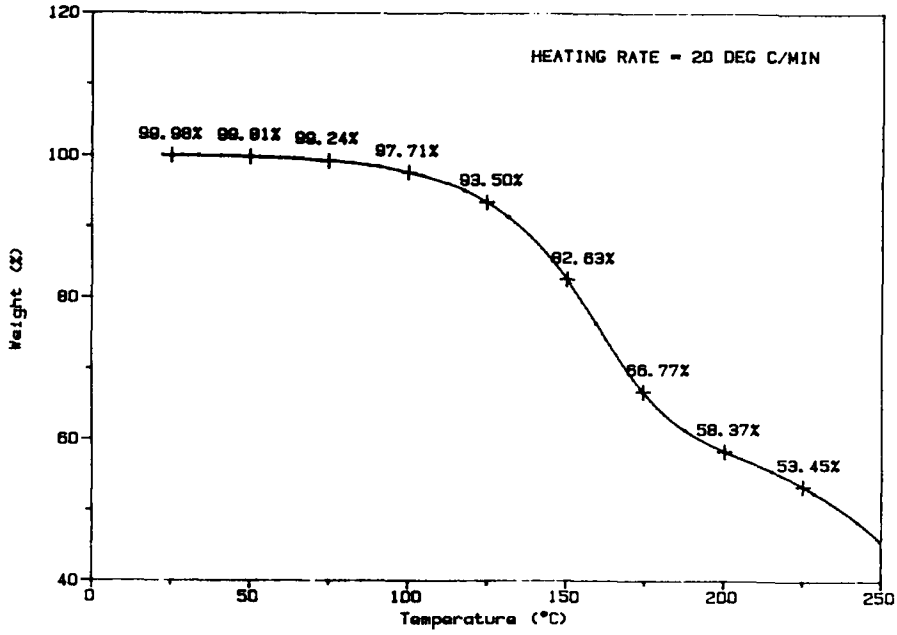

Figure 13 Thermogravimetric Isotherms For Solder Paste Flux

Sample: SOLDER FLUX PASTE
Size: 22.7600 mg
Method: 20 TO 100 C HOLD 2.5 HR
File: SOLD100.01
Operator: HOELLER

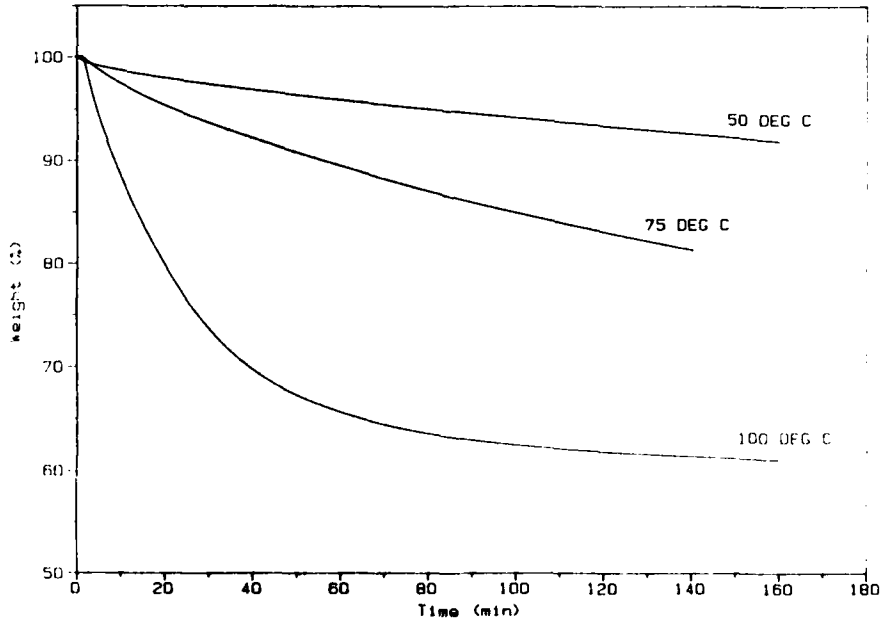

Figure 14a FTIR Plot For Solder Paste Flux at 75 C, Time = Zero

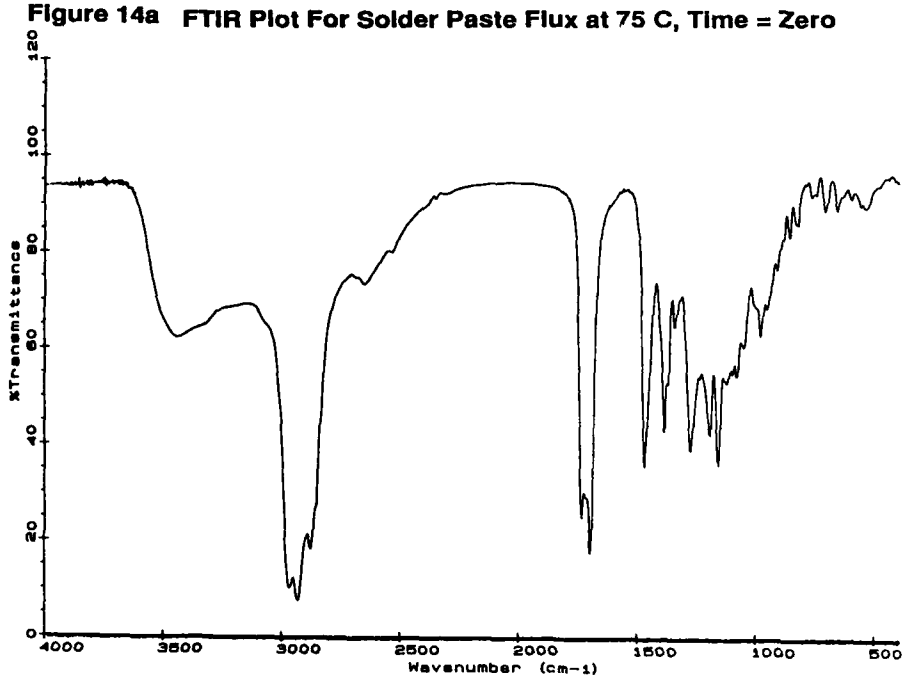

Figure 14b FTIR Plot For Solider Paste Flux at 75 C, Time = 20 Minutes

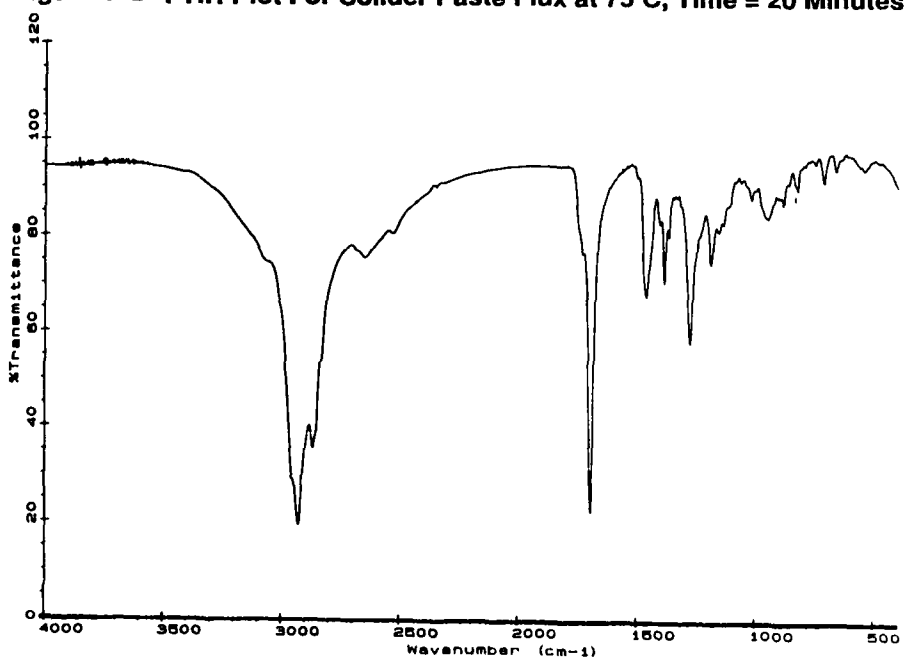

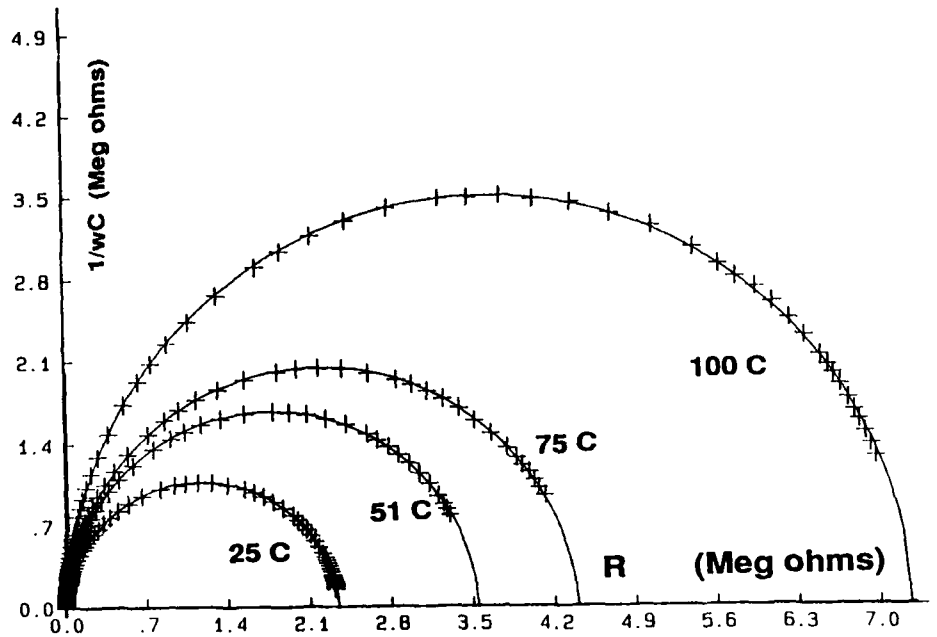

Figure 15 Complex Impedance Plots For Solder Paste Flux

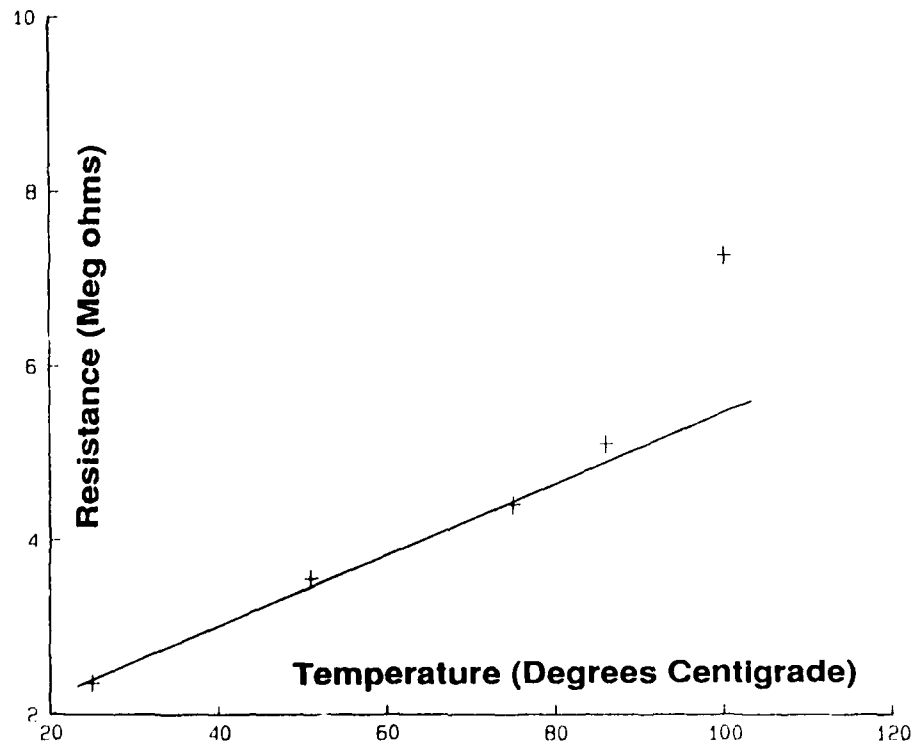

Figure 16 Resistance vs. Temperature For Solder Paste Flux

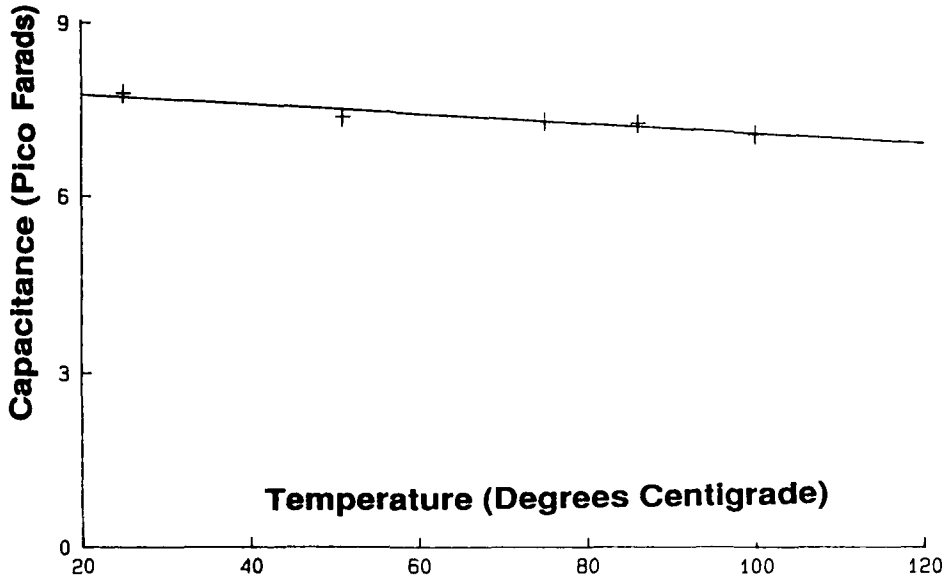

Figure 17 Capacitance vs. Temperature For Solder Paste Flux

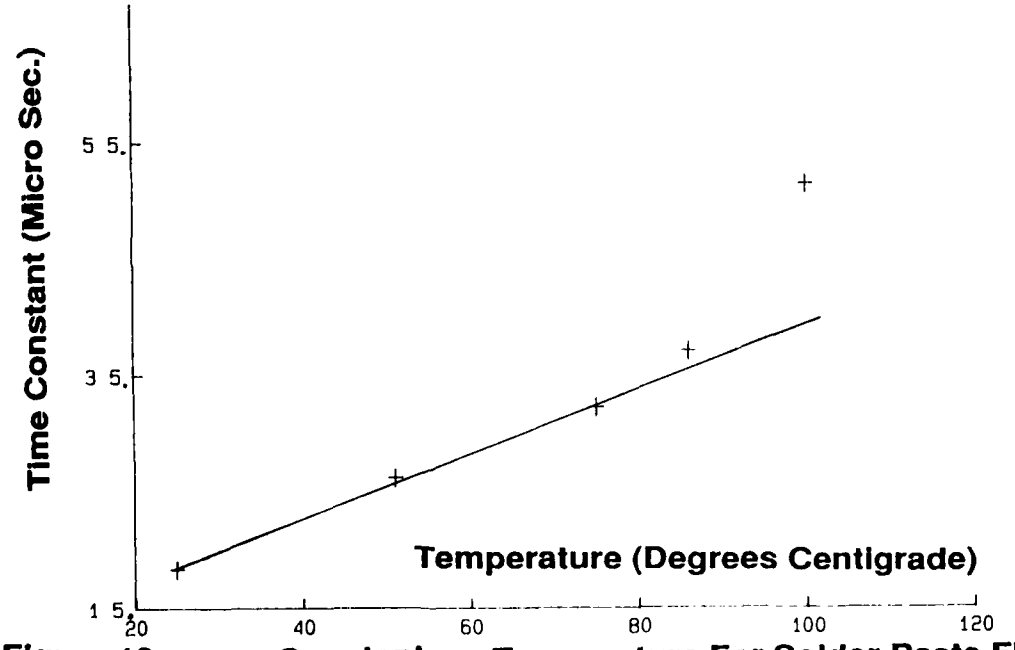

Figure 18 Time Constant vs. Temperature For Solder Paste Flux

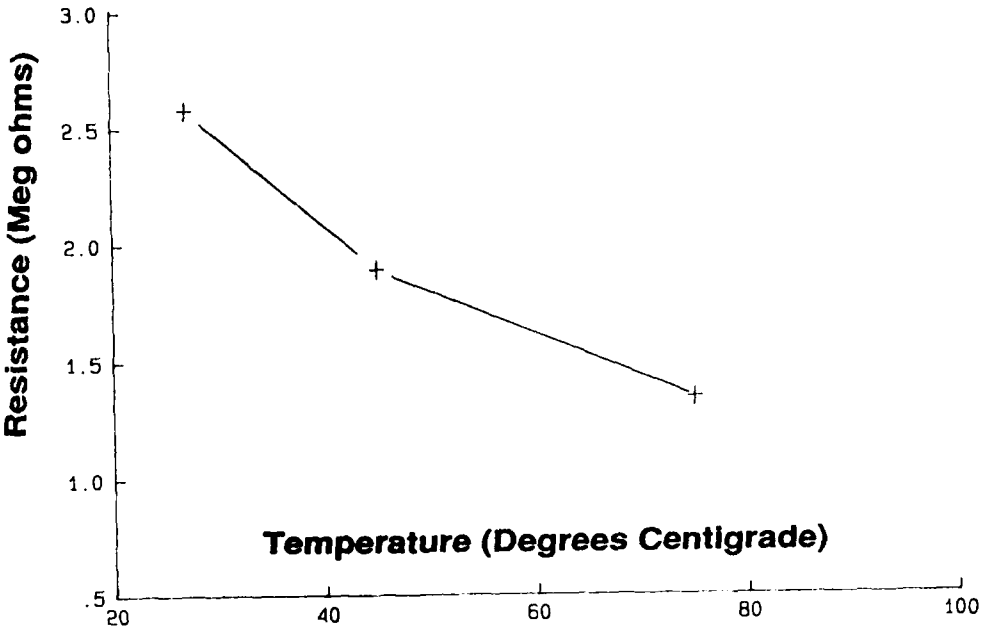

Figure 19 Resistance vs. Temperature, Measured at Temperature

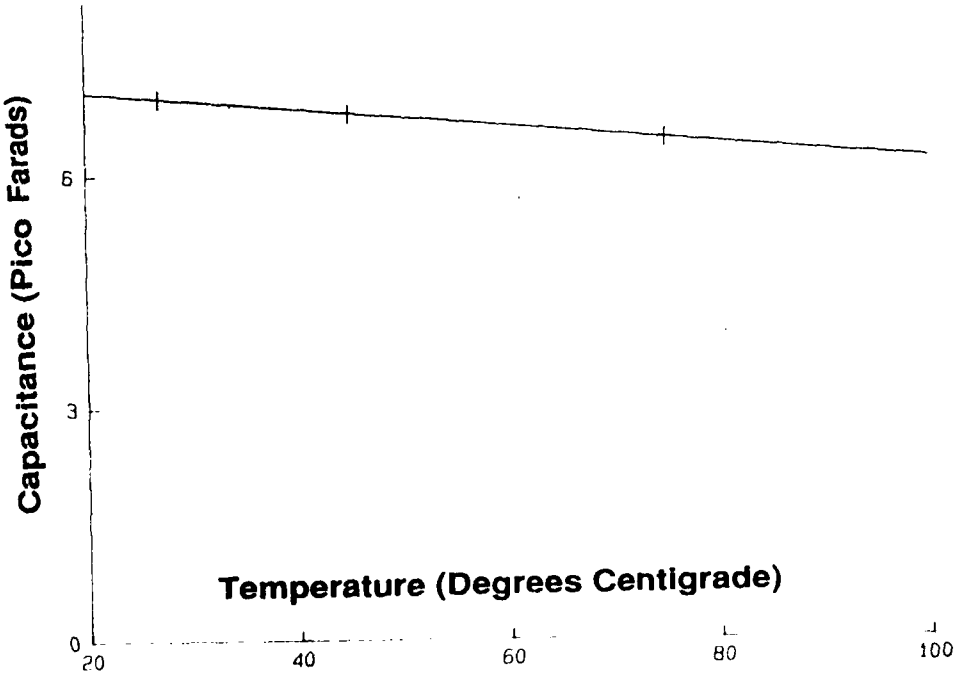

Figure 20 Capacitance vs. Temperature, Measured at Temperature

Mark Polczynski is the Manager of Materials Research at Eaton Corporation. He has worked in SMT assembly for 4 years, hardware and software design for 6 years, and quality control for 2 years.

Mark holds a BS degree and a Ph.D. in Electrical Engineering from Marquette University.

Address: Eaton Corporation
H-341, 4201 N. 27th St.
Milwaukee, WI 53216

Automatic Three Dimensional Solder Joint Quality Measurement

by
Raymond Swenson
Group Engineer
Advanced Manufacturing Technology
General Dynamics Air Defense Systems
Pomona, California

Abstract

An evaluation was performed to determine the measurement repeatability of a three dimensional solder quality measurement system. Discriminant analysis was used to determine which measurement variables from over 100 possible variables were significant in measuring solder quality. Discriminant functions were derived to reduce eleven "significant" solder quality variables into easily interpreted two dimensional solder quality graphs suitable for statistical process control. The basis for determining the discriminant functions was the use of "good" and "bad" solder joints as determined by two category C inspectors.

Technical Problem

Visual solder joint inspection criteria are subjective, and do not quantitatively measure variables such as wetting angle, volume of solder, and solder fillet curvature. Wetting angle characteristics are an excellent measure of the metallurgical quality of a solder joint. Lead size and spacing reductions limit the ability of an inspector to "see" the joints since the interconnections reside under packages or between tightly spaced packages and devices. Visual inspection data is subjective, requires manual data gathering, and is difficult to correlate with quantitative process parameters.

Production of high reliability electronic circuitry under present military standards requires 100% visual inspection of solder joints. The well known problem of inconsistency between visual calls (attributes) for two or more inspectors and rising costs due to unnecessary rework has fostered the development of various methods of automatic solder joint inspection. The justification for automated solder joint inspection systems has been well documented in the literature; unfortunately, automatic solder inspection methods available today (infrared thermal signature response, x-ray/vision system technology, and vision system technology) all have inherent strengths and weaknesses in terms of throughput speed, machine programming, calibration requirements, and the output format of the inspection data . With the exception of a few military contractors working on waivers, automatic solder joint inspection systems are primarily used in commercial low mix/high volume manufacturing environments.

Overall Project Objectives:

1) Estimate the variable measurement repeatability of the equipment on multiple runs of the same part for "key" solder joint dimensions (variables).

2) Determine variable signatures (frequency distributions for "good, bad, and marginal joints") for 9 solder joint process indicator variables (for example wetting angle, volume of solder, and solder fillet curvature).

3) Utilize discriminant analysis techniques for identification of "key" statistically significant variables to be used for quality assurance purposes.

4) Develop discriminant functions to be used for classification (prediction) of solder joint quality based on solder joint dimensional measurements and discriminant models.

Technical Approach

Initial set-up

Optimization of the automatic joint scanning operation was accomplished by measuring nominal solder joint dimensions and tolerances(pad thickness and width, lead length, and solder fillet height) for "good" joints as determined by visual inspection, and programming the circuit board solder joint locations and board levels . Ranking value interval widths (extra small, small, nominal, medium, and large) were assigned and input to the system for variables including wetting angle, fillet height, solder volume, and solder curvature. Sensitivity settings for factors including bump, dewet, hole, poor wet, and distortion were also entered into the system. Ranking values establish discrete intervals which are used by the system uses to "map" continuous random variables. These parameters were optimized for dual inline packages (DIPS). This operation is basically an iteration process where the solder joint ranking values and sensitivity factors are adjusted until accurate repeatable solder joint measurements and attribute calls are made by the system.

Repeatability testing

A test was performed to determine the repeatability of solder joint geometric measurements and solder joint attribute defect calls produced by the RVSI HR-2000 solder joint inspection system. Multiple inspection runs were performed on circuit card assemblies having 690/1260 programmed solder joints connections. All seven boards were of the same design, but five of the seven boards received five separate inspection scans at 690 solder joint locations, and the remaining two CCA's were inspected five times each at 1260 solder joint locations. A utility program was written to access and compare data files for each comparison. Each test run has been compared to all other test runs for a given part. In other words, five inspection scans of each circuit board resulted in ten sets of comparisons (Figure 1). This procedure was performed for both variables and attributes.

The PWB technology was multilayer plated through hole and the leads inspected were of the dual in line package variety (DIPS). Pin number one was omitted from the data analysis for each package during the preliminary work since pin one has a square pad as opposed to around pad. Pin one could be characterized in the same manner as the other joints. A utility program was written to compare inspection result files to all other files for a given circuit board. Figure 1 outlines the sequence of comparisons for each circuit board.

BOARD RUN			
cca run one to cca run two	cca run one to cca run three	cca run one to cca run four	cca run one to cca run five
	cca run two to cca run three	cca run two to cca run four	cca run two to cca run five
		cca run three to cca run four	cca run three to cca run five
			cca run four to cca run five

Figure 1. Inspection scan comparison sequence. A series of 5 inspection scans results in a set of 10 comparisons.

As the table shows, each set of five inspection runs for a particular circuit board resulted in ten comparison groups. These comparisons were used to test repeatability for both variable data and attribute data. The results are discussed in the next two sections.

Repeatability of variable measurements

Testing variable measurement repeatability for the solder joint variables (5 scans per CCA) resulted in ten comparisons per solder joint for each of twenty one dimensional variables. Repeatability of the systems own internal A.I system was also made. These ten comparison groups were performed on seven separate boards yielding a total of seventy comparison groups. Since five of the seven boards had 690 inspections and two of the boards had 1260 solder joints inspected, the potential number of comparisons totals 59,700. In the case of attributes, all 59,700 comparisons were made. In the case of variables, not all comparisons were available for data analysis. The system outputs an empty variable file when the system is not properly generating three dimensional solder joint image data. This can occur from poor tooling (large variation in point to point board elevations), non uniform solder mask, improper input of the nominal solder joint dimensions, or a grossly defective solder joint. When an empty file is created, code D15 (undefined defect) is output without performing the normal joint segmentation and calculation of variables. The RVSI system defaults to this mode to increase overall software code execution speed; whenever geometric dimensional data is out of tolerance; when the segmentation process is not functioning properly; and when solder joints are grossly defective. The percentage of solder joint variables omitted for a given comparison ranged between 5.3% and 18.9% (Figure 2). Identification codes for the variables tested are as follows:

1) Left fillet mean fillet solder height (LFMH),
2) Left fillet mean pad wetting angle (LFMPWA),
3) Left fillet mean fillet top wetting angle (LFMTWA),
4) Left fillet mean fillet curvature (LFMFC),
5) Left fillet mean fillet solder volume (LFMSV),
6) Left fillet distortion pad wetting angle distortion (variation of pad/fillet wetting angle measurements) (LFDPWA),
7) Left distortion fillet top wetting angle distortion (variation of fillet/lead wetting angle measurements) (LFDTWA)
8) Right fillet mean fillet solder height (RFMH),
9) Right fillet mean pad wetting angle (RFMPWA),
10) Right fillet mean fillet top wetting angle (RFMTWA),
11) Right fillet mean fillet curvature (RFMFC),
12) Right fillet mean fillet solder volume (RFMSV),
13) Right fillet distortion pad wetting angle distortion (variation of pad/fillet wetting angle measurements) (RFDPWA),
14) Right distortion fillet top wetting angle distortion (variation of fillet/lead wetting angle measurements) (RFDTWA),
15) Toe fillet mean fillet solder height (TFMH),
16) Toe fillet mean pad wetting angle (TFMPWA),
17) Toe fillet mean fillet top wetting angle (TFMTWA),
18) Toe fillet mean fillet curvature (TFMFC),
19) Toe fillet mean fillet solder volume (TFMSV),
20) Toe fillet distortion pad wetting angle distortion (variation of pad/fillet wetting angle measurements) (TFDPWA),
21) Toe distortion fillet top wetting angle distortion (variation of fillet/lead wetting angle measurements) (TFDTWA).

Figure 3 presents the average measurement difference for the twenty one variables mentioned above. The average difference between variable measurements comparisons ranged between 0.12 and 7.55%.

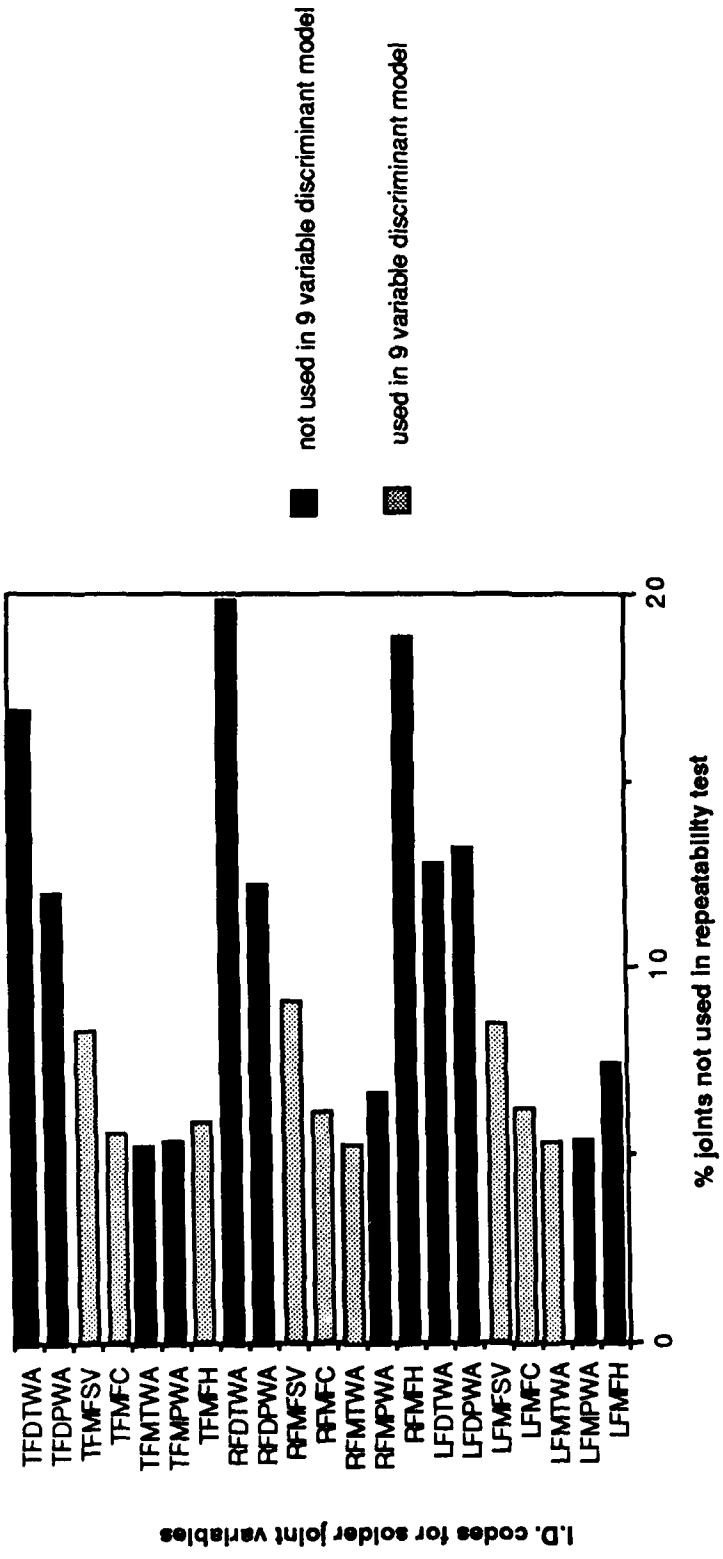

Figure 2. Percentage solder joint comparisons not used in determining overall inspection repeatability.

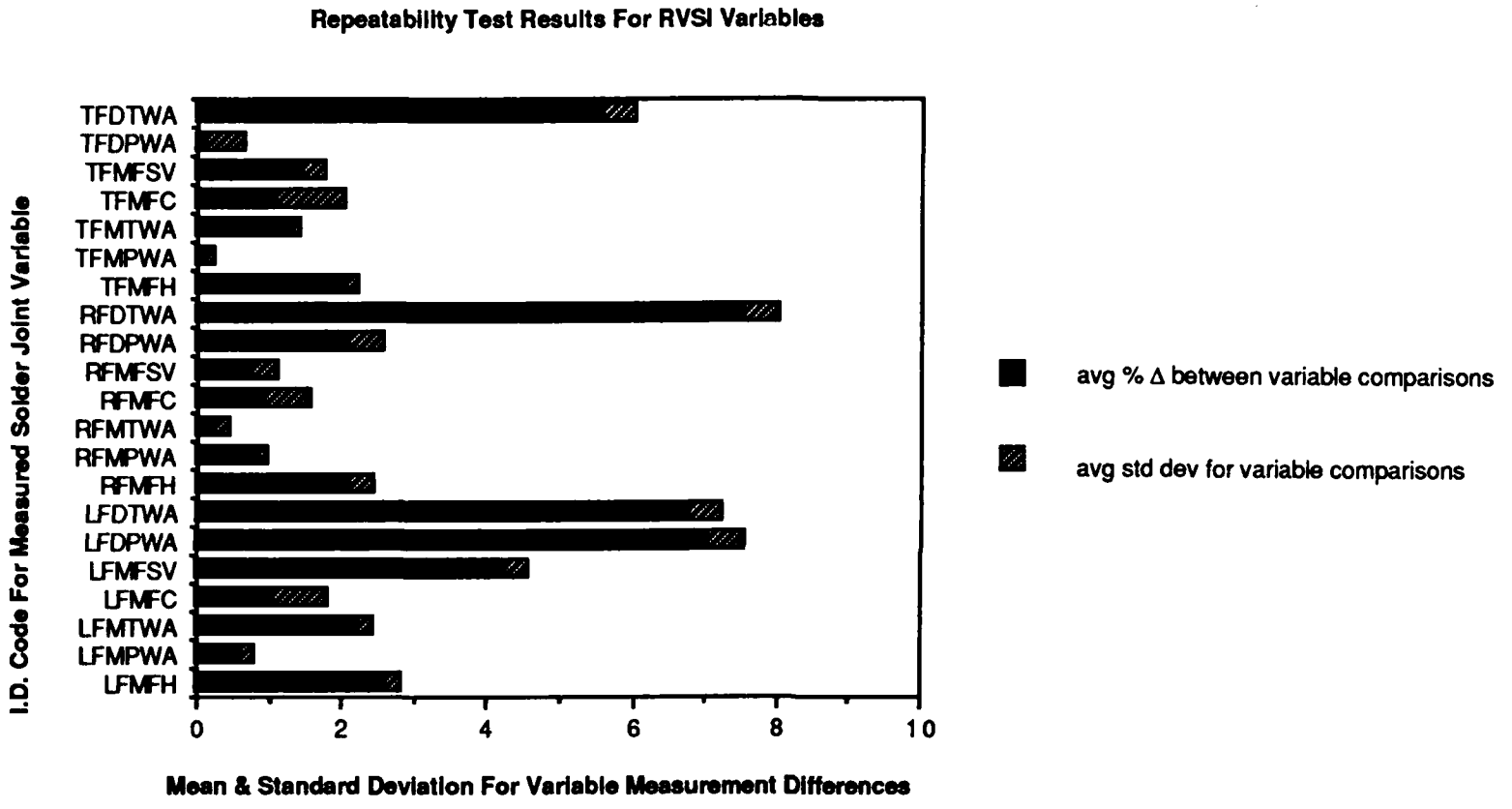

Figure 3. Repeatability test for solder joint variable measurements. The major portion of the bars represent the average percentage difference in readings when two solder joints are compared. The striped ends of the bars present average standard deviations.

Repeatability measurements of defect attributes

Repeatability of attribute inspection data (as determined by artificial intelligence system) was also tested. Unlike the variable repeatability test, all test data were used in the repeatability analysis (D 15 's - undefined defects were included). The attribute repeatability evaluation was based on the following three tests:

1) Does the system consistently call either "A* or D* or nothing" (ie A* or D* or nothing indicates a "good" joint), or does the system consistently call D (D is considered a "bad" joint)? No attempt was made to classify the defect attribute type. *RESULT - 98.0 % REPEATABILITY*

2) Does the system consistently call A*-A*, D*-D*, no defect-no defect, or D-D with no regard to correctly classifying the defect attribute type? *RESULT - 73.6 % REPEATABILITY*

3) Does the system consistently call A*(plus defect code#)-A*(plus defect code#), D*(plus defect code#)- D*(plus defect code#), or D(plus defect code#)-D (plus defect code#)? *RESULT - 72.3 % REPEATABILITY*

When considering the results of test three, it should be emphasized that the majority of attribute defects (visual criteria) were insufficient solder (A*1, D*1, D1) for all CCA's in the the sample, so effectively the RVSI A. I. system was tested for one type of attribute defect only. Repeatability for other attribute types may be better or worse. Figure 4 summarizes the results for the defect attribute repeatability testing.

	no defect code (good)	A* marginally acceptable	D* marginally rejectable	D rejectable	Repeatability percentage
Test one (detection)	no code = A* = D*	no code = A* = D*	no code = A* = D*	D = D	98%
Test two (severity)	no defect = no defect	A* = A*	D* = D*	D = D	73.6%
Test three (detection & severity)	no defect = no defect	A* = A* includes code A*1,2,+ ··· 15	D* = D* includes code D*1,2,+ ···15	D = D includes code	72.3%

1) INSUFFICIENT SOLDER	8) NO SOLDER	A*	MARGINAL ACCEPTABLE
2) EXCESS SOLDER	9) MISREGISTRY		
3) POOR WETTING	10) NO LEAD	D*	MARGINAL REJECTABLE
4) BRIDGING	11) NO HEEL		
5) PEAKS, BUMPS > 4 mils	12) OVEREXTENDED LEAD	D	REJECTABLE
6) HOLES/PITS > 4 mils	13) ABSNT/MISDR CLINCH		
7) DEWETTING	14) ABNRML CLINCH LNGTH		
	15) UNDEFINED DEFECT		

Figure 4. Attribute repeatability test criteria and repeatability results.

Analysis of solder joint inspection data

The three dimensional inspection system can output over one hundred measurements for each solder joint ; however, storage, retrieval, and interpretation of this much information for hundreds and even thousands of solder joints per assembly would severely limit the usefulness of the system in a production setting. The calibration for the discriminant analysis models was obtained from the the inspection results from two independent category "C" inspectors. Figure 5 shows a high degree of agreement (98%) when the solder joints are considered "good" by the visual inspectors; however, when the joints are "bad" or rejectable in quality, the agreement as to what is rejectable is only 38%. Possible reasons for the low level of agreement are interpretation of solder quality specifications and the tendency of human inspectors to make relative quality comparisons between solder joints on a given circuit card assembly rather than against "fixed" standards. A key objective of the project was to minimize the number of solder quality indicator variables necessary to monitor and control the soldering process. Additionally, it would be desirable to isolate or identify components or materials that possess solderability problems so that a statistical data base could be established. Attribute or qualitative data such as excess solder, insufficient solder, and not smooth and shiny indicate cosmetic problems with specific solder joints, but do not provide numbers that could be used to rank or compare specific solder joints to other similar joints produced under the same process parameters. Selection of variables for the original discriminant model was based on experience, intuition, and trial and error from a pool of 21 "key" variables listed in the RVSI operational manual. Means and standard deviations for the 21 variables as measured by the system are presented in Figure 6. The basis for variable selection or elimination was the canonical correlation coefficient. The 9 variable model developed will be discussed in the next section, but is mentioned here to explain the selection of 9 specific solder measurement variables. Means for the nine variables used in the discriminant model are presented graphically in Figure 6. An additional bar is used in Figure 7 to compare the original model development data means to a test board with "good" joints. As can be seen from the graph, the "good" means for the arbitrary test board are comparable to the "good" means from the development data.

Discriminant analysis is a statistical tool that can be used to study differences between two or more groups with respect to multiple variables. Discriminant analysis is actually a broad class of related statistical activities. In a typical application, discriminant analysis is used for identifying group (classification cases) differences with respect to variable measurements and for developing functions to be used for classifying cases (such as "good", "bad", or "marginal solder joint quality) into groups. The idea is to discriminate between groups (for example discrete solder quality groups) on the basis of multiple measurement variables and to identify which measurement variables have the the most discriminating power; and secondly, one is interested in classifying new cases into specific groups through the use of quantitative measurements (variables) and discriminant functions. Several important assumptions must be made when analyzing data by discriminant analysis:

(1) two or more groups: $g \geq 2$
(2) at least two cases per group: $n_i \geq 2$
(3) any number of discriminating variables,
provided that it is less than the total number of cases minus two: $0 < p < (n_. - 2)$
(4) discriminating variables are measured at the interval level
(5) no discriminating variable may be a linear combination of other discriminating variables
(6) the covariance matrices for each group must be"approximately" equal
unless special formulas are used on the discriminating variables

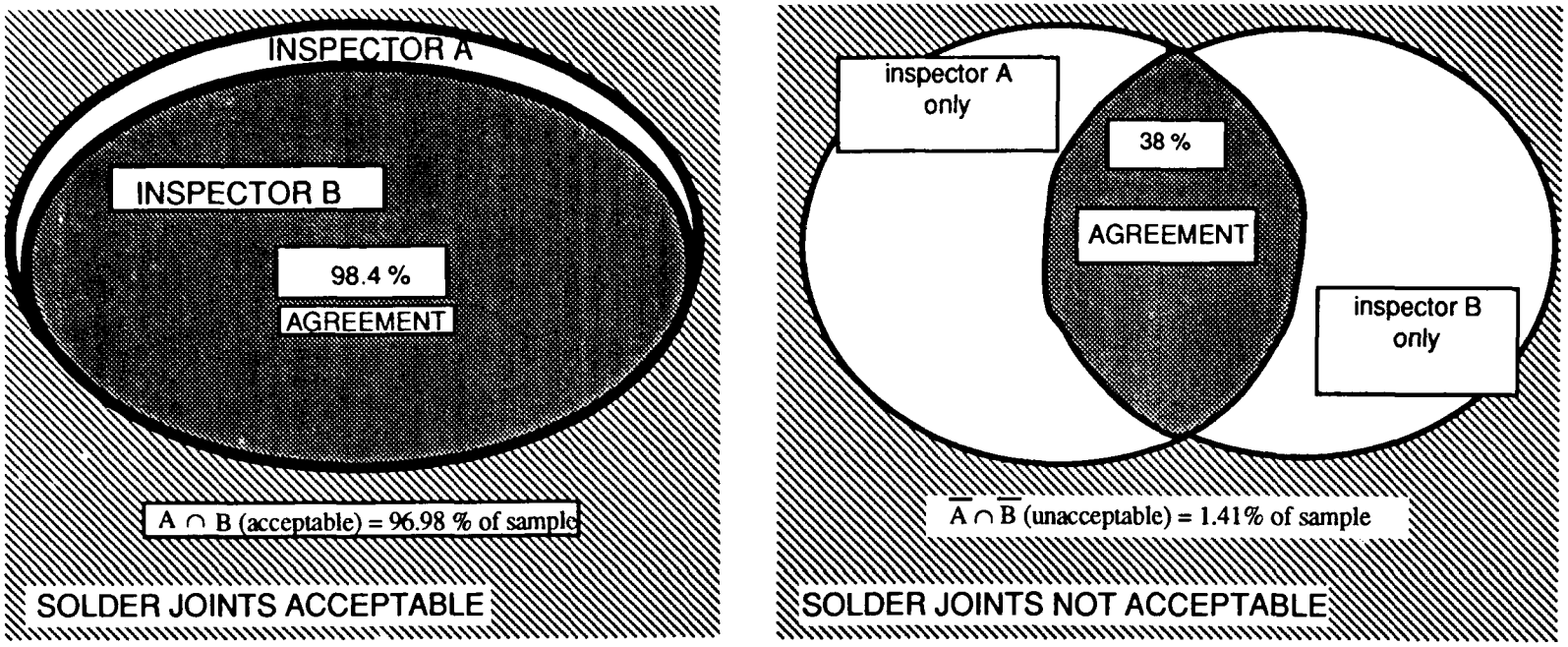

Figure 5. Correlation of two category C inspectors. A (left) - a high level of correlation exsisits for solder joints perceived to be "good" (98.4 %). B (right) - For "bad" or marginal solder joints, the agreement is much less (38 %).

VARIABLE I.D.	MEAN "GOOD"	MEAN "BAD"	MEAN "DISAGREE"	STD DEV "GOOD"	STD DEV "BAD"	STD DEV "DISAGREE"
LFMH	173.58	185.94	182.64	32.102	34.579	35.965
LFMPWA	13.029	22.736	16.800	1.5225	11.642	7.6473
LFMTWA**	51.273	60.966	57.778	9.3923	10.070	12.154
LFMFC**	-89.806	-23.483	-59.022	29.129	52.569	54.480
LFMSV**	10256	16556	14702	4239.6	7142.1	7645.3
LFDPWA	6.0648	16.954	9.5333	4.7931	14.831	10.826
LFDTWA	21.374	16.690	18.444	12.594	12.664	11.267
RFMFH	162.12	181.57	170.29	30.484	52.849	32.631
RFMPWA	13.511	20.782	17.222	2.1106	9.6418	6.6646
RFMTWA**	50.353	61.276	55.178	8.6266	12.764	12.865
RFMFC**	-81.424	-32.851	-53.844	24.944	50.592	49.411
RFMFSV**	9173.8	18233	13527	3534.3	7990.3	7667.9
RFDPWA	3.9640	12.149	9.4222	3.3695	13.445	10.217
RFDTWA	14.388	13.598	12.844	7.8144	10.698	7.3977
TFMFH**	168.83	184.29	176.33	33.121	34.129	27.822
TFMPWA	12.640	19.057	15.089	1.2336	13.274	7.8272
TFMTWA	54.353	60.138	58.889	8.2091	11.9351	11.769
TFMFC**	-67.173	-33.425	-49.178	20.756	58.348	46.843
TFMFSV**	10728	16252	15989	4754.5	6134.4	5990.3
TFDPWA	2.3813	12.184	5.9333	1.7993	19.681	12.040
TFDTWA	9.2158	11.816	9.3111	4.3949	10.649	7.5312

** Also used in Statgraphics Discriminant Model

Figure 6. Mean and standard deviations for 21 key RVSI variables. "Good", "bad", and "disagree" category designations are based on the visual inspection results of two category "C" inspectors. "Good" and "bad" designations require agreement between both inspectors: whereas, "disagree" results when disagreement whether to reject or accept exists between the two inspectors. No attempt to correlate defect attribute calls was made.

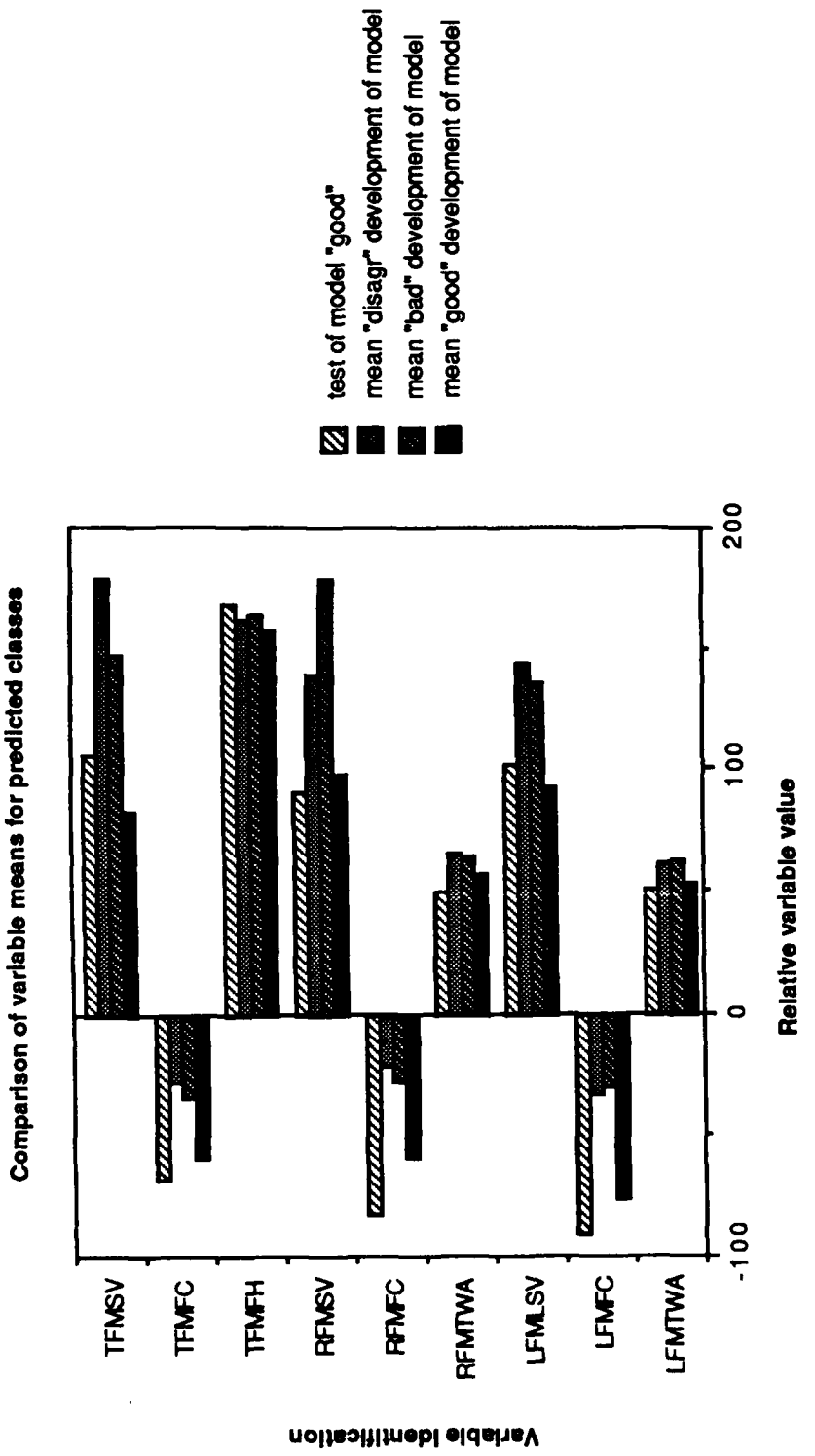

Figure 7. Comparison of means for the nine variables used to develop the discriminant analysis model described later in this report. In each group the three lower bars represent the categories coded "good", "bad", and "disagreement" by conventional visual inspection. The upper bar in each group represents solder joints from an independant test board where all solder joints were classified as "good" by visual inspection. Notice that the mean values for the "good" solder joints used in developing the discriminant analysis model are comparable to the "good" joints from a board used to test the model.

Testing Variable Distributions For Normality

A key assumption in the use of discriminant analysis is that each group originates from a population having a multivariate normal distribution for the discriminating variables. It is understood that a multivariate normal distribution implies univariate normal distributions; however, it is theoretically possible for normal univariates to result in a non normal multivariate distribution. The situation of a non-normal multivariate distribution with normal univariate distributions is highly unlikely in the "real world", so histograms and Chi Square tests were performed on key measurement variables to demonstrate that the assumption of multivariate normality was reasonable.
Histograms for the solder joint measurement variables were made from solder joints ranked "good", "bad", and "grey area" by category C inspectors. The following criteria were used to designate the three categories: "good" joints, "bad" joints, and "grey" area joints.

1) $(A \cap B) \Rightarrow$ INSPECTORS A & B AGREE THAT SOLDER JOINTS ARE "GOOD"
2) $(\bar{A} \cap \bar{B}) \Rightarrow$ INSPECTORS A & B AGREE THAT SOLDER JOINTS ARE "BAD"
3) $(A \cap \bar{B}) \cup (\bar{A} \cap B) \Rightarrow$ "GREY AREA" INSPECTORS A & B DO NOT AGREE.

Histograms were generated for the nine variables used in the discriminant model, and goodness of fit tests were performed on select dimensional data to test the normal distribution assumption. During inspection, each solder joint is divided into three 120° sectors; and, the three sectors are designated left fillet, right fillet, and toe fillet. The histograms generated for the nine variables describing "good", "bad", and "disagreement" joints are similar in appearance for the left fillet, right fillet, and the toe regions of the solder joints. The chi square goodness of fit test was performed on "good", "bad", and "disagreement" solder joint data from the left mean fillet information. The data in Figure 8 supports the assumption that that the individual variables are normally distributed is considered reasonable.

Variable Tested	Chi Square Value χ^2	Chi Square Critical with α = 0.01	Conclusion
LFMTWA "GOOD"	17.1185 with 9 d. f.	21.7	accept H_0: normal dist.
LFMTWA "BAD"	5.2334 with 7 d. f.	18.5	accept H_0: normal dist.
LFMTWA "DISAGREE"	7.1454 with 3 d. f.	11.3	accept H_0: normal dist.
LFMSV GOOD"	13.7359 with 10 d. f.	23.2	accept H_0: normal dist.
LFMSV "BAD"	2.0429 with 6 d. f.	16.8	accept H_0: normal dist.
LFMSV "DISAGREE"	3.7667 with 3 d. f.	11.3	accept H_0: normal dist.
LFMFC "GOOD"	16.0261 with 10 d. f.	23.2	accept H_0: normal dist.
LFMFC "BAD"	17.7103 with 6 d. f.	16.8	reject H_o/accept H_a:**
LFMFC "DISAGREE"	1.0140 with 3 d. f.	11.3	accept H_0: normal dist.

**can accept H_o: at α=0.005 level

Figure 8. Chi Square test for normality of the solder joint measurement variables. Test hypothesis is as follows:

H_o: The data are normally distributed $\quad \chi^2_{calculated} > \chi^2_{k,\ a=.01}$

H_a: The data are not normally distributed $\quad \chi^2_{calculated} > \chi^2_{k,\ a=.01}$

The normality assumption has been found to be reasonable and the discriminant analysis of the inspection data is reported in the next section.

ANOVA was used to test the hypothesis that the "good", "bad", and "disagreement" means do not differentiate between data classes and are in fact from the same population for the nine variables used in discriminant analysis model one.

Mathematical Overview of Discriminant Analysis using Canonical Functions

This section is intended to provide a brief overview of the mathematics underlying discriminant analysis using Canonical Discriminant Functions. Canonical discriminant functions are linear combinations of the discriminant variables that can be modified to accomplish various tasks such as: identification of significant discriminant variables, comparison of the relative contribution of each discriminant variable to the discriminant model, and sorting solder joints into classes of quality based on variable measurements and a discriminant model. These functions and several types of discriminant coefficients were obtained through the use of software packages including Statgraphics and SAS. The mathematical form of the discriminant function is as follows:

$$f_{km} = u_0 + u_1X_{1km} + u_2X_{2km} + \cdots + u_pX_{pkm}$$

f_{km} = the score on the canonical discriminant function for case m in the group k;

X_{ikm} = the value on discriminating variable X for case m in group k; and

u = coefficients that produced desired outputs from function.

The coefficients (u's) are derived in such as way as to maximize the difference between group means. More than one unique discriminant function can be derived, and the number of possible functions depends on the number of groups minus one. In other words, three separate groups can produce two unique discriminant functions. In addition to maximizing the difference between group means, the u's are derived so that values from the second function are not correlated with values from the first function. The number of possible functions is based on the number of groups minus one, a two dimensional plot of the two most significant functions can often be used to discriminate between the groups. When multiple variables are involved in discriminating between the groups, the reduction of variables into two dimensions (for example two discriminant functions) greatly simplifies interpretation of the information.

Results of Discriminant Analysis

The Statgraphics software package was used to generate an initial discriminant model based on nine variables. The variables entered into the model were selected because of their intuitive appeal; for example, soldering literature typically refers to wetting angle as a good indictor of solderability. Manko[6] states that high reliability solder joints will have a dihedral angle (wetting angle) less than 75°. Fillet curvature and solder volume were also chosen for use in the model because much of the conventional visual inspection criteria could be verified by the use of dimensional measurements of fillet curvature and solder volume. The Statgraphics package was run on an IBM PS 2 model 50. Initial attempts to include more variables than nine in the discriminant model caused the system to "bomb", so a trial and error procedure using a pool of 21 different types of measurement variables was used to manually optimize the choice of variables. Selection of variables was based on the resulting canonical correlation coefficients and the Wilks Lambda values when variables were added or removed from the model.

Discriminant analysis using Statgraphics software produced a nine variable model and two discriminant functions, the model coefficients are listed in Figure 9.

Variable	classifi-cation function 1	classifi-cation function 2	classifi-cation function 3	unstandard. discrim coeffs function 1	unstandard discrim coeffs function 2	standard. discrim coeffs function 1	standard. discrim coeffs function 2
LFMTWA	1.51385	1.55325	1.566162	0.02063	0.03281	0.20844	0.33155
LFMFC	-0.112011	-0.074181	-0.103242	0.01755	-0.01654	0.74806	-0.70514
LFMLSV	-0.490665	-0.504434	-0.46552	-0.00467	0.04268	-0.02778	0.25372
RFMTWA	1.50981	1.54901	1.49554	0.01722	-0.04690	0.18725	-0.50996
RFMFC	-0.365867	-0.375431	-0.363062	-0.00413	0.01068	-0.16238	0.41980
RFMSV	0.205043	0.351346	0.239883	0.06791	-0.06272	0.41132	-0.37989
TFMFH	0.506654	0.509777	0.488719	0.00031	-0.02553	0.01013	-0.83059
TFMFC	-0.103721	-0.124384	-0.110851	-0.00972	0.00600	-0.39866	0.24611
TFMSV	-0.553544	-0.408113	-0.308081	0.08040	0.21064	0.43425	1.13764
constants	-138.386	-146.606	-140.747	-3.68293	2.56965		

Figure 9 A. Classification function coefficients, unstandardized discriminant coefficients, and standardized discriminant coefficients (nine variable model based on Statgraphics output).

Discriminant function	Eigenvalue	relative percentage	canonical correlation	
one	0.8720301	91.42	0.68251	
two	0.0818777	8.58	0.27510	
functions derived	Wilks Lambda	Chi-Square	df	Sig. level
0	0.4937521	185.60479	18	0.00000
1	0.9243189	20.69762	8	0.0800

Figure 9B. Discriminant analysis statistics for Statgraphics nine variable discriminant model.

A comparison of discriminant function predictions and human visual inspection calls is presented in Figure 10. This graphic shows that a high level of agreement concerning "good" joints exists between two category C inspectors and the discriminant model predictions; on the other hand, agreement for the categories "bad" and "disagreement" between model and inspectors is considerably less. Figure 11 is a composite of solder joints used to develop the model and another test circuit panel of the same configuration used to provide raw data for testing the model.

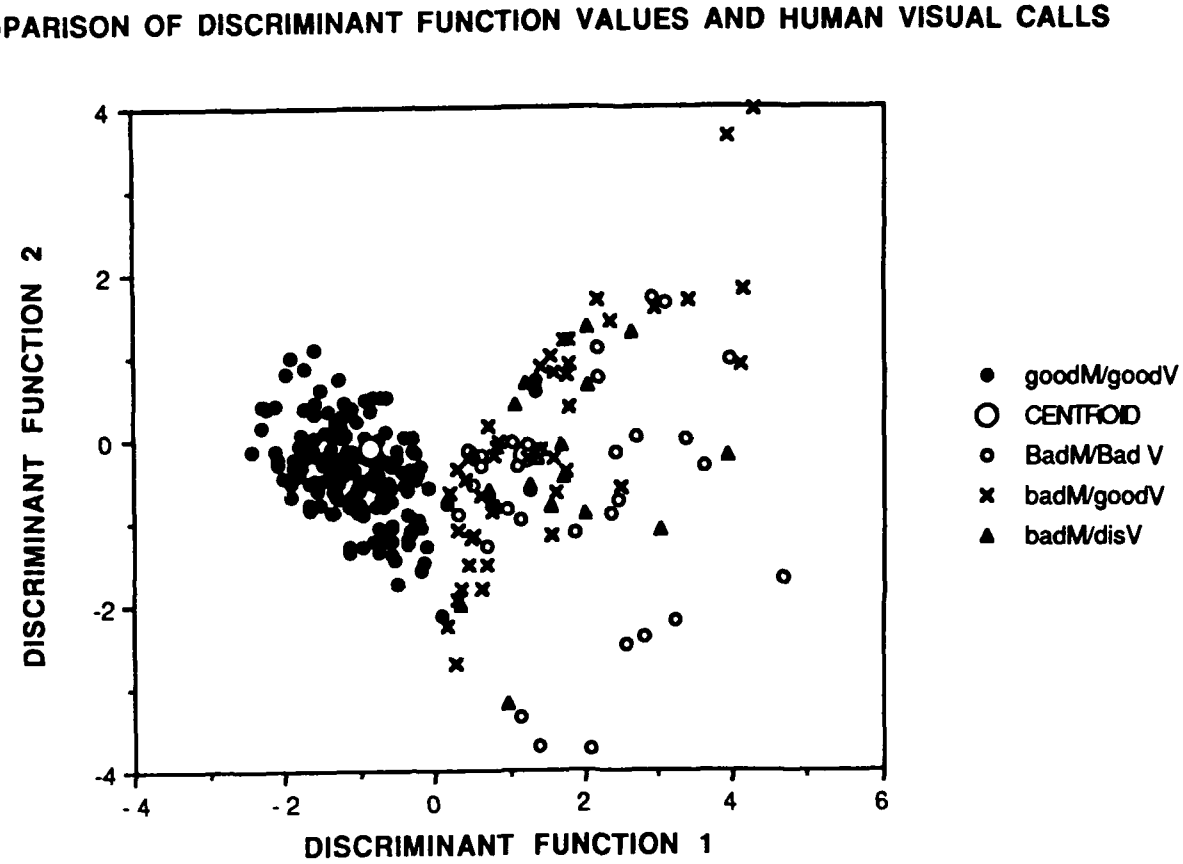

Figure 10. Solder joint data cases as calculated by discriminant functions 1 & 2. Legend indicates corresponding solder joint quality judgement by two category C inspectors. Agreement between discriminant function data cases and visual inspection is high (tightly clustered about "good" centroid region), but iss dispersed in the "grey" and "bad" solder joint regions.

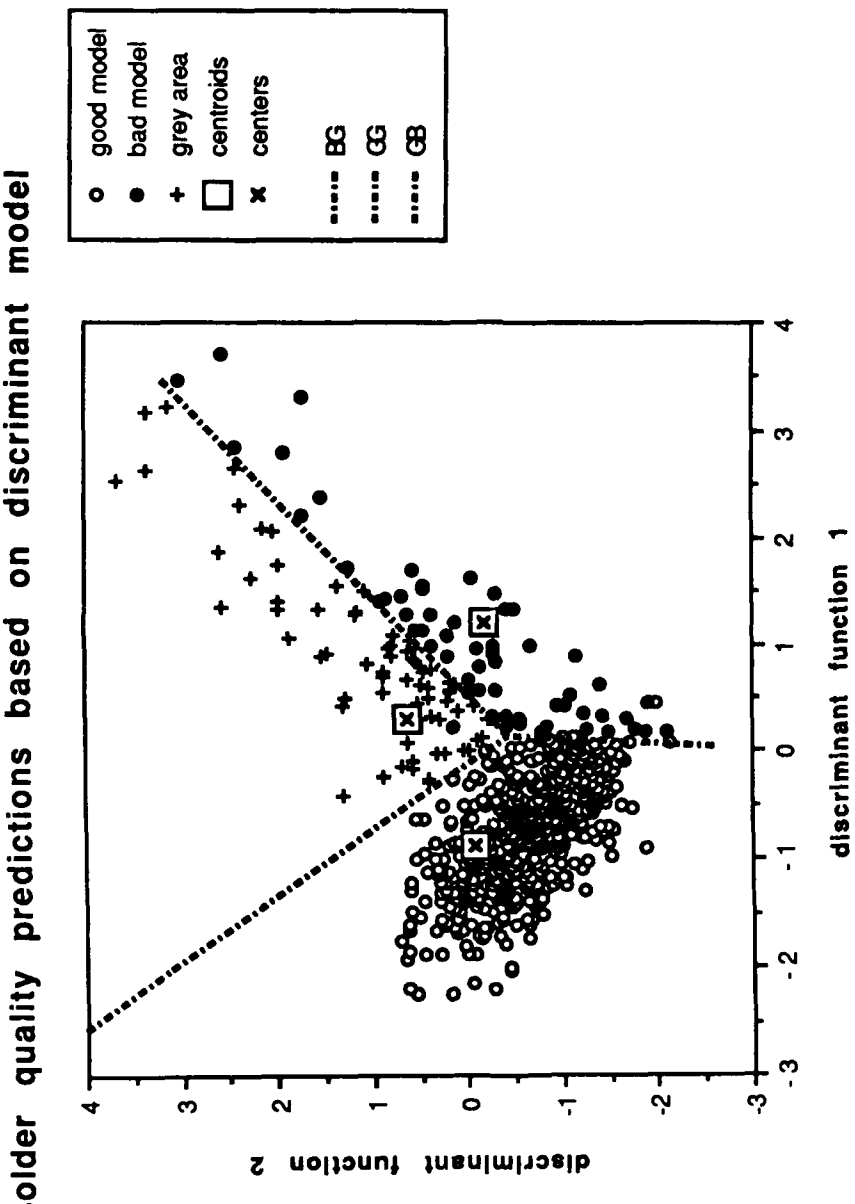

Figure 11. Two function plot showing centroids and predicted solder joint cases. This plot is based on a composite of solder joints used to develop the model and solder joints from a test CCA not used in developing the discriminant model.

Attempts to use more than 9 variables with the Statgraphics software package caused the system to "bomb", and it was decided to evaluate 21 variables with SAS software and the mainframe computer system. A stepwise procedure using SAS was performed to determine which of the 21 variables entered into the software are the most significant. The SAS stepwise procedure resulted in an eleven variable model using the variables listed in Figure 12.

	NUMBER IN	F STATISTIC	WILK'S LAMBDA
LFMFC **	1	65.269	.672458
TFMFSV **	2	23.031	.573518
TFDPWA	3	12.147	.525522
RFMFSV **	4	10.490	.486969
RFDPWA	5	10.957	.449645
TFMTWA	6	6.365	.428850
TFMFH **	7	4.933	.413320
RFMTWA **	8	3.051	.403877
LFDPWA	9	2.360	.396676
RFMFH	10	2.639	.388754
TFMPWA	11	2.509	.381338

** Also used in Statgraphics Discriminant Model

Figure 12. Best choice of 21 variables as determined by SAS stepwise discriminant analysis software.

Figure 13 provides the unstandardized and standardized discriminant coefficients obtained from use of the stepwise discriminant software package. It is concluded that several possible models using different variable or combinations of variables will provide similar prediction results. Both the nine variable and eleven variable model are presented in the next section for comparison purposes.

Variable	unstandard. discrim coefficients function 1	unstandard. discrim coefficients function 2	standard. discrim coefficients function 1	standard. discrim coefficients function 2
LFMTWA6	.01304852	.000116793	0.48380	-0.00987
TFMFSV22	.01398602	-.03767339	0.52047	-1.16019
TFDPWA23	-.00955487	.001201490	0.20538	0.16817
RFMFSV15	.03661687	-.02885719	0.39867	-0.43225
RFDPWA16	.00011136	-.00005298	0.43858	0.25789
TFMTWA20	.03702294	.01677572	0.41132	-0.37989
TFMFH18	-.05571071	-.02355195	-0.27091	-0.68569
RFMTWA13	-.02713154	-.01550199	0.23856	-0.22981
LFDPWA9	-.06409442	.02437955	0.24530	-0.47492
RFMFH11	.00007781	.00023667	0.16352	0.15710
TFMPWA19	.03164474	-.00167516	0.08455	-0.21016
constants	2.40239	2.12922		

Figure 13. Classification function coefficients, unstandardized discriminant coefficients, and standardized discriminant coefficients for stepwise eleven variable model (developed through SAS software).

Figure 14 presents a plot of discriminant functions one and two using the SAS recommended eleven variable solder quality prediction model. Figure 15 is a similar plot with the addition of solder joint quality prediction using the SAS eleven variable model. The test solder joints were all designated "good" by two category C inspectors. As would be expected, most of the data points are superimposed over the solder joint model "region of good joints".

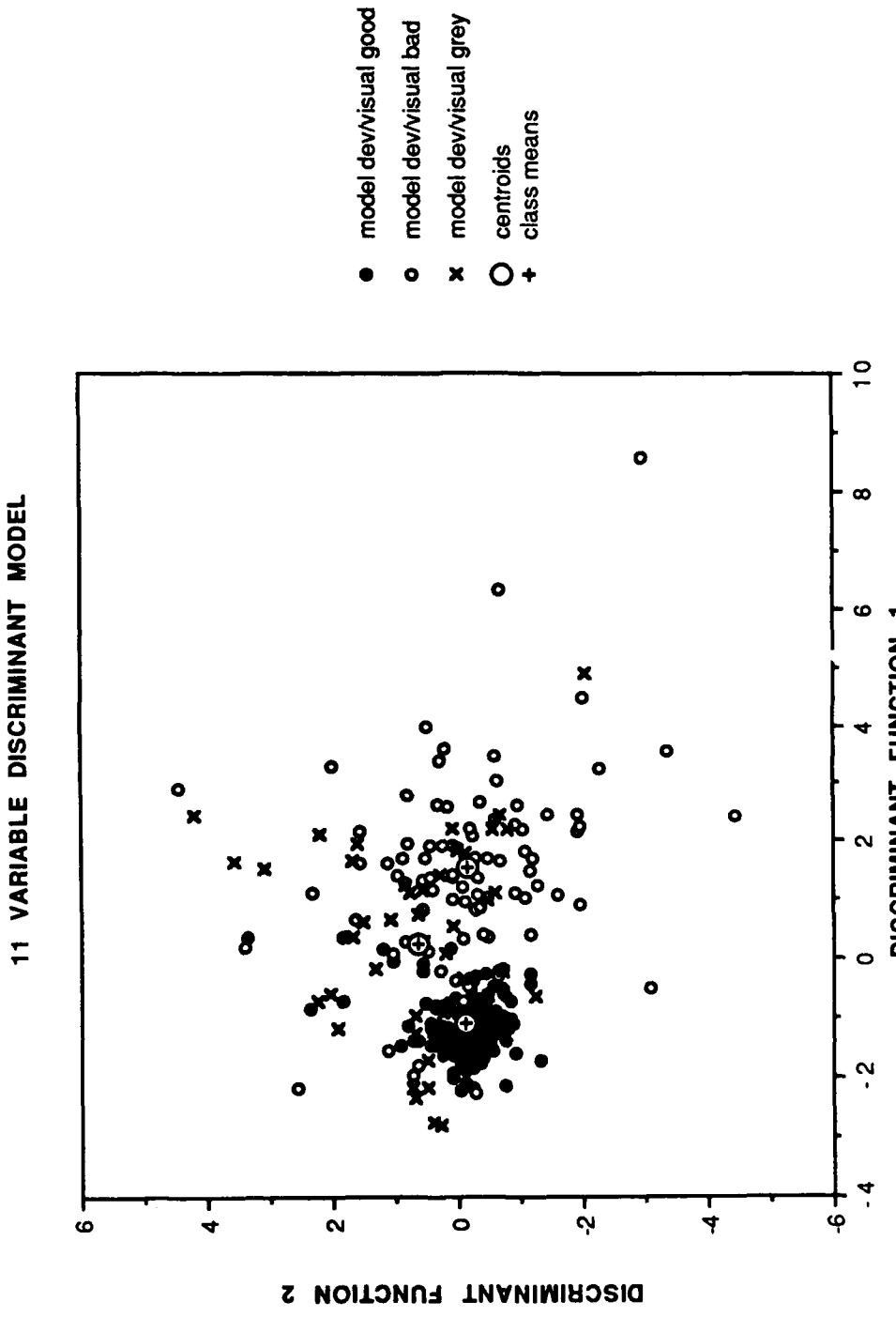

Figure 14. Eleven variable discriminant analysis model developed with SAS™ stepwise discriminant analysis and SAS™ canonical discriminat analysis.

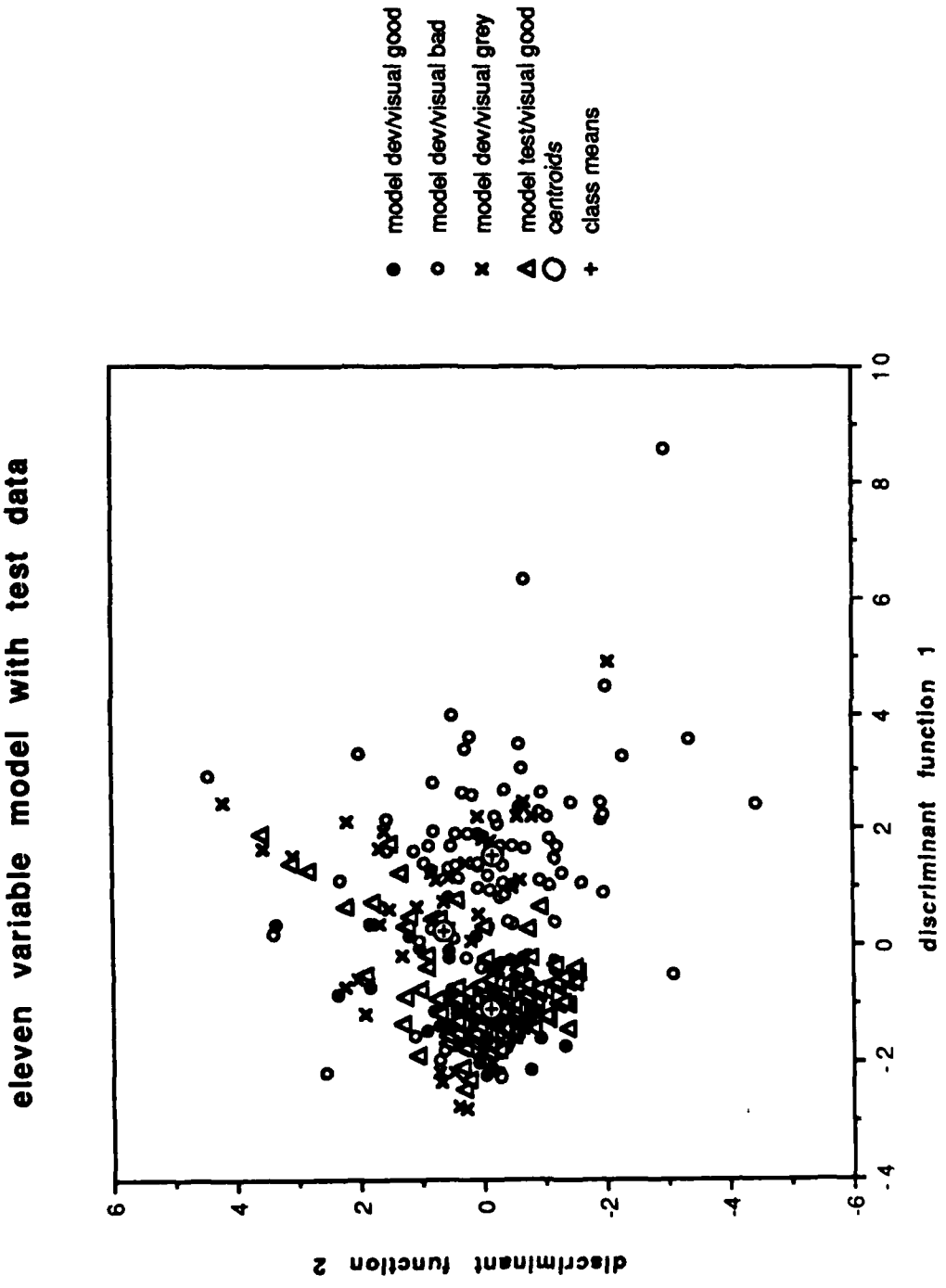

Figure 15. Eleven variable step wise discriminant analysis model with test data.

Summary of Results and Recommendations:

Results

1) A high degree of correlation exists for visual inspectors when solder joints are considered "good" - 98.4%; however, only 38% agreement as to what is considered "bad" was obtained from a sample of 7 CCA's with approximately 1200 joints each. These two solder joint agreement samples were used to calibrate the solder quality model (Figure 5).

2) The average difference between variable measurement comparisons ranged between 0.12 and 7.5?%. Solder joints considered grossly defective or out of tolerance by the 3D solder joint inspection system are not dimensioned by the software; as a result, the percentage of solder joints omitted from the repeatability test ranged between 5.3 and 18.9% for the 21 measurement variables tested (Figures 2 & 3).

3) A nine variable discriminant model for use in predicting solder joint quality was developed through the use of Statgraphics™ discriminant analysis software and nine solder joint dimensional variables selected due to their technical relevance to solder quality (for example wetting angle, fillet curvature, and solder volume: Figures 9, 10, 11).

4) An eleven variable model was derived through the use of SAS™ stepwise discriminant analysis and SAS™ Canonical analysis. SAS™ stepwise discriminant analysis is an iteration process that systematically enters and removes variables from the solder quality model and tests the statistical significance of the model after each variable addition or removal. Stepwise discriminant analysis was performed for the purpose of developing a set of equations that provide the best description of solder joint quality with a minimum number of statistically significant variables (Figures 12, 13, 14, 15).

Conclusions

1) Solder joint dimensional variables and discriminant functions provide a marked advantage over visual criteria in terms of statistical process control data because the results are quantitative, repeatable, and are more easily transformed into management summary reports used for material and process control.

2) Data file design and management, design of an easy to interpret report format, and factory implementation of the automatic three dimensional solder quality measurement system as a solder quality measurement tool are key issues that must be addressed if a realization of quality improvement, reduction in inspection costs, and increased reliability through the elimination of unnecessary rework are to be realized.

3) Several variable combinations have been used to derive models for predicting and measuring solder joint quality, but variables common to all solder joint quality indicator models include wetting angle, fillet curvature, and solder volume. Other variables specific to certain regions of the pad or component lead show promise in differentiating between solderabilty (material) problems as opposed to process control problems.

REFERENCES

1. Klecka William R. (1980) *Discriminant Analysis; Quantitative Applications in the Social Sciences.* Sage University Papers # 19 (Sage Publications Beverly Hills & London).

2. Kwoka Mark A. & Mullenix Paul D. (1990) *"Using Wetting Balance Parameters with Discriminant Analysis to Classify Visual Coverage and Defect Categories" 14th Annual Electronics Manufacturing Seminar Proceedings.* NWC TP 7066 Naval Weapons Center China Lake, Ca 93555-6001 Feb 21-22, 1990 p. 269 - 293.

3. Ludovic Lebart, Morineau Alein, Warwick Kenneth M. (1984) *Multivariate Descriptive Statistical Analysis.* (Wiley Series in Probability and Statistics: John Wiley & Sons New York).

4. Manko Howard H. (1979) *Solders and Soldering Second Edition.* (McGraw Book Company New York).

5. Muirhead Robb J. (1982) *Aspects of Multivariate Statistical Theory.* (Wiley Series in Probability and Statistics: John Wiley & Sons New York).

6. Mullenix Paul D. Gerker R. David & Kwoka Mark A. (1989) *"Assessing Solderability Performance with Wetting Balance Indices and Discriminant Analysis" 13th Annual Electronics Manufacturing Seminar Proceedings.* NWC TP 6986 Naval Weapons Center China Lake, Ca 93555-6001 Mar 1-3, 1989 p. 7 - 29.

7. Raby Jim D. (1987) *"Elimination of the P3 of Solder Joint and Assembly Inspection" 11th Annual Electronics Manufacturing Seminar Proceedings.* NWC TP 6789 Naval Weapons Center China Lake, Ca 93555-6001 Feb 18-20, 1987 p. 245 - 251.

8. Zazekas Daniel A. (1987) *"Report of the Fleet Hardware Assessment Project- A Survey of the Soldering Problems Observed in Navy Weapons Systems" 11th Annual Electronics Manufacturing Seminar Proceedings.* NWC TP 6789 Naval Weapons Center China Lake, Ca 93555-6001 Feb 18-20, 1987 p. 245 - 251.

Acknowledgements

Dang, Ann T.	Unix utilities, Ethernet Interface, and other communications software.
Lind, Jackie	Visual Solder Joint Inspection.
Harlow, Marcie S.	Visual Solder Joint Inspection.
Tran, Dao N.	Data File Format conversions involving Sun 386, IBM PS 2 Mainframe, and Macintosh II Systems.

Raymond Swenson is a Group Engineer with General Dynamics Air Defense Systems Division where he devotes his efforts to R&D work specific to electronics. Previously he worked in the areas of solderability, cleaning, automatic solder-joint inspection, interconnection technology, and laser and waterjet profiling of rigid and flexible substrates. His manufacturing development work over the past 10 years also includes cutting, forming, and joining methods for advanced metals, alloys, composites, and ceramics.

Ray received a BS degree in Metallurgical Engineering from Montana Tech and at the present time is completing courses for an MS degree in Management Science from California State University, Fullerton.

Address: General Dynamics
Air Defense Systems Division
P.O. Box 2507
Pamona, CA 91769-2507

DESIGN OF EXPERIMENTS (DoE) FOR THE "LAYMAN" ENGINEER

by

David P. Urban
Sr. Quality Engineer
Simmonds Precision
Aircraft Systems Division
ASQC CQE

ABSTRACT

Once limited in use to those with advanced mathematical (statistical) backgrounds, such as scientists, educators and top engineers, **Design of Experiments (DoE)** is now heralded by many as a tool for process improvement in a wide variety of industries. Although rapidly gaining in popularity, DoE is still eschewed by many as "too complex".

This paper is an introduction to the concepts and applications of DoE, providing the reader with enough understanding to implement DoE techniques for their own applications. Theoretical concepts are reinforced through direct relation to an actual designed experiment performed at the author's facility. The case presented is optimization of an electronic component solder tinning process for printed wiring assemblies, however the innumerable possible applications are stressed.

The key concepts of DoE are presented, including selection of factors and levels to be examined, use of orthogonal arrays, data reporting, analysis of results (ANOVA and S/N ratios), and confirmation of the experiments' resulting optimum conditions. The paper discusses the various types of DoE from full and fractional factorials through Taguchi techniques, including explanation of the "loss function".

The benefits derived from performance of a designed experiment are expounded as compared to "trial and error" methods of process evaluation.

INTRODUCTION

Many "tools" are available to today's Quality and Process Engineers to assist in controlling the variety of processes in manufacturing the Printed Wiring Assembly (PWA). Some of these tools are tangible items we can touch and see, such as computerized data acquisition systems, SPC Charts and Pareto diagrams while others are less tangible but equally as beneficial. One often overlooked tool is Design of Experiments (DoE).

Though gaining in popularity here in the United States of late, DoE has been shunned by many as "too complicated", or "too difficult to understand the results". However, with the advent of high-power, sophisticated computer software for statistical analysis that is user friendly, virtually anyone who is technically familiar with a process can use DoE.

Planning and Development of an Experiment

There are some simple rules or steps involved in designing, performing and analyzing the results of an experiment (see Figure 1). The planning and development stage may be the most important in determining the success or failure of the experiment. Without careful consideration given to just what the specific goals and objectives are, one may consume much time and effort which will result only in useless data.

Many techniques for developing the goals and objectives are available, with the "Brainstorming" technique perhaps the most common and most productive. For those who may not be familiar with brainstorming, its rules are outlined in Appendix A. Basically, the concept is to allow those individuals with intimate knowledge of the process under study to freely offer ideas or suggestions for improvement of the process, i.e., areas to examine for improvement. These ideas are then pared down by committee to those remaining which are most apt to result in a process improvement.

Although some knowledge of the basics of DoE is helpful, all one really needs to know are the parameters to be measured, and at what levels (conditions) the parameters are to be tested. As many parameters and levels to be tested as desired are possible, however to keep the analysis realistic, they should be confined to those that are likely to have the greatest impact on the process. Note at this time that no specific process has been defined. The experiment could examine machine component insertion techniques, the soldering operation, conformal coat, or any other process. For illustrative purposes, an actual experiment for tinning electronic components at ASD is presented.

Tin Dip Experiment Example

In this experiment, the objective or goal was to optimize the tinning operation of components for greatest solderability (refer to Appendix B). Lacking a formal solderability test program and a controlled storage environment as well as a "First In, First Out" stock system, all electronic components were tinned just prior to assembly to the printed circuit board. Approximately 95% of all tinning was performed using a semi-automated machine process, with the remaining 5% hand dipped in solder pots.

The accepted military standard test for solderability of discrete components (resistors, caps, diodes, etc.) is MIL-STD-202, Method 208.[1] This test is somewhat subjective however, requiring one to determine 95% solder coverage of the lead with no defects. We therefore elected to use tinning thickness (in relative numbers), as our measurement standard, using a microscope at 800X and micro-section analysis techniques. Indeed, the thickness measurement technique has been successfully employed previously.[2] It is noted here that extreme attention to detail and methods used in preparing the lead microsection samples is imperative to insure that accurate representations of solder tinning are obtained, and are not impaired by the preparation process. We found that a cut, polish, etch, micropolish procedure yielded the most accurate results, though this method is very time consuming and requires an experienced technician. There are other, more precise methods for determining solder coating thickness, such as Wet Chemical, X-Ray Fluorescence Spectometry, and Differential Scanning Calorimetry (DSC).[3] However, for purposes of expediency, the microsectioning technique was used.

A team was formed consisting of the tin dip Manufacturing Process Engineer, PWA Quality Engineer, a Metallurgist and Lab Technician. This team's charter was to define, perform and analyze the results of the experiment. (Refer to Appendix B). After determining which parameters were to be examined and at what levels (Table 1), this data was brought to our Statistician who defined the type of experiment best suited to most efficiently achieve our objectives.

DESIGN TYPES

There are many types of experimental designs, each with their own set of advantages and disadvantages. These design types include what are known as "Classical" designs, such as full and fractional factorials, multi-level, block, nested and latin square, and more recently gaining in popularity, "Taguchi Techniques". Genichi Taguchi was a Japanese Quality Engineer who modified fractional factorial experimentation with what he calls "The Loss Factor", basically, "the loss to society imparted by something performing less than it should". Taguchi also employs "Orthogonal Arrays". An Orthogonal Array is basically a matrix that identifies combinations of factors and levels in a manner that provides for independent analysis of each factor and all interactions between all factors. Taguchi techniques find widespread use throughout industry but full explanation of their workings is beyond the scope of this paper. Interested parties are encouraged to seek further information by referring to the selected reading list on the subject as listed in Appendix C.

The order and quantity of "Runs" of the experiment are established, resulting in a matrix. In statistical terms, the "order" is called a "treatment combination", or "tc" for short, and a "Run" is termed a "replication". The Statistician chooses the design type based on the factors (variables) to be tested and the levels (conditions) of test such that that the most information can be obtained using the least amount of actuals "Runs" or experiments to be performed. If a Statistician is not accessible, there are many good texts on Design of Experiments available, which define in layman's terms how to select the correct design type to use for a given set of factors and levels. Most of these texts also explain how to analyze the resultant data. One such text is "Quality by Experimental Design" by Thomas B. Barker.[4] This text even includes proven computer program listings in BASIC for determining arrays and analysis of data, useable on any MS-DOS PC.

There are also many commercially available software packages that perform a variety of functions such as assistance in selecting the correct design type, storing experiment parameters and data, as well as the statistical analysis of results. The ability of these programs to perform the statistical analysis with great speed and accuracy alone makes them quite desirable. One such software package for Taguchi techniques is called "Quest" tm, marketed by Technicomp as part of their comprehensive video instruction course "Taguchi Methods for Quality Optimization".[5] Another is "Taguchi Consultant" from Texas Instruments".[6]

ORTHOGONAL ARRAYS

In our case, the Statistician decided that a Taguchi experiment was most appropriate. The Orthogonal Array (OA) selected was an L8 Array, shown in Figure 2.

One of the chief advantages of the Taguchi approach is its use of the Orthogonal Array. The Orthogonal Array provides the same amount of information from an experiment as a full factorial but with far less actual experimental trials. Using our tin dip L8 Array example, a full factorial examining 7 factors at 2 levels would require 2^7 or 128 trials to test all possible combinations. The L8 Array derives the same information with only 8 trials, a 94% savings!

The benefits of this type of experimental trial savings is lucidly clear as the number of factors and levels increase as depicted in Table 2.

One might argue that such large factor and level experiments have no practical use, but indeed an L64 has been used in examining a wave solder process for improvement.[7]

The OA is relatively simple to read. For example, in Figure 2, Line 3 is read as: Solder Temp., Level 1 (475°F), Preheat Time, Level 2 (30 Secs), Solder Dwell Time, Level 2 (5.0 Secs), and Withdrawal Rate, Level 1 (5). Other lines are similarly defined by referring back to the Variable and Levels shown in Table 1. The runs or tc's are then performed in the order given according to their definition in the array. In our case, the components were tin dipped per the conditions of Table 1, then carefully microsectioned for measurement of the thickness of the deposited solder.

ANALYSIS OF RESULTS

At this point one is well advised to have a Statistician available, or alternatively in his/her absence, a good working knowledge interpreting a computer software package's analysis of the data. As stated earlier, many software programs will give you conclusions and optimum conditions to use based on the inputted data. However, care must be taken to understand the statistical assumptions the software's algorithm's use in making decisions and drawing conclusions from the data. Usually, a sound understanding of basic ANOVA (Analysis of Variance) techniques is sufficient. The table of resulting thicknesses from the tin dip experiment is shown in Figure 3, and a representative cross section shown in Figure 4.

In our tin dip example, a plot of the average S/N ratio for each factor and level is shown in Figure 5. This type of plot is used to analyze results of Taguchi experiments, and is referred to as the responses of the main effects. The S/N ratio is calculated using the formula shown in Figure 3 for quality characteristic "The Bigger the Better". The expression in brackets is the Mean Square Deviation (MSD), so the S/N ratio is $-10 \log_{10}$ (MSD). The MSD calculation varies with the quality characteristic used. The formulas for MSD for the three quality characteristics are given at the bottom of Appendix "D". The response of the main effects as depicted in Figure 5 is a simple representation of what the optimum conditions are based on the data obtained from the experiment. For example, Factor A (Solder Temp) at Level 1 (475°F), Factor B (Preheat Time) at Level 1 (60 secs), Factor C (Dwell Time) at Level 1 (3.0 secs) and Factor D (Withdrawal Rate) at Level 1 (5) are the optimum conditions for our tin dip example. These optimum conditions are verified by a confirmation run at these levels.

ANALYSIS OF RESULTS

A vital part of any DoE Experiment is the "Confirmation Run". This is another trial or run (tc) using the optimum conditions obtained from analysis of the data gathered from the experiment. The confirmatin run is significant because the optimum conditions most often will not have been one of the trials of the experiment. The confirmation run indicates whether analysis of data was correct, or points out any anomalies that may have occurred while performing the runs of the experiment. If such anomalies are indicated, another set of trials (runs) as defined by the orthogonal array is in order. If the anomalies persist in the new data analysis, some "detective" work may be required to locate the source. Possibilities include an incorrect machine setting, abnormal environmental conditions, inconsistency of operator, unexpected material variances, or unplanned interaction of factors. Such anomalies are usually rare however, (with the exception of unplanned interaction of factors perhaps) and the confirmation run normally does just what its name implies by confirming the validity of the optimum conditions defined by the data analysis.

From here, process changes reflecting the results of the experiment can be implemented, which will result in overall process improvement. Experimentation on a given process does not have to end here. In fact, in our tin dipping example, we used the results of this experiment to narrow parameters (ie, eliminate some parameters), and define a second experiment which is currently in progress.

TAGUCHI'S LOSS FUNCTION

Another benefit of Taguchi techniques is the ability to quantifiably measure quality process improvements through calculation of "The Loss Function". Taguchi asserts that society suffers a loss when an item or service is poorly designed or produced. He further maintains that such loss can be quantified, and thus a measurable degree of quality is obtained. He uses this loss function as a means of quantifying product or process improvement in two ways:

TAGUCHI'S LOSS FUNCTION

1)
Calculation of savings from improvements;

2)
Calculation of product tolerances as defined by actual customer requirements vs. manufacturer processes.

There are three basic characteristics of the loss function.

1)
There is no loss when the quality characteristic equals the target value;

2)
The loss is greater as the quality characteristic deviates further from the target value;

3)
The loss function is a continuous function of target value deviation.

The loss function is a true mathematical function, and its formulae can be derived using Taylor's theorem on the function of values.

There are unique formulas for single and multiple units, as well as for each of the three quality characteristics (nominal is best, the bigger the better, the smaller the better). Specific application of these formulae is beyond the scope of this paper, however the formulas themselves are given in Appendix D for those interested in further exploration.

SUMMARY

DoE is superior to "Trial and Error" and 1-F.A.T. Methods in supplying statistically valid, scientific information on process variables and levels. Data is turned into usable information, and requires far less time and effort than the aforementioned methods.

The techniques used in planning, organizing, performing and analyzing the results of a designed experiment are not as complex as many believe. Although some statistical background is essential to a successful analysis of experimental results, one does not need be a Statistician per se to succeed. High power computers and sophisticated software packages perform the most difficult tasks.

There are several good courses and seminars offered each year on DoE and Taguchi methods at various locations throughout the country. Armed with a little knowledge and training on DoE, the "Layman" Engineer can become quite dangerous to out of control processes!

APPENDIX A

BRAINSTORMING GUIDELINES

- Members can be volunteers, appointees, or both
- Members should have a familiarity with process under study
- Solicit ideas, one at a time from all members, "Round Robin" style, then repeat until all ideas are exhausted
- Impose NO limitations on ideas - The wilder the better
- Individuals may pass on any given turn
- No commenting on anyone's idea by any other member, however building on another's idea is allowed
- Relate ideas generated into process-under-study factors
- As a group, analyze list of factors
- Eliminate those that the group agrees to
- If list is still long, select those most likely thought to have greatest effect on process for first experiment. Include as many as feasible.
- For Taguchi experiments, classify factors as controllable (signal) or uncontrollable (noise)
- Keep remaining factors on another list - They may be needed later!

APPENDIX B

HOT SOLDER COAT(TIN DIP) EXPERIMENT DEFINITION

GOAL

TO REDUCE PRINTED WIRING ASSEMBLY(PWA) DEFECTS DUE TO POOR SOLDERABILITY OF COMPONENTS.

OBJECTIVE

TO OPTIMIZE THE HOT SOLDER COAT(TIN DIP) PROCESS FOR MAXIMUM SOLDER COAT ON COMPONENT LEADS.

METHODOLOGY

- o USING TAGUCHI TECHNIQUES WITH THE QUALITY CHARACTERISTIC "THE BIGGER THE BETTER", ANALYZE THE MAIN EFFECTS AND PRIMARY INTERACTIONS AMONG FOUR(4) CONTROLLABLE AND ONE(1) UNCONTROLLABLE FACTORS AT TWO LEVELS.
- o EMPLOY A TRUNCATED L8 ORTHOGONAL ARRAY
- o ANALYZE RESULTS USING SIGNAL TO NOISE RATION(S/N) OF

$$S/N = -10 \log_{10} \left[\frac{1}{n} \sum \frac{1}{y^2} \right]$$

APPENDIX C

TAGUCHI METHOD REFERENCES

ORTHOGONAL ARRAYS AND LINEAR GRAPHS, Forward by Yuin Wu and Shin Taguchi, ASI Press ISBN 0-941243-X.

PHADKE, MADHAV, QUALITY ENGINEERING USING ROBUST DESIGN, Prentice-Hall, 1989. ISBN 0-13-745167-9.

ROSS, PHILIP, TAGUCHI TECHNIQUES FOR QUALITY ENGINEERING, McGraw Hill, 1987. ISBN -0- 07053866-2

TAGUCHI, EL SAYED & HSIANG, QUALITY ENGINEERING **IN PRODUCTION SYSTEMS**, McGraw Hill, 1988, ISBN 0-07-062830-0.

TAGUCHI, GENICHI, INTRODUCTION TO QUALITY ENGINEERING, Asian Productivity Institute, 1986, ISBN 92-833-1084-5.

TAGUCHI, GENICHI, SYSTEM OF EXPERIMENTAL DESIGN, UNIPUB- Kraus International Publications, 1976. ISBN 0-527-91621-8.

SOURCE: Sammy Shina, Univ. of Lowell, "Quality and Productivity Improvements in Soldering Processes" Seminar, Lowell, MA November 1989.

APPENDIX D

LOSS FUNCTION FORMULAE[8]

SINGLE UNITS

NOMINAL IS BEST

$$L(Y) = k(Y-Y_0)^2$$

WHERE:

Y = Measured value of quality characteristic (inches, FT-LBS, relative value on a scale of 1 to10, etc.)

Y_0 = Target value of quality characteristic

k = Constant dependent upon cost methods of an operation or organization, which equals

$\frac{L_0}{^2}$, where L_0 = Cost to correct failure or cost of exceeding tolerance zones, and ^{2} = Limits of variation (tolerance zone) squared.

BIGGER THE BETTER

SMALLER THE BETTER

APPENDIX D

LOSS FUNCTION FORMULAE[8]

MULTIPLE UNITS

NOMINAL IS BEST

$$L(Y) = k(MSD)$$

$$MSD =$$

BIGGER THE BETTER

$$L(Y) = k(MSD) \qquad MSD =$$

SMALLER THE BETTER

$$L(Y) = k(MSD) \qquad MSD =$$

TABLE 1

TIN DIP EXPERIMENT EXAMPLE

FACTORS AND LEVELS (CONDITIONS)

FACTOR (VARIABLE)		LEVEL 1	LEVEL 2
A	SOLDER TEMP(°F)	475	500
B	PRE-HEAT TIME(secs)	60	30
C	SOLDER DWELL TIME(secs)	3.0	5.0
D	LEAD WITHDRAWAL RATE	5	1

NOISE FACTORS

PART NUMBER AND DATE CODE

TABLE 2

BENEFITS OF ORHTOGONAL ARRAYS

		NO. OF TRIALS REQUIRED	
FACTORS	LEVELS	FULL FACTORIAL	ORTHOGNAL ARRAY
2	2	4	4
3	2	8	4
4	2	16	8
7	2	128	8
15	2	32,768	16
63	2	9.22×10^{18}	64
9	3	19,683	32

FIGURE 1

STEPS OF A DESIGNED EXPERIMENT

o ESTABLISH GOALS AND OBJECTIVES

o DETERMINE FACTORS AND LEVELS TO BE TESTED

o DETERMINE TYPE OF DoE TO BE USED

o PERFORM EXPERIMENT TRIALS(TREATMENT COMBINATIONS)

o ANALYZE RESULTS

o CONFIRM RESULTS

o IMPLEMENT PROCESS CHANGES

FIGURE 2

TIN DIP EXPERIMENT EXAMPLE

ORTHOGONAL ARRAY

TRIAL	A	B	C	D
1	1	1	1	1
2	1	1	1	2
3	1	2	2	1
4	1	2	2	2
5	2	1	2	1
6	2	1	2	2
7	2	2	1	1
8	2	2	1	2

FIGURE 3

TIN DIP EXPERIMENT EXAMPLE

RESULTS TABLE WITH S/N RATIO

	REPLICATE		
TRIAL	R1	R2	S/N RATIO
1	4.94	6.00	14.63
2	5.25	6.00	14.94
3	5.21	4.67	13.83
4	4.50	4.38	12.94
5	4.69	4.63	13.36
6	5.32	4.25	13.44
7	6.61	5.30	15.33
8	3.40	4.50	11.67

$$S/N = -10 \log_{10} \left[\frac{1}{n} \sum \frac{1}{y^2} \right]$$

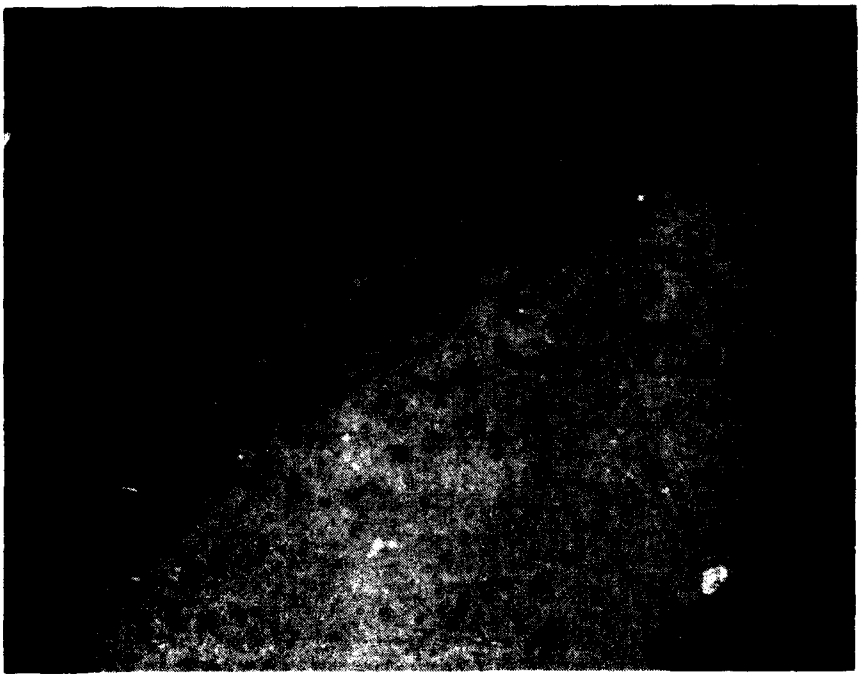

Figure 4. Cross section of capacitor lead showing outer solder coating from hot tin dip process, tin-lead layer from manufacturer, intermetallic compound and base material.(800x)

FIGURE 5

TIN DIP EXPERIMENT EXAMPLE

MAIN EFFECTS

RESPONSES

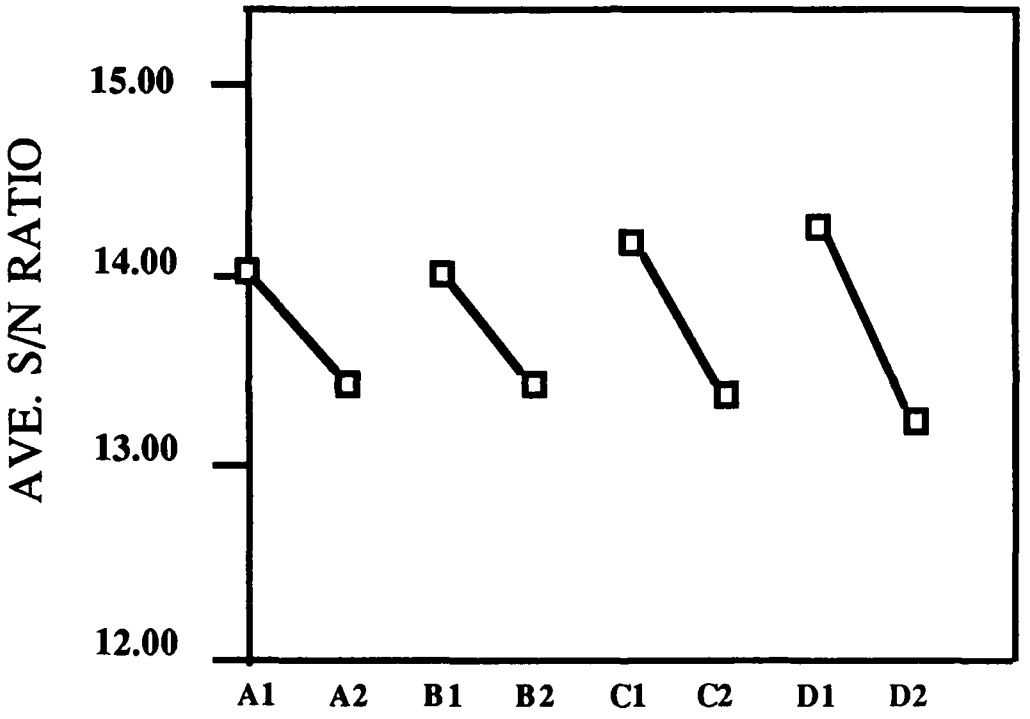

Dave Urban is Senior Quality Engineer with the Aircraft Systems Division of Simmonds Precision. Dave has been in quality engineering for more than 12 years, with emphasis for the past 4 years on all aspects of printed-wiring assembly and soldering technology.

He is a Certified Quality Engineer—American Society for Quality Control, as well as a member of IPC. He holds an AS degree in Communications Electronics and is doing further study in Industrial Engineering at Syracuse University.

Address: Simmonds Precision
Aircraft Systems Division
M/S 1 PRA Panton Rd.
Vergennes, VT 05491-1099

THE EFFECTS OF TEMPERATURE CYCLING ON SOLDER CONNECTIONS SURFACE APPEARANCE VERSUS INTERNAL REALITY

by
William J. Porteous
Senior Quality Engineer
Quadri Electronics Corporation
Chandler, Arizona

ABSTRACT

Extensive tests were performed to establish a correlation between the surface deterioration of solder connections due to thermal "aging" and the integrity of the solder structure.

The extent of surface disturbance was found to vary widely with factors such as the thermal transition rate and hardness of the conformal coating used. Most important, the onset of surface deterioration was found to occur far sooner than any discernable affect on the internal structure of the solder joint. It is concluded that the results indicate a need to establish separate accept/reject criteria for visual inspection of thermally aged solder.

INTRODUCTION

In 1987, the government imposed rigorous inspection and testing at the supplier level to reduce failures in government purchased electronic equipment. By 1988, government representatives were rejecting product because it did not meet the visual accept/reject criteria imposed by MIL-STD-454, WS6536, DOD-STD-2000 and MIL-STD-2000. These standards require that soldered connections be "smooth, shiny and not have a dull, grainy or gray appearance". While these standards are useful for new product, they do not address the purely visual degradation of solder due to thermal aging.

Thermal aging results from thermal cycling of an assembly, often done intentionally in order to eliminate parts with infant mortality or assemblies with workmanship problems. A thermal cycle is defined as the transfer of a product from +25°C to a cold temperature, to hot and then back to +25°C over a designated time profile. The process causes changes in the surface of the solder which we shall call "disturbed" solder. (See Figure 1)

Thermal cycling has been used by most companies to reduce delivered product failures, but what is not widely known is that excessive thermal cycling can cause solder fatigue.

Three articles have described the affect of different types of thermal cycling on solder. H.D. Solomon's "Fatigue of 60/40 Solder" (Reference 1), is based on the Coffin-Manson fatigue law that relates excessive thermal cycling to changes in the internal solder structure. In Reference 2, "Research on the Mechanism of Thermal Fatigue in near-Eutectic Pb-Sn Solders," J.W. Morris et al address thermal aging caused by the cycling of power applied to the assembly. In the third study (Reference 3), J. L. Marshall addresses the combined effects of numerous thermal cycles on various types of solder.

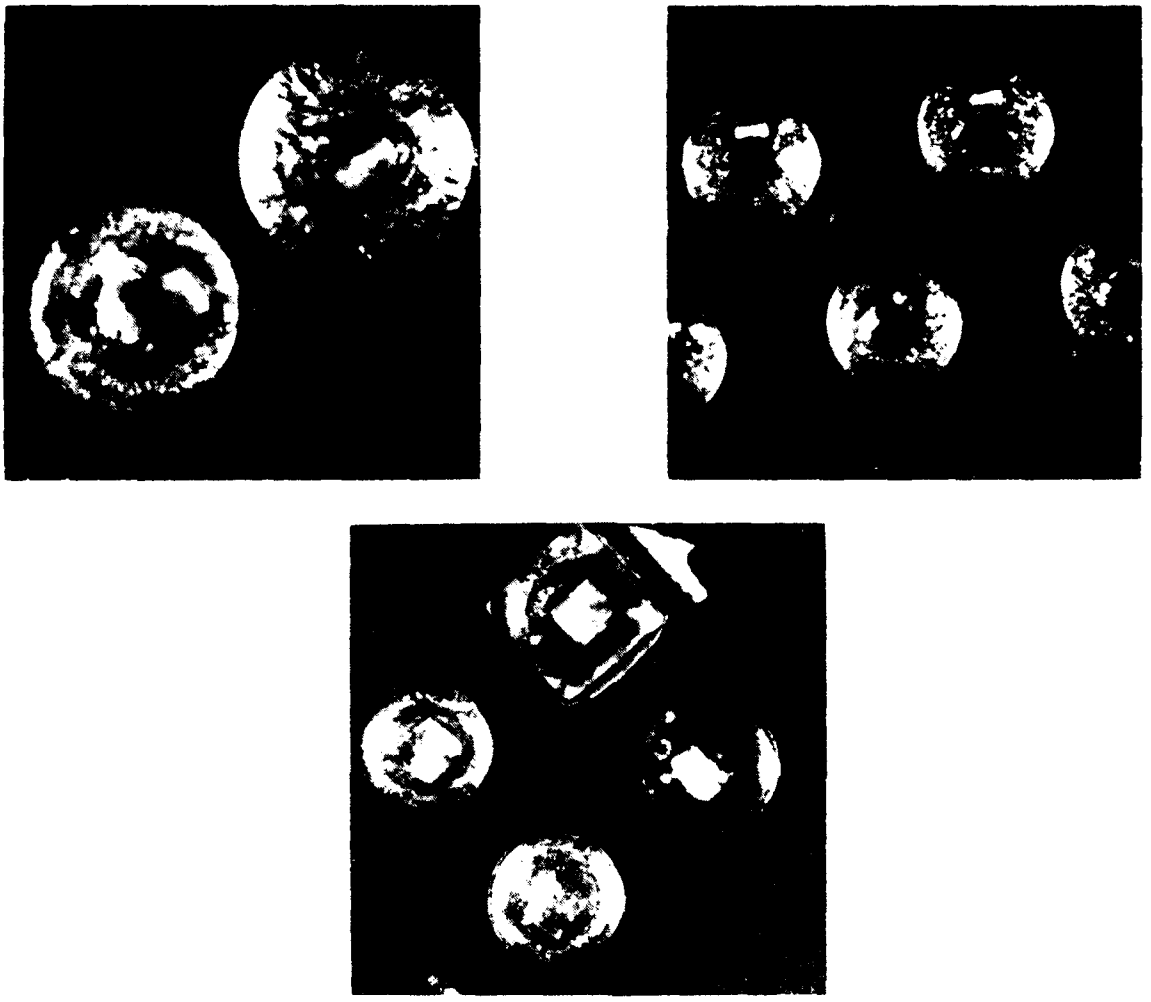

FIGURE 1. Typical Disturbed Solder Appearance After 110 Thermal Cycles

All three articles describe what can happen internally to the solder connection with excessive thermal cycling. They do not, however, deal with the affects on the solder *surface* of even fewer thermal cycles.

How soon into thermal cycling is the disturbed solder syndrome apparent? Does this aging process pose a threat to the internal integrity of the solder connection? Is the surface disturbance cause for rejection if the product initially passed inspection? The following four experiments were conducted to answer these questions:

I. An assembly was thermal cycled to observe and record the disturbed solder phenomenon at various stages. A portion of the board was microsectioned.
II. A second assembly with a known history of thermal cycling was microsectioned and evaluated.
III. Assemblies from other manufacturers were thermal cycled and evaluated.
IV. Two alternate conformal coatings were evaluated as a means of slowing the aging process.

EXPERIMENT I

One half of an assembly was coated with Silicone Resin conformal coating (Dow Corning 1-2577). The other half was left uncoated. This assembly was placed in a chamber which was transitioning on a 5-hour cycle from -55°C to +85°C. The transition rate was maintained between 5 to 10 °C per minute.

OBSERVATION

Photographs were taken to record changes in the appearance of solder connections. Figure 2 shows the coated portion at zero cycles. By the 117th cycle the solder surface had changed significantly (Figure 3). It exhibited a rough and grainy appearance and would not pass visual inspection. It was also noted that the non-coated area was significantly more disturbed than the coated area. Thermal cycling was continued to the 195th cycle (Figure 4), at which point a portion of the board was microsectioned. The microsection (Figure 5) showed the rough solder surface but revealed no change in the internal structure.

FIGURE 2. Experiment I at Zero Cycles.

FIGURE 3. Experiment I at 117 Cycles.

FIGURE 4. Experiment I at 195 Cycles.

FIGURE 5. Experiment I Microsections After 195 Thermal Cycles.

EXPERIMENT II

An assembly (Figure 6) which was conformally coated with Silicone Resin was removed from a system after more than 143 thermal cycles.* The system had been cycled from -55°C to +85°C at intervals ranging from 5 to 8 hours. The same transition rate of 5 to 10 degrees per minute used in Experiment I had been maintained.

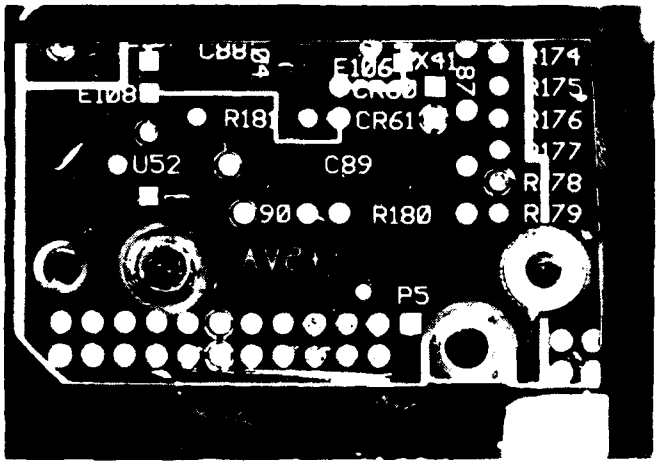

FIGURE 6. Assembly Used in Experiment II.

* The cycling of applied power, if taken into account, would have increased the "aging" to 286 cycles.

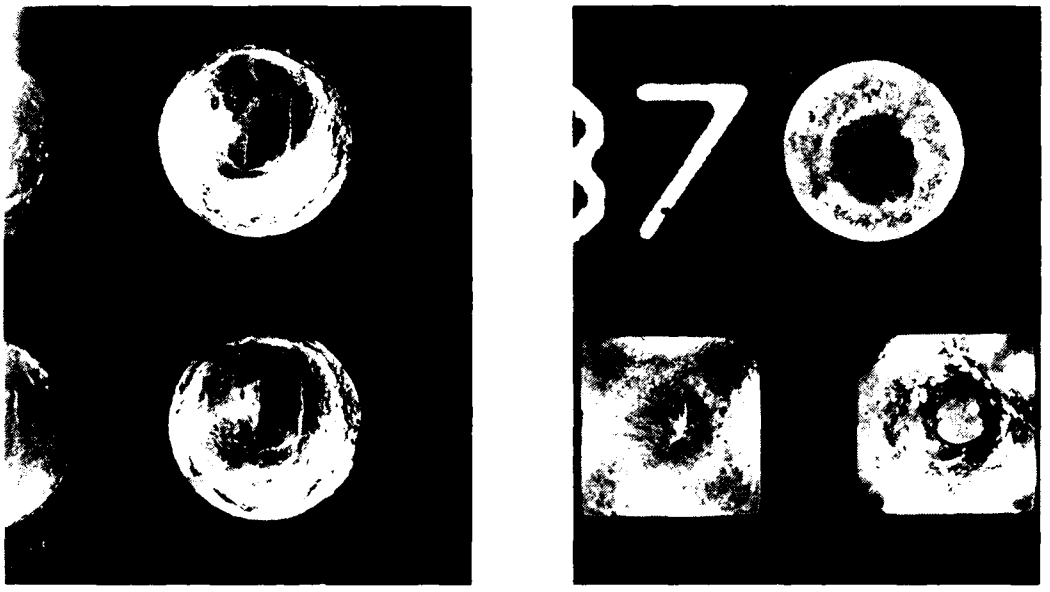

FIGURE 7. Area Selected for Microsectioning in Experiment II.

OBSERVATION

Various areas (Figure 7) were selected for microsectioning to determine the structural integrity of the solder connections. An outside lab was used to conduct a SEM/EDX analysis of the solder structure and to verify that the tin/lead ratio had not changed. The lab findings showed that the structural integrity of the solder connections was retained regardless of the extent of surface disturbance (Figures 8). The 63/37 tin/lead content was unchanged and no grain separation of the tin and lead was observed.

EXPERIMENT III

It was not known whether other manufacturers' assemblies would exhibit the disturbed solder phenomenon (i.e., whether some process or solder problem unique to Quadri was responsible for our observations). Three such assemblies were evaluated, two of which were uncoated. The third was coated with Parylene. The assemblies were subjected to temperatures varying between -55°C and +85°C in 5-hour thermal cycles. Again, the transition rate between hot and cold temperatures was maintained at 5 to 10°C per minute.

OBSERVATION

Experiment III confirmed that, as in Experiments I and II, the disturbed solder surface appeared, in this case by the 100th cycle in the uncoated assemblies. The Parylene-coated assembly did not exhibit any surface disturbance.

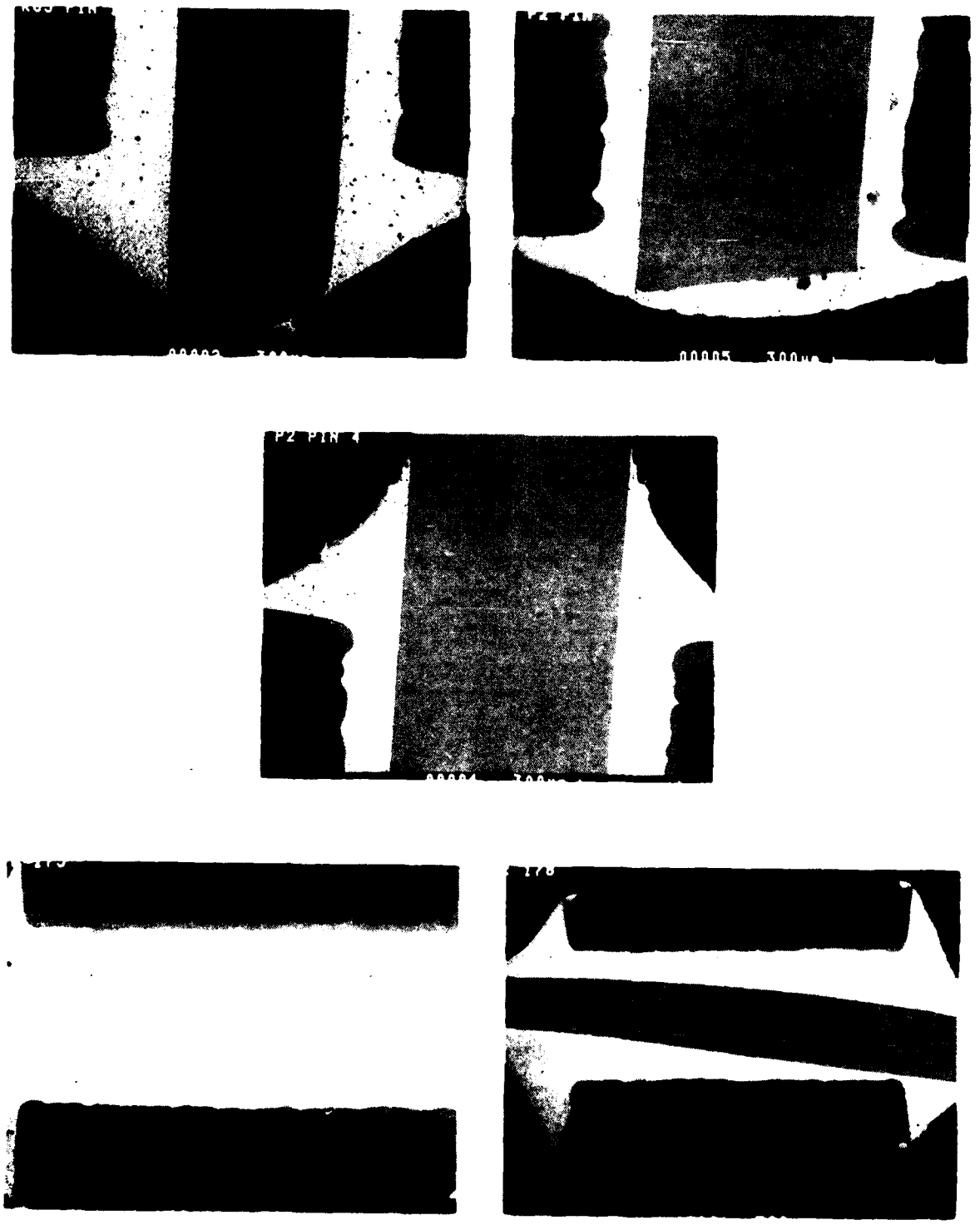

FIGURE 8. Microsections From Experiment II.

Cycling of the coated assembly was continued until the 238th cycle; still there was no disturbed solder. The coating was then removed from five solder connections and thermal cycling was continued. When the assembly was removed at 320 cycles, just 82 cycles later, the uncoated portions had deteriorated to a rejectable state. The Parylene-coated area had not changed.

The Parylene-coated assembly never did change, even after more than 800 thermal cycles. When microsectioned, it showed solder cracks as predicted by the article written by James L. Marshall (Reference 3).

EXPERIMENT IV

The Parylene-coated assembly used in Experiment III provided the first clue that the type of conformal coating used had a significant effect on solder surface condition. Experiment IV was conducted to evaluate the affect of two other conformal coatings on the solder surface condition. Three similar assemblies were used. One was uncoated and two were conformally coated, one with Silicone Resin coating (Dow Corning 1-2577), and the other with Urethane (Hysol PC18M). All three were subjected to temperatures ranging from -55 (-0+4)°C to +85 (+0-4)°C with three hour thermal cycles. The transition rate was slowed to 2-3 degrees per minute. No power was applied to the assemblies.

OBSERVATION

The first observation was taken at the 103rd cycle. All three assemblies exhibited the beginnings of the disturbed solder look. They were not, however, rejectable as yet.

The second observation was taken at the 205th cycle. There was rejectable disturbance on the solder of all three assemblies. The uncoated assembly exhibited the greatest disturbance, followed by the Silicone resin coated assembly. The Urethane resin coated assembly showed the least disturbance. Solder connections involving large holes showed little solder disturbance.

SUMMARY

Experiments I and II were conducted to determine if there was any correlation between an external surface disturbance and the internal integrity of the solder connection. It was verified that the presence of a surface disturbance does not necessarily imply a problem with the internal solder.

Experiments III and IV verified that the product of other manufacturers could be expected to exhibit the same disturbed solder condition if subjected to repetitive thermal cycling.

It was also determined that the hardness of the conformal coating reduced the extent of visible solder surface disturbance. Each coating has a durometer hardness called Shore hardness, when measured in accordance with ASTM-D-2240-86. All QPL 46058 approved conformal coatings have a Shore hardness rating.

The following are approximate hardness ratings for several commonly used coatings:

AR - Acrylic resin - SHORE HARDNESS 16D
SR - Silicone resin - SHORE HARDNESS 30D
UR - Urethane resin - SHORE HARDNESS 40D
XY - Parylene resin - SHORE HARDNESS 70D
ER - Epoxy resin - SHORE HARDNESS 75D

Based on our experiments, there seems to be a strong correlation between Shore hardness and resistance to solder surface degradation due to thermal aging.

CONCLUSION

Disturbed solder due to thermal aging will remain a cause for product rejection until separate criteria are established for inspection of thermally cycled solder. Present guidelines stress the "smooth-and-shiny" principle, which is adequate for newly manufactured assemblies. There is, therefore, a need for the Government to give industry specific guidelines for inspection of solder after thermal cycling, thereby avoiding needless rework, potential scrapping of good product or, even worse, an actual deterioration of reliability due to the rework.

While it was found that conformal coatings with greater Shore hardness result in less solder disturbance than do softer coating materials, adopting a harder coating material can ultimately create more costly manufacturing and rework processes. Hence, this is not necessarily a recommended solution.

It was also observed that reducing the thermal transition rate slowed the onset of the disturbed solder phenomenon. When the transition rate was reduced to 2-3°C per minute, surface deterioration was slower than at a 5-10 degree per-minute rate. This suggests an alternate method of reducing the visual aging effect.

---

1. H. D. Solomon, "Fatigue of 60Sn/40Pb Solder", *Proceedings of 36th Electronic Component Conference*, IEEE, 1986. Pp 622-629.

2. J.W. Morris, JR. D. Grivas, D. Tribula, T. Summers and D. Frear. "Research On The Mechanism Of Thermal Fatigue In Near-Eutectic Pb-Sn Solders", *13th Annual Electronics Manufacturing Seminar Proceedings*, 1-3 March 1989. Pp. 275-297.

3. James L. Marshall. "Characterization Of Solder Fatigue In Electronics Packaging", *12th Annual Electronics Manufacturing Seminar Proceedings*, 17-19 February 1988. Pp. 389-411.

William Porteous is with Quadri Electronics Corporation and has been Senior Quality Engineer with them since 1981. From 1969 until he joined Quadri, Bill was with Analog Devices serving as supervisor of field quality. He is certified for WS 6536E Category H and MIL-STD-2000 Category C.

Bill is a member of the American Society for Quality Control.

Address: Quadri Electronics Corporation
300 N. McKemy Ave.
Chandler, AZ 85226

THE USE OF HCFC SOLVENTS IN MILITARY ELECTRONICS CLEANING: A WORKING EXAMPLE *

by

Dr. Olexander Hnojewyj
Manager - Materials and Process Engineering
Litton Applied Technology
San Jose, CA 95150

and

Dr. J. K. "Kirk" Bonner
Manager - Applications and Process Development Engineering
Allied-Sig[illegible] Inc.
Genesolv/Baron-Blakeslee
Melrose Park, IL 60160

ABSTRACT

Solvents based on CFC-113 are in the process of being replaced by alternative technologies due to the ban on CFCs under both the Montreal Protocol and Title VI of the Clean Air Act. In electronics defluxing this has resulted in replacing chiefly CFC-113 in azeotropic blends and mixtures. DoD electronics defluxing applications, in particular, have relied heavily on CFC-113-based solvents, principally because of the many advantageous properties that CFC-113-based solvents offered. This paper describes one viable alternative technology to be used in military electronics defluxing applications. This technology is cleaning with hydrochlorofluorocarbons (HCFCs). HCFCs are described, and details involving the usage of this technology for military electronics cleaning by a major contractor are presented.

*This paper/presentation does not and is not intended to address the environmental or worker health risk or safeguard issues associated with the use of HCFCs.

1.0 INTRODUCTION

It is clear at this point that the usage of chlorofluorocarbon (CFCs) solvents will cease by the end of the century, if not sooner. Under the initial agreement of the Montreal Protocol, the production of CFCs was to be cut back to 50% of the 1986 levels by 1998. Now the London Amendments (June 1990) to the Protocol are even more restrictive. All CFCs will be phased out of production by the year 2000, and it is conceivable that this timetable may be accelerated. In addition, under the London agreement, 1,1,1-trichloroethane (methyl chloroform) and carbon tetrachloride will be phased out by the year 2005.

2.0 HYDROCHLOROFLUOROCARBONS (HCFCs)

With the pressure to reduce or eliminate the usage of CFC-113 (1,1,2-trichloro-1,2,2-trifluoroethane), new materials and process technologies are being developed. Among the most promising of these are a family of substances known as hydrochlorofluorocarbons, or HCFCs for short. These substances, in addition to containing the elements carbon (C), chlorine (Cl), and fluorine (F), also contain the element hydrogen (H). One of the most important HCFCs for solvent applications is HCFC-141b (1,1-dichloro-1-fluoroethane). This material shows excellent stability and compatibility with a wide variety of materials, and it can form azeotropes with different substances such as lower molecular weight alcohols, e.g., methanol (methyl alcohol). Another important HCFC is HCFC-123 (1,1-dichloro-2,2,2-trifluoroethane). The two dimensional structural formulas of these two substances are shown in Figure 1 along with the structural formulas of CFC-113 and 1,1,1-trichloroethane.

The chief advantages of HCFCs over CFC-113 in solvent applications are (1) their substantially lower ozone depletion potentials (ODPs) and (2) their substantially lower greenhouse warming potentials (GWPs). In addition, solvents blended from one or more of the aforementioned HCFCs typically have lower boiling points (b.p.). Many of the other properties of HCFC solvents are very similar to those of solvents based on CFC-113. Table 1 contrasts a typical solvent based on HCFC-141b with one based on CFC-113.

Because of their advantages, HCFCs are clearly adequate replacements in many solvent applications where previously CFC-113 or CFC-113 plus other ingredients was the solvent of choice. However, the HCFCs, like CFC-113, contain the element chlorine

(Cl); therefore, they do have a residual ozone depletion potential. Because of this they are subject to regulation both by the London Amendments to the Montreal Protocol and Title VI of the Clean Air Act (U.S.). Under the London Amendments HCFCs should be phased out by the year 2020 and no later than 2040; by Title VI of the Clean Air Act there is to be a production freeze on HCFCs starting in 2015 and usage after that until 2030 to be limited to refrigerants. There is to be a total production ban on all HCFCs by 2030. Hence, HCFCs are perceived as useful transitional substances. They will be the technological bridge between solvents based on CFC-113 and newer solvents having very little (<0.05 ODP) or zero ODPs. These latter substances are expected to appear sometime during the first decade of the next century. So although HCFCs will only have a finite service lifetime, that lifetime is projected to be twenty years or better in solvent applications.

3.0 HCFC APPLICATIONS

Like CFC-113 based solvents, solvents based on HCFC-141b have a broad usage range. See Table 2. For electronics defluxing, the HCFC-141b can be combined in an azeotropic formulation with lower molecular weight alcohols like methanol and ethanol. One important azeotropic formulation for defluxing contains HCFC-141b, methanol, and nitromethane; another contains HCFC-123 added to the HCFC-141b, methanol, and nitromethane in either an azeotropic mixture or in a blend of these particular constituents. These formulations demonstrate equal and in many cases superior cleaning performance to CFC-113-based solvents [1,2,3,4,5,6,7]. In addition, these formulations have passed the Phase 2 test making them suitable alternative cleaning technologies for DoD electronics defluxing applications [8,9]. See Section 4.0, Phase 2 Tests.

For metal degreasing and precision cleaning, formulations containing varying amounts of HCFC-141b and HCFC-123 are suggested [10]. See tables 3 and 4. In many cases nitromethane is not added to such blends since it can be shown that blends of HCFC-141b and HCFC-123 by themselves demonstrate sufficient stability in a wide variety of metal cleaning operations. In the case of metal degreasing involving an emulsifiable or semi-emulsifiable oil, a solvent based on HCFC-141b and containing methanol may prove superior to a blend having no alcohol. Other potential applications for HCFC-based solvents are: deposition, drying, dry cleaning, and individual pressurized containers.

4.0 PHASE 2 TESTS

In response to the threat of CFCs to stratospheric ozone, a number of alternative technologies have arisen as possible substitutes for defluxing applications. Some of these technologies have been around a long time, such as water soluble fluxes. Some of them are more recent, such as the hydrochlorofluorocarbons (HCFCs) and "no clean" fluxes. In order to facilitate acceptance of these alternative technologies by the military, the EPA arranged for a consortium of EPA, military, and industry to tackle the problem of military acceptability of new technologies. This consortium is know as the EPA/DoD/IPC Ad Hoc Solvents Working Group. This group of people, drawn from the EPA, the military, and industry, got together to define and specify both a suitable printed wiring assembly test board and a detailed test procedure for cleaning performance acceptance of alternative technologies.

4.1 PHASE 1 AND PHASE 2 TESTING

The EPA/DoD/IPC Ad Hoc Solvents Working Group elaborated a standard test procedure to be used for cleanliness performance acceptance of alternative defluxing technologies for the purpose of replacing CFC-113 in defluxing and cleaning operations [11]. This document outlines in detail the procedures that were followed in the Phase 1 test; these same procedures must be followed by anyone performing a Phase 2 test. The Phase 1, or Benchmark, test was performed at two government facilities, EMPF in Ridgecrest, CA,* and NAC in Indianapolis, IN. The results of the Phase 1 test are available from the IPC [12]. All manufacturers of alternative technologies who wish to have their material accepted by the military must undergo a Phase 2 test with their alternative technology.

4.2 PURPOSE

The Phase 2 test was designed by the EPA/DoD/IPC Ad Hoc Solvents Working Group as a test for evaluating alternative cleaning technologies for reducing the level of CFCs (chlorofluorocarbons) used in electronics manufacturing cleaning processes. The Phase 1, or Benchmark, test defined by the IPC Cleaning and Cleanliness Testing Program specified the use of a batch cleaning operation and employing as the cleaning agent the nitromethane-stabilized azeotrope of CFC-113 and methanol (note: commercially available as Freon TMS).

---

* The EMPF is now located in Indianapolis, IN.

4.3 PROCESS SEQUENCES

Five process sequences were run. These were; A boards, B1 boards, B2 boards, C assemblies and D assemblies. The definition of each of these are;

A boards. A boards are boards that are precleaned and tested. No other processing operation os performed on them.

B1 boards. B1 boards are boards having the specified solder paste screened on the bare board substrate and subsequently vapor phase reflowed. They are tested, but they are not cleaned.

B2 boards. B2 boards are boards having the specified solder paste screened on the bare board substrate and subsequently reflowed. They are also exposed to the wave soldering operation using the specified wave solder flux. They are tested, but they are not cleaned.

C Assemblies. C assemblies are assemblies having components attached to the bare board substrate using the specified solder paste and vapor phase reflow. They are then cleaned and tested.

D Assemblies. D assemblies are assemblies having components attached to the bare board substrate using the specified solder paste and vapor phase reflow. They are also exposed to the wave soldering operation using the specified wave solder flux. They are cleaned twice - once after vapor phase soldering and once after wave soldering. They are tested after the two cleaning operations.

The only boards used for the official criteria were the A, C, and D boards. The B1 and B2 boards were used for reference only.

4.4 CLEANING PROCESS

The cleaning process followed at Allied-Signal Inc. during their Phase 2 test was identical to the batch process used in Phase 1 (Benchmark) with the exception of the solvent. In place of the stabilized azeotrope of CFC-113 and methanol, the stabilized azeotrope of HCFC-141b, HCFC-123, and methanol was used instead for the first Allied-Signal Phase 2 test. For the second Allied-Signal Phase 2 test the stabilized azeotrope of HCFC-141b and methanol was used. No other process change was made. Essentially, the cleaning cycle consisted of (1) 30 seconds vapor equilibration, (2) 3 minutes direct boil sump immersion, (3) 1 minute rinse sump immersion, (4) 30 seconds vapor equilibration.

4.5 PHASE 2 TEST RESULTS

Three official cleanliness test methods were used to ascertain cleanliness. These were:

1 ionic contamination test
2 residual rosin test
3 surface insulation resistance (SIR).

For the ionic contamination test, a tester having spray headers in the test tank and heated test solution was used (Omega Meter 600 SMD). For the residual rosin test a UV/VIS spectrophotometer was employed. The SIR data are for reverence only. They are presented in the complete Allied-Signal Phase 2 Reports [8,9] but not here.

The results for the official Allied-Signal Phase 2 test for the stabilized azeotrope of HCFC-141b, HCFC-123, and methanol (Note; which will be commercially available as Genesolv®2010) are given in Table 5. This was the first Phase 2 test to be performed; it was performed on 7-8 September 1989. Again, it must be stressed that the only difference between the Benchmark, or Phase 1, test and Allied-Signal Phase 2 test was the solvents used. The Benchmark test employed the stabilized azeotrope of CFC-113 and methanol and the Allied-Signal Phase 2 test employed the stabilized azeotrope of HCFC-141b, HCFC-123, and methanol. The entire Phase 2 test was repeated with the stabilized azeotrope of HCFC-141b, HCFC-123, and methanol. However, batch cleaning was not used. Rather, the material was run in an in-line conveyorized defluxer with the same pressure parameters as previously used. The conveyor speed was 4 ft/min. The results are presented in Table 6. The results for the official Allied-Signal Phase 2 for the stabilized azeotrope of HCFC-141b and methanol (Note; which will be commercially available as Genesolv®2004) are given in Table 7. This Phase 2 test was performed 10-11 May 1990; the batch cleaning process was again used.

5.0 DoD AND ALTERNATIVE TECHNOLOGIES

When the Montreal Protocol was initially promulgated (1987), it was realized by members of the electronics industry that DoD military standards called out in a number of instances the use of CFC-113-based solvents. Not only were these standards necessary for military contractors, they were in many instances *de facto* standards throughout the industry. As was pointed out in Section 4.0 dealing with the Phase 2 test, a group of people from the EPA, DoD, and the industry formed a working committee known as the

EPA/DoD/IPC Ad Hoc Solvents Working Group. Now that Phase 2 testing is well underway and have been completed for seven different cleaning agents, the issue now becomes how best to implement alternative technologies in actual situations where CFC-113 based solvents are currently being used by military contractors.

To meet the problem of replacing CFCs in DoD applications, the United States Congress established under the Defense Authorization Act for Fiscal Year 1990-91, Section 356, the DoD CFC Advisory Committee. This committee has a maximum of 15 members and consists of DoD staff, defense contractors, and EPA staff members. This committee is conducting a study for the Secretary of Defense to report to Congress by June 1991 on DoD efforts to phase out CFCs and other substances harmful to the ozone layer.

In addition to the DoD CFC Advisory Committee the Military Electronics Technology Advisory Group (METAG), although not specifically formed because of the ozone issue, also reviews military standards and specifications and has formed a subgroup to examine the issue of CFC alternatives for DoD electronics cleaning.

Both of these groups operate at high levels. An alternative approach is to obtain the necessary approvals at the individual contractor level. This approach is being pursued by Litton Applied Technology, which obtained a deviation to employ several new HCFC-based solvents in their cleaning operations. Litton Applied Technology's efforts are described below in Sections 7.0 and 8.0.

6.0 COMPATIBILITY OF HCFCs

Solvents based on HCFC-141b, in general, show excellent compatibility. Although they are slightly more aggressive that CFC-113-based solvents, they are nowhere nearly as aggressive as 1,1,1-trichloroethane. Tables 8 and 9 show compatibility data for HCFC-141-based solvents.

7.0 HCFC APPROVAL AT LITTON APPLIED TECHNOLOGY DIVISION

Litton Applied Technology Division's soldering process criteria meet the requirements of Navy Process Specification WS-6536. This specification defines the approved materials, methods, and inspection standards for producing high reliability quality electrical soldering workmanship [13]. Section 3.3.3 of WS-6536 specifies approved solvents and cleaners. Use of alternative solvents requires approval of the customer, Naval Air Systems Command.

To obtain customer approval to use HCFCs, Material and Process Engineering at Litton Applied Technology initiated the following negotiations and formal requests:

1. Obtained supporting documentation and recommendations from the:

   a. Soldering Technology Training Director (Code 3681), Naval Weapons Center, China Lake, CA.

   b. Electronics Manufacturing Productivity Facility (EMPF), Ridgecrest, CA (See Note, p. 4).

   c. Ad Hoc Solvents Work Group.

   d. Institute for Interconnecting and Packaging Electronics Circuits (IPC), Lincolnwood, IL.

2. Contacted the Litton Applied Technology Program Office.

3. Requested approval from the Naval Weapons Center, China Lake, CA.

4. Requested approval from the Naval Air Systems Command, Washington D.C.. Litton's request to use HCFCs was approved.

This paragraph provides additional detail on how Litton Applied Technology obtained approval for using HCFCs. Supporting documentation and recommendations basically followed the recommendations of the Military Electronics Technology Advisory Group (METAG): "...that the Phase 1 Benchmark become the acceptance criteria for cleanliness for all electronic assemblies ...", and "...that any environmentally safe and compatible process proven capable of cleaning materials to the Benchmark be allowed for military electronic assemblies, even if a contract modification is required ...". The Litton Applied Technology Division Program Office submitted Deviation Number 335D007C1 for review and approval

to use Phase 2 approved HCFCs under WS-6536. All supporting documentation was attached with the Deviation request. The Deviation was approved by Naval Air Systems Command, Code AIR-54625F, on 20 September 1990. This entire process, from initiation to final Deviation approval, took approximately seven weeks.

8.0 HCFC PERFORMANCE DATA AT LITTON APPLIED TECHNOLOGY DIVISION

Preliminary comparative cleaning testing results are presented for CFC and HCFC solvents. Two CFC solvents (DuPont Freon® TMS, Blaco-Tron® TMS Plus) and two HCFC solvents (Genesolv® 2004 and Genesolv® 2010) were tested. Two cleanliness test methods were used to compare the cleaning processes. The test methods included:

1. Residual Rosin testing, and

2. Ionic contamination testing.

8.1 RESIDUAL ROSIN TESTING

The extractive technique for removing residual rosin uses straight isopropyl alcohol (IPA) in a stainless steel tank with the aid of ultrasonics. This extractive technique has been described by Bonner and Banasiak [14]. For residual rosin determination, a UV/VIS spectrophotometer (Perkin-Elmer Lambda 6) was employed.

Table 10 lists the equipment with the corresponding cleaning solvent that was tested. A Baron Blakeslee MLR-216 Low Emission (LE) Cleaning and Degreasing Systems with the Automated Rotating Multiaxis (ARM) Handling System was specifically designed to handle HCFCs. Eight different PWAs were cleaned. Based on a limited sampling, results indicate improved cleaning with HCFCs. Table 11 describes the cleaning process conditions.

8.2 IONIC CONTAMINATION TESTING

Litton Applied Technology Division uses a Model 300 Omega Meter II ionic contamination tester to determine quantitative measurements of residual ionic contamination on PWAs after post wave soldering cleaning operations. The unit uses a 75-80% solution of reagent grade isopropyl alcohol (IPA) and deionized water for removal of residual flux. Cleanliness measurements are taken first in resistive values then converted to mg NaCl/sq-in* for the final cleanliness reading.

---

* 1 milligram (mg) = 1000 micrograms (µg); therefore, a reading of 0.003 mg NaCl/sq-in = 3µg NaCl/sq-in.

For the comparative cleaning tests, 40 single-sided through-hole type production boards of varying component load density were wave soldered using Kester 1587 MIL flux. The boards were then divided into 4 groups of 10 each. The individual groups were cleaned using the equipment and corresponding solvent listed in Table 11. All 40 boards passed the ionic contamination test with an average reading of 0.003 mg NaCl/sq-in, with no one reading exceeding 0.005 mg NaCl/sq-in. The maximum ionic contamination level allowable per MIL-P-28809 is 0.01 mg NaCl/sq-in. Negligible difference was seen between equipment/cleaning solvent efficiency with respect to ionic contamination levels.

9.0 CONCLUSIONS

Military customer approval to use HCFCs can be obtained. One of the methods to obtain approval is by submitting a Deviation to an existing specification at the individual contractor level. The military contractor's Program Manager should submit the Deviation to the customer with supporting documentation.

Based on a limited sampling, rosin residual results indicate improved cleaning with HCFCs.

Negligible difference was seen between the efficiency of equipment/cleaning solvent and ionic contamination levels.

While there is not direct drop-in substitute available for CFC-113, solvents based on HCFC-141b present the nearest technological replacements to CFC-113-based solvents in terms of their overall properties and cleaning performances. Equipment is readily available for these new solvents, and in some cases existing equipment in the field may be retrofittable to contain them. Since for more than 40 years the flame limits of 1,1,1-trichloroethane did not hinder its successful use of a wide variety of industrial applications, the very similar flame limits of HCFC-141b are likewise not perceived as a detriment to its being used successfully in a similar range of industrial operations. To date there is not toxicological evidence to suggest that the PEL of HCFC-141b shouldn't be 500 ppm. Hence, solvents based on HCFC-141b represent the best overall choice for situations requiring the replacement of solvents based on CFC-113.

REFERENCES

1. J. K. "Kirk" Bonner, "New Solvent Alternatives," Printed Circ. Ass., Vol. 3, 9, Sept. (1989), 36-38.

2. J. K. "Kirk" Bonner, "Solvent Defluxing of Printed Wiring Board Assemblies and Surface Mount Assemblies: Materials, Processes, and Equipment" in L. Hymes, ed. Cleaning Printed Wiring Assemblies in Today's Environment (New York: Van Nostrand Reinhold, 1990) Chap. 3.

3. J. K. "Kirk" Bonner, "Cleaning Surface Mount Assemblies; The Challenge of Finding a Substitute for CFC-113" in J.E. Morris, ed. Electronics Packaging Forum, Vol. 2 (New York; Van Nostrand Reinhold, 1990) Chap. 11.

4. J. K. "Kirk" Bonner, "Two HCFC Solvents for Replacing CFC-113," Proc. of 1st CFC Alternatives Conf., San Francisco, CA, June 26-27 (1990).

5. R. S. Basu and J. K. Bonner, "Alternatives to CFCs: New Solvents for the Electronics Industry," Surf. Mount Tech., Vol. 3, 8, Dec. (1989) 34-37.

6. A. N. Merchant and M. C. Wolff, "Screening and Development of Ozone/Greenhouse Compatible Cleaning Agents," Proc. Nepcon West '89, Anaheim, CA, March 6-9 (1989) 756-758.

7. J. K. "Kirk" Bonner, "Cleaning Surface Mount Assemblies: The Challenge of Finding a Substitute for CFC-113," Proc. Nepcon West '89, Anaheim, CA, March 6-9 (1989) 1051-1058.

8. Phase 2 Test: Final Report/Genesolv® 2010 (Melrose Park, IL; Allied-Signal, 1989).

9. Phase 2 Test: Final Report/Genesolv®2004 (Melrose Park, IL: Allied-Signal, 1990).

10. J. K. "Kirk" Bonner, "New Solvent Alternatives to CFCs for Precision Cleaning," Proc. Inst. Environ. Sciences, New Orleans, LA, April 23-27 (1990).

11. No author. "Cleaning and Cleanliness Testing Program: A Joint Industry/Military/EPA Program to Evaluate Alternatives to Chlorofluorocarbons (CFCs) for Printed Board Assembly Cleaning," March 30 (1989) - available from the IPC.

12. No author. "Cleaning and Cleanliness Test Program: Phase 1 Test Results," IPC-TR-580, Oct. (1989).

13. WS-6536, "Naval Air Systems Command Department of the Navy Process Specification Procedures and Requirements for Preparation and Soldering of Electrical Connections".

14. Bonner, J.K., and Banasiak, R.M., "A Comparison of Rosin Residue Determination by the IPA Extraction Technique with the Supplemental Ultrasonic Extraction Technique", 14th Ann. Elec. Mfg. Sem. Proc., Naval Weapons Center, China Lake, CA., 21-22 Feb. (1990) 193-197.

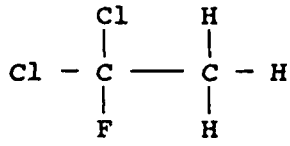

(1) 1,1-dichloro-1-fluoroethane (HCFC - 141b)

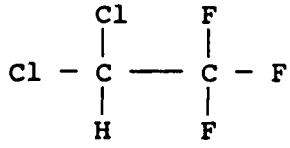

(2) 1,1-dichloro-2,2,2-trifluoroethane (HCFC - 123)

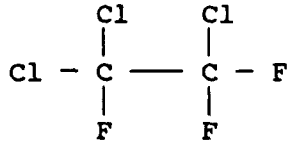

(3) 1,1,2-trichloro-1,2,2-trifluoroethane (CFC-113)

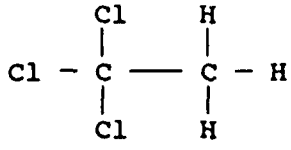

(4) 1,1,1-trichloroethane (methyl choloroform)

Figure 1. The structural formulas of (1) HCFC-141b, (2) HCFC-123, (3) CFC-113, (4) 1,1,1-trichloroethane.

Table 1. Key Comparison of HCFC-141b Solvents vs. CFC-113

	CFC-113 Based	HCFC-141b + Methanol
Boiling point	100-117° F	84.9° F (29.4° C)
Compatibility	Very Good	Very Good
Stability	Very Good	Very Good
Flash point	None	None*
Toxicity (TLV)	500-1000	400**
Recyclable	Yes	Yes
Flame limits		
Lower limit (Vol. %)	None	7.6 ***
Upper limit (Vol. %)	None	17.7 ***
ODP	0.8	0.1
GWP	2.3	0.14

* ASTM D 1310-87 or ASTM D 56-82
** Preliminary Value
*** Values for pure HCFC-141b

Table 2. Soils Removed by HCFC-141b-Based Solvents

HCFC-141b/HCFC-123	HCFC-141b/HCFC-123/MeOH* & HCFC-141b/MeOH
Silicone Oil	Solder Flux
Hydrocarbons	Solder Paste
Straight Cutting Oils	Silicone Oil
	Hydrocarbons
Some Fluorolubricants	Straight Cutting Oils
	Water-Soluble Oils
	Glycols
Grease	Grease

* MeOH = Methanol

Table 3. Metal Degreasing Contrasting CFC-113 with an HCFC-141b-Based Solvents

SOIL	SOLVENT	% OIL REMOVED
Petroleum Base	CFC-113	99.1 ± 0.4
	HCFC-141b/HCFC-123	98.3 ± 0.8
Semi-Synthetic	CFC-113	87.8 ± 1.3
	HCFC-141b/HCFC-123	99.9 ± 0.3
Synthetic	CFC-113	19.0 ± 8.0
	HCFC-141b/HCFC-123	54.4 ± 7.9

Test Substrate: Cold-Rolled Steel
Aging: 200° F
Cleaning Cycle: Vapor Only (15 Seconds)

Table 4. Case Study of CFC-113 and HCFC-141b/HCFC-123

Substrate: - Aluminum Fins

Soil: - Omicron Oil, Upsilon Oil

Method: - Extraction of residual organics in Isopropanol

- Detection by UV/VIS Spectrophotometry

Solvent	Oil Concentration ppm*	
	Set 1	Set 2
HCFC-141b/HCFC-123	0.75	0.90
CFC-113	1.39	2.16

TABLE 5

Allied-Signal First Phase 2 Test Results Contrasted with the Benchmark Results

	Benchmark (Phase 1) CFC-113/Methanol Azeotrope		Phase 2* (Allied-Signal) HCFC-141b/HCFC-123/Methanol Azeotrope**	
Assembly Type	Ionic Residue ($\mu g/in^2$)	Rosin Residue (μg)	Ionic Residue ($\mu g/in^2$)	Rosin Residue (μg)
A	2.0	301	0.6	47
C	3.8	3,135	2.5	3,128
D	10.7	3,945	8.1	1,536

* Test officially monitored by TMVT members on site.

** Genesolv®2010 = HCFC-141b/HCFC-123/Methanol Azeotrope

TABLE 6

Allied-Signal Phase 2 Test Results Contrasted with In-Line Results

	Phase 2* (Allied-Signal) Batch Unit HCFC-141b/HCFC-123/Methanol Azeotrope		Phase 2 (Allied-Signal) In-Line (Liquid Seal) Conveyorized Defluxer HCFC-141b/HCFC-123/Methanol Azeotrope**	
Assembly Type	Ionic Residue ($\mu g/in^2$)	Rosin Residue (μg)	Ionic Residue ($\mu g/in^2$)	Rosin Residue (μg)
A	0.6	47	0.7	2
C	2.5	3,128	1.6	155
D	8.1	1,536	4.1	237

* Test officially monitored by TMVT members on site.

** Genesolv®2010 = HCFC-141b/HCFC-123/Methanol Azeotrope

TABLE 7

Allied-Signal Second First Phase 2 Test Results Contrasted with the Benchmark Results

	Benchmark (Phase 1) CFC-113/Methanol Azeotrope		Phase 2* (Allied-Signal) HCFC-141b/Methanol Azeotrope**	
Assembly Type	Ionic Residue ($\mu g/in^2$)	Rosin Residue (μg)	Ionic Residue ($\mu g/in^2$)	Rosin Residue (μg)
A	2.0	301	1.1	76
C	3.8	3,135	3.3	2,937
D	10.7	3,945	8.5	610

* Test officially monitored by TMVT members on site.

** Genesolv®2004 = HCFC-141b/Methanol Azeotrope

Table 8. HCFC-141b-Based Solvents Compatibility

Compatible	Incompatible	Test Compatibility
PTFE	Butyl Rubber Adhesive	ABS
Phenolic	Polystyrene	Polyphenylene Oxide
PCFE	Acrylic	Polycarbonate
HDPE	Cellulosic	
Polypropiene		
Polyester		
PVC		
Acetal		
Epoxy		
Nylon		
Polyetherimide		
Polyhenylene Sulfide		

Table 9. Elastomer and Gasket Compatibility with HCFC-141b/HCFC-123/MeOH

	Linear Swell %	Extractables %
Polyurethane	50	4
Acrylonitrile-Butadiene	16	24
Styrene-Butadiene	6	11
Isobutylene-Isoprene	9	8
Polyester TPE	14	1
Chlorosulfonated Polyethylene	15	2
Natural Polyisoprene	30	6
Polychloroprene	7	19
Ethylene/Propylene Terpolymer	-2	32
Polysiloxane	32	3
Polysulfide FA	8	3
Polysulfide ST	9	2
Fluoroelastomer A	18	5
Fluoroelastomer B	17	<1
Perfluoroelastomer	0	<1

TABLE 10: RESIDUAL ROSIN
CFC and HCFC Cleaning at LATD.
(Flux: Kester 1587 MIL) [1]

EQUIPMENT	SOLVENT	CONTAMINATION [2] µg/sq-in			PERCENT [3] REMOVAL
		Sample 1	Sample 2	Average	
Electrovert SC-500 In-Line Degreaser	DuPont Freon TMS (CFC)	887	448	668	96.1
Degreastill LP-1618 Batch Vapor Degreaser	Blaco-Tron TMS Plus (CFC)	690	992	806	95.3
Baron Blakeslee MLR-216 LE Batch Vapor Degreaser with ARM Handling System	Genesolv 2004 (HCFC)	219	240	230	98.6
Baron Blakeslee MLR-120 Batch Vapor Degreaser	Genesolv 2010 (HCFC)	548	267	408	97.6
Not Cleaned Control	None	16997	17447	17222	0.0

NOTES:

(1) Type RA per MIL-F-14256

(2) RESIDUAL ROSIN $= \frac{\text{ppm Rosin (UV/VIS)} \times \text{S.G. of IPA} \times \text{VOL. of IPA} \times 100}{\text{Surface Area of PWA}}$

$= \frac{\text{ppm Rosin (UV/VIS)} \times 0.785\ \text{g/cc} \times 1500\text{cc}}{\text{Surface Area of PWA}}$

(3) % Removal $= \frac{\text{(Avg. Unclean Contamination) - (Avg. Sample Contamination)}}{\text{Avg. Unclean Contamination}} \times 100$

$= \frac{17222 - \text{(Avg. Sample Contamination)}}{17222}$

TABLE 11: CLEANING PROCESS CONDITIONS

EQUIPMENT /SOLVENT	BELT SPEED	BOIL SUMP DIP EXPOSURE TIME	SPRAY WASH EXPOSURE TIME	FINAL CLEAN WELL DIP EXPOSURE TIME	TOTAL PROCESS TIME
Electrovert SC-500 In-Line Degreaser/Dupont Freon TMS (CFC)	2 fpm	2.5 min	2 min @ 30-40 psi @ 200-220 psi	2.5 min	7 min
Degreastill LP-1618 Batch Vapor Degreaser/ Blaco-Tron TMS Plus (CFC)	N/A	3 min	N/A	1 min	4 min
Baron Blakeslee MLR-216 LE Batch Vapor Degreaser / with ARM Handling System Genesolv 2004 (HCFC)	N/A	3 min *Plus 1 Min vapor dwell	N/A	1 min * Plus 1 min conden-sation dwell	5 min
Baron-Blakeslee MLR-120 Batch Vapor Degreaser/ Genesolv 2010 (HCFC)	N/A	3 min	N/A	1 min	4 min

* Steps are intended for solvent loss prevention and protection of clean well flux drag-in.

Dr. Olexander Hnojewyj is Manager of Material and Process Engineering at Litton Applied Technology Division. He has 5 years' experience in the electronics industry. Before joining Litton he was associated with the 3M Company for approximately 14 years. He has extensive experience in adhesive and polymer coating products and in associated process developments.

Olex holds a B.Ch.E. degree from the University of Minnesota and both an M.S. degree and a Ph.D. in Chemistry from North Dakota State University. He is a member of the Society of Manufacturing Engineers (SME) and is the Litton Applied Technology representative to the Institute for Interconnecting and Packaging Electronic Circuits (IPC).

Address: Litton Applied Technology
4747 Hellyer Ave.
San Jose, CA 95150-7012

J. K. "Kirk" Bonner is Manager of Applications and Process Development Engineering at Allied-Signal Inc. He has 13 years' experience in the electronics industry, including manufacturing processes and the automation of printed-wiring and surface-mount assemblies.

He was awarded an MBA degree from Florida Institute of Technology and a Ph.D. from The Johns Hopkins University. He is a Certified Manufacturing Engineer and a member of SME, IEPS, ACS, and SMTA. Kirk has authored or co-authored more than 25 technical papers in his field, including those delivered at these Seminars.

Address: Allied-Signal Inc.
2001 N. Janice Ave.
Melrose Park, IL 60160

ULTRASONIC CLEANING OF MILITARY PWAs

by

Bill Vuono and Tim Crawford
Electronics Manufacturing Productivity Facility
Indianapolis, IN

ABSTRACT

Ultrasonic cleaning is a successful method for cleaning printed wiring assemblies (PWAs) to a level required by both industry and military standards. Unfortunately, it is also a controversial technique due to possible component damage. Studies performed in the 1950s determined that ultrasonic energy can damage fragile wire interconnects between the die and the terminal of microelectronic devices. Based on these studies, the Department of Defense (DOD) has not allowed ultrasonics to be used when cleaning military PWAs. However, recent technological changes in both component manufacturing and board assembly have caused the military to reevaluate this position.

The Electronics Manufacturing Productivity Facility (EMPF), in cooperation with industry, has taken the initiative to conduct a comprehensive study to determine the effects of ultrasonic cleaning on PWAs. Metal-cored boards affixed with leadless chip carriers (LCCs) and compliant pin surface mount devices were subjected to ultrasonic energy during cleaning. The assemblies were then subjected to various environmental tests to observe detrimental effects that ultrasonic energy may have on sensitive components. These findings and the potential application for ultrasonic cleaning on military hardware are presented in this paper.

INTRODUCTION

The increasing trend toward surface mount technology has added new challenges in the area of cleaning electronics. Dense packaging and smaller component standoff heights have created areas that are large enough to entrap corrosive flux, but too small to clean using conventional solvents and equipment. Surface tensions prevent most solvents from penetrating small areas to dissolve and remove contamination. Capillary action can sometimes aid in drawing the solvent to the contamination, but then the softened residue is too viscous to be removed by simple draining. Additional force is needed to

get solvent both into and back out of tight spacing in order to achieve a satisfactory level of cleanliness. Ultrasonics may be that force.

In addition to surface mount technology creating spaces too tight to clean, fine pitch technology has created a need to remove even the smallest amounts of contamination. Ultrasonics has long been recognized as an efficient method for removing even minute particles of surface contamination.

Though an effective cleaning technique, ultrasonics has been prohibited for use on military PWAs for nearly forty years. Earlier studies showed that ultrasonic frequencies were causing wire bonds to vibrate enough to fatigue and eventually break. In addition, PWA technology at that time was less dense and had higher component standoffs; therefore, special cleaning techniques were not needed to attain an acceptable level of cleanliness. Since the need could not be justified and component damage was evident, ultrasonic cleaning was banned from military use.

At present, wire bonding techniques and ultrasonic equipment have improved since the 1950s, as has our understanding of ultrasonic energy. We know that using ultrasonics at the proper frequencies and times will yield a clean product without putting unneeded stress on fragile wire bonds. This knowledge, combined with increasingly difficult to clean technologies, prompted the EMPF to begin a three year study to determine the effects of ultrasonic cleaning on PWAs.

BACKGROUND

A component analysis was performed in Phase I to find the extreme component wire bond dimensions. The wire lengths were calculated based on measurements made of loop height, separation between the bonds, and the difference in height of bonds (see figure 1). Finite element modeling of the interconnect structure was then performed to predict resonant frequencies for the first four modes of vibration based on user choices of loop height, diameter, type of wire and package configuration.[1] If the calculated resonant frequency of a component fell in the operating range of the cleaners, this component was "theoretically susceptible" to ultrasonic damage. All components selected for the functional test have 0.001" aluminum interconnect wires with calculated resonant frequencies that range from 37.7 to 41 KHz.

These components were then designed into a functional board in Phase II. A 10" X 10" copper / molybdenum / copper cored board was used to minimize the coefficient of thermal expansion (CTE) during thermal shock testing. Edge connectors on all four sides of the test board enabled each wire interconnect of each component to be monitored individually.

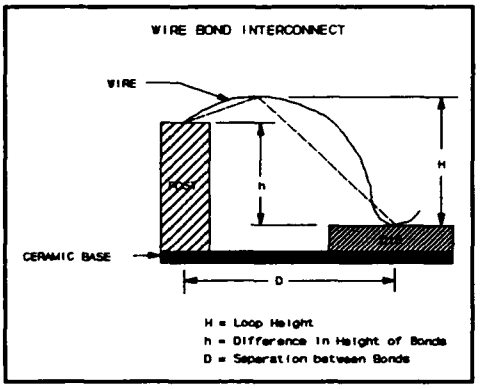

Figure 1
Wire Bond Configuration

In addition, Phase II also used common, commercially available ultrasonic cleaning equipment to document cleaning times, efficiency and process control. The first two phases were completed and published (EMPF TB0008) in August of 1989.

The third and final phase determined if ultrasonics degraded component wire bonds to the point that reliability is questioned. Laboratory testing is complete and a report should be available in the Spring of 1991.

CLEANING

Phase II measured the effectiveness of ultrasonics in removing contamination from under brass plates machined to yield different standoff heights. Plates were used in place of components to allow a known amount of contamination to be easily covered and uncovered for testing. Still, there was a need to establish the effectiveness of ultrasonic cleaning on this board design in Phase III. The first series of tests measured how much contamination was being applied to the test board. A rosin activated (RA) paste was used in this test to give a worst case cleaning situation.

Three polyimide test boards were cleaned and tested to a zero contamination level. In order to prevent contamination from being trapped and therefore not measured, no components were used on these test boards. Solder paste was stenciled onto the boards and then reflowed one at a time using infrared (IR) heat. Following a 15 minute cool, each board was placed into an ionic contamination tester to measure the amount of residue. Results showed an average of 8.2 micrograms per square inch of sodium chloride equivalent present on the PWAs.

The next step measured how well ultrasonics would clean under the components selected for this phase. The components and three more polyimide test boards were cleaned and checked to a zero contamination level. After paste was applied, the components were placed using a robot pick-and-place system. Each assembly was then reflowed and allowed to cool for 15 minutes. The assemblies were individually cleaned in a batch solvent machine using 1,1,1-trichloroethane for one minute at the mildest setting (11 watts/liter). Each component was then carefully removed from its test board using a hot air rework station. The test board and the components were inspected for visible residues then tested for ionic contamination. The average result was 2.23 micrograms per square inch of sodium chloride equivalent present on the board and components.

Even at the mildest setting, one minute of ultrasonics proved sufficient time to achieve satisfactory results on this particular board design. It is important tc realize however, that different board geometries may require longer cleaning times.

COMPONENT DEGRADATION

Three ultrasonic cleaning machines were retained from Phase II for further testing. Two batch aqueous units, one operating at 66 KHz and the other in the 39-41 KHz range, were tested using water with 5% saponifier at 60° C. The third machine, a batch solvent unit operating at 43.75 KHz, used 1,1,1-trichloroethane just below the boiling point at 70° C.

When all of the components were procured and received at the EMPF, they were inspected and solderability tested. A control sample of each component type was delidded and pull tested to provide baseline wire interconnect strengths prior to testing. Table 1 shows the average initial bond pull strength of each component selected.

Tight process controls were used to assemble the test boards and every precaution was taken to prevent component damage due to electrostatic discharge (ESD). In order to maintain consistency throughout the study, the same RA paste used earlier for the cleaning study was also used during this test. Fresh paste was stenciled onto metal cored boards and components were placed using a pick-and-place robot. Reflow was accomplished using an in-line IR system.

Table 1			
Component Catalog #	Device	Description	Pull Test Results in Gram Force
30003	54LSO4	Hex Invertor	7.3
30007	54LS20	Dual 4-Input AND Gate	6.8
30102	54LS74A	Dual D Flip-Flop	7.2
30107	54LS175	Quad D Flip-Flop	7.0
30501	54LS32	Quad 2-Input OR Gate	6.5
30502	54LS86	Quad Exclusive OR Gate	6.3
30702	54LS139	Dual 1-of-4 Decoder/Mux	7.5
30908	54LS253	Dual 4-Input Mux	4.5
31001	54LS11	Triple 3-Input AND Gate	6.8
31004	54LSO8	Quad 2-Input AND Gate	6.7
31504	54LS161A	4-Bit Binary Counter	7.4

Once assembled, each test assembly was electrically tested to assure all bonds were functional. If all checked well, the assemblies were placed in storage until they were ready to be cleaned. (Note: It is not common to assemble, then store prior to cleaning. Since damage was being measured and not cleaning efficiency, it was more important to stabilize the cleaning machines and have the assemblies available when the machines were ready.)

Since the purpose of this phase was to determine if ultrasonic energy damages wire bonds, the cleaning equipment was set to the harshest settings based on Phase II testing. The two aqueous units were set at 33 and 42 watts/liter and the solvent unit was set at 16 watts per liter. Though one minute proved to be sufficient to clean our test board, it would not be uncommon for a manufacturer to use three minutes as a "typical" cleaning time. A worst case manufacturing condition was established at five cleaning cycles, for a total cleaning time of 15 minutes. Additional test times were set at 60 minutes and 180 minutes. The 180 minute time gave a safety margin of 60 times that of a "typical" cleaning cycle.

A full factorial experiment was designed using the following variables:

- Machines (One, Two, Three)
- Time (15, 60, 180 minutes)

A total of 480 wire interconnects were tested at each setting. In addition, a control group was exposed to boiling 1,1,1 trichloroethane for three hours, with no ultrasonics. Pull test results for the control sample are listed in Table 2.

After being exposed to ultrasonics, and prior to delidding, the assemblies were again functionally tested to assure all bonds were intact. This information, combined with data gathered after delidding, would identify whether the bond was broken during cleaning or during the delidding process. Each bond of each component was individually pull tested and the results were documented. The data listed in Tables 2, 3 and 4 show the **average** pull test result of each component type cleaned in each machine. Also listed in the tables are the pull test results performed on new components as received.

Table 2

Machine One Test Results (Solvent, 43.75 KHz)

Component Type	Ultrasonic Exposure Time in Minutes				
	New	Control	15	60	180
30003	7.3	7.1	7.1	7.2	6.3
30007	6.8	6.9	7.0	7.3	6.9
30102	7.2	7.3	7.2	7.2	7.3
30107	7.1	6.4	6.9	7.2	6.9
30501	6.5	6.5	6.7	6.3	6.2
30502	6.3	N/A	6.2	5.6	6.2
30702	7.5	7.3	7.2	6.8	7.1
30908	4.5	4.5	4.0	4.3	4.4
31001	6.8	7.0	6.6	6.6	6.6
31004	6.7	6.7	6.4	6.6	6.8
31504	7.4	8.5	7.8	6.6	8.0

Values represent **average** pull test in gram force

Table 3

Machine Two Test Results (Aqueous, 66 KHz)

Component Type	Exposure Time in Minutes			
	New	15	60	180
30003	7.3	6.7	7.1	6.3
30007	6.8	6.9	6.7	6.9
30102	7.2	7.3	6.8	7.2
30107	7.1	6.9	7.0	6.9
30501	6.5	6.7	6.8	6.8
30502	6.3	6.7	5.8	6.2
30702	7.5	6.6	7.6	6.9
30908	4.5	4.9	3.8	4.7
31001	6.8	6.4	6.4	6.7
31004	6.7	6.4	6.5	6.9
31504	7.4	6.8	6.8	8.2

Values represent **average** pull test in gram force

Table 4

Machine Three Test Results (Aqueous, 39-41 KHz)

Component Type	Exposure Time in Minutes			
	New	15	60	180
30003	7.3	6.6	7.1	5.8
30007	6.8	6.7	6.9	7.1
30102	7.2	7.2	7.2	7.9
30107	7.1	7.6	6.8	6.8
30501	6.5	6.8	6.6	6.5
30502	6.3	6.2	6.2	6.6
30702	7.5	6.5	7.1	7.2
30908	4.5	5.5	4.4	4.8
31001	6.8	6.8	6.7	6.5
31004	6.7	7.0	6.3	6.9
31504	7.4	7.5	7.3	8.2

Values represent **average** pull test in gram force

Pull test results show that little or no difference exists between wire bonds exposed to ultrasonics and those that were not. It can also be noted that the 30908 component had lower pull test measurements than the other components. This was consistent on all bonds of all 30908 components regardless of ultrasonic exposure time, frequency, solvent or temperature. For this reason, the low readings are attributed to component manufacturing.

The results show that wire interconnects are just as strong after ultrasonics as they were before. All of the interconnects tested exceed the minimum military requirement of a 1.5 gram force units.

In addition to measuring the force required to break each bond, test results noted and documented the location of each break (see figure 2). Tables 5, 6 and 7 describe how time affects break location when components were cleaned in each of the three machines. Also noted in these tables are bonds that were broken after ultrasonic exposure and prior to delidding.

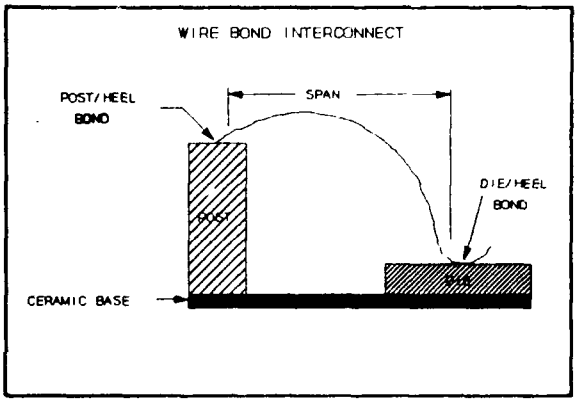

Figure 2
Wire Bond Configuration

Table 5				
Machine One Test Results (Solvent, 43.75 KHz)				
Component Type	Exposure Time in Minutes			
	New	15	60	180
Die/Heel	15%	19%	15.7%	17.3%
Post/Heel	8%	12%	18.3%	8.6%
Span	76%	69%	66.0%	74.1%
*Broken	0%	0%	0.0%	0.0%

* broken after being exposed to ultrasonic energy and prior to delidding.

Table 6 Machine Two Test Results (Aqueous, 66 KHz)				
Component Type	Exposure Time in Minutes			
	New	15	60	180
Die/Heel	15%	10.6%	15.6%	11.9%
Post/Heel	8%	11.9%	8.1%	5.8%
Span	76%	77.5%	76.3%	82.0%
*Broken	0%	0%	0.0%	0.3%

* broken after being exposed to ultrasonic energy and prior to delidding.

Table 7 Machine Three Test Results (Aqueous, 39-41 KHz)				
Component Type	Exposure Time in Minutes			
	New	15	60	180
Die/Heel	15%	19.6%	16.5%	13.6%
Post/Heel	8%	13.3%	15.4%	6.4%
Span	76%	67.0%	67.9%	79.7%
*Broken	0%	0.0%	0.2%	0.3%

* broken after being exposed to ultrasonic energy and prior to delidding.

As expected, most of the breaks were found at the span of the wire, while the rest were split between the die/heel bond and the post/heel bond. This same trend was noted on components that were exposed to ultrasonic energy as well as those that were not.

This observation shows that the bonds at both ends of the span are just as strong after ultrasonics as they were before. In most cases, wire interconnects did not appear measurably fatigued even after resonating for three hours under severe conditions. Four minor failures did occur, however, at high power densities (33 and 42 watts/liter). This observation correlates with a study performed at GEC Hirst in England.[2]

RELIABILITY

Testing thus far has shown no immediate effect of ultrasonics on the wire interconnect of components used in this study. Additional testing was then done to assess the components reliability.

Another group of test assemblies was prepared using the same procedure performed earlier. All three machines were set at their harshest settings and the assemblies were exposed for three hours. All assemblies were functionally tested prior to cleaning, after cleaning, and after each stress test.

The test assemblies were divided into four groups. Group 1 was subjected to humidity testing for 48 hours at 40° C and 95% relative humidity. Group 2 was thermal shocked from -65° to +125° C for ten cycles, ten minute dwell times, eight second transfer time. Group 3 was subjected to random vibration of 20-2000 Hz for two hours at room temperature. The final group was subjected to all three environmental stress tests.

The original test plan required all test assemblies to be powered up and monitored during stress testing to document when a component failed. However, time restrictions required multiple assemblies to be stress tested at the same time. All assemblies being humidity tested were done at one time. Thermal shock was performed five at a time and vibration was done two at a time. Though not all of the test assemblies were individually monitored, one representative assembly was powered and monitored during each test.

Each assembly was functionally tested for continuity after stress testing. The components were then delidded and each wire bond pull tested. Table 8 represents data from boards cleaned in machine one only. Data from machines two and three are not available at this time.

Table 8

Machine One Test Results (Solvent, 43.75 KHz)

Comp. Type	New Comps	Cleaned Only	Humidity Only	Shock Only	Vib. Only	All Tests
30003	7.3	6.9	7.3	7.4	6.7	6.3
30007	6.8	7.4	7.1	7.1	7.3	6.9
30102	7.2	7.4	7.4	7.6	7.0	7.3
30107	7.0	7.0	7.1	7.0	7.2	6.9
30501	6.5	7.2	7.0	6.7	6.6	6.2
30502	6.3	6.2	6.2	6.3	6.4	6.2
30702	7.5	7.3	7.1	7.7	7.0	7.1
30908	4.5	5.0	4.6	4.7	4.7	4.4
31001	6.8	6.5	7.1	7.0	7.0	6.6
31004	6.7	N/A	6.8	6.8	6.9	6.8
31504	7.4	7.2	8.6	8.8	7.8	8.0

Values represent **average** pull testing in gram force.

CONCLUSIONS

Until recently, using chlorofluorocarbon (CFC) based solvents in an in-line or batch vapor degreasing system was the most common technique for cleaning military PWAs. Due to environmental concerns, the Montreal Protocol has established goals for a worldwide phaseout of all CFC production by the year 2000. Saponified water, with the aid of ultrasonic energy, could fill the void created by the ban on CFCs. Ultrasonic energy allows water and other solvents to penetrate tight spaces to dissolve and remove even minute particles of surface contamination.

One minute proved to be sufficient time to remove most solder paste contamination from our test board design. By cleaning, an average of 8.2 micrograms of sodium chloride equivalent per square inch was reduced to a level of 2.23 micrograms of sodium chloride equivalent per square inch. No visible residue was noted under the components.

Components that were "theoretically susceptible" to ultrasonics were subjected to ultrasonic energy for as much as three hours at 16, 33 and 42 watts/liter. The three hour time frame represents a safety margin of 60X over

"typical" exposure times necessary for ultrasonic cleaning. After cleaning, the wire interconnects were pulled until broken and the force necessary to break each interconnect was recorded. No components failed the military minimum pull test requirement of 1.5 gram force. The location of the wire interconnect breaks was generally at the span rather than at the bond. The percentage of breaks at the span versus either weld was nearly identical to that percentage in non-exposed (new) components. No significant wire bond damage or trends were noted at any of the three frequency ranges tested.

Humidity, thermal shock, and vibration did not appear to have an obvious weakening effect on wire bond strengths. No electrical failures were detected on assemblies that were powered and monitored during thermal shock or humidity testing.

During vibration testing, 8 of the 7,840 wire interconnects that were powered and monitored exhibited continuity failures. Pull test results showed no weaknesses in four of these bonds, so they were attributed to defective solder joints. The other four continuity failures noted during vibration were actual breaks. It is interesting to note when these failures were observed. No failures occurred at the weakest power density (16 watts/liter), one failure occurred after three hours at 33 watts/liter, and three failures (one at one hour and two at three hours) occurred at the harshest power density (42 watts/liter). Therefore, caution should be used at power densities greater than 30 watts/liter.

In addition to the four continuity failures that were attributed to solder joints, two unmonitored chips were lost during vibration testing. A possibility exists that ultrasonics may have contributed to the weakening of some solder joints, but since no inspection was performed after reflow, these defects could also have been caused by insufficient solder or poor wetting.

The 30908 chip consistently had a lower pull force during testing. Since these low readings were consistent even on new components, they appear to be related to manufacturing.

RECOMMENDATIONS

This study has shown that ultrasonics is an effective cleaning technique and, when used correctly, will not damage component wire bonds. Though no significant damage was measured on the component wire bonds used in this study, it is important to note that not every type of component was tested (e.g. pin grid arrays, hybrid circuits, crystal oscillators, etc.). As the military allows the use of ultrasonic cleaning PWAs, each user will have to perform preliminary testing to prove ultrasonics is not damaging his products. In addition, cleaning times will have to be established based on the complexity of each board design.

The EMPF will send a copy of the final report to the Navy Solder Working Group along with the following recommendation:

> *A recent study performed by the EMPF proves that ultrasonic energy does prove to be a better cleaning medium than conventional techniques. No significant damage or trends were detected; however, ultrasonics should not be blanketly approved. Though components thought to be "susceptible to ultrasonics" were used to obtain a worst case situation, there are some components that were not tested such as pin grid arrays, crystal oscillators and hybrid circuits.*
>
> *We recommend that ultrasonic cleaning be allowed on military hardware provided the user conducts his own internal testing and has documentation available showing that ultrasonic energy does not damage his product. Also, internal process controls need to be established for their product lines. This would be similar to the allowance for alternative cleaning solvents.*

REFERENCES

1. Electronics Manufacturing Productivity Facility. "Ultrasonic Cleaning For Military PWAs," Ref. EMPF TB 0008, August 1989.

2. Richards, Burton and Footner, "The Effects of Ultrasonic Cleaning on Device Degradation," GEC Hirst Research Centre, Wembley, Middlesex, England.

Bill Vuono is no stranger to this area or to these Seminars. He was with the Electronics Manufacturing Productivity Facility locally and moved with them to the Naval Avionics Center where he heads the Materials and Process Research Branch.

Bill holds a BS degree in Chemistry and an MS degree in Materials Science, and has 10 years' experience in soldering technology.

Address: Electronics Manufacturing
Productivity Facility
Naval Avionics Center (D/460)
6000 E. 21st St.
Indianapolis, IN 46219-2189

CONTINUOUS PROCESS IMPROVEMENT AND TEAMWORK REPLACE EXPERIMENTATION FOR LOW VOLUME, HIGH MIX SOLDERING PROCESS

by

Howard S. Feldmesser
Robert S. Strider
Engineers
The Johns Hopkins University
Applied Physics Laboratory
Laurel, Maryland

INTRODUCTION:

The use of the wave soldering process at APL is relatively new. Although the machine is about five years old, it has had what is, for us, extensive use only in the last twelve to eighteen months. During 1989 we have produced approximately 300 printed wiring assemblies consisting of over 663,000 solder joints. Although this seems like an extraordinarily large number of solder joints in our terms, the rest of the electronics fabrication industry would consider the quantity small. Therefore, the tools used by them to develop their processes and ensure minimum rework are not practical for us.

Typically, a process development engineer designing the process for wave soldering would have tens of assemblies to use to fine tune the process before placing the deliverable hardware on the machine (Reference 1). Initially, the machine would be adjusted to have the operating parameters set as dictated by experience and the first trial boards would be run. Each one would be painstakingly examined for defects. The defect type and quantity would give the technician clues to what adjustments, if any, were appropriate. After adjustments, the next trial boards would be soldered and examined. Further process adjustments would then be made. When the defect rate on the trial boards was within the shop standards, the deliverable assemblies would finally be soldered.

When hundreds or thousands of like assemblies are run as a group, this practice is practical and warranted. In our environment, however, we normally assemble only ten or fewer boards. There are rarely test boards available on which to try the process and make the adjustments. We must have the adjustments optimized before soldering any assemblies since they are all deliverable. We had concluded that there was no way for our small but talented

our low volume and sporadic use of the wave solder machine.

We saw a description of the process of continual improvement (Reference 2) using statistical process control (SPC) which would allow us to refer to previous runs of printed wiring assemblies and learn from the performance of the process during those runs. This learning would be applied to future runs if good data is kept on all phases of the operation. Our implementation of this method involves keeping a log of the process parameters set into the machine when a run is made and then recording the quantity of the most common defects while these defects are corrected by a manual operation.

It must be noted here that the quality of our wave soldering process was not in question. Our average defect rate measured before beginning our SPC program was approximately 1%. The process is considered to result in reliable solder joints if the rework rate is less than 6% (Reference 3). Our desire was to improve the productivity of the operation and achieve a comfortable feeling that we were truly doing the best that could be done in our environment. We knew that it was very unlikely that we would achieve defect rates as low as those in the mass production industries, but we felt the need to use <u>every</u> tool at our disposal to reduce the rate.

Further, we strongly felt a mandate provided by several customer surveys taken within the Laboratory community on behalf of our Branch (Reference 4) and our Group. In each survey, our customers reported that their primary concern was quality. Even though they were generally satisfied with the quality of the product they received, we felt that it was of the utmost importance to maintain or improve on the quality of our hardware because of the customer's priorities.

By performing this exercise, we hoped to uncover the effects caused by fabrication processing, the machine settings, and the input from the engineering and design functions. Specifically, we wanted to know - quantitatively - the effect of preprocessing the printed wiring board, preprocessing the components before soldering them, and certain designed-in characteristics. Each of these effects could be easily fed back to the people who controlled the causes for inclusion in the design/fabrication scheme of operation. This feed forward type of operation was as close to concurrent engineering as we felt a small volume, large diversity operation such as ours could come. Although we would never be able to cure all the ills before they struck in fabrication (a very worthwhile ideal), we would systematically discover any causes for less than 100% yield, plant them in the corporate memory as either process specifications or design rules, and eliminate them from future fabrication efforts. Such a process had been described (Reference 5) but, to our knowledge, not yet used in an environment like ours.

HISTORY:

There were several attempts to train the staff and begin using statistical process control on parts of the Electronic Fabrication Group's operations previous to beginning the wave solder program. Staff resistance, poorly documented process specifications, infrequent use of the process, etc. all prevented the acceptance and use of the new tool. Undaunted, work with the consultants continued in order to find a process which appeared to be able to benefit from SPC and had a reasonable chance for staff acceptance. This would serve the Laboratory in all the manners for which SPC is known, such as preventing waste (Reference 6), as well as serving as an object lesson for the staff and management.

The use of the wave soldering machine was just beginning to achieve regularity, people new to this part of the operation were just coming aboard, and these people seemed open and excited to be in the forefront of the use of a new tool. Several "old hands" would be remaining with the operation in order to bring their considerable experience to bear to help reduce the struggle of bringing the process along and to also learn the techniques and values of SPC. There was still some skepticism all around because the feeling that SPC was a tool only for high volume fabrication efforts pervaded the thoughts of the staff.

A task force was established during several sessions held before any hardware was run over the solder wave. The first task was a careful look at the early data which had been used to measure the existing defect rate. The rate was good, but it seemed clear that it could be made better. The task force operated in the Nominal Group Technique (Reference 7) which ensured that all members had ample opportunity to contribute their ideas and equal weight in the proceedings.

Obviously, it was imperative that the defect rate must always be tracked in order to give notice of problems occurring in the process. What was appreciated is that there is considerable additional information that can be garnered from the defect rate if the defects were categorized as they were corrected at the rework stations. A defect scoring chart, Figure 1, whose categories represented the opinions of the team members of the defects most likely to occur was developed. The process log, Figure 2, was maintained as it was with no changes. Even the process was to remain unchanged; the intention was only to look at it differently. In general, the group became convinced that the current process was inherently good; the only desire was to make it better by that last increment while proving to the operators, inspectors, managers, and customers that it was as good as it could be.

Finally, the first run of PWA's was made on the wave solder machine. The run consisted of ten assemblies of one part number with 1,700 solder joints formed in the wave solder process on each board. (Other solder joints would be made by hand later when special parts were assembled onto the boards.) The defects fell

into only three categories: four boards had evidence of skipped joints (no solder at all in the hole); all ten had some number of joints judged to have insufficient solder in them; and seven of the boards had joints with pinholes or voids. The defects were totalled for each board and the results were plotted with the control limits on the Group 1 control chart (Figure 3).

It was quickly noted that one board clearly had a defect rate that lies outside the control limits, indicating that some special cause was in existence. The overall average defect rate for the run was 1.2%, very near the previously accepted norm, but, obviously, something had gone awry somewhere. Also noted was the fact that the defect rate without considering this one board was 0.92%, a pleasing value. What followed was a problem solving session wherein an attempt was made to ascertain the special cause.

The search for the special cause began with the group brainstorming onto a fishbone diagram all of the causes of defects occurring during wave soldering. The concentration was on causes for insufficient solder and pinholes and voids, the defects most prevalent on the board whose defect level lies outside the control limits. That fishbone diagram, Figure 4, provided insight, but did not lead to the actual cause. The search went to the process log to see if any changes in the process parameters were made during the run. The operators noted that they indeed had made some parameter changes after the first board was passed over the wave. This represented a normal mode of operation; using one board to verify and fine tune the process (a variation on the tens of boards used in production level facilities) and did not surface earlier as a potential cause of defects. If the board whose defect rate was outside the control limits was the first board run, the special cause was identified. Unfortunately, there was no way of verifying this possibility beyond all doubt, but all agreed that the scenario fit the results extremely well. The solution was to serialize the boards before soldering them and noting in the log the order in which they were run so that if the position in the run was a significant cause of changing defect rate, it would become known.

Additionally, it was discovered that the original assessment of the kinds of defects expected to be was not entirely correct. Further, some room for those who count and rework the defects to write comments that might aid later problem solving could prove to be a real boon. As a result, the defect chart was reworked. Figure 5 is the newer, and current, chart. Two classes of defects were added: off center pins and floating pins. These additions were to provide a finer detail level for the causes of insufficient solder on the boards that were soldered. It was possible that some of the defects were not related to anything the people or the machine did to or on the PWA's. If this was true, it was necessary to have the capability to locate these causes; if not, the extra space on the form came at no cost.

The next run of PWA's followed a short time later. Fortunately, these boards were the same part number as the earlier run.

There were twelve assemblies to be soldered and the usual routine was going to be followed. Good results were expected. Unfortunately, the high expectations were not borne out. As Figure 6, the Group 2 Control Chart, indicates, the average defect rate was 1.2%, higher than before, and three PWA's had defect rates above the upper control limit. Another problem solving session was necessary to resolve the special cause(s).

The defect chart was examined very closely during the problem solving meeting. Notably, only four defect types - icicles, insufficient solder, pinholes/voids, and off center pins - appeared at all. Of the 251 recorded defects on the 20,400 joints, only a total of 46 were in the last two categories. This low level of occurrence led to the decision that these two defects were "in the noise" and were not of concern. Insufficient solder defects represented a relatively large portion of the total defects and were examined first. Referring back to the original fishbone diagram (Figure 4), it was not exceptionally difficult to prove that the small size of the pads on these boards reduces the boards' solderability and that a high moisture content would exacerbate the problem. Since the pad size did not change from the earlier run to this one, it was not the special cause but the PWB designers would be asked to include a larger pad on future designs. The team's analysis noted that an increase in moisture content was caused by insufficient bake out of the assemblies prior to soldering. Bake out with appropriate parameters would be included in the standard process.

The search for the cause of the icicles was much more problematic since none of the team members had much exposure to them. There was a fear that earlier searches for the causes of errors did not include sufficient inputs to locate the special cause in this run. Another search for error causes was made, concentrating on the causes for icicles. The resultant fishbone diagram is Figure 7. By itself, however, even this fishbone diagram does not provide sufficient information to determine the special cause(s) that occurred during the second run. The collected intelligence of the group, coupled with the notations made in the comments column of the defect chart provided the necessary synergism to elicit the problem causes. The notations showed that there was a relationship between the boards whose defect rates were above the control limit and those that had notably more icicles than the others. Also, according to the observations, the icicles were much more prevalent around several integrated circuit sockets (on all of the boards) than around all of the other sockets. Examination of those sockets showed that they had much longer leads than those which did not collect icicles. Thus, the special cause was identified. Buying sockets with lead lengths properly chosen would prevent the reappearance of this problem. Removing the three assemblies exhibiting the special cause from the control chart yields an average defect rate of 0.90%, better than before and an indication that the application of previously gained knowledge was yielding improvements.

The third group of assemblies contained two different part types. One had only 1,000 joints per board and the other was the same type of board as in the first two runs with 1,700 joints per board. Analysis was a problem because the control charts from which the earlier conclusions were drawn are c-charts, graphing the number of nonconformities on each unit as attribute data (Reference 6). This type of chart would no longer suffice because the important measure is truly the ratio of defects to non-defects which balances the values from one unit to the next. The p-chart is used when examining ratio data when the number of samples is still small (Reference 8). All of our charts were promptly converted to this mode. Now, all process effects could be related without being misled by the number of solder joints produced on any board. When the data from this run was plotted in Figure 8, one of the boards indicated a special cause and no amount of individual or group thinking could identify that cause. In general, the results were pleasing since the average defect rate was below 1% and the process was almost within statistical control.

The fourth run proved enlightening in unexpected ways. The control chart, Figure 9, was, taken by itself, unremarkable. It clearly indicated that the process was in statistical control for the complete run and that there were no special causes to locate and remove. Further perusal of the data indicated that the average defect rate for the run was extremely low, 0.23% instead of the more usual 1%. This is, by definition, a special cause worthy of further research (Reference 8). The team did its research which initially revealed that the person responsible for loading the components onto the board had pre-tinned the component leads prior to insertion, a practice not usually followed unless dictated by specifications external to our operation. It seemed obvious, especially considering the results of many others, that this procedure should be followed on a regular basis. However, what seemed so obvious at the initial stages was found to be erroneous after further analysis. When the data from the third run was separated into two parts, one for the board type with 1,000 joints and one part for the other type, the board with 1,000 joints, which is the same part as the board in the fourth run, has an average defect rate of 0.51%, not very far from the average rate for this run. The team concluded from this data that the actual special cause was the design of the board and the components. This board has normally sized pads, and the components have the proper lead lengths. It is still possible that pre-tinning the component leads has some positive effect, but it will take further experimentation to prove the hypothesis.

When looking at the shape of the control chart for the fifth run, Figure 10, it shows that only one point is indicated as outside the control limits. The remainder of the points are well inside the limits of this run. However, when considering the entirety of all of the assemblies we have produced, the upper control limit is 2.8%; the majority of the points for this run are outside the control limits. Further, the average defect rate of 2.6% is much higher than for earlier runs, (although still well

within the limits set by Mil-HDBK-217). During this run we processed 33 boards of a new design placed on panels of six boards each with 172 solder joints on each board. The rework rate exhibited a significant departure from our accepted norms and considerable thinking to find the cause and solve the problems was required and justified.

Although solder bridges appeared for the first time, their numbers were low enough to be considered in the noise level. However, the quantities of joints with insufficient solder were significant. Since serializing each board was the normal process after the first run was made, any correlation between the position of the boards on the panel and the defect levels could be ascertained. The data from the defect log indicated that the boards that were on the outer edges of the panel had many more defective joints than those that were centrally located. A recreation of the actual process showed that these boards were at the margins of the wave where the solder has a significantly lower level than at the center. The special cause will be eliminated by not allowing panels, or wide single boards, to exceed a determinable width. The original parameters given to the design group (who performed that panelization at that time) for maximum panel width were excessive for this wave solder machine.

CONCLUSIONS:

The process of recording and analyzing defect rate data for our shop has enabled us to feed back valuable information to our own process as well as the engineering and design personnel. We have learned that pads that are too small, component leads that are too long, and joints soldered too close to the margins of the wave all lead to increased rework which adds costs and delays If the rework rate exceeds a limit value, the reliability of all solder joints made becomes questionable.

We have learned that, even if we do not have all the answers, we can get them by meticulously recording our results. This clearly means that we will no longer make the same mistake twice. The methods we followed also prevent us from coming to false conclusions and, perhaps, adding a process step where none is warranted. Although no harm is likely to be done to quality and reliability, such an occurrence will add cost and delay unnecessarily.

It seems unfortunate that the last data gathered shows a higher defect rate than earlier runs. In bygone days, when we simply recorded the defect rate without using the tools of SPC charting, defect logging, and process logging, this occurrence would have been the cause of much teeth gnashing and brow beating. We would not have had a clue to help us find the cause and effect the repair. With the tools that proved to be so instrumental in reducing the defect rate to the levels experienced in the fourth run, we know precisely what caused the increase in defect rate and

will go forward with full confidence that this assignable cause will never rear its ugly head again.

It is clear to us that without this well conceived plan for recording data and analyzing it in an orderly fashion, we would never be able to continue reducing, or even maintaining, the wave solder rework rate. We would have been vulnerable to either reductions in productivity or, quite possibly, increases rework rates to levels that exceed the limit for claiming that our process was reliable. On the contrary, there is now a great deal of confidence in our own facility that our wave soldering operation results in the highest quality and lowest cost possible. In addition, as our knowledge and technology increase, we now have the tools in place to continue to improve in a scientific and orderly fashion. We have proved that the synergy created by combining staff personnel with technical expertise, operators of the machine, and those responsible for on-line inspection and rework and giving them management support, seemingly insurmountable problems can be solved.

1. J.R. Wooldridge. "Wave Solder Parameter Optimization Using a Statistical Experimental Design," in Proceedings of the 13th Annual Electronics Manufacturing Seminar, China Lake, CA: Naval Weapons Center, 1-3 March 1989.

2. General Requirements for Implementation of Statistical Process Control, IPC-PC-90, Proposal dated April 1989.

3. MIL-HDBK-217.

4. K.A. Potocki and D.M. Saunders. "Quality Services Using Customer Research," in Proceedings of the 42nd Annual Quality Congress, Dallas, TX: American Society for Quality Control, May 1988.

5. J.G. Davy. "Closed Loop Soldering,", in Proceedings of the 14th Annual Electronics Manufacturing Seminar, China Lake, CA: Naval Weapons Center, 21-22 February 1990.

6. Continuing Process Control and Process Capability Improvement, Ford Motor Company, Corporate Quality Education and Training Center.

7. A.L. Debecq, A.H. Van de Ven, and D.H. Gustafson, Group Techniques for Problem Planning: A Guide to Nominal Group and Delphi Processes, Glenview, IL: Scott, Foresman & Co., 1975.

8. W.J. Latzko, Quality and Productivity for Bankers and Financial Managers, New York, NY, Marcel Dekker, Inc.

Wave Soldered Joint Defect Chart

Date	Part Number	Serial Number	Number of defects: Icicles	Bridges	Insufficient Solder	Excess Solder	Dewetted Joint	Pinholes/ Voids	Blowhole

FIGURE 1. Defect Log

WAVE SOLDERING MACHINE – DAILY OPERATING LOG

DATE/TIME	PART NUMBER	FLUX DATA	PREHEAT SETTING	SOLDER TEMP	CONVEYER SPEED	MAINTENANCE	OPERATOR

FIGURE 2. Process Log

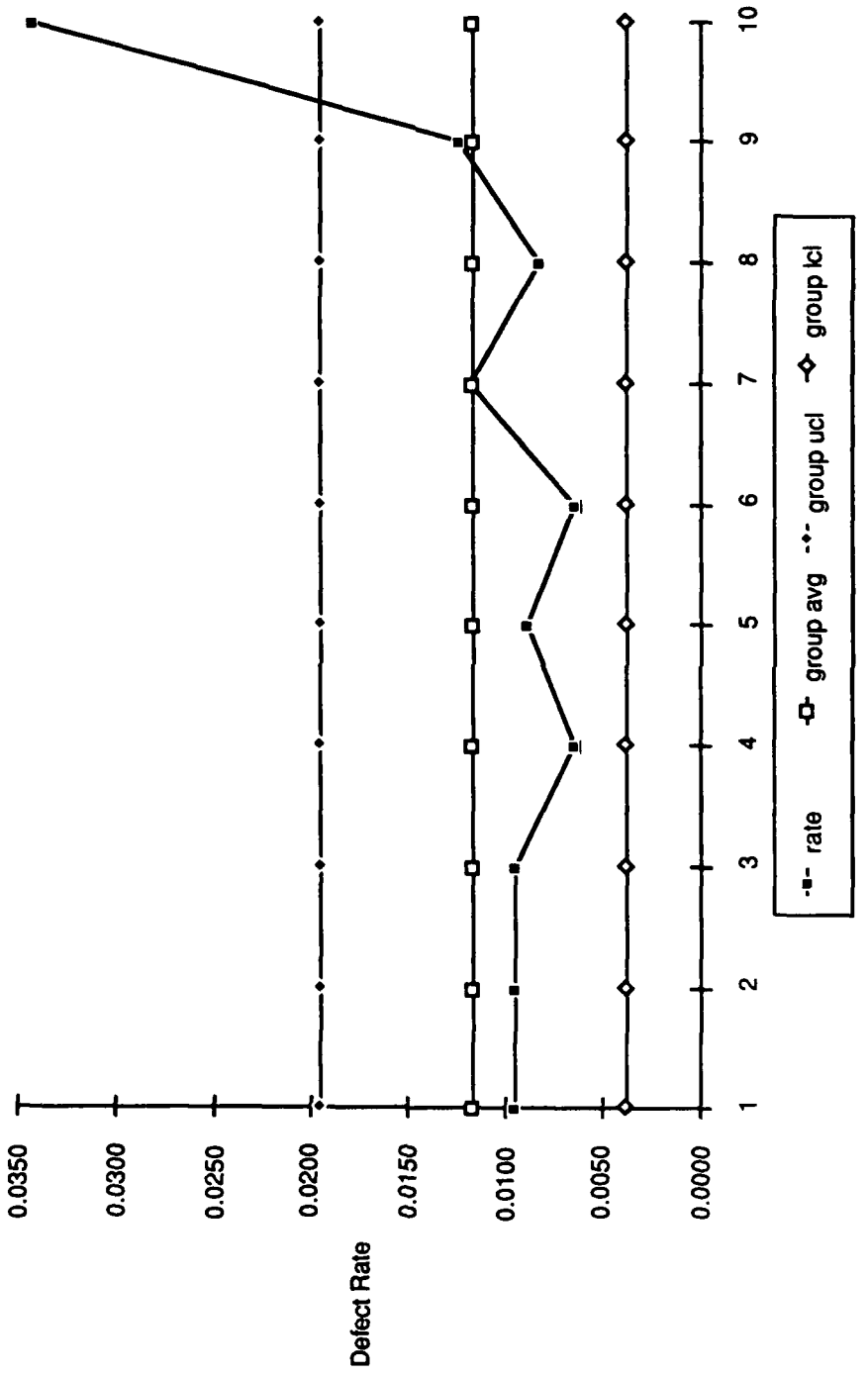

FIGURE 3. Group 1 Control Chart

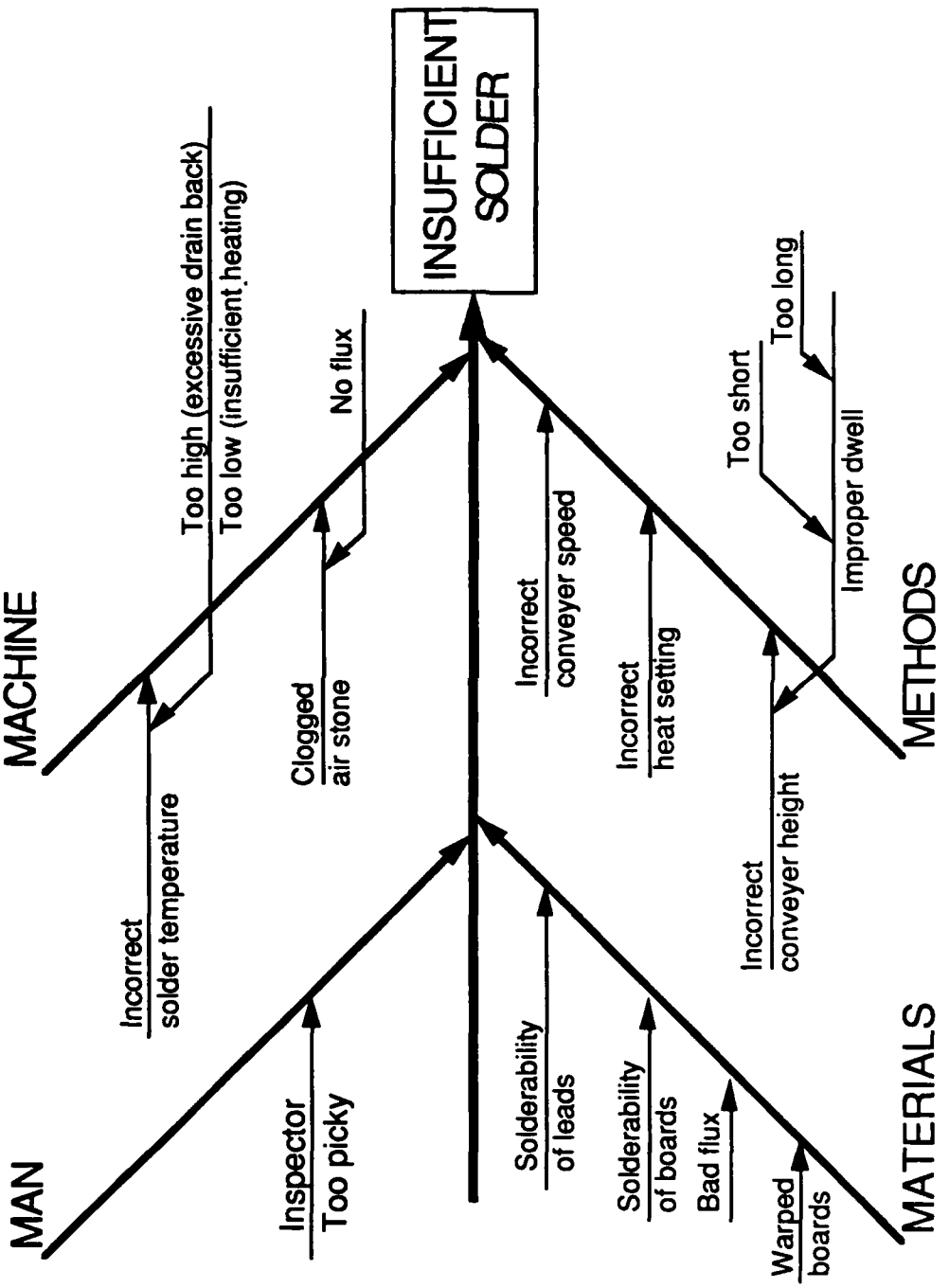

FIGURE 4. Insufficient Solder Fishbone Chart

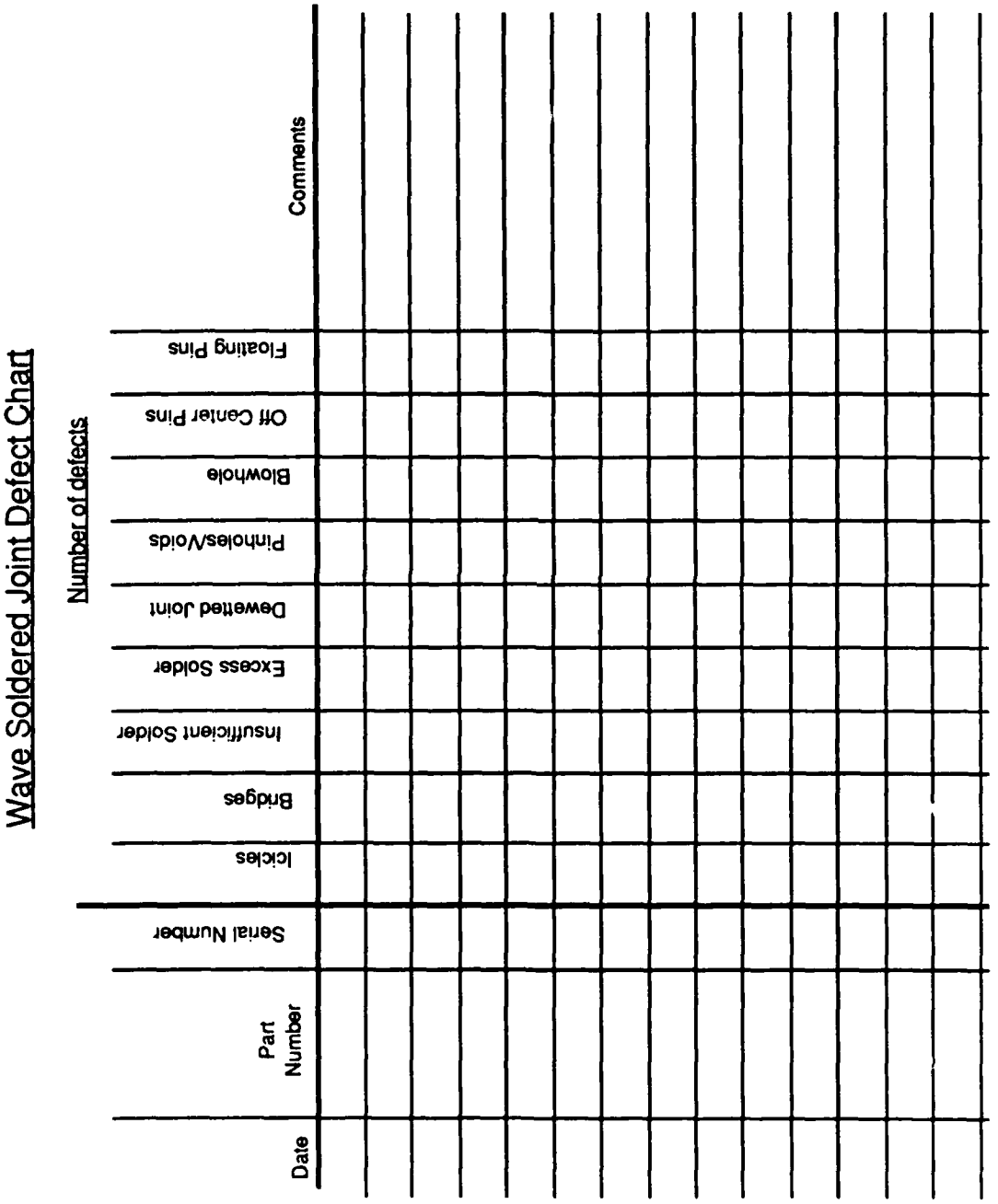

FIGURE 5. Modified Defect Log

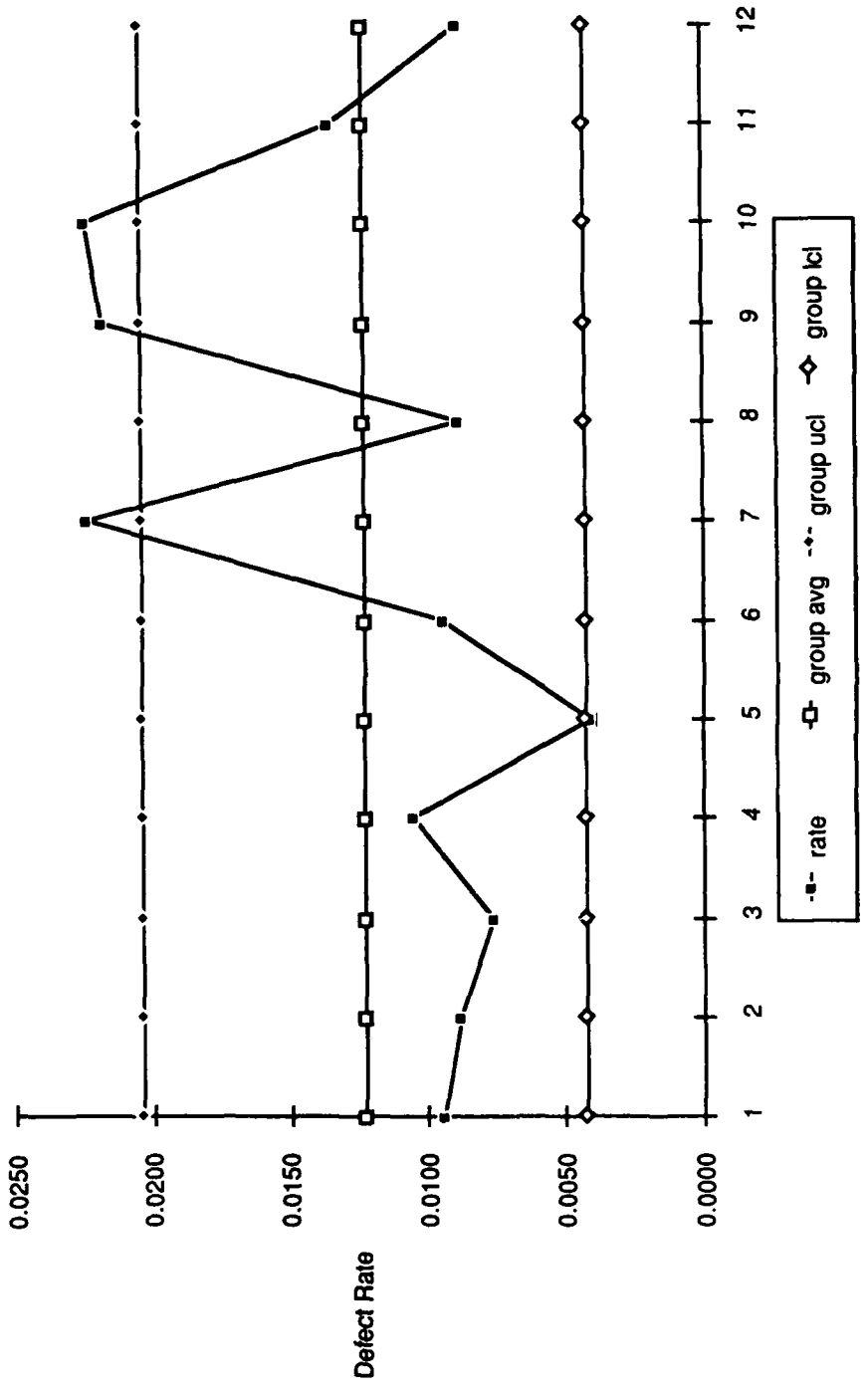

FIGURE 6. Group 2 Control Chart

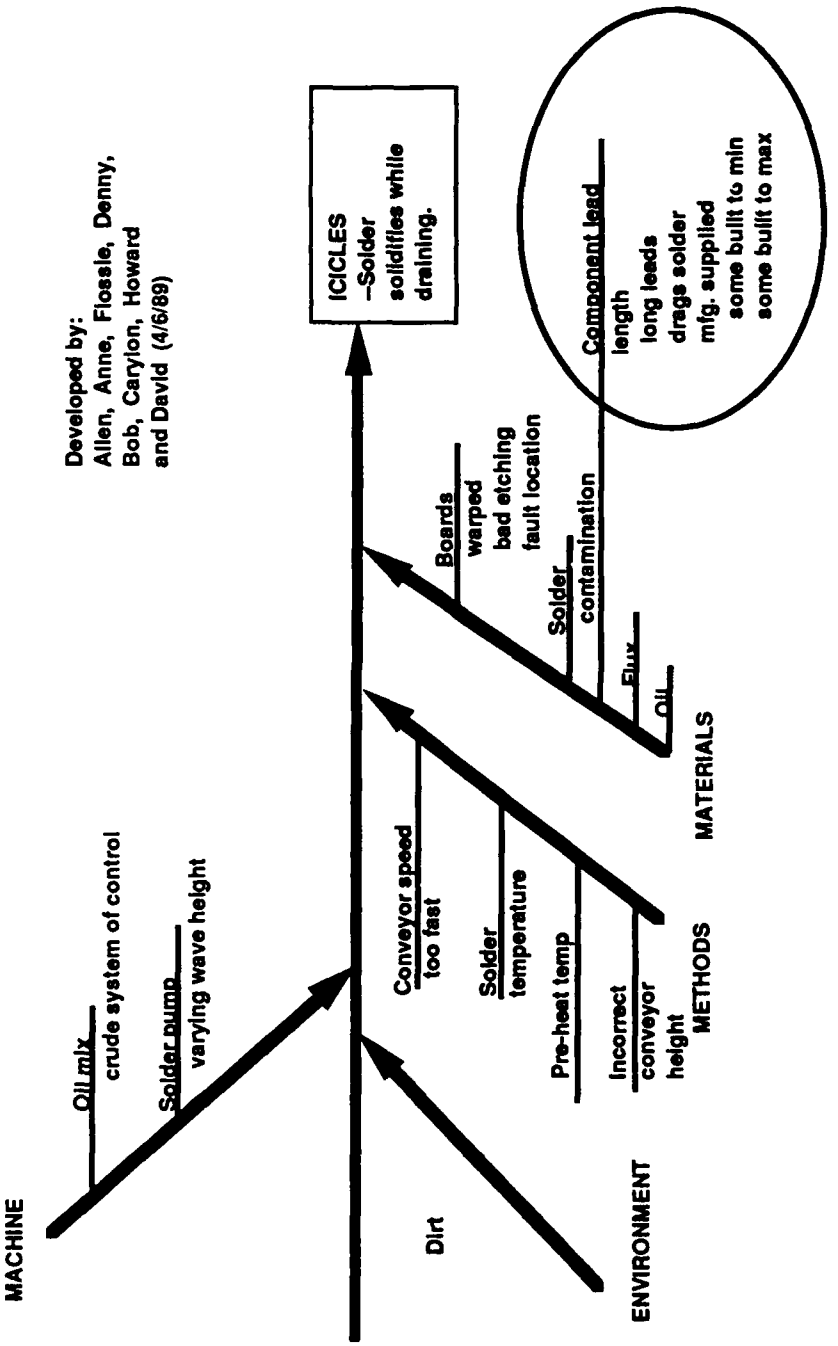

FIGURE 7. Icicles Fishbone Chart

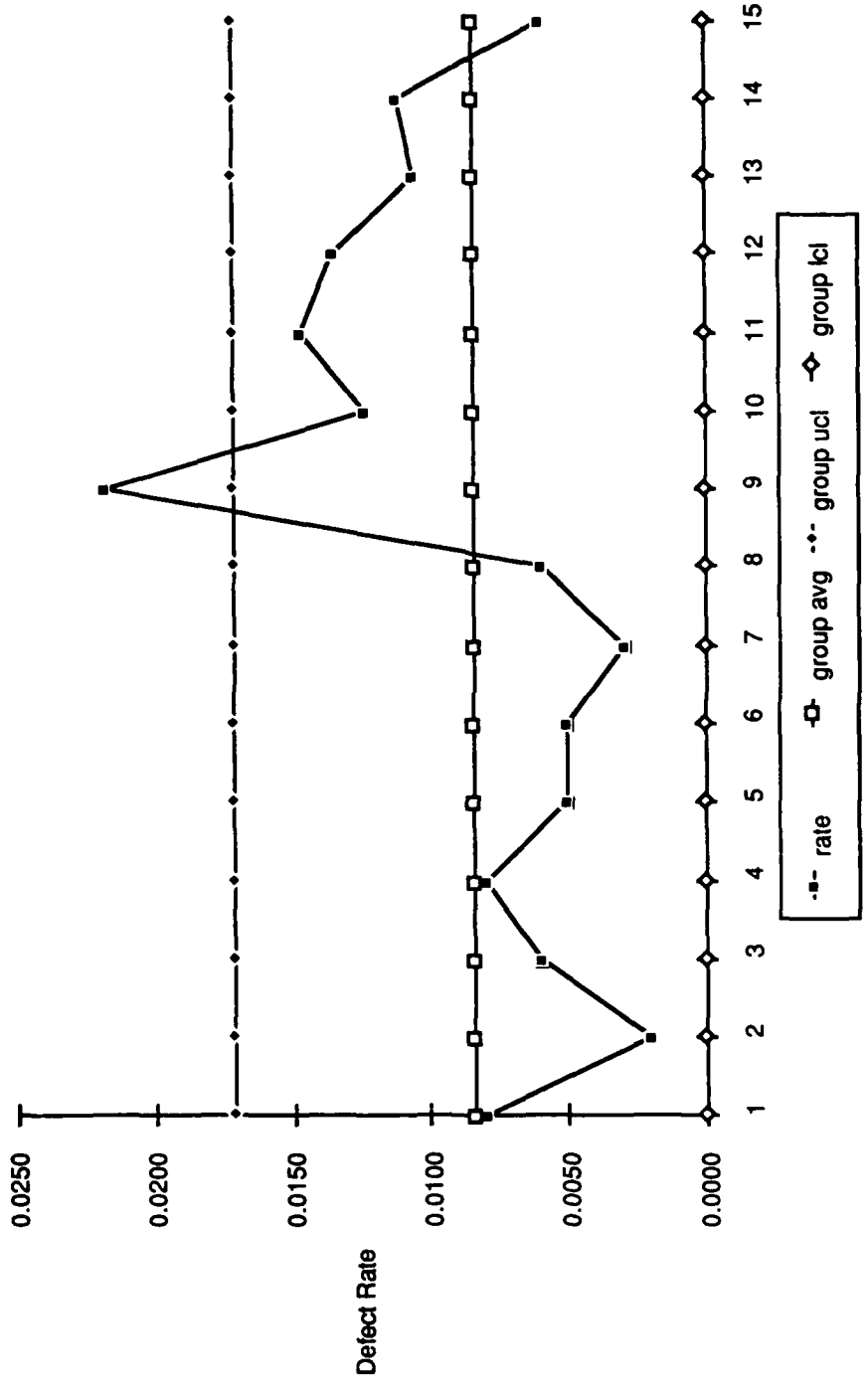

FIGURE 8. Group 3 Control Chart

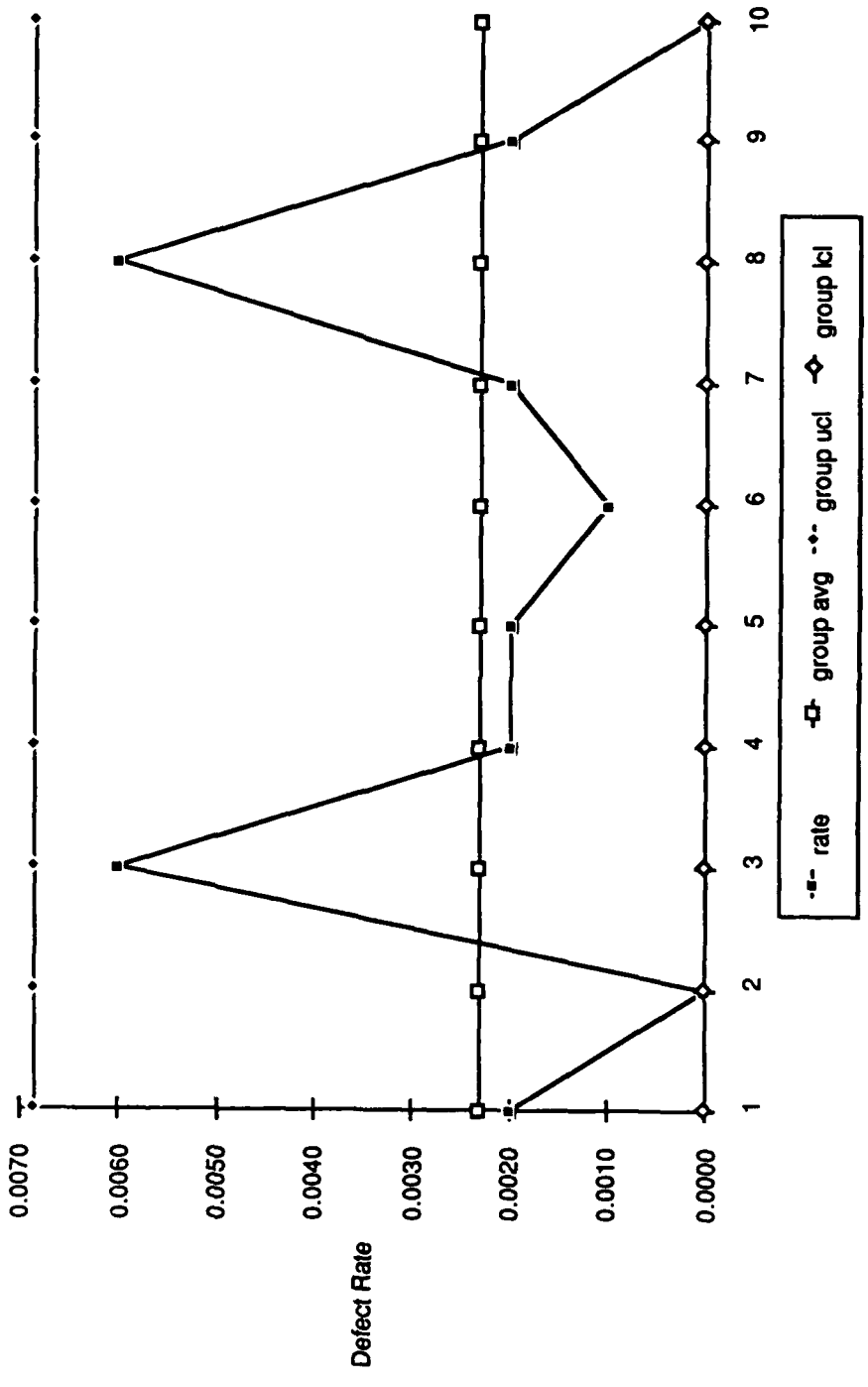

FIGURE 9. Group 4 Control Chart

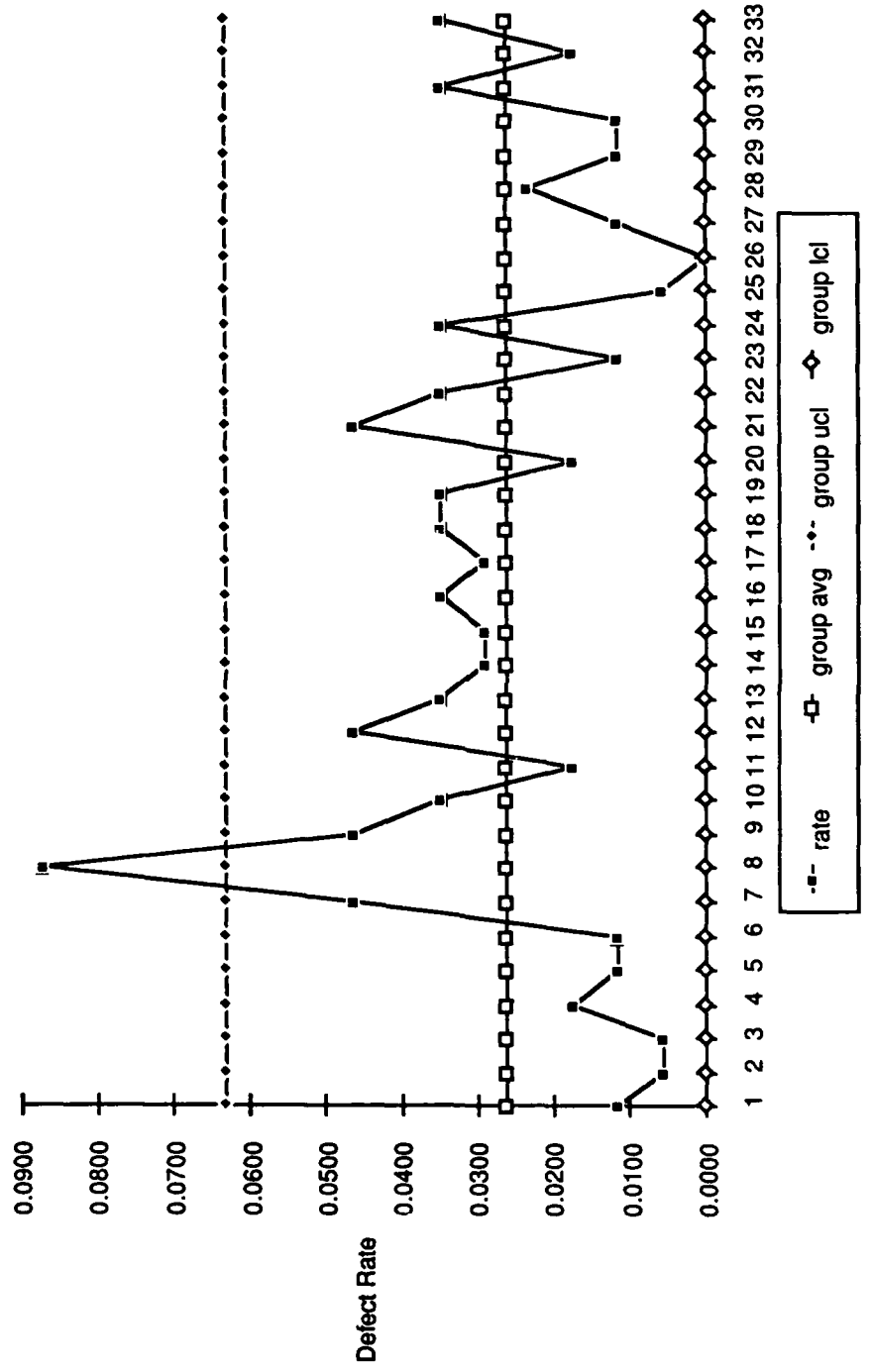

FIGURE 10. Group 5 Control Chart

Howard Feldmesser is a Group Supervisor/Engineer with the Applied Physics Laboratory/The Johns Hopkins University. He has more than 20 years' experience as an electronic design engineer and manager of electronic fabrication operations. His design background includes high-power radar transmitters, television systems, and high-voltage power supplies. He is also experienced in the fabrication of medical imaging systems, as well as military and space electronic hardware fabrication.

Howard received a BSEE degree from Rutgers University and an MSEE degree from The Johns Hopkins University. He is the holder of a U.S. Patent and is a member of the IPC Assembly and Joining Handbook Subcommittee and Heat Sink Attachment Task Group.

Address: Applied Physics Laboratory/
The Johns Hopkins University
Johns Hopkins Road
Laurel, MD 20723-6099

A COMPARISON OF CFCs, HCFCs AND SEMI-AQUEOUS AGENTS FOR CLEANING PRINTED WIRING BOARDS

by
B. Carroll Smiley and T. Randall Fields
E.I. du Pont de Nemours & Co., Inc.
Research Triangle Park, N.C.

ABSTRACT

The planned phase-out of CFCs set forth in the Montreal Protocol has required CFC-113 users to examine alternative technologies for cleaning printed wiring boards (PWBs). HCFC and semi-aqueous cleaning represent two major classes of alternative technologies.

This paper compares the properties and performance of an HCFC blend (consisting of 62.2% HCFC-141b, 35% HCFC-123, 2.5% methanol and 0.3% stabilizer) and a hydrocarbon-based, semi-aqueous agent to those of CFC-113/methanol. Both of these alternatives have exceeded the performance of CFC-113/methanol for removing ionic contamination and residual rosin in EPA Ad Hoc Phase II testing.

This paper also discusses the equipment and process design considerations for these two CFC alternatives. Generally, both alternative technologies require new equipment vs. CFC-113/methanol vapor degreasers/defluxers; some existing equipment can be retrofitted for HCFC use.

And finally, this paper compares the ecology of CFC-113/methanol, the HCFC blend and the hydrocarbon-based agent for semi-aqueous cleaning, presenting the advantages and trade-offs of each.

INTRODUCTION

Over the last 30 years, CFC-113 has gained widespread acceptance for cleaning PWBs due to its numerous desirable characteristics. It is nonflammable, chemically and thermally stable and low in toxicity. In addition, CFC-113 operates at low temperatures, provides selective solvency, is easily recovered and, most importantly, is an extremely effective cleaner. Used in the time-proven vapor degreasing/defluxing process, CFC-113/methanol achieves high levels of cleanliness, removing contaminants from under tightly spaced, surface mount components on PWBs.

However, because of its high ozone depletion potential (ODP) and global warming potential (GWP), CFC-113 is no longer considered an "ideal" cleaning agent. In fact, under the provisions of the Montreal Protocol, CFC-113-based cleaning agents will be phased out by the year 2000. In the interim, supplies will

diminish and costs will increase significantly. Therefore, CFC-113 users are examining more environmentally acceptable alternatives, such as HCFC and semi-aqueous cleaning agents.

This paper compares an HCFC blend for use in a modified vapor degreasing/ defluxing process and a hydrocarbon-based agent for use in the semi-aqueous cleaning process to traditional CFC-113/methanol cleaning.

HCFCs VS. CFCs: A PROPERTY COMPARISON

Comparative Properties

HCFC alternatives can be designed to retain many of the desirable characteristics of CFCs. In 1989, an HCFC blend, consisting of 62.2% HCFC-141b, 35% HCFC-123, 2.5% methanol and 0.3% stabilizer, was introduced by Du Pont for PWB cleaning. The properties of this HCFC azeotrope-like blend compared to those of CFC-113/methanol are shown in Table 1.

This HCFC blend has a lower boiling point, and hence, higher vapor pressure at comparable temperatures than the CFCs it would replace. Thus, it necessitates using new vapor degreasing/defluxing equipment or modifying existing equipment, as discussed in the following section (HCFC Equipment and Process Design Considerations). However, the low surface tension and viscosity of this formulation prove extremely helpful in cleaning PWBs.

Since the HCFC blend is constantly boiling, it exhibits azeotrope-like behavior under the conditions used in a vapor degreaser for cleaning PWBs. In addition to compositional stability, this blend is extremely chemically stable. In reflux corrosion tests, it exhibited excellent chemical stability due to its carefully designed stabilizer package.

Comparative Environmental Impact

From an environmental standpoint, this HCFC blend offers significant advantages over CFCs in both ODP and GWP. The addition of hydrogen atoms to the CFC molecule dramatically reduces the atmospheric life, and hence the ODP of this compound. The atmospheric life of CFC-113 is approximately 90 years, compared to eight years for HCFC-141b and only two years for HCFC-123. The shorter atmospheric life of these compounds translates into an order of magnitude decrease in the ODP of the HCFC blend compared to CFCs.

The HCFC blend also has a significantly lower GWP than CFCs -- 0.08 compared to 1.35. Even though CFCs are responsible for less than 10% of the GWP, substituting shorter life HCFCs for CFCs will reduce the concentration and contribution of these compounds to the earth's warming.

TABLE 1. Comparative Properties of an HCFC Blend[a] and a CFC-113/Methanol Azeotrope.

Property	Units	HCFC Blend[a]	CFC-113/ MeOH
Boiling Point	° F (° C)	86.0 (30.0)	103.5 (39.7)
Vapor Pressure at 77° F (25° C)	psia	12.7	8.3
Liquid Density at 77° F (25° C)	lb/gal g/cc	10.70 1.28	12.33 1.48
Latent Heat of Vaporization at Boiling Point	BTU/lb	92.6	90.7
Surface Tension at 77° F (25° C)	dynes/cm	18.5	17.4
Viscosity at 77° F (25° C)	cp	0.42	0.70
Estimated Ozone Depletion Potential (CFC-11 = 1)	--	0.07	0.75
Global Warming Potential	--	0.08	1.35
Flammability	--	No	No
Estimated Toxicity	ppm by vol	105 (AEL)[b]	475 (AEL)[b]

[a] This HCFC blend consists of 62.2% HCFC-141b, 35% HCFC-123, 2.5% methanol and 0.3% stabilizer.

[b] An Acceptable Exposure Limit (AEL) is the recommended time-weighted average concentration of an airborne chemical to which nearly all workers may be exposed during an 8-hr day, 40-hr week without adverse effect, as determined by the Du Pont Company for compounds that do not have a Threshold Limit Value (TLV®).

HCFC EQUIPMENT AND PROCESS DESIGN CONSIDERATIONS

One trade-off of HCFC-141b/123-based products used in vapor degreasing and defluxing equipment is their relatively low boiling points compared to CFC-113. To minimize solvent losses, new equipment or retrofitted existing equipment needs to incorporate provisions for controlling emissions due to leaks, dragout and diffusion, as discussed below.

Controlling Leaks

To minimize solvent emissions due to leakage, the equipment itself should be fabricated from materials that are chemically compatible with the cleaning agent. Type 304 and Type 316 stainless steel are the preferred materials of construction for equipment. Copper and brass may be acceptable for valves and piping in degreasers, if they are compatible with the soils being removed. They should not be used for process piping in defluxing equipment since the copper may dissolve and contaminate the PWB to be cleaned. Welded or soldered joint piping, with flanged connections for removing accessories, is recommended.

Seals and gaskets should also be chemically compatible with the cleaning agent. (Refer to the HCFC Compatibility with Plastics and Elastomers section.)

Controlling Dragout

Dragout can be minimized by designing methods of handling PWBs that minimize solvent entrapment and maximize solvent drainage during cleaning. In addition, the flow of PWBs through the degreaser/defluxer should be controlled to avoid disturbing the vapor/air interface during PWB insertion and removal. The recommended maximum speed for PWB entry and removal is 10 ft/min.

However, even with these measures, PWBs removed from a degreaser/defluxer contain a thin liquid film that evaporates, resulting in vapor emission. One way to minimize or even eliminate this dragout is to dry the PWB in the freeboard zone, using superheated vapor drying. This technology subjects the PWB to solvent vapor heated above its normal boiling point in the freeboard zone. This superheated vapor evaporates any entrapped solvent and the liquid film, allowing the PWB to emerge dry.

Controlling Diffusion

In a vapor degreaser/defluxer, relatively stagnant gas in the freeboard zone is sandwiched between a layer of 100% solvent vapor (extending from the condenser downward) and a layer of 100% air (extending upward from the top of the machine). This causes diffusion to occur as the solvent vapor migrates from an area of high vapor concentration to an area of low vapor concentration. To minimize the rate of diffusion, deeper freeboards and lower condenser temperatures compared to CFC-113 equipment are needed.

HCFC COMPATIBILITY WITH PLASTICS AND ELASTOMERS

In general, this HCFC blend is more aggressive than CFC-113 and less aggressive than chlorinated solvents, such as 1,1,1-trichloroethane. It is compatible with a wide range of plastics, elastomers and metals. In addition, it is compatible with most cured epoxy and polyimide substrates, as well as with acrylic and epoxy solder masks. Since compatibility is affected by material variations, critical components should be tested under actual conditions before switching to this cleaning agent.

Generally, it is gentle enough for cleaning PWB assemblies having components made of many common plastics. Table 2 shows the compatibility of this HCFC blend with various plastics.

Elastomeric gaskets and seals used in the construction of cleaning equipment are exposed to the cleaning agent for long time periods. Table 3 shows the compatibility of this HCFC blend with various elastomers.

TABLE 2. Plastic Compatibility of an HCFC Blend[a] under Typical Cleaning Conditions.[b]

Plastic	Tradename	HCFC Blend[a]	CFC-113/ MeOH
ABS	Kralastic®	3	0
Acetal	DELRIN®	0	0
Acrylic	LUCITE®	3	0
Cellulosic	Ethocel™	3	3
Epoxy	--	0	0
Fluorocarbon	TEFLON® TFE, FEP, PFA	0	0
Ionomer	SURLYN®	1	1
Nylon	ZYTEL®	0	0
Polycarbonate	Tuffak®	3	0
Polyester	RYNITE®, Valox®	0	0
Polyetherimide	Ultem®	0	0
Polyethylene	ALATHON® HDPE	0	0
Polyphenylene Oxide	Noryl®	2	0
Polyphenylene Sulfide	Ryton®	0	0
Polypropylene	--	0	0
Polystyrene	Styron™	3	2
Polysulfone	--	0	0
Polyvinyl Chloride	--	0	0

[a]This HCFC blend consists of 62.2% HCFC-141b, 35% HCFC-123, 2.5% methanol and 0.3% stabilizer.
[b]Test Conditions: Samples immersed in boiling liquid for 5 min.
Key: 0 = Compatible; 1 = Probably Compatible; 2 = Probably Incompatible; 3 = Incompatible

TABLE 3. Elastomer Compatibility of an HCFC Blend[a] under Typical Cleaning Conditions.[b]

Elastomer	Common/ Tradename	HCFC Blend[a]	Extractables (%) CFC-113/ MeOH
Polyurethane	ADIPRENE®	3	3
Acrylonitrile-butadiene	Buna N	23	11
Styrene-butadiene	Buna S	12	8
Isobutylene-isoprene	Butyl	8	4
Chlorosulfonated Polyethylene	HYPALON®	1	--
Polyester TPE	HYTREL®	2	2
Natural Polyisoprene	Natural	5	4
Polychloroprene	Neoprene	20	8
Ethylene/Propylene Terpolymer	NORDEL®	32	21
Polysiloxane	Silicone	3	2
Polysulfide	Thiokol FA	2	1
	Thiokol ST	2	1
Fluoroelastomer	VITON® A	5	< 4
	VITON® B	0.4	--
Perfluoroelastomer	KALREZ®	0.2	--

[a]This HCFC blend consists of 62.2% HCFC-141b, 35% HCFC-123, 2.5% methanol and 0.3% stabilizer.

[b]Test Conditions: HCFC blend was immersed in boiling liquid for at least 8 hrs. Data for CFC-113/methanol were extrapolated from experience with CFC-113 or from actual use conditions.

SEMI-AQUEOUS VS. CFCs: A PROPERTY COMPARISON

Comparative Properties

A hydrocarbon-based agent for semi-aqueous cleaning of PWBs, commercially available from Du Pont, combines polar and nonpolar components to yield a proper balance of selective solvency, high flash point, low toxicity, maximum biodegradability and other important characteristics. Its hydrocarbon base component is non-aromatic and non-terpene. In addition to low toxicity, high flash point and mild odor, the hydrocarbon base was selected for its ready and abundant availability and for its consistent quality on a large-volume basis and for its quick separation from water.

Hydrocarbon blends used in the semi-aqueous process are compositionally more flexible than CFC-113-based azeotropes. This allows their solvency to be adjusted to match the soils to be removed. Table 4 compares the physical properties of a hydrocarbon-based agent for semi-aqueous cleaning to those of CFC-113/ methanol. In contrast to CFC-113-based cleaners, the hydrocarbon-based, semi-aqueous agent has a very low vapor pressure. It also has slightly higher viscosity and surface tension. These differences are exploited by agitation and heating to ensure good cleaning in tight spacing.

Comparative Environmental Impact

Semi-aqueous cleaning agents have zero ODP and GWP, making them attractive for replacing CFC-113 and other ozone-depleting solvents, such as methylchloroform, which will be phased out by the year 2005.

Additionally, the semi-aqueous process has several advantages over aqueous cleaning. Since the organic soils dissolve in the semi-aqueous agent, they can be separated from the aqueous effluent, minimizing the load on treatment facilities. The hydrocarbon-based cleaning agent and the soils can be incinerated as fuel. And since the hydrocarbon-based, semi-aqueous process operates at a neutral pH, it does not dissolve metals and is considered a non-hazardous waste under RCRA standards.

The aqueous effluent, which contains very low levels of biodegradable components, can be recycled in a closed loop system or sent to the drain in most parts of the world. Furthermore, waste water treatment using existing technologies can reduce organic output by more than 95%.

Rinse water containing the hydrocarbon-based agent is non-toxic and non-inhibitory to bacteria. As with all organic fluids, however, it should not be a major portion of the feed to a biological waste treatment plant.

TABLE 4. Comparative Properties of a Hydrocarbon-Based Agent for Semi-Aqueous Cleaning and a CFC-113/MeOH Azeotrope.

Property	Units	Hydrocarbon-Based Agent for Semi-Aqueous Cleaning	CFC-113/ MeOH
Boiling Point	° F (° C)	N/A	103 (39.7)
Vapor Pressure	mm-Hg	0.2	429
Flash Point (TCC)	° F (° C)	159 (71)	None
Viscosity	cp	1.4	0.70
Surface Tension	dynes/cm	28	17.4
Specific Gravity		0.85	1.48
Estimated Ozone Depletion Potential (CFC-11 = 1)		0	0.75
Global Warming Potential		0	1.35
Estimated Toxicity	ppm by vol	None established	475 (AEL)[b]

N/A = Not Applicable.
[a]Measured at 77° F (25° C).
[b]An Acceptable Exposure Limit (AEL) is the recommended time-weighted average concentration of an airborne chemical to which nearly all workers may be exposed during an 8-hr day, 40-hr week without adverse effect, as determined by the Du Pont Company for compounds that do not have a Threshold Limit Value (TLV®).

SEMI-AQUEOUS EQUIPMENT AND PROCESS DESIGN CONSIDERATIONS

To obtain optimum performance requires equipment designed for semi-aqueous cleaning. Figure 1 shows a schematic of an early semi-aqueous system, which involved dissolving the soil in the solvent; rinsing the solvent/soil mixture from the surface with water; and drying the parts. Generally, an air knife was used after the solvent stage to remove the excess solvent/soil mixture from the parts. This limited the contamination introduced to the rinsing system, and hence, to the aqueous effluent.

Several improvements to this process have adapted semi-aqueous cleaning to the modern industrial environment. The first improvement establishes consistent, stable process control, while the others improve the ecology of the process.

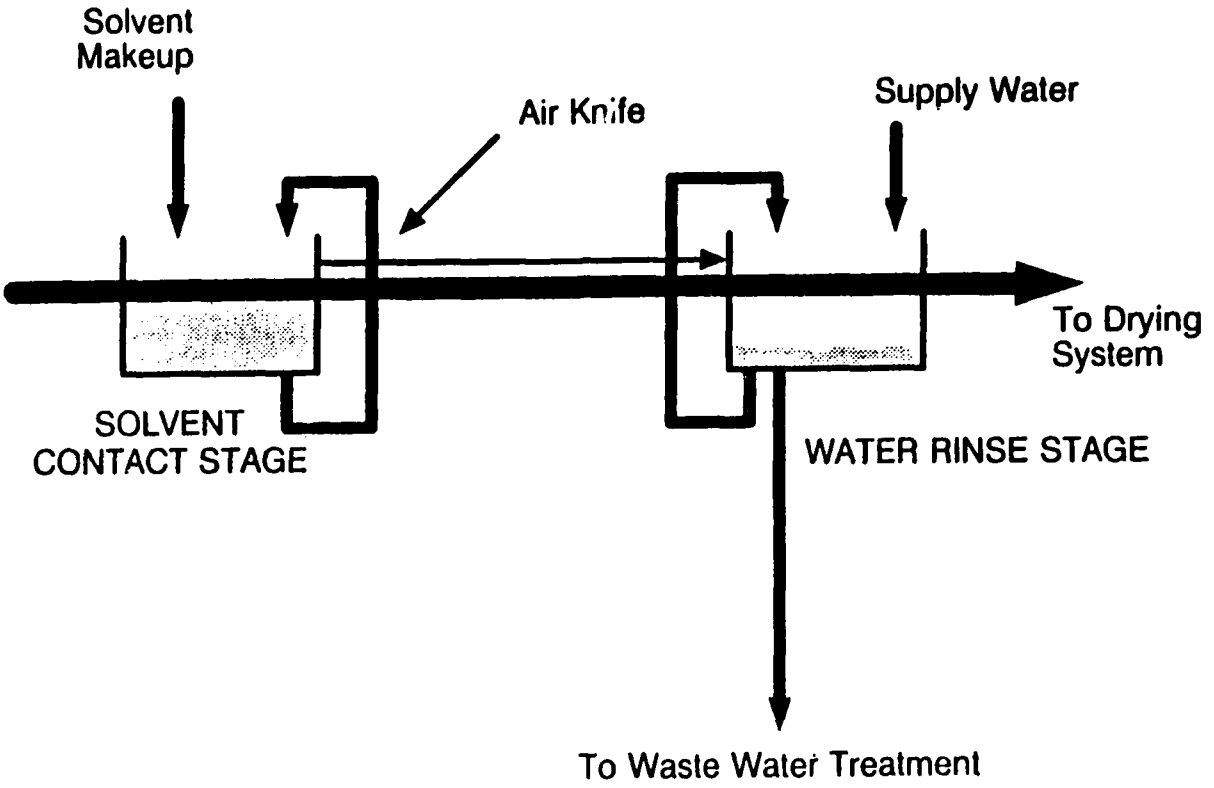

FIGURE 1. Early Semi-Aqueous Cleaning Process.

Achieving a Steady-State Solvent Stage

In early semi-aqueous equipment designs, the air knife used in the solvent stage reduced the organic loading in the water effluent. However, it introduced an unsteady state in the bath. More soil was added to the bath than removed. Hence, the soil concentration constantly increased and the bath eventually became too contaminated to clean. This made cleaning performance dependent upon the bath's life cycle. In fact, cleaning efficiency initially increased with small concentrations (approximately 10%), but eventually decreased as flux concentrations became very

high (40% to 50%). Hence, cleaning efficiency of a new bath rose, tapered off and eventually fell substantially. This meant that contaminant concentration required monitoring and that the bath had to be dumped periodically (Figure 2a).

The preferred situation is to equalize the dragout of the contaminants with the amount of contaminants being introduced. This can be accomplished by controlling the effectiveness of the air knife. In this case, the contaminant concentration reaches an equilibrium condition at a low contaminant concentration, where the bath is at an enhanced state of cleaning effectiveness. Stable process control is established and the need for bath changes is eliminated (Figure 2b).

Measuring the specific gravity of the cleaning agent, as shown in Figure 3, is the only control required. The air knife can then be adjusted to maintain the desired contamination level in the cleaner (taking care not to mist the agent with the air knife).

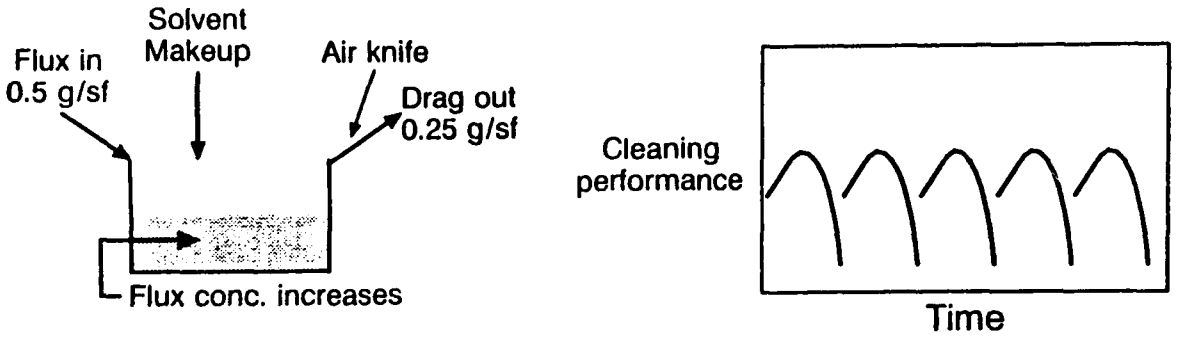

(a) Use of an Air Knife Produces Unsteady State.

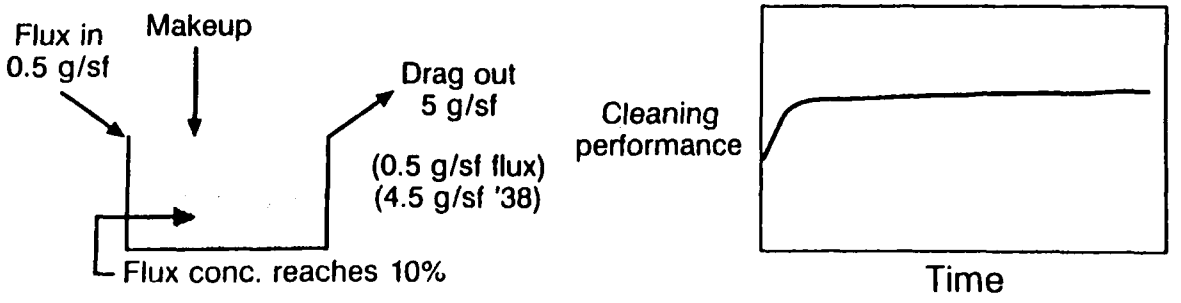

(b) Natural Dragout Produces Steady State.

FIGURE 2. Use of an Air Knife vs. Natural Dragout in the Semi-Aqueous Cleaning Process.

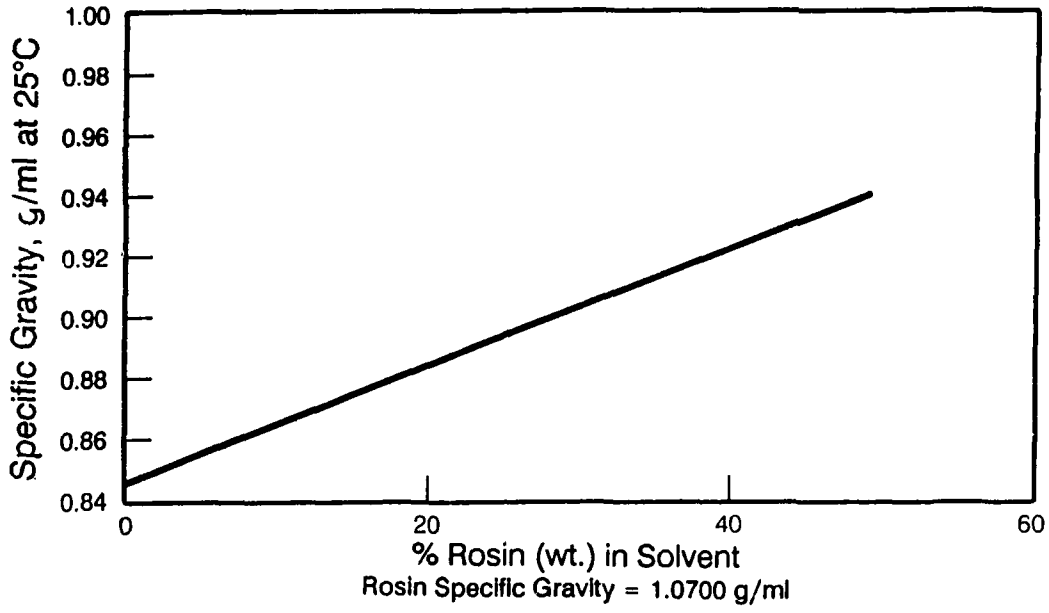

FIGURE 3. Specific Gravity of a Hydrocarbon-Based Agent for Semi-Aqueous Cleaning vs. Percent Rosin.

Reducing Organics in the Effluent

If the air knife is controlled, reducing organics in the aqueous effluent can be accomplished by establishing an emulsion in the first rinse stage, where the dragout from the solvent stage is removed with water (Figure 4). Since the organic concentration of the cleaning agent/soil is relatively low in the emulsion, the organic dragout to subsequent rinse stages is reduced by 80% to 95%. As the organic concentration increases in the emulsion stage, it can be removed to a decanter and allowed to separate into two layers. Once separated, the decanter water can be recycled into the emulsion stage.

This approach separates the contaminants generated in the cleaning process from the aqueous effluent. Contaminants collect in the hydrocarbon layer separated in the decanter. The organic in the water is primarily entrapped cleaning agent.

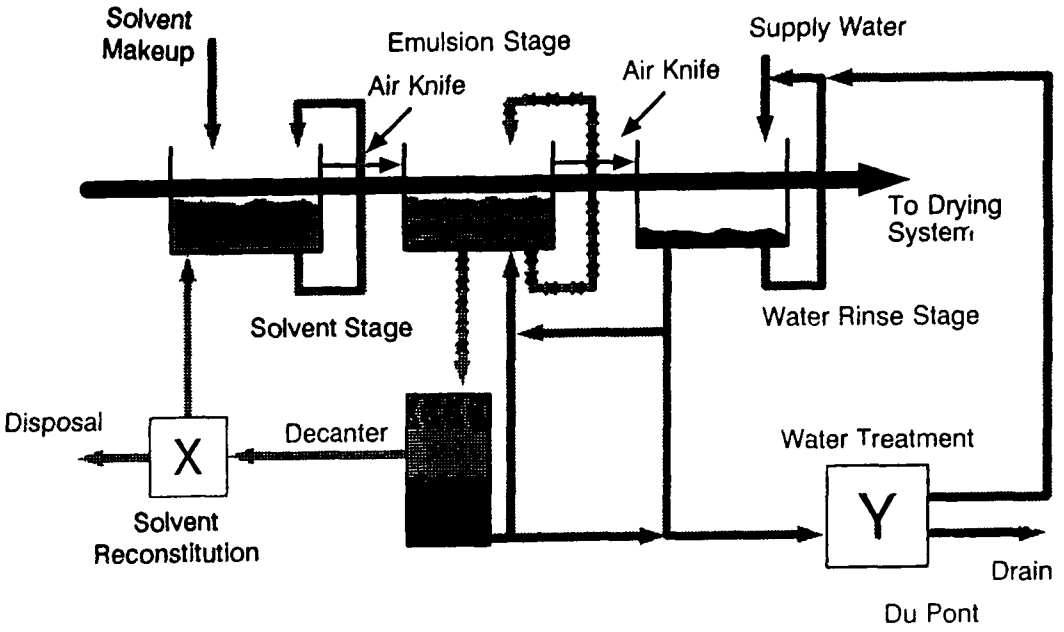

FIGURE 4. Reducing Organics by Establishing an Emulsion in the First Rinse Stage by the Dragout from the Solvent Stage.

Recycling Rinse Water

To make the semi-aqueous cleaning process even more environmentally attractive, three well-known technologies are currently being evaluated for their effectiveness in removing contaminants from the rinse water.

Tests with membrane technology have provided very positive results. Mixtures of 1% hydrocarbon-based agent for semi-aqueous cleaning (containing flux residues) have been evaluated by UV spectroscopy, COD and conductivity after treatment with three different membranes. Each of the three membranes resulted in water that was greater than 95% clean.

The effectiveness of these same membranes in treating decanter water, a worst case situation, has also been evaluated. After treatment, the decanter water was greater than 70% clean. Tests with two commercially available membranes are underway, and to date have yielded waste water that is more than 95% clean after two weeks of processing.

Another approach called advanced oxidation, which uses peroxide and UV light to destroy the organics, is also being studied. In initial tests with decanter water, advanced oxidation eliminated 87% of the organics.

A third approach, involving carbon treatment/ion exchange technology, is under evaluation as well. In initial tests, it shows promise for removing 90% of the organics.

How clean does the water have to be for recycling? To answer this question, experiments were performed with final rinsing in recycled water. The process provides excellent cleaning performance with recycled water. Figure 5 shows the consistently low levels of ionics measured on boards (4" x 4" with 800 unplated holes) cleaned with a hydrocarbon-based agent and recycled water. After 10 recyclings of the aqueous effluent, the ionics remained low, even though the chemical oxygen demand increased linearly from 0 ppm for the first recycling to 1,500 ppm for the tenth recycling. Apparently, relatively modest amounts of organics in the aqueous effluent do not adversely effect cleaning performance.

Since 100 ppm organics in the water can be obtained with all three water-cleaning technologies, other factors, such as equipment and operating costs, will determine which system is best for a given application.

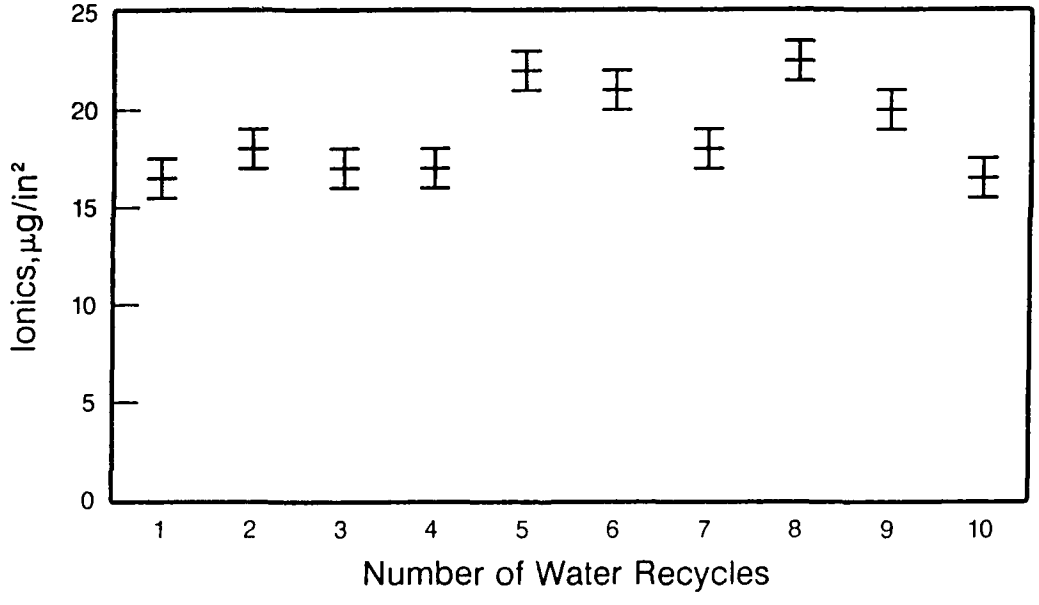

FIGURE 5. Effect of Rinse Water Recycling on Ionic Levels.

SEMI-AQUEOUS COMPATIBILITY WITH PLASTICS AND ELASTOMERS

In general, the hydrocarbon-based cleaning agent is more aggressive than CFC-113 and less aggressive than chlorinated solvents, such as 1,1,1-trichloroethane. It is compatible with a wide range of plastics, elastomers and metals. In addition, it is compatible with most cured epoxy and polyimide substrates, as well as with acrylic and epoxy solder masks. Since compatibility is affected by material variations, critical components should be tested under actual conditions before switching to this cleaning agents.

Generally, it is gentle enough for cleaning PWB assemblies having components made of many common plastics (Table 5). It is also compatible with most elastomers used for gaskets and seals in semi-aqueous equipment (Table 6). Specific recommendations are available for suitable gasket and seal materials for operating equipment.

TABLE 5. Plastic Compatibility of a Hydrocarbon-Based, Semi-Aqueous Cleaning Agent Under Typical Cleaning Conditions.[a]

Material	Tradename	Hydrocarbon-Based, Semi-Aqueous Cleaning Agent	CFC-113/ MeOH
ABS	Kralastic®	2	0
Acetal	DELRIN®	0	0
Acrylic	LUCITE®	2	0
Cellulose	Ethocel™	3	3
Epoxy	--	0	0
Fluorocarbons			
PTFE	TEFLON®	0	0
PVDF	KYNAR®	0	
Ionomer	SURLYN®	2	1
Nylon	ZYTEL®	0	0
Polyacrylate	Arylon®	3	--
Polycarbonate	Tuffak®	3	0
Polyester			
PBT	Valox®	0	0
PET	RYNITE®	0	0
Polyetherimide	Ultem®	0	0
Polyethylene	ALATHON®	1	0
Polyimide	KAPTON®	0	--
Polyphenylene Oxide	Noryl®	2	0
Polyphenylene Sulfide	Ryton®	0	0
Polypropylene	--	2	0
Polystyrene	Styron™	3	2
Polysulfone	--	0	0
Polyvinyl chloride	--	2	0
Chlorinated Polyvinyl Chloride	--	2	

[a]Test Conditions: 1-day immersion at 50° C (122° F).

Key: 0 = Compatible
1 = Probably compatible
2 = Probably incompatible
3 = Incompatible

TABLE 6. Elastomer Compatibility of a Hydrocarbon-Based, Semi-Aqueous Cleaning Agent.[a]

Material	Hydrocarbon-Based, Semi-Aqueous Cleaning Agent	
	% Wt. Change	% Linear Swell
SBR	25	7
Butyl	100	30
Natural	150	40
EPDM NORDEL®	25	10
ADIPRENE®	40	10
NBR	90	25
HYPALON®	30	15
Neoprene	40	10
ALCRYN®	40	15
HYTREL®	15	6
Silicone	90	25
Thiokol FA	3	0.4
Thiokol ST	15	6
VAMAC®	80	25
VITON® A	25	9
VITON® B	20	6
KALREZ®	0.3	0.3
VITON® GF	8	5
VITON® VT-R-6186	2	0.2

[a]Test Conditions: 1-week immersion at 50° C (122° F).

HCFCs AND SEMI-AQUEOUS VS. CFCs: COMPARATIVE CLEANING EFFECTIVENESS

The HCFC blend and the hydrocarbon-based, semi-aqueous agent both provide a very effective, consistent way of removing ionic contamination; removing oxidized rosin that causes "white residue;" maintaining high surface insulation resistance (SIR); and cleaning under tight-spaced surface mount assemblies.

In military qualification testing, the overall performance of the HCFC blend was better than traditional vapor degreasing/defluxing using the CFC-113/methanol azeotrope. Similarly, the hydrocarbon-based, semi-aqueous agent consistently provided better cleaning performance than CFC-113/methanol.

EPA Ad Hoc Phase II Testing

Since CFCs are used extensively to clean PWBs for military electronics, a joint program between industry, the military and the EPA was undertaken to evaluate new cleaning agent candidates. Phase I, completed in 1989, established two criteria for measuring PWB cleanliness -- ionic levels (for inorganics) and residual rosin (as measured by UV spectroscopy and High Performance Liquid Chromatography) -- of both surface mount (C) and surface mount/plated through-hole (D) boards. SIR results, while measured, were not used as a pass/fail criterion.

In Phase II, cleaning alternatives are compared to the benchmark results for CFC-113/methanol. For an alternate material/process to be considered as good as the benchmark, its mathematical means for processes C and D must fall between the lower limit and the upper limit for the mean of the ionic contamination and residual rosin tests. In addition, the sample-to-sample variance of the alternate must be less than the benchmark upper limit for variance. If the alternate's mean values are less than the lower limit, then the material/process is considered to be better than the benchmark; if the alternate's mean values are greater than the upper limit, then the material/process is considered to be worse than the benchmark. Both the HCFC blend and the hydrocarbon-based, semi-aqueous agent were judged better than the CFC-113/methanol azeotrope in Phase II testing.

Tables 7 and 8 compare the effectiveness of the HCFC blend and the hydrocarbon-based, semi-aqueous agent, respectively, in removing ionic contamination vs. CFC-113/ methanol. Tables 9 and 10 compare the effectiveness of the HCFC blend and the semi-aqueous agent, respectively, in reducing residual rosin vs. CFC-113/methanol.

TABLE 7. Comparison of Ionic Contamination for CFC-113/MeOH to an HCFC Blend.[a]

Process Sequence	Phase I CFC-113/MeOH				Phase II HCFC Blend[a]			
	Lower Limit for Mean	Bench-mark Mean	Upper Limit for Mean	Upper Limit for Variance	Minimum Reading	Mean	Maximum Reading	Variance
A	1.5	2.0	2.5	1.7	0.0	0.0	0.0	0.0
C	2.8	3.8	4.8	6.7	0.2	0.3	0.4	0.1
D	9.4	10.7	12.0	10.1	4.6	5.0	5.5	0.1

[a]HCFC blend consisting of 62.2% HCFC-141b, 35% HCFC-123, 2.5% MeOH and 0.3% stabilizer.

Note: The cleaning cycle, conducted in a Branson PSD 1210 vapor degreaser, was as follows: 30 sec of vapor dwell, 3 min in the boil sump, 1 min in the rinse sump and 30 sec of vapor dwell.

TABLE 8. Comparison of Ionic Contamination for CFC-113/MeOH to a Hydrocarbon-Based, Semi-Aqueous Agent.

Process Sequence	Phase I CFC-113/MeOH				Phase II Hydrocarbon-Based, Semi-Aqueous Agent			
	Lower Limit for Mean	Bench-mark Mean	Upper Limit for Mean	Upper Limit for Variance	Minimum Reading	Average	Maximum Reading	Variance
A	1.5	2.0	2.5	1.7	0.0	0.0	0.0	0.0
C	2.8	3.8	4.8	6.7	0.0	0.2	0.5	0.0
D	9.4	10.7	12.0	10.1	4.4	4.6	5.0	0.1

Note: The cleaning cycle was as follows: 10 min cleaning in the semi-aqueous agent at room temperature in an ECD 6307 cleaner; 2 min rinse in hot (140° F [60° C]) tap water in an ECD 6300B; 1 min rinse in hot (140° F [60° C]) tap water in an ECD 6300B; 1 min rinse in hot (140° F [60° C]) tap water in an ECD 6300B; 1 min rinse in room temperature deionized water in an ECD 6300B; and 20 min drying in a Blue M oven at 250° F (121° C).

TABLE 9. Comparison of Residual Rosin for CFC-113/MeOH to an HCFC Blend.[a]

Process Sequence	Phase I CFC-113/MeOH				Phase II HCFC Blend[a]			
	Lower Limit for Mean	Mean	Upper Limit for Mean	Variance	Minimum Reading	Mean	Maximum Reading	Variance
A	217	301	385	44,135	0	5.0	12.5	38
C	2,852	3,135	3,418	535,961	1,465	1,712	2,243	74,417
D	2,481	3,945	5,410	13,696,891	936	1,233	1,546	54,876

[a]HCFC blend consisting of 62.2% HCFC-141b, 35% HCFC-123, 2.5% MeOH and 0.3% stabilizer.

Note: The cleaning cycle, conducted in a Branson PSD 1210 vapor degreaser, was as follows: 30 sec of vapor dwell, 3 min in the boil sump, 1 min in the rinse sump and 30 sec of vapor dwell.

TABLE 10. Comparison of Residual Rosin for CFC-113/MeOH to a Hydrocarbon-Based, Semi-Aqueous Agent.

Process Sequence	Phase I CFC-113/MeOH				Phase II Hydrocarbon-Based, Semi-Aqueous Agent			
	Lower Limit for Mean	Bench-mark Mean	Upper Limit for Mean	Variance	Minimum Reading	Average	Maximum Reading	Variance
A	217	301	385	44,135	0.0	12.8	64.0	656
C	2,852	3,135	3,418	535,961	1,231	1,342	1,559	12,882
D	2,481	3,945	5,410	13,696,891	186	338	467	12,027

Note: The cleaning cycle was as follows: 10 min cleaning in a hydrocarbon-based agent for semi-aqueous cleaning at room temperature in an ECD 6307 cleaner; 2 min rinse in hot (140° F [60° C]) tap water in an ECD 6300B; 1 min rinse in hot (140° F [60° C]) tap water in an ECD 6300B; 1 min rinse in hot (140° F [60° C]) tap water in an ECD 6300B; 1 min rinse in room temperature deionized water in an ECD 6300B; and 20 min drying in a Blue M oven at 250° F (121° C).

SUMMARY

Table 11 compares the three PWB cleaning technologies discussed in this paper -- CFCs, HCFCs and semi-aqueous. Both the HCFC blend and the hydrocarbon-based, semi-aqueous agent discussed in this paper have demonstrated cleaning effectiveness superior to CFC-113/methanol in EPA Ad Hoc Phase II testing.

Like CFCs, both HCFCs and hydrocarbon-based, semi-aqueous agents employ a very effective cleaning strategy; they dissolve the soils in a solvent. In the semi-aqueous process, however, subsequent rinsing and drying steps are required. For applications requiring precision cleaning without rinsing and drying, this makes HCFCs the technology of choice.

Both of the CFC alternative technologies require new equipment, with the caveat that some existing vapor degreasing/defluxing equipment can be retrofitted for HCFCs.

From an environmental standpoint, the two CFC alternatives differ. The HCFCs offer significantly reduced ODP and GWP compared to CFC-113/methanol. Though it is widely agreed that HCFCs, such as the blend discussed in this paper, will fill many immediate needs and represent an essential part of the solution to the CFC/ozone issue, it is recognized that they will have a limited life cycle. A non-binding resolution to the Montreal Protocol calls for phasing out HCFCs by 2040, and possibly by 2020. In addition, like CFCs, HCFCs require disposal as a hazardous waste.

Semi-aqueous cleaning with a hydrocarbon-based agent offers significant long-term ecological advantages over currently available vapor degreasing/defluxing agents. Unlike CFC-113-based cleaners, semi-aqueous cleaners have zero ODP and GWP, and do not require disposal as a hazardous waste. In addition, soils removed in the semi-aqueous process are easily separated from water rinses, greatly reducing treatment requirements. The aqueous effluent can be recycled in a closed loop system to reduce water consumption or it can be sent to the drain. In addition, the spent cleaning agent can be disposed of by incineration to generate energy for other operations.

TABLE 11. Alternative PWB Cleaning Technologies vs. Vapor Degreasing/Defluxing with CFC-113/Methanol.

	Vapor Cleaning with CFC-113/MeOH	Vapor Cleaning with an HCFC Blend[a]	Semi-Aqueous Cleaning with a Hydrocarbon-Based Agent/Water
Overall Cleaning Effectiveness vs. CFC-113/Methanol	--	Better Than[b]	Better Than[b]
Cleaning Strategy	Soils dissolved in solvent	Soils dissolved in solvent	Soils dissolved in solvent and rinsed away
Drying Step	No	No	Yes
Process Control	Easy	Easy	Easy
New Equipment vs. CFC-113/MeOH	--	Yes	Yes
Aqueous Waste	None	None	Does not contain soils or hydrocarbons; can be recycled
Non-aqueous Waste	Requires disposal as hazardous waste	Requires disposal as hazardous waste	Is separated from aqueous waste; ready for incineration (15,000 BTU/lb fuel value)
Estimated Toxicity (ppm by vol)	475 (AEL)[c]	105 (AEL)[c]	None Established
Ozone Depletion Potential	0.75	0.07	0
Global Warming Potential	1.35	0.08	0

[a]HCFC blend consisting of 62.2% HCFC-141b, 35% HCFC-123, 2.5% methanol and 0.3% stabilizer.
[b]As determined by EPA Ad Hoc Committee Phase II Testing.
[c]An Acceptable Exposure Limit (AEL) is the recommended time-weighted average concentration of an airborne chemical to which nearly all workers may be exposed during an 8-hr day, 40-hr week without adverse effect, as determined by the Du Pont Company for compounds that do not have a Threshold Limit Value (TLV®).

B. Carroll Smiley is a Senior Development Engineer with the Du Pont Company. He has been with Du Pont for 16 years and has 9 years' experience in cleaning electronic assemblies.

Address: Du Pont Company
14 T. W. Alexander Dr.
Research Triangle Park, NC 27709

USING MACHINE VISION TO AUTOMATE SOLDERABILITY INSPECTION

BY

STEPHEN KAISER

MARK BROWN

LAVAUGHN DAWSON

FACTORY AUTOMATION ENGINEERS

TEXAS INSTRUMENTS

LEWISVILLE, TEXAS

ABSTRACT

Component solderability is an industry wide issue which if not detected, can result in excessive board joint rework and system failures. In the Defense Industry, the majority of military contracts require that samples from component lots be inspected for solderability per MIL-STD-202, Method 208. This inspection task is highly labor intensive and susceptible to human error. To improve the accuracy, repeatability and cycle time of this inspection operation, Texas Instruments (TI) developed an automated system capable of inspecting axial components. This system named the *Automated Solderability Inspection Station (ASIST) uses a custom developed illumination chamber, machine vision, and custom analysis algorithms to locate, measure and document the solderability defects on axial component leads. Texas Instruments is currently evaluating the performance of ASIST in a production environment while actively pursuing the application of the developed technology to other component package types.

* Patent Pending

INTRODUCTION

Texas Instruments has historically sought continuous improvement in the quality of it's products. This effort allowed TI to be the first company to provide an extensive warranty on weapon systems sold to the government. A recent quality improvement made by TI deals with the assurance of component solderability. Poor component solderability can result in costly rework and system failures. The trend toward higher density boards and smaller components is compounding rework and failure problems. TI is developing the tools required to address this problem at the beginning of the manufacturing operation where it is most cost effective and has the greatest impact on quality. TI determined that automating the solderability inspection operation would result in a direct reduction of man hours required to perform the operation. An additional benefit would be increased yield and quality of solder connections down stream in the manufacturing area. To accomplish this, a system was developed that utilizes a patent pending lighting technique, machine vision, and custom analysis algorithms to accurately calculate the percent solder coverage on components.

PROBLEM DESCRIPTION

Many of the military contracts require that all components that have solder connections must pass specified solderability testing requirements before the parts are used. Typically, samples of the components to be tested are selected and tested under military specified conditions to gauge the solder wetting ability on the component leads. The most common test requirement for components with leads is MIL-STD-202, Method 208. This document specifies the operational requirements for all the equipment to be used in the test and the evaluation criteria to determine if the solder dipped components pass or fail. The critical area of the evaluation process is the visual examination of the solder coverage on the leads after the solder dip operation. The requirements specify that a specially trained and certified inspector perform a "visual" measurement of the solder coating at 10 power magnification with a "shadowless" light source. The 1-inch portion of the dipped lead nearest the component, or the whole lead if it is less than 1 inch long, is examined. If the new solder coating doesn't cover at least 95% of the lead then the specimen has failed the test. Visual determination of the solder coverage makes it very hard to get accurate and repeatable results . Even though a limited number of components are selected from each lot, the inspection operation through a microscope is very tedious. The only "tool" that has been available to help in this measurement is a grid reticule that fits in the eyepiece of a microscope. This requires the inspector to count the squares that the defects occupy and gauge against the 95% coverage criteria. Unfortunately, the grid is not very effective at the required 10x magnification.Figure 1shows a scale representation of a typical component lead and the grid reticule. The defects shown are equal to 5% of the lead area.

CRITICAL FACTORS

The examination of each component requires inspectors to visually measure the total solder coverage. Components failing to meet a minimum of 95% solder coverage or

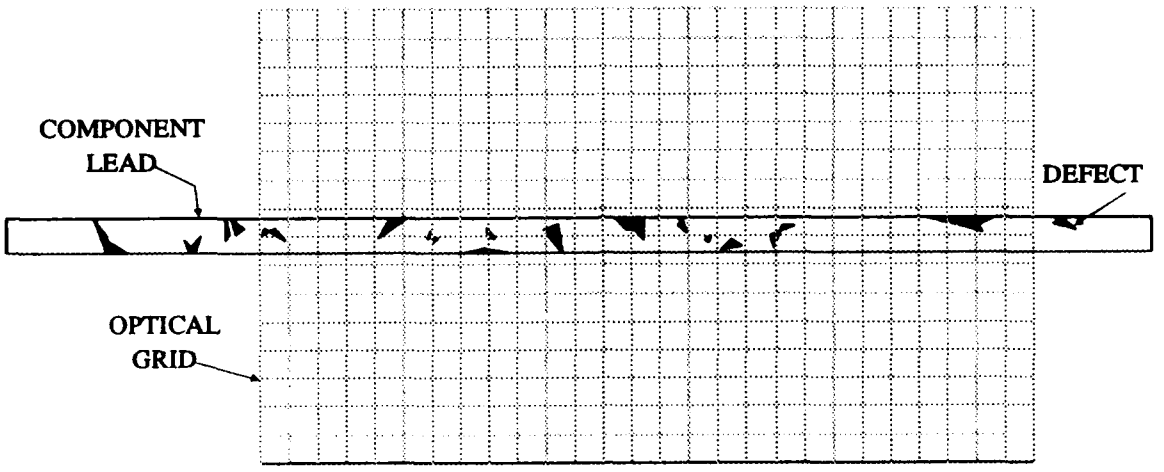

FIGURE 1

components with large defect regions are rejected. When the length or diameter of the leads change it is even more difficult for the inspector to gauge the percent coverage. Another problem TI identified in the inspection is the inspection lighting . A number of lighting techniques commonly used, such as ring lights and multi-point light sources, make it very difficult to identify surface defects on the lead. See Figure 2, left view. The right view of Figure 2 shows the same component area with the new lighting.

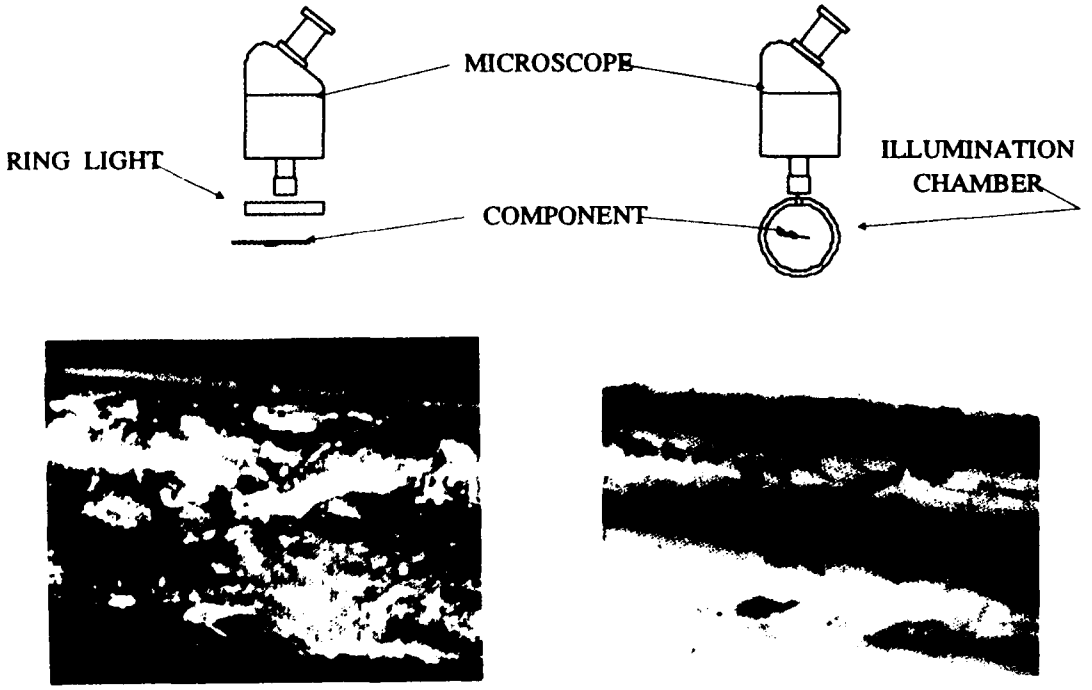

FIGURE 2

DESCRIPTION

LIGHTING AND OPTICS

ASIST utilizes a custom designed chamber which produces even, diffused lighting on all surfaces of the component being inspected. The light chamber is cylindrical in shape, and machined out of a translucent plastic. The plastic was selected to provide a consistent light diffusing characteristic and easy machining properties. An inspection port is machined into the chamber to allow the illuminated lead to be imaged by a solid state camera. One problem encountered with the developed lighting was how to view the lead without degrading the performance of the chamber. This problem was solved by placing a viewing hole away from the area being examined and setting the optics so that the desired lead area is imaged. Mounted to the outside of the chamber is a fiber optic ring used to illuminate the chamber. A high intensity, constant voltage light source was used for this application to ensure consistent light intensity over the expected life of the incandescent bulb.

The optical system selected was a stereo microscope with a 7-20x magnification range and optics certified to meet resolution requirements for military inspection criteria. The microscope was purchased with a trinocular body to allow use of a solid state video camera. This microscope was chosen instead of custom designed optics because it allowed direct visual observation of the components and was approved for the inspection operation and did not require extra testing or certification.

ELECTRONICS

Shown in Figure 3 is the block diagram of the system. The main controller of ASIST is an 80286, PC compatible computer with 2 megabytes of main memory, a 40 megabyte hard drive, two floppy drives, two serial, and two parallel ports. The computer has four 8 bit and six 16 bit slots to hold computer cards. The machine vision system consists of a set of boards that plug directly into the PC buss and is able to use all the peripherals of the PC. The vision board image buffer has four 512x512 pixel frame buffers and a complete library of standard vision analysis functions.The computer uses one parallel port for a standard dot matrix printer and the other port for the video image printer. The high resolution video image

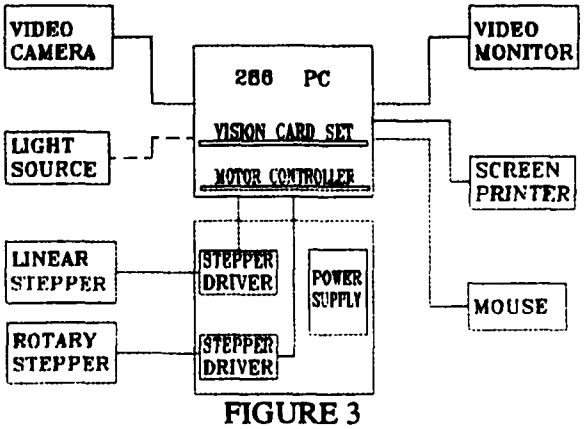

FIGURE 3

screen printer can print pictures of the component lead being inspected or images that have been stored on disk. A mouse is connected through one of the serial ports as the user interface device.

Critical to the inspection accuracy of this system was the selection of a camera. The camera required high pixel resolution and the capability to accurately resolve the gray levels on the lead surface. A black and white, solid state camera with 780 x 540 pixel imager resolution and low level light sensitivity was selected after extensive testing. The user control panel for the system consists of a standard three button digital mouse and a high resolution color monitor for displaying easy to follow menu screens. The video monitor allows switching between the standard PC video output and the machine vision video output. The video monitor can also provide a display of the image being printed by the video image printer. A special, multi axes stepper controller card is used by the PC to control the component positioning system. The stepper motor controller is capable of controlling four axis of motion. In its present application, ASIST (Figure 4), utilizes both a linear and rotational stepper motor for parts handling.

FIGURE 4

TOOLING

The ASIST tooling consists of a two finger, parallel gripper with two degrees of freedom (linear and rotational). Positioning of the gripper is controlled through the computer by standard linear and rotational stepper motors. Special care was taken to ensure that the tooling was static safe for components. The gripper is capable of holding axial components with body diameters ranging in size from 0.06 to 0.5 inches. The gripper is manually operated and holds the component by the body. A slip clutch was developed to prevent damage to the component body when the gripper is closed. During operation, the tooling will position each part so the entire circumference of a one inch long lead can be inspected. The ends of the grippers were designed to prevent interference with the lighting of the component and to allow the vision system to locate the end of the component body.

SOFTWARE

The software was written in the C programming language to allow maximum portability across different computers and machine vision systems. The code is in a modular format with each module responsible for a very limited number of actions. The main modules for the system are the menu, motion control, light calibration, error checking, image capture, and image analysis.

The menu system is designed to display the operating menus grouped by functional operations. In a normal inspection cycle the system will display the appropriate choices for the operator. Extended functions are not displayed unless specifically requested and properly authorized. Control of the component positioning system is performed with software interrupts that allow real time response of the computer to the conditions of the system. The hardware and software make it possible to perform some of these operations concurrently to reduce overall cycle time.

The machine vision code which performs the defect identification and area calculations was developed in stages. First, sample leads were analyzed for defect characteristics. General vision algorithms were then developed to locate and measure the defects. Next the Category C inspector came in to compare his identification of defects to that of the machine. The software engineers and the inspectorthen went through a tuning procedure to make the computer duplicate the defect selection criteria of the inspector.

Operation

Operation of the system has been simplified through the use of operating menus to allow proficient operation after 1 hour of training. Machine vision or computer operating expertise is not required. The first step in inspecting a component lead is loading the part. Since the current system does not have automatic parts loading, parts must be manually inserted into the gripper. Once the desired part is loaded, the execute command is selected on the menu screen and the system verifies the inspection chamber lighting. If not correct, the system displays a setup screen that allows the operator to interactively set the correct lighting level. The system will then move the part into the illumination chamber. As the part enters the field of view of the camera, the vision system establishes a reference point on the edge of the component body and performs a calibration procedure. This calibration procedure ensures that the system begins inspecting the lead 50 mils from the component body, which is one of the MIL-STD-202 requirements. The computer then begins inspecting the component lead. The part positioning system moves an area of the lead under the microscope for inspection. The vision system analyzes the viewed portion of the lead and determines the percent defect area. This process is repeated until the entire lead is inspected. Upon completion of the inspection operation, the system displays the total solder coverage on the monitor, prints desired statistical data on a dot matrix printer (i.e. largest defect found, defect density, per field of view solder coverage, etc...), and returns the part to home position so the next part can be loaded.

SYSTEM EVALUATION/TESTING

To verify that ASIST could meet both the requirements of MIL-STD-202F and those of TI Production and Quality control, the following test plan was developed by the quality group and the TI MIL-STD instructor who is certified for solderability inspection training.

TEST

Ten axial components were selected by Procurement Assurance for the test. The parts varied in size and shape and were representative of the following types of defects:

- Non-wetting
- Pin holes
- Dewetting
- Foreign Contamination
- Pits
- Voids
- Unpretinned areas

All parts were inspected by a Category C examiner. To assure maximum accuracy the defects were carefully mapped onto graph paper. Each component mapping took more than one hour to complete. The total solder coverage of each part was calculated using the graphical mapping. The results of the inspection were used as the actual baseline numbers. A Category R inspector was selected to inspect the same parts in a normal way. The computer then inspected the components.

ACCURACY

The test parts were given to a Category R inspector who determined the percent defect area using the standard inspection setup for components. The same parts were then run through the ASIST system ten times without removing the components from the gripper. This was done to reduce the chance for mechanical tolerances affecting the accuracy to impact the measurement. The results of both tests were then compared with those of the Category C inspector.

REPEATABILITY

The repeatability of ASIST and the Category R inspector was determined by inspecting each part a number of times. The Category R inspector checked each part three times. Each inspection was about one week apart and the parts were not labeled to ensure "new" results each time. The parts were run through ASIST ten different times. The parts were physically removed from the gripper and reloaded for each run. ASIST had more inspection runs than the Category R person because of time limitations. Also, we wanted a larger test data base for the machine.

CYCLE TIME

The cycle time of ASIST and the inspector was determined by measuring the duration of each inspection with a stop watch.

EASE OF USE

The relative ease of operation of the system was a qualitative test performed by the production line operators. Five operators were selected to run the system on production components and then fill out a survey sheet at the end of two weeks

Solderability coverage Measurement Factor	ASIST	Current Manual	Percent Improvement
Accuracy (Percent defect area vs. benchmark measurement)	±1.3%	±2.7%	51.8
Range/Repeatability (Measurement consistency)	±0.4%	±0.7%	42.3
Cycle Time (Minutes/lead - includes inspection, load and unload)	1.8	3.5	48.6

TABLE 1

TEST RESULTS

The results of this test (Table 1) proved ASIST was superior to the "standard" manual inspection method in each of the measured categories. In the accuracy test, ASIST was able to locate each defect mapped by the Class C inspector. The accuracy of the manual inspection varied depending on the number and size of the defects. For example, leads with small pinhole defects widely scattered were harder to inspect than leads with a few large nonwetted defect areas. In the repeatability test, ASIST found the same defects in each of the ten runs and measured the solder coverage with little variance. The repeatability of the manual inspection varied, with defects either not being found or measured consistently. The cycle time measurements showed ASIST was faster than for this test. Although faster cycle times are possible with the manual method, accuracy and repeatability performance are sacrificed.

The qualitative portion of the test showed ASIST was simple to operate and was a viable tool for production. Enhancements were requested regarding the system speed, parts loading and documentation features. These enhancements will be incorporated into the production systems.

IMPLEMENTATION

Lighting

The developed lighting technique has been fanned out within TI in two forms. The first of these designs is a cylindrical diffuser*, illuminated with a standard fluorescent ring lamp

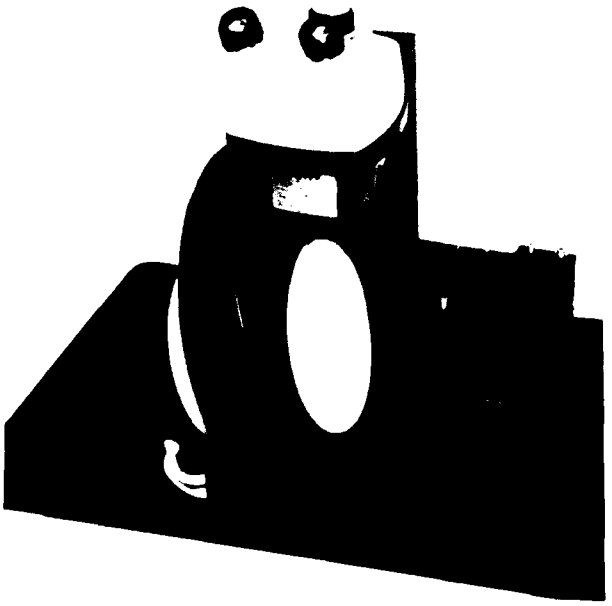

FIGURE 5

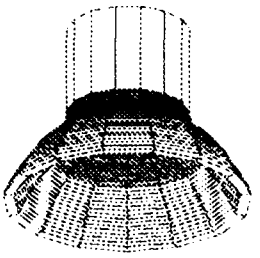

FIGURE 6

(Figure 5). This light chamber is used in conjunction with a standard microscope and allows a wide assortment of components to be inspected. The light source provides optimum solder to non-solder coverage contrast while producing no glare. The second design is a hemispherical diffuser (Figure 6). This design is used for inspecting solder joints on circuit boards. One version of the diffuser threads into the bottom of a microscope and holds a standard ring light in place. This configuration produces a high contrast, glare free image of board solder joints. Both light diffusers reduce operator eye fatigue, and improve the accuracy and repeatability of the manual solderability inspection process.

* Patent Pending

Automated system

The Automated Solderability Inspection Station was moved to TI's Central Incoming Inspection Facility after the test results proved its capability. Work is under way with our internal organizations to have the test system officially certified for production use. TI is also working with the Naval Weapons Center to allow use of the system for inspection of components used on the High Speed Antiradiation Missile (HARM) project. The system is being used in the incoming pretin operation to allow the inspectors to evaluate the operation of the system under factory conditions. The inspectors use ASIST on to verify solderability calculations on a wide range of axial components. The process is providing valuable feedback on the functionality of the system and helping to identify areas for improvement for the "productionized" system. Two "productionized" inspection systems are currently being developed for TI's Central Incoming Inspection Facility (Figure 7). Planned improvements for these systems include: higher speed vision board set, higher resolution images, faster parts positioning system, automatic multiple component queuing, new light source with electronic feedback, reduced system package size and improved system calibration software.

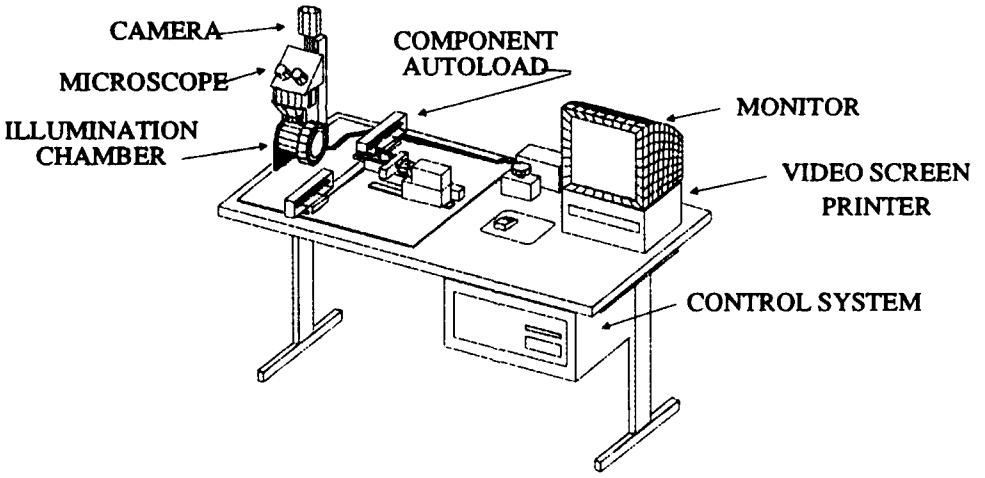

FIGURE 7

PLANS

Texas Instruments first goal is to gain formal approval for ASIST and implement the system at key internal locations. This task will begin with certification by an internal quality control group and then approval from the Naval Weapons Center. Once the system is approved for production use, two fully productionized, automated inspection systems will be built and installed at TI's Central Incoming Inspection facility. The automated systems will be high speed and have automatic parts loading to allow queuing of component lot samples. The desired outcome is to provide highly automated systems that can perform the inspection operation and document the results with minimal operator intervention.

A second goal is to integrate ASIST with the automated lead pretinning systems currently used by TI. ASIST would be used as a process control tool to detect solderability problems and provide a feedback loop for optimizing the pretin process. TI knows it is critical that the variables associated with pretinning be controlled so component related problems can be isolated.

TI's third goal is to implement ASIST at key component supplier locations and link these systems with those at TI's Central Incoming Inspection Facility. Texas Instruments currently has a computer network link between all its sites to facilitate message and data transfer. The network could be expanded to include supplier sites, providing transmission of inspection images and data between locations to identify and document component problems before shipping and receiving occurs. By working closely with suppliers, component process problems can identified and corrective action taken to reduce future defect count. Once the systems are successfully implemented, the component manufacturers can be designated as "certified" suppliers and the TI incoming inspection work will be reduced.

A fourth goal is to develop the inspection systems for the other major component package types. High risk components include radial components and dual inline packages (DIP). Radial components are difficult to inspect because the multiple leads can be bent and interfere with the inspection process. The inner side of DIP leads are a problem to inspect because it is difficult to illuminate the area without shadows. The industry trend however, toward surface mount components and larger DIPs should reduce illumination problems.

SUMMARY

The labor intensive and subjective solderability inspection test required by many military contracts is being successfully addressed with new lighting and machine vision technology. ASIST is a machine vision based automatic inspection system capable of measuring solder coverage on axial component leads. Through an extensive test, ASIST was proven superior to trained operators in accuracy and repeatability. User feedback is being used to incorporate design enhancements in the development of production ready systems. Plans are underway to gain formal approval for ASIST from the Naval Weapons Center. The technology is being developed to allow computer inspection of other component types. Ti is also investigating the possible fanout of this technology to component manufacturers.

Stephen Kaiser is a member of the Group Technical Staff involved with Automation Engineering at TI. He has worked in the TI factory-automation group for the past 9 years, specializing in the use of machine vision systems.

Address: Texas Instruments
P.O. Box 405, MS 3491
Lewisville, TX 75067

EVALUATION OF SOLDERING PROCESS FOR 20 MIL PITCH COMPONENTS

by

Jacqueline G. Jones

ABSTRACT

Due to increasing performance demands of surface mounted integrated circuits, printed wiring assembly design changes to facilitate these demands must take place. The implementation of fine pitch technology will be necessary. Integrated circuit components with lead spacings of 25 mil, 30 mil and higher have been in use in industry for some time. The new generation of electronic assemblies will need integrated circuits with 15 mil and 20 mil lead spacing and finer. The implementation of this type of component will, in turn, place greater demands on the fabrication and assembly processes. Printed wiring board fabrication and assembly processes must be upgraded to efficiently and cost effectively produce assemblies with these new requirements. For these reasons, a Design -of- Experiment (DOE) evaluation of the soldering process for components with 20 mil center to center lead spacing (pitch) has been performed . The purpose of the evaluation is to identify the most significant variables in the process, quantify them, and make recommendations of optimal parameters to obtain the highest quality and reliability, with maximum yield. A designed experiment is an effective, low cost method of process evaluation. It requires fewer experimental runs than the "one variable at a time" approach and the results are more representative of the actual process because variable interactions are also examined. Performance of this type of evaluation prior to implementation of designs will allow for consideration of the variables resulting in a more producible design, as well as reduce the time required for production implementation.

The experiment performed determined that for the fabrication process used, plated solder thickness was the most important parameter in determining strength and yield, however, pad width also had some effect on yield. Use of the parameter values optimized in this study for future designs for this type of

component will result in high quality soldered assemblies which are easily manufactured.

INTRODUCTION

For the next generation of electronic assemblies, finer pitch components will be required in order to meet the increasing performance demands of future electronic systems. In order to best evaluate the impact of the proposed design changes the following issues must be addressed:

1) How will the incorporation of fine pitch components in new designs affect costs and producibility?

2) Are there design considerations which can be incorporated to enhance the producibility of these components.

In this study, the use of simultaneous engineering and design of experiment techniques have been fundamental in addressing these issues. This paper describes the methodology used to evaluate the impact of one type of component on a specific assembly process.

SIMULTANEOUS ENGINEERING

The use of the Simultaneous or Concurrent Engineering methodology helps to bridge the gap between the design function and the manufacturing function. Historically, the method for design and manufacture of hardware did not incorporate any interaction of personnel outside of their functional area. The design would be completed and given to manufacturing to implement regardless of cost. In some instances, all of the design requirements would not be able to be implemented as provided, therefore, some redesign would be have to take place. In order to be competitive in today's marketplace, the

simultaneous engineering methodology should be incorporated in our every day working considerations. Based on the proposed use of finer pitch components in new designs, an evaluation of the soldering process for 20 mil pitch components has been performed concurrrently with the design effort. Performance of this study at this time has resulted in the following:

1) Reduction in the total design/manufacturing implementation cycle time.

2) Allowance of manufacturing constraints to be considered during the design process resulting in a more easily manufactured (less costly) product.

DESIGN OF EXPERIMENT

The Design of Experiment methodology is an efficient technique for process evaluation. The technique uses statistical methods to quantify the effects of variables on process responses. The classical factorial design is an experiment which controls several factors and quantifies their effects at two or more levels (more levels allow for computation of higher order models). It is very useful because, unlike the one variable at a time approach, it also quantifies the effects of the interaction among variables. This is beneficial because not only is more information derived from the limited number of experimental runs, but the information most closely resembles the actual process. A two factor two level (2^2) full factorial experiment design will result in a linear model which will quantify the effects of the two factors and the interactions between them. A design of this type could have been used in this study, however, the addition of a third level in one of the factors was chosen instead to allow for computation of a quadratic model with only two more experimental runs. Based on previous experimentation, a quadratic model was determined to be more representative of the process in question. This constitutes a D-Optimal experiment design (see Figure 1).

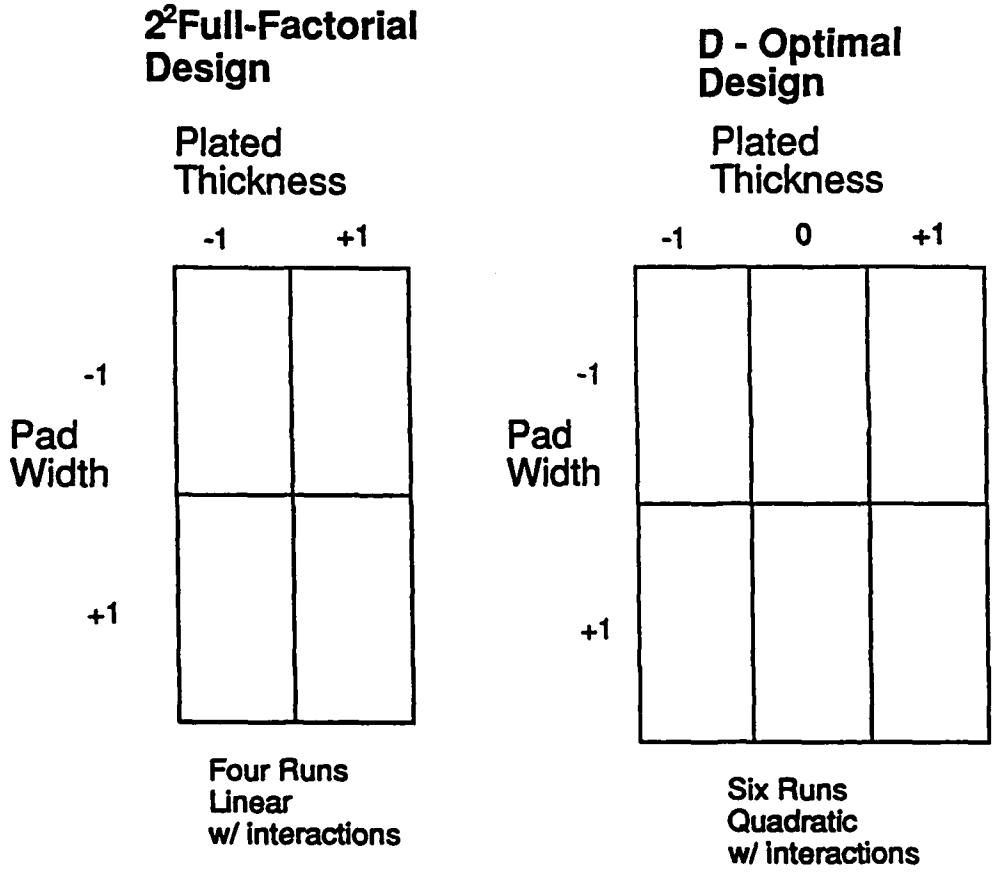

FIGURE 1 - EXPERIMENT DESIGN

Based on knowledge of the process currently used to solder quad packs, it was expected that because the leads of the 20 mil pitch components were finer than the components historically used, during the soldering operation the leads would be buried within the soldered terminations or otherwise damaged. Also it was expected that there would be extensive lead bridging/ misalignment due to the narrow pad spacing. For these reasons, the factors chosen for study were plated solder thickness and pad width.

The responses chosen were those determined to best represent solder joint reliability and ease of manufacture. The most reliable solder joint was determined to be the one that is most resistant to the thermal and mechanical stresses induced during service. Throughout the industry, mechanical breaking strength is considered to be correlated with reliability. The most easily manufactured solder joint was determined to be the assembly with the highest total yield after visual inspection in accordance with the current manufacturing requirements.

The solder thickness was studied at three levels and the pad width at two levels. The pad patterns used for the experiment consisted of 256 pads, 128 of these were at each of the two pad widths (see Figure 2). This enabled both lead/pad geometries to be soldered using the same component. The soldering operation was performed using the semi-automated heater bar reflow soldering equipment. One component was soldered on each of the three panels. The relative solder thickness values chosen for the study were 25%, 100%, and 166% of a selected solder thickness. However, plated solder thickness was found to be a quadratic function of plating time, pad area, and position (within the pattern). The amount of variation, as much as 50%, of the actual plated thickness made this variable difficult to use in the analysis. For this reason, plating time replaced solder thickness as the variable for analysis. Solder thickness values were calculated from established relationships after the results

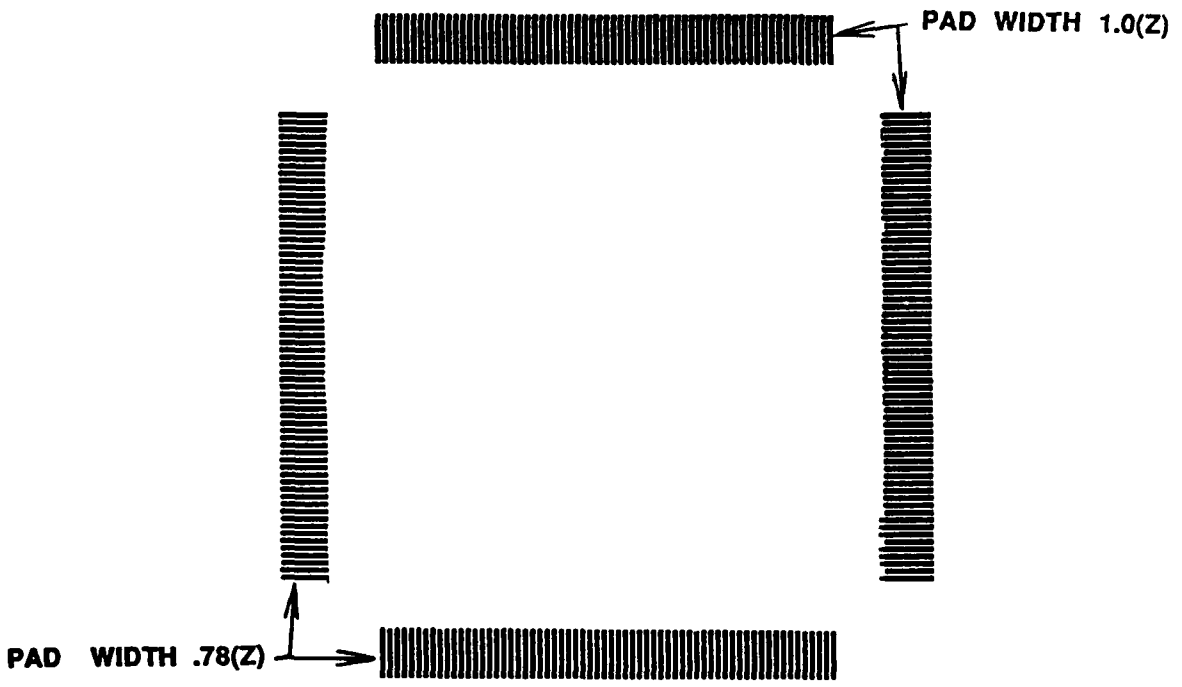

FIGURE 2 - DIAGRAM OF TEST COMPONENTS

were obtained. The relative plating times used and the resulting average thickness values are included in Table I.

TABLE I - RELATIVE SOLDER THICKNESS VALUES

Target Thickness (X)	Plating Time (Y)	Pad Width (Z)	Actual Average Thk.
.25(X)	.26(Y)	.78(Z) 1.0(Z)	.35(X) .30(X)
1.0(X)	1.0(Y)	.78(Z) 1.0(Z)	.90(X) 1.08(X)
1.66(X)	1.73(Y)	.78(Z) 1.0(Z)	1.46(X) 1.55(X)

ANALYSIS

The responses in the experiment were yield and pull strength. Yield was quantified by dividing the 128 leads for each pad width per component into eight sections of 16 adjacent leads. The defect observations for each section were calculated. This was equivalent to eight replications of each experimental treatment. The accept/reject criteria for the yield inspection was based on current requirements. The strength measurements were performed using wire bond pull test equipment.

Upon initial analysis, the original yield data results were not found to be normally distributed. Normal distribution of data is one of the basic assumptions for the application of analysis of variance (ANOVA) techniques. Proportions or percentages (attribute-type) as response data typically follow a binomial

distribution. Therefore, in order to correctly apply ANOVA, the data should be transformed[2]. The purpose of the transformation is to stabilize the variance in the data. In this study arc sine $\sqrt{p}$, where p is the number of defective observations, was used as the transformation function. The model generated for the transformed yield response determined that plating time is the most statistically significant variable with respect to yield and strength. The yield would be maximized at a relative plating time of .66(Y) and the strength would be maximized at 1.06(Y). The optimum value for processing is chosen to be .66(Y) because the reduction in joint strength with respect to plating time is less severe and (less costly) than the corresponding reduction in yield (see Figure 3).

RESULTS

The soldering process used for the evaluation was semi-automated reflow heater bar soldering. This most closely resembles the process that would be used for the most cost effective assembly method. The variables chosen for the study were plated solder thickness, and pad width. The responses were solder joint yield and solder joint breaking strength (we assume that solder joint breaking strength is correlated with reliability). These responses were used to determine the best manufacturing parameters to provide the most reliable (strongest) solder joint and the highest yield.

Solder thickness was found to be the most significant parameter with regard to yield and strength (the two responses studied). Solder thickness below the .68(X) level produced a higher quantity of joints with insufficient solder. Even for those solder joints where the solder fillets were acceptable , when microsectioned it was revealed that at best a minimal amount of solder was on the bottom portion (foot) of the connection. This condition results in decreased pull strength. Solder thickness above the .68(X) level produced an

[2]Hicks,C.R.,"Fundamental Concepts in the Design of Experiments,"New York: Holt,Rinehart and Winston (1982).

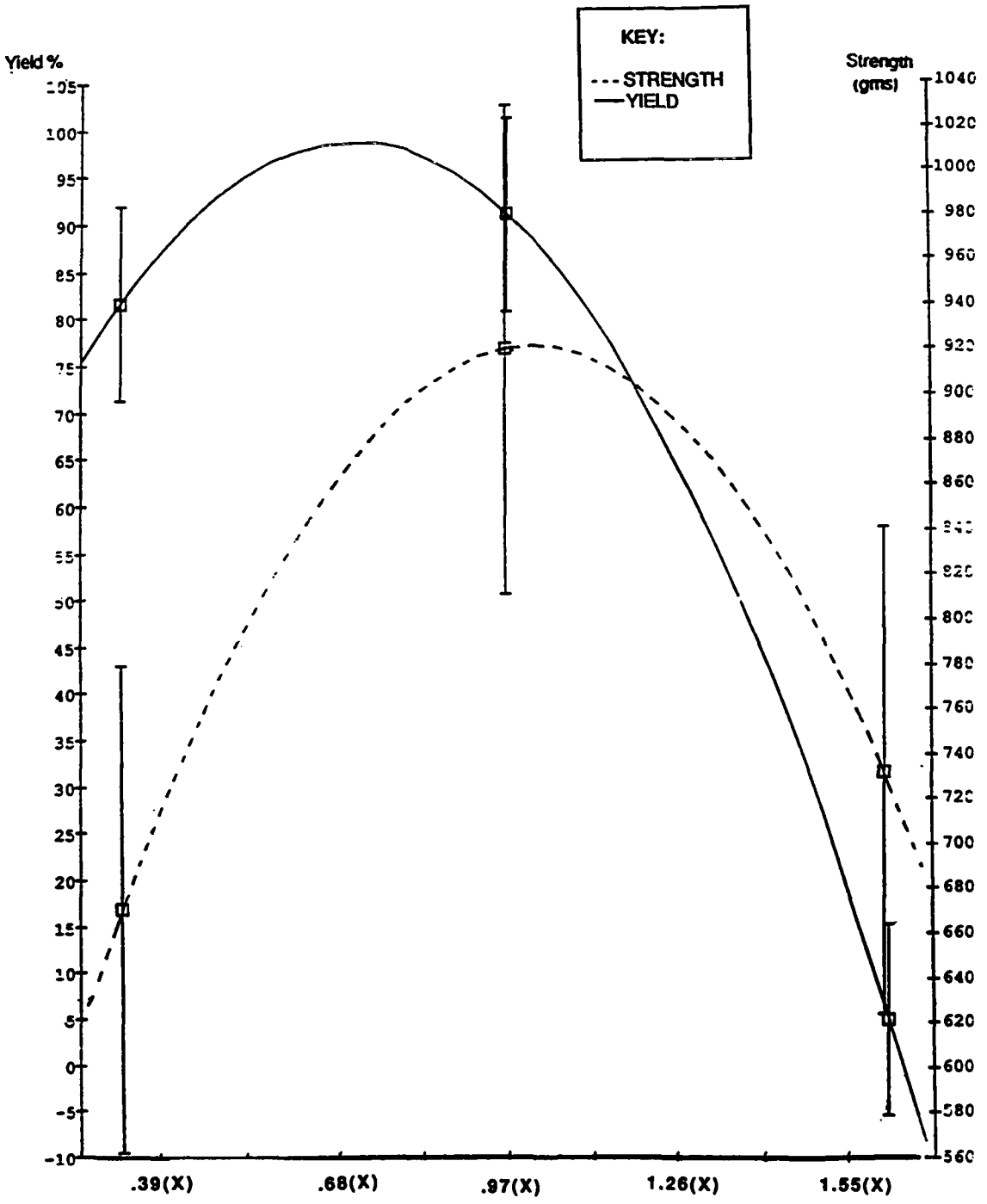

AVERAGE PLATED THICKNESS (IN TERMS OF A SELECTED VALUE X)
PAD WIDTH 1.0(Z)

FIGURE 3 - 20 MIL PITCH SOLDER EVALUATION RESULTS

increased quantity of solder joints which exhibited bridging and/or misalignment. Because of the narrow pad width necessary for this design, plating excessively thick solder causes the pads to be mounded. This condition is most apparent on the .78(Z) width pads. Upon reflow of the solder, the pressure of the heater bar causes the leads to slide sideways. The thicker the solder (the solder plated thicker on the narrower pads) the farther the lead would travel.

This study did not reveal any reduction in strength (decreased reliability) with the use of .78(Z) width pads as opposed to 1.0(Z) width pads. However from an assembly producibility standpoint a 1.0(Z) width is preferred. The narrower pads are less accommodating to misalignment than the 1.0(Z) width pads. Another consideration for alignment is the relationship of the component leads to the pad pattern. Variations in the alignment of the leads to the component body should be minimized as much as possible. Due to the large size of the components any variation allowed is magnified from end to end. Because of the required closeness of the pad spacing these variations could result in misalignment. The experimentation performed determined that solder thickness was the most important parameter in determining strength and yield, however, pad width also had some effect on yield. The optimum levels of the parameters studied are as follows:

SOLDER THICKNESS	.68(X) (average)
PAD WIDTH	1.0(Z)

RECOMMENDATIONS

In order to facilitate the implementation of 20 mil pitch components the following recommendations were made:

Change the current requirement for plated solder thickness to .68(X) average and minimize variation between PWB plating baths. A range of ± .21(X) would result in an approximate 95% solder joint yield. Other processes for adding solder should be considered to eliminate this pad position variation due to electro-plating effects.

ACKNOWLEDGEMENTS

The author would like to thank Peter J. Savagian for his direction on this project. And a special thank you to Tyrone U. Jones for his never-ending support.

Jacqueline Jones is the Technical Supervisor of the Assembly Technology organization of Product Engineering at the Hughes Aircraft Company Radar Systems Group. Her previous experience includes 8 years in materials and process engineering support. Her responsibilities include providing manufacturing engineering support to electronic assembly production operations and producibility support to product design operations.

Ms. Jones was awarded a BS degree in Ceramic Engineering from Georgia Institute of Technology.

Address: Hughes Aircraft Co.
Radar Systems Group
P.O. Box 92426, Bldg. R1, MS 3A3
Los Angeles, CA 90245

NEW X-RAY TECHNOLOGY TO INSPECT SURFACE MOUNT ASSEMBLIES

by

Dr. Richard Albert
President
and
Joseph Fjelstad
Consultant
Digiray Corporation
San Ramon, California

ABSTRACT

A novel x-ray imaging technology for the inspection of soldered surface mount assemblies is reviewed. The new technology, based on a principle of reverse geometry, provides crisp, first generation images while significantly reducing image degradation due to x-ray scatter, a problem common with standard techniques. Other unusual capabilities of the technology are discussed and include 3-D (stereoscopic) viewing, panning, zooming and the uses of psuedo color to enhance defect indentification.

BACKGROUND

Surface mount technology has experienced an excellent growth rate in recent years. Fueled by the many advantages the technology offers (outlined in Table 1), surface mounting of electronic components has apparently become the method of choice for many new electronic designs. It should be noted, however, that surface mount technology has taken a long time to gain the broad acceptance it enjoys today.

As with any new technology, surface mount technology presented early users with a host of technical problems, from lack of adequate assembly equipment to ill defined processes that yielded sporatic success. To compound their difficulties users had to overcome problems with solder joint reliability, stemming from the mismatch in the coefficients of thermal expansion between the printed wiring board and the surface mount devices.

Years of concerted effort by equipment and process suppliers and manufacturers have resulted in great improvements being made. There remains, however, opportunity and need for continued improvement in materials and processes to achieve the part per million defect levels sought by today's quality conscious manufacturers and users. This is especially true as surface mount technology transitions into fine pitch technology.

A NEW X-RAY INSPECTION TECHNIQUE

As has been frequently cited by surface mount technology experts, inspection of surface mount assemblies is an important but difficult task. The concern about hidden or subtle defects continues to be a subject of near constant discussion. While defect prevention is the ultimate objective of any assembly process, it cannot be made to happen without adequate detection methods. Put another way, we don't normally set about correcting problems we don't know we have!

Detecting the subtle defects associated with surface mount assembly (listed in Table 2) represents a great challenge to reliability and test engineers. To aid them in their efforts a host of techniques have been employed. Among them are:

Laser/Infrared Inspection, wherein solder joints are individually heated by a laser and thermally profiled against a standard to detect the subtle differences between excess and insufficient solder.

Scanning Accoustic Microscopy, where parts are immersed in liquid and profiled for their accoustical responses to ultra sonic energy.

X-Ray, the original and extremely versatile test method which has many variations, from real time fluoroscopy to 3-D laminography to computer aided tomography. It is from the category of x-ray methods that the new technology has evolved.

REVERSE GEOMETRY X-RAY (RGX)

Conventional x-ray technology and its variants, in essence, use a point source which is directed at the object of interest. The x-rays pass through the object and the image is recorded either on silver halide film or picked up by an image intensifier and video camera for monitoring on a video screen. The resulting image often lacks sharpness due to the scattering of x-rays that occurs as they impact the various elements of the object under inspection. In contrast, the new technology uses a scanning beam of photons that travel throughout the object and converge on a small detector. The

small detector is significantly less prone to picking up the scattered radiation that tends to contaminate ordinary x-ray viewing (see Figure 1). Data from the detector is then digitized and sorted in a 1024 x 1024 pixel array maintaining full detail, and images are available for immediate viewing on a video monitor. The image obtained is first generation quality and exhibits superior sharpness. It is capable of distinguishing density differences of less than 0.5% This feature can be of great value in determining critical variations in solder thickness (see Figure 2).

There are over 4000 shades of gray available which can be drawn up to aid evaluation, 256 at a time. If the subtleties between shades of gray become too similar for visual distinction it is possible to convert the image to psuedo color to heighten the distinction between various solder thicknesses.

3-D (STEREOSCOPIC) IMAGING

The new technology is also capable of providing 3-D or stereoscopic images of the device under inspection when two detectors are used simultaneously. This should prove to be of great benefit to those charged with discerning the subtle defects in surface mount assemblied by providing the viewer with a third dimension so that depth can be sensed, helping to distinguish relative location.

Finally, the zoom and pan features of the system speed up facilitate inspection by allowing the operator to move from location to location over a wide area. One can view nearly 80 square inches at one time, zooming in on features of interest without having to touch the printed wiring assembly.

CONCLUSION

While Reverse Geometry X-Ray has not yet been adapted for automatic inspection, its features are well suited for such an application because the data is already digitized (in fact, a development effort is currently under way). However, even in a manual mode the higher quality imaging capabilities of RGX should make it a welcome addition to the store of non-destructive test methods now employed for ensuring the quality of surface mount assembly processes and products. The new system will enable process and quality engineers to see and interpret soldering quality in an entirely new way and in another dimension.

TABLE 1. Surface Mount Technology Advantages

Item	Advantages
Denser Packaging	Surface Mount Technology offers more function per unit area and unit volume than its thru hole counter parts and, in fact, can accommodate devices on both sides of the circuit board.
Greater Operating Speeds	The close spacing of devices provides the advantage of shorter signal paths, resulting in high speed capability.
Smaller and Lighter Electronic Packages	The small sized and light weight of surface mount technology devices contribute significantly to the reduction in weight and size of the overall package.
Lower Cost Assembly	Systems for pick and place of surface mount devices for assembly are extremely efficient and keep assembly costs low.
Improved Reliability	System complexity can be reduced and reliability improved by minimizing both the number of printed wiring assemblies and the number of interconnects in the system.

TABLE 2. Surface Mount Assembly Defects

Defect	Characteristics
Visible	Insufficient solder (dewetting, non-dewetting)
	Excessive solder
	Lifted devices leads
	Device rotation
	Tomb stoning
	"Grainy" solder
	Cold solder joints
	Insufficient solder rise in fillets and castellations
	Surface solder balls
	Solder bridging (gull wing leaded)
Invisible	Solder voids in joint
	Solder voids under device leads
	Hidden lead bridging abscured by proximity of other devices especially with "J" leaded devices
	Solder thickness inconsistencies
	Solde: balls under devices

TABLE 3. Reverse Geometry X-Ray Advantages

Advantages	Characteristics
Very Small Density Changes are Detectable	- 4096 Gray levels are stored - 256 Gray levels are viewable at a time - < 0.5% density changes are detectable
Clearer Images are Presented for Viewing	- Reverse geometry technology precludes most scattered x-rays from degrading image quality
Fine Image Definition On High Resolution Monitor	- Focal spot is < 0.001" with the monitor containing more than one million pixels.
Quicker Board Inspection Capability	- No physical motion of any kind is required. Any part of a board up to 10" on the diagonal can be viewed, targeted, and enlarged while the assembly being inspected remains stationary.
Real Time 3-Dimensional Stereo Viewing	- The perception of depth reduces the clutter of multiple layers of circuitry and overlying surface mount devices.

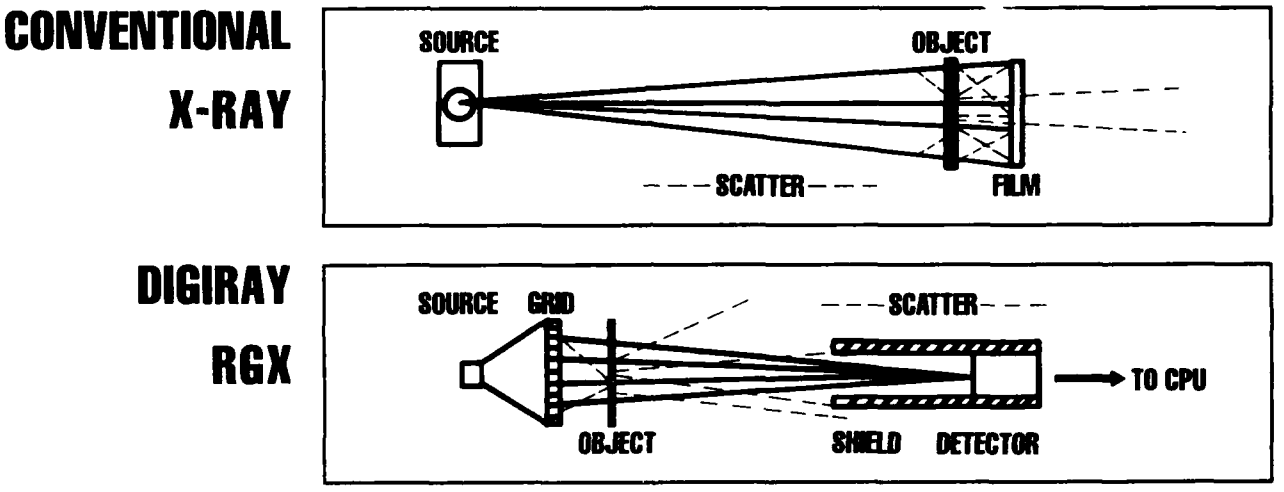
CONVENTIONAL
X-RAY
SOURCE
OBJECT
SCATTER
FILM
DIGIRAY
RGX
SOURCE
GRID
SCATTER
TO CPU
OBJECT
SHIELD
DETECTOR

Figure 1

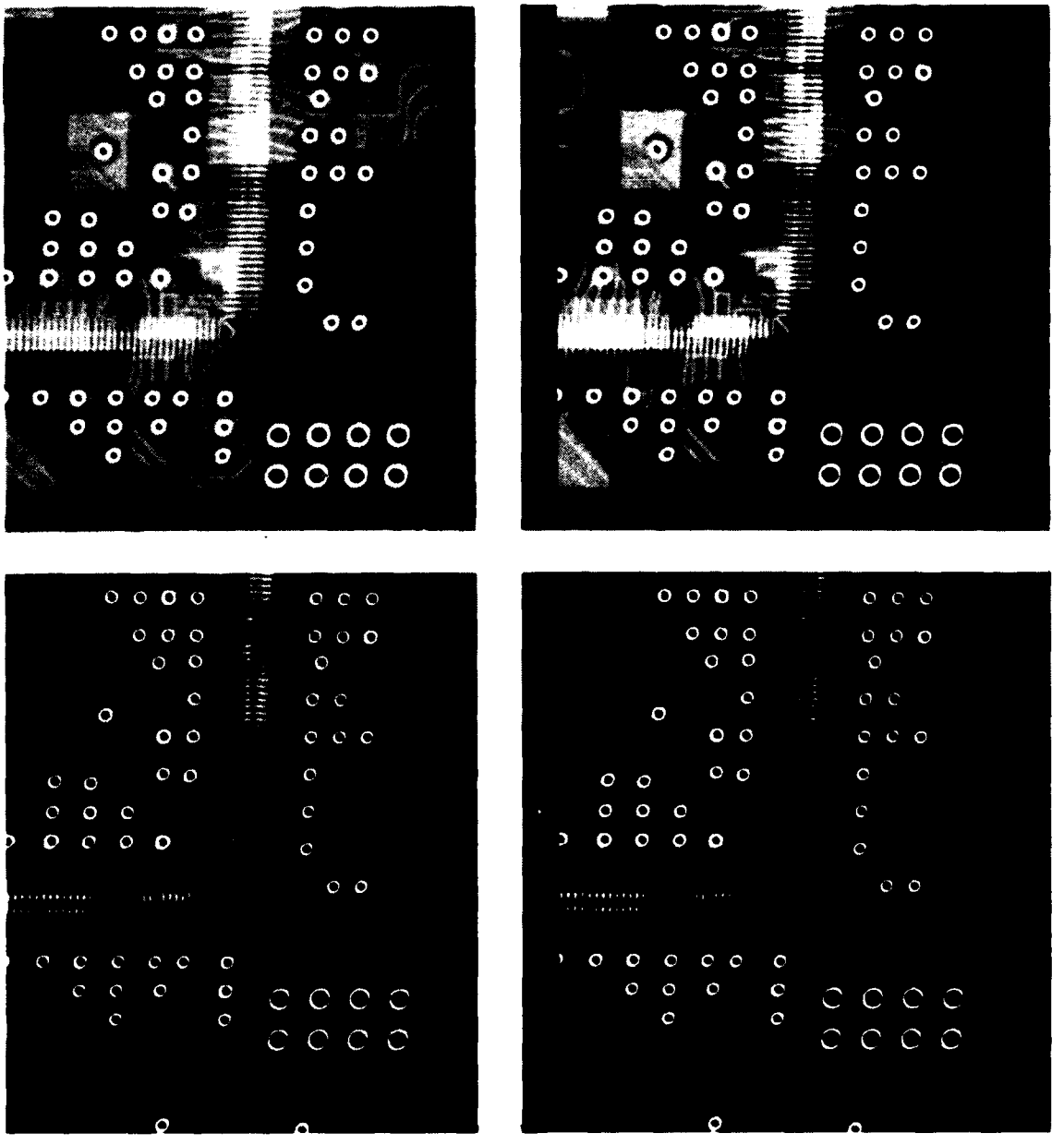

Figure 2

Joseph Fjelstad is a Consultant with Digiray Corporation. He was previously associated with Boeing Aerospace: Printed Circuit Builders, Inc., and as a Process Engineer with them, specialized in imaging, plating, and lamination operations. While at Boeing he invented and had patented an electrochemical deburring process. He has worked in the field of electronic interconnections since 1972.

As the Educational Director for the Institute for Interconnecting and Packaging Electronic Circuits, he is responsible for the Technical Workshop Program and is a frequent instructor at industry workshops on microsectioning and evaluation, multilayer board hole preparation techniques, PWB basics, and flexible circuit technology.

Joe has served on various technical committees, including the recent Industry Blue Ribbon Committee on Small Plated Thru Hole Reliability, the Guidelines for Chip on Board Implementation, and the Tape Automated Bonding and Fine Pitch Assembly Technical Assessment. He has authored and published many technical papers and contributed to the Electronic Materials Handbook, Volume 1, Packaging.

Address: Digiray Corporation
2239 Omega Road Ste. 3
San Ramon, CA 94583

ENVIRONMENTAL STRESS SCREENING AND USE ENVIRONMENTS --THEIR IMPACT ON SURFACE MOUNT SOLDER JOINT AND PLATED-THROUGH-HOLE RELIABILITY

by

Werner Engelmaier
Engelmaier Associates, Inc.
Mendham, NJ 07945
(201) 543-2747

ABSTRACT

Electronic assemblies are subject to cyclic thermo-mechanical loading conditions due to system-external temperature variations and imposed operating conditions, as well as due to environmental stress screening (ESS) and burn-in procedures. The accumulating fatigue damage resulting from these and other causes, e.g. vibration, can lead to the premature failure of the solder attachments of the components as well as the plated-through-hole-vias. Inappropriate ESS of undue severity or/and duration can consume a large fraction of the available fatigue life of solder joints and PTH-vias. Evaluation methods of the accumulating damage are given and the effects of inappropriate testing is illustrated using the history of the Magellan spacecraft.

INTRODUCTION

Electronic assemblies are subject to cyclic thermo-mechanical loading conditions due to system-external temperature variations and imposed operating conditions, as well as due to environmental stress screening (ESS) and burn-in procedures. The accumulating fatigue damage resulting from these and other causes, e.g. vibration, can lead to the premature failure of the solder attachments of the components as well as the plated-through-hole (PTH)-vias, because fatigue damage accumulates until the material's capability to accommodate it is exhausted.

For high-density electronic assemblies the long-term reliability can be assured only by a deliberate 'Design for Reliability' that considers the specific damage mechanisms threatening the reliability. Knowledge of the fatigue behavior of solder joints (Reference 1)and PTH-via barrels (Reference 2), and of what constitutes realistic use environments (Reference 3) are the prerequisite in the successful 'Design for Reliability' of high-performance,

high-density electronic assemblies based on the desired design life and the maximum acceptable failure risk level. This knowledge is also essential in the establishment of ESS programs that successfully weed out 'weak' assemblies without significantly damaging good assemblies.

Inappropriate testing of undue severity or/and duration prior to service can consume a large fraction of the available fatigue life of solder joints and PTH-vias. On the other hand, designs for reliability based on unrealistic use conditions can result either in designs unable to meet reliability expectations or in limitations of the design options available for the design.

USE ENVIRONMENTS

Electronic assemblies, depending on their intended application, have to function in vastly different environments, for significantly different product lives, and without exceeding very different acceptable reliability risk levels. In Table 1 realistic, but worst-case, use environments for electronic assemblies divided into nine use categories (Reference 3) are given.

In Table 1 accelerated test condition producing the same fatigue damage mechanisms, although not the same amount of damage per cycle, as the corresponding use environment temperature cycles are given also.

ENVIRONMENTAL STRESS SCREENING AND BURN-IN -- PURPOSE AND CAVEATS

Environmental Stress Screening. The purpose of ESS is to cause overstressing of 'weak' parts of an assembly to the point of failure. Once having failed, the part can be detected and either repaired, replaced, or discarded. However, this overstressing needs to be accomplished without significant damage to the 'normal' parts of the assembly. Significant damage means in this context damage to an extent that function and/or reliability no longer meet expectations.

While the above stated purpose appears obvious, many environmental stress screening (ESS) procedures, functional acceptance tests (FAT), quality tests, thermal cycling tests, reliability assurance tests, etc. are applied to product, not prototypes, without purposeful rationale or thought of detrimental consequences. Improper screening procedures can systematically destroy good product to the point that it becomes useless before installation in the field. Both the rationale for the procedure as well as the damage consequences need to be understood to avoid failures of the product even before shipment or prematurely in the field. This requires a thorough understanding of the properties and behavior of the materials involved in the assembly as well as their interactions with each other. This means, that such procedures cannot be required on a routine basis for all products; in many cases these procedures require specific tailoring to the product and its needs.

TABLE 1. Realistic Worst-Case Use Environments and Appropriate Accelerated Testing for Surface Mounted Electronics by Use Categories.

USE CATEGORY	WORST USE ENVIRONMENT					Years of Service	ACCELERATED TESTING			
	Tmin °C	*Tmax* °C	ΔT [1] °C	t_D hrs	Cycles/ year		*Tmin* °C	*Tmax* °C	ΔT[2] °C	t_D min
1 CONSUMER	0	+60	35	12	365	1-3	+25	+100	75	15
2 COMPUTERS	+15	+60	20	2	1460	~5	+25	+100	75	15
3 TELECOMM	-40	+85	35	12	365	7-20	+25	+100	75	15
4 COMMERCIAL AIRCRAFT	-55	+95	20	2	3000	~10	0	+100	100	15
5 INDUSTRIAL& AUTOMOTIVE -PASSENGER COMPARTMENT	-55	+95	20 &40 &60 &80	12 12 12 12	185 100 60 20	~10	0	+100	100	15
							& "COLD[3]"			
6 MILITARY GROUND&SHIP	-55	+95	40 &60	12 12	100 265	~5	0	+100	100	15
							& "COLD[3]"			
7 SPACE leo	-40	+85	35	1	8760	5-20	0	+100	100	15
7 SPACE geo				12	365					
							& "COLD[3]"			
8 MILITARY AVIONICS a	-55	+95	40	2	500	~5	0	+100	100	15
8 MILITARY AVIONICS b			60	2	500					
8 MILITARY AVIONICS c			80	2	500					
			&20	1	1000		& "COLD[3]"			
9 AUTOMOTIVE -UNDER HOOD	-55	+125	60	1	1000	~5	0	+100	100	15
			&100	1	300					
			&140	2	40		& "COLD[3]" & "LARGE ΔT[4]"			

& = in addition

(1) ΔT represents the maximum temperature swing, but does not include power dissipation effects; for power dissipation calculate ΔT_e; power dissipation can make pure temperature cycling accelerated testing significantly inaccurate.

(2) All accelerated test cycles shall have temperature ramps <20°C/min and dwell times at temperature extremes shall be 15 minutes measured on the test boards. This will give ~24 cycles/day.

(3) The failure/damage mechanism for solder changes at lower temperatures; for assemblies seeing significant cold environment operations; additional "COLD" cycling from perhaps -40 to 0°C with dwell times long enough for temperature equilibration and for a number of cycles equal to the "COLD" operational cycles in actual use is recommended.

For additional table footnotes see next page.

Burn-In Testing. Burn-in testing, while frequently also applying environmental stresses, can and should be carried out on product in routine fashion. The fundamental difference between ESS and burn-in testing is in their goals. While ESS should be specifically aimed at screening out specific defects using short-term applications of severe stresses, burn-in testing is routinely applied without specific purpose sometimes for hundreds of hours of normal, perhaps worst-case but still realistic, operational environments. In purpose it resembles the shake-down cruise of a ship.

PLATED-THROUGH-HOLE-VIAS

With the ever increasing density demands on printed circuit boards, multilayer boards (MLBs) with 16 or more layers are no longer rare and result in MLB thicknesses in excess of 4.0 mm (160 mils). At the same time PTH-via diameters are decreasing to 0.25 mm (10 mils) and below. Thus, PTH-vias with MLB-thickness/PTH-diameter aspect ratios of higher than 10 to 1 have found their way into product.

The reliability of small-diameter PTH-vias has been studied extensively in an IPC-sponsored Round Robin Study (Reference 4). One finding of that IPC study was that PTH-vias with aspect ratios (MLB thickness divided by PTH diameter) of larger than 3 to 1 and plated with standard electrolytic acid copper show decreasing thermal cyclic reliability. It was found that the copper plating process window narrows as the PTH aspect ratio increases and that the standard electrolytic plating processes become inadequate even with optimum process control. These findings agree with earlier studies investigating the effects of plating current density and agitation level on copper deposit quality in PTH-vias (Reference 5). In this study it was shown that inadequate electrolyte replacement rates, which can clearly occur in high-aspect-ratio PTH-vias, will lead to mass-transport-limited copper plating conditions. Under these conditions, in combination with the non-uniform plating current densities that also get worse with increasing aspect ratios, the copper deposit quality rapidly deteriorates with increasing aspect ratios. The decline in physical properties is frequently accompanied by increasing 'dogboning' (copper deposit thinning at the PTH-via barrel center) as well.

Plated-through-hole-vias with small diameters are also subject to entrapment of air bubbles near the center of the PTH-via barrels during plating. This causes deposits of copper to be either absent altogether or very thin in combination with a stress and strain concentration due to the bubble shape.

---

(4) The failure/damage mechanism for solder is different for large cyclic temperature swings traversing the stress-to-strain -20 to +20°C transition region; for assemblies seeing such cycles in operation, additional appropriate "LARGE ΔT" testing with cycles similar in nature and number to actual use is recommended.

The PTH-vias must survive up to five (5) thermal shock excursions to solder reflow temperatures {(1) fusing of tin/lead plating, (2) solder levelling, (3 & 4) component solder attach, (5) rework/repair} during normal production and assembly. In use, depending on the application and the resulting use environments they can be subjected to many, sometimes severe, thermal cycles.

Combined, these effects are likely to cause failures in the course of the necessary solder reflow operations or shortly after being place into service due to the subsequent operational thermal cycles. It id therefore imperative, that these defective MLBs be removed from the product population.

BEHAVIOR OF PTH-VIAS WITH 'AIR BUBBLE' PLATING DEFECTS

This defect is by far the more serious of the defect conditions previously described. When it occurs, it does so at about the 10 ppm/PTH level. It almost invariably causes the initiation of cracks, if not the complete fracture, of the PTH-via barrels in the first excursion to solder reflow temperatures due to the z-direction thermal expansion of the MLB dielectric material. Subsequent solder reflow processes or operational thermal cycles will cause the propagation of these cracks to completion. Thus, it is imperative when this condition occurs, that product with this defect be screened out of the normal product population.

The IEC Hot Oil Thermal Shock Test is designed to simulate the processes involving solder reflowing, while thermal cycling simulates and accelerates the effects of operational temperature cycles. In the IPC study (Reference 4) both types of tests were employed.

The IEC (International Electrotechnical Commission) Specification 362-2, Test C, which is designed to simulate repetitive solder reflow operations, consists of alternating immersions of the samples into silicon oil at 260±3°C and 20±5°C for 20 seconds. During the test the PTH-via electrical resistance is continuously monitored. Failure is defined as a resistance increase of 100% or larger.

The MIL-T-CYCLE test performed for the IPC study (Reference 4) consists of air-to-air thermal cycles from -65 to +125°C with 30 minutes dwell times at the temperature extremes. During the test the PTH-via resistance is continuously monitored. Failure is defined as an electrical open.

In Table 2 the results obtained in the IPC study from these tests for 'typical' MLBs are given together with estimates of the stresses and strain ranges occurring during these tests, and estimates of the tensile properties resulting from an analysis of these test results using Equations 1 through 8 in the following section. The tensile properties are determined by keeping the tensile strength constant and calculating the copper ductility; the fatigue life results show, that for both tests ductility-dependent low-cycle fatigue

TABLE 2. Estimates of Tensile Properties of PTH-Via Barrel Copper Deposits Based on the Results of the IPC Round Robin Study (Reference 4).

Test	ΔT [°C]	Fatigue Life N_f [cycles]	Barrel Stress σ [MPA\ksi]	Strain Range $\Delta\varepsilon_{max}(eff)$ [%]	Tensile Strength S_u [MPa\ksi]	Minimum Ductility D_f [%]
IEC Hot Oil Thermal Shock	235	~30	219\31.8	4.5	281\40.7	20.6
MIL-T-CYCLE Thermal Cycling	190	~150	177\25.7	2.2	281\40.7	23.3

predominates. The close agreement in the ductility results from the two tests gives confidence in the approach for engineering purposes.

FATIGUE RELIABILITY ANALYSIS

The fatigue behavior of metals can be described by (References 6 and 7)

$$\overline{N_f}^{-0.6} D_f^{0.75} + 0.9\frac{S_u}{E}\left[\frac{\exp(D_f)}{0.36}\right]^{0.1785\log\frac{10^5}{\overline{Nf}}} - \Delta\varepsilon = 0, \qquad (1)$$

where $\overline{N_f}$ = mean fatigue life, cycles-to-failure
D_f = fracture ductility, plastic strain at fracture
S_u = tensile strength
E = modulus of elasticity
$\Delta\varepsilon$ = total cyclic strain range.

The relationships underlying Eq. 1 were developed to be able to predict the fatigue life from tensile properties and brought about a unified approach (Reference 8) for the ductility-dependent low-cycle fatigue and the quite different strength-dependent high-cycle fatigue. Equation 1 has been used for some major study programs (References 9, 10, and 11) and the development of test methods (References 12 and 13).

The accurate determination of the stresses and strains in the PTH-via barrel requires a complex and expensive Finite Element Analysis (Reference 11) which goes significantly beyond the scope of this paper. However, for our purpose the stresses and strains can be estimated with adequate accuracy using the approach taken in the IPC study (Reference 4). Depending on the magnitude of the PTH-via barrel deformation, the stresses are calculated by

$$\sigma = \frac{(\alpha_E - \alpha_{Cu})\Delta T A_E E_E E_{Cu}}{A_E E_E + A_{Cu} E_{Cu}}, \text{ for } \sigma \le S_y \qquad (2)$$

or

$$\sigma = \frac{\left[(\alpha_E - \alpha_{Cu})\Delta T + S_y \frac{E_{Cu} - E_{Cu}'}{E_{Cu}E_{Cu}'}\right] A_E E_E E_{Cu}'}{A_E E_E + A_{Cu} E_{Cu}'}, \quad \text{for } \sigma > S_y, \tag{3}$$

where

$$A_E \equiv \frac{\pi}{4}\left[(h+d)^2 - d^2\right] \quad \text{and} \quad A_{Cu} \equiv \frac{\pi}{4}\left[d^2 - (d-2t)^2\right] \tag{4 \& 5}$$

and where

- σ = lumped maximum PTH-via barrel stress,
- S_y = PTH-via barrel copper yield strength, ~172 MPa\25 ksi assumed,
- α_E = coefficient of thermal expansion of MLB in thickness direction, for FR-4 epoxy ~65 ppm/°C @ $< T_g$, ~315 ppm/°C @ $> T_g$,
- α_{Cu} = coefficient of thermal expansion of copper, ~18 ppm/°C,
- ΔT = temperature range of thermal excursion/cycling,
- A_E = cross-sectional area of influence of MLB,
- A_{Cu} = cross-sectional area of PTH-via barrel,
- E_E = modulus of elasticity of polymer, for FR-4 epoxy ~3.5×10^3 MPa\$0.5 \times 10^6$ psi,
- E_{Cu} = modulus of elasticity of PTH copper, ~8.3×10^4 MPa\$12 \times 10^6$ psi,
- E_{Cu}' = modulus of plasticity of PTH copper, ~690 MPa\$0.1 \times 10^6$ psi,
- h = thickness of MLB,
- d = drilled PTH-via diameter,
- t = thickness of copper deposit in PTH-via barrel,
- T_g = glass transition temperature, for FR-4 epoxy ~125°C.

The strains in the PTH-via barrel are determined from

$$\Delta\varepsilon = \frac{\sigma}{E_{Cu}}, \quad \text{for } \sigma \le S_y \quad \text{and} \quad \Delta\varepsilon = \frac{S_y}{E_{Cu}} + \frac{\sigma - S_y}{E_{Cu}'}, \quad \text{for } \sigma > S_y, \tag{6 \& 7}$$

where $\Delta\varepsilon$ = cyclic strain range during thermal excursion/cycling.

It has been found (References 4 and 11) that the barrel strains thus calculated need to undergo a correction for the stress concentrations occurring due to the uneven PTH-via barrel geometries. An effective maximum strain range can be found from

$$\Delta\varepsilon_{max}(eff) = K_\varepsilon \Delta\varepsilon \tag{8}$$

where K_ε = strain concentration coefficient, ~2.5.

For thermal shock conditions, as they occur during solder reflow processes, this strain concentration effect is not effective to the same extent,

if at all, as it is for thermal cycling. Thus, for the solder reflow temperature excursions $K_\varepsilon \cong 1.0$.

Given the results in Table 2, the minimum fatigue lives for the typical MLB PTH-vias can be estimated. In Table 3 estimates of the minimum fatigue lives for a number of typical electronic use environments from Table 1 are given together with the pertinent information on the use conditions and the resulting stresses and strains.

TABLE 3. Estimates of the Fatigue Life and Time to Failure of Multilayer Board Plated-Through-Hole-Vias in Some Typical Use Environments.

Use Environment	ΔT [°C]	Estimated Maximum Annual Cycles	Barrel Stress σ [MPa\ksi]	Strain Range $\Delta\varepsilon$ [%]	Effective Strain Range $\Delta\varepsilon_{max}(eff)$ [%]	Minimum Fatigue Life [cycles]	Estimated Time to First Failure [years]
Computers	20	1460	67\9.7	0.08	0.20	8.0×10^6	5 500
Telecomm	35	365	117\16.9	0.14	0.35	75 000	205
Industrial	60	250	173\25.1	0.28	0.71	2 900	12
Automotive/ Military	80	365	174\25.2	0.38	0.95	1 200	3.3

Multiple cyclic load histories (e.g. "COLD" temperature fatigue cycles combined with higher temperature creep/fatigue cycles (see Table 1) combined with vibration) all make their contributions to the cumulative fatigue damage. Under the assumption that these damage contributions are linearly cumulative -- the assumption underlies all fatigue analyses -- and that the simultaneous occurrence or the sequencing order of these load histories makes no significant difference, the Palmgren-Miner's rule (Reference 14) can be applied

$$\sum_{1}^{i} \frac{N_i}{N_{f,i}} \leq 1 \tag{9}$$

where

N_i = actually applied number of cycles at a specific cyclic load level,

$N_{f,i}$ = fatigue life at the acceptable failure probability from the specific cyclic load level i alone.

Equation 9 can be used with the allowable sum of the fatigue damage fractions less than unity to provide margins of safety.

ESS PROCEDURE AND EFFECTS ON LONG-TERM RELIABILITY

A possible ESS procedure would consist of five (5) thermal shock cycles of the same nature as those in the IEC Hot Oil Thermal Shock test (Reference 4). AS in the IEC test, monitoring the electrical resistance of the PTH-vias will separate 'good' from 'bad' product.

This ESS procedure, together with the solder reflow processes necessary for production, will result in no more than ten (10) thermal shock cycles. By applying the cumulative damage principles underlying Equation 9, these ten (10) thermal shock cycles will result in a reduction of the remaining fatigue life by about 33% based on the IEC Hot Oil Thermal Shock test results showing ~30 cycles to first failure for high-aspect ratio PTH-vias. Given the results in Table 3, this reduction in life is only significant and of consequence for the more severe use environments. This perhaps is not too high a price for eliminating early failures due to "air bubble" thin plating defects. Of course, elimination of the defect source by assuring flow of the plating solution through the PTH-vias, is much preferred.

SURFACE MOUNT SOLDER JOINTS

The solder joints in electronic assemblies with surface mounted components not only have the function of providing the electrical interconnection between component and circuit board, but also are the sole mechanical attachment of the component to the board and serve a heat-removal function as well. The solder joints frequently connect materials of highly disparate properties, causing global thermal expansion mismatches (References 1, 15, 16 and 17), and are made of a material, solder, that itself has often properties significantly different than the bonding structure materials, causing local thermal expansion mismatches (References 17 and 18). The severity of these thermal expansion mismatches depends on the design parameters of the assembly and the use environment (see Table 1).

BEHAVIOR OF DEFECTIVE SOLDER JOINTS

It has been shown that the variations of the solder joint attributes within accepted workmanship standards (References 19 and 20) have no measurable correlation with long-term fatigue reliability (Reference 21); deviations need to be gross before having detrimental effects on reliability.

Grossly defective solder joints not only result in reduced fatigue reliability, but also have reduced structural integrity and strength. Solder joint strength -- as measured with pull or shear tests -- has no correlation with fatigue reliability; this is not to say that solder joint strength is not important foe applications with vibrational or shock (mechanical or thermal) loading conditions. However, grossly defective solder joints show a reduction in both fatigue reliability and strength, which permits the successful

application of ESS procedures without significant detrimental effects on solder joint fatigue reliability.

Solder readily creeps and stress relaxes at temperatures above about 0°C, a tendency that increases with further increases in temperature (Reference 22). Solder at these temperatures can be thought of as a load-bearing material on a strictly temporary basis only. Thus, loading solder joints at elevated temperatures for ESS purposes does not make much sense, because even for grossly defective and weakened solder joints overstressing to failure cannot be consistently assured. At lower temperatures however, the tendency to creep and stress relax is greatly reduced and becomes insignificant (Reference 22). Thus, applied loads build up stresses in the solder joints, rather than cause stress relaxing plastic flow, and result in failure-inducing overstresses in the weak solder joints.

It has been shown (Reference 23) that the fatigue life, $N_f(x\%)$, at a given acceptable failure probability, x, and thus the reliability, of surface mount (SM) solder attachments can be predicted to engineering accuracy by (Reference 1)

$$N_f(x\%) = \frac{1}{2}\left[\frac{F}{2\varepsilon_f'}\frac{L_D\,\Delta\alpha\,\Delta T_e}{h}\right]^{\frac{1}{c}}\left[\frac{\ln(1-0.01x)}{\ln(0.5)}\right]^{\frac{1}{\beta}} \qquad (10)$$

for stiff leadless SM solder attachments and for compliant leaded solder attachments (the scaling coefficient for metric units is 1.38 MPa instead of 200 psi) by

$$N_f(x\%) = \frac{1}{2}\left[\frac{F}{2\varepsilon_f'}\frac{K_D\,(L_D\,\Delta\alpha\,\Delta T_e)^2}{(200\text{ psi})Ah}\right]^{\frac{1}{c}}\left[\frac{\ln(1-0.01x)}{\ln(0.5)}\right]^{\frac{1}{\beta}} \qquad (11)$$

where

$$c = -0.442 - 6\text{x}10^{-4}\overline{T_S}_J + 1.74\text{x}10^{-2}\ln\left(1+\frac{360}{t_D}\right) \qquad (12)$$

and where

- A = effective solder joint area (≡ 2/3 solder-wetted lead area vertically projected to solder pad),
- c = fatigue ductility exponent,
- F = empirical "non-ideal" factor indicative of deviations of real solder joints from idealizing assumptions and accounting for secondary and frequently intractable effects such as cyclic warpage, cyclic transients, non-ideal solder joint geometries, solder microstructure, brittle intermetallic compounds, Pb-rich boundary layers, and local solder/bonded material expansion differences, as well as in accuracies and uncertainties in the parameters in Equations 10 and 11; $1.5 > F > 1.0$ for column-like

leadless solder attachments, $1.2 > F > 0.7$ for castellated chip carriers, chip components and leadless solder attachments with fillets, $F \approx 1$ for solder attachments utilizing compliant leads,

h = solder joint height, for leaded attachments $h \equiv 1/2$ of solder paste stencil depth,

K_D = "diagonal flexural stiffness of unconstrained (not soldered) component lead, determined by strain energy methods or finite element analysis,

$2L_D$ = maximum distance between component solder joints measured from solder joint centers,

$N_f(x\%)$ = number of operating cycles to $x\%$ failure probability,

T_C, T_S = steady-state operating temperature for component, substrate ($T_C > T_S$ for power dissipation in component),

$T_{C,0}, T_{S,0}$ = lower steady-state operating temperature for component, substrate, for non-operational (power off) half-cycles $T_{C,0} = T_{S,0}$,

$\overline{T_{SJ}}$ = $(1/4)(T_C + T_S + T_{C,0} + T_{S,0})$, mean cyclic solder joint temperature,

t_D = half-cycle dwell time in minutes, average time available for stress relaxation at T_C/T_S and $T_{C,0}/T_{S,0}$,

x = acceptable cumulative failure probability for the component under consideration after N cycles, %,

α_S, α_C = coefficient of thermal expansion (CTE) for substrate, component,

β = Weibull shape parameter, slope of Weibull probability plot, typically 4 for stiff leadless attachments and 2 for compliant leaded attachments,

ΔT_C = cyclic temperature swing/excursion for component,

ΔT_e = $|(\alpha_C \Delta T_C - \alpha_S \Delta T_S)/\Delta\alpha|$, equivalent cycling temperature swing, accounting for component power dissipation effects as well as component-external temperature variations,

ΔT_S = cyclic temperature swing/excursion for substrate (at component),

$\Delta\alpha$ = absolute difference in coefficients of thermal expansion of component and substrate, CTE-mismatch, ΔCTE,

ε_f' = fatigue ductility coefficient, $2\varepsilon_f' \approx 0.65$ for eutectic and 60% Sn-40% Pb solder.

Equations 10 and 11 contain all the first-order parameters influencing the shear fatigue life of solder joints. They come from a generic understanding of the response of surface mount solder joints to cyclically accumulating fatigue damage resulting from shear displacements due to thermal expansion mismatches between component and substrate. These shear displacements cause time-independent plastic strains and time-, temperature-, and stress-dependent creep/stress-relaxation strains (References 1 and 23), which together on a cyclic basis form visco-plastic strain energy hysteresis loops whose area is indicative of the cyclical accumulating fatigue damage. In Equations 10 and 11, A, h, K_D, and L_D are physical design parameters, $\Delta\alpha$ depends on the material properties of component and substrate, ΔT_e reflects the component-external environmental and thermal conditions as well as the component-internal power dissipation, c

in Equation 12 accounts for the degree of completeness of the cyclically recurring stress relaxation process in the solder joints (the coefficients in c as well as ε_f' are dependent on the solder composition -- the values given are for 60% Sn-40% Pb and eutectic Sn-Pb solder), and β is the slope of the Weibull statistical failure distribution. In this context, failure is defined as the interruption of electrical continuity (>300 Ω) even for only very short durations (>1 μsec) (Reference 24). The "non-ideal" factor, F, is the only parameter reflecting specific design- and processing-induced influences on fatigue reliability and needs to be determined empirically from the difference in the predicted fatigue life from Equation 10 or 11 for idealized solder attachments (F = 1), and the fatigue life obtained empirically from appropriate accelerated testing. It should be noted that it is not altogether clear whether the F-values obtained from accelerated tests are necessarily the same for cyclic use environments, which typically allow more complete cyclic stress relaxation.

It should also be noted, that for leaded components with lead materials that have CTEs significantly lower than copper alloy materials, e.g. Kovar, Alloy 42, the results from Equation 11 will be optimistic, since the fatigue damage contributions from the solder/lead material CTE-mismatch are not included.

ESS PROCEDURE AND EFFECTS ON LONG-TERM RELIABILITY

For ESS procedures for weak solder joints, temperature cycling, perhaps even air-to-air thermal shock cycling, from room temperature to -40°C or below for five (5) to ten (10) cycles should be adequate to cause failure to grossly weakened solder joints without fracturing 'good' joints.

This ESS procedure would cause only negligible fatigue damage to 'good' solder joints based on Equations 9 through 11; depending on the design parameters, for most designs the ESS procedure suggested would consume less than 2% of the available solder attachment fatigue life.

Another possible ESS procedure is vibrational loading at temperatures of -40°C or below.

IMPROPER ESS PROCEDURES AND EFFECT ON LONG-TERM RELIABILITY

Unfortunately, ESS and verification procedures that have been applied do not always reflect the necessary understanding to accomplish the screening out of weak parts without jeopardizing good product.

Magellan/Galileo Spacecraft Solder Joint Failures

Fractured solder joints have been found in the Magellan/Galileo spacecrafts (Reference 25). The prime reason for these failures is the pre-launch exposure of the flight electronics to the thermal cycles given in Table 4 for the Magellan spacecraft. Some of this severe and extensive thermal

cycling is a direct result of the delays and mission changes necessitated by the Challenger disaster. The devices with solder joints most exposed to fatigue damage are 16 I/O ceramic DIPs manually converted to SM gullwing lead configurations, mounted to G-10 aluminum-backed circuit boards, and covered with Solithane conformal coating. For the calculations performed for the results in Table 4, the following design parameters were used: L_D = 10.1 mm\0.4 in, h = 0.13 mm\0.005 in, K_D = 35 N/mm\200 lb/in, A = 0.5 mm^2\800x10^{-6} in^2, $\Delta\alpha$ = 12 ppm/°C.

TABLE 4. Pre-Launch and Mission Thermal-Cycle Exposure for the Magellan Spacecraft Electronics.

Cause of Cycles	ΔT [°C]	T_0 [°C]	T_C, T_S [°C]	$\overline{T_{SJ}}$ [°C]	t_D [hrs]	Applied Cycles, N	Leadless $\overline{N_f}$ cycles	Leadless N_f (10%) cycles	Leadless % of Life	Leaded $\overline{N_f}$ cycles	Leaded N_f (1%) cycles	Leaded % of Life
Functional	85	0	+85	42.5	~24	9	45	16	56	180	21	43
Verification	65	+25	+90	57.5	~24	8	74	25	32	500	59	14
Thermal	50	+25	+75	50	~12	1	144	51	2.0	1 800	210	0.5
Tests	40	+25	+65	45	~12	1	240	86	1.2	5 000	600	0.17
Curing	25	+25	+50	37.5	~12	25	730	260	9.6	44,000	5 300	0.48
On/Off Test	15	+25	+40	32.5	~8	1 075	2 600	900	119	520,000	62,000	1.7
Test Sum	--	--	--	--	--	--	--	--	**220**	--	--	**60**
Space Mission	3	+25	+28	26.5	~6	4 000	115,000	40,000	**9.9**	980x10^6	118x10^6	**0.003**

While for the observed solder joint failures the high-thermal-expansion Solithane underneath the DIPs is the direct cause, it is the excessive thermal cycling which has a strong contributory effect. Because the leads of DIPs converted to SM gullwings are very stiff, it is not clear whether the resulting solder joints behave like compliant leaded solder attachments or stiff leadless attachments. Therefore, Table 4 shows the results of treading them as both attachment types. From the results it is evident, that these solder attachments do not behave like leadless joints; treating them as compliant leaded attachments produces reasonable results in line with the observed limited solder joint failures. The results show that while the actual space mission is indeed very benign as far as the solder attachments are concerned, about 60% of their life at a 1% failure probability level has been consumed by the testing. At the 0.1% failure probability level, life has been exhausted. It is clear that the rationale for these tests need to be reexamined.

SUMMARY

Some prior work on the reliability prediction for plated-through-hole-vias and surface mount solder attachments has been reviewed with the aim of of reliable high-density circuit boards. It has been shown that the reliability

of high-density circuit boards need to be assured by deliberate 'Design for Reliability' procedures. These, as well as the design of proper ESS procedures, require an understanding of the specific damage mechanisms threatening reliability. 'Design for Reliability' and ESS procedures for both PTH/vias and SM solder joints have been suggested. The detrimental effects of improper ESS procedures on long-term reliability of heretofore good product has been demonstrated.

---

1. Engelmaier, W., "Performance Considerations: Thermal-Mechanical Effects," in Section 6: Soldering and Mounting Technology, Electronic Materials Handbook, Volume 1, Packaging, ASM International, Materials Park, OH, 1989, p. 740.

2. Engelmaier, W., in "Round Robin Reliability Evaluation of Small Diameter Plated Through Holes in Printed Wiring Boards, " IPC Technical Report IPC-TR-579, The Institute for Interconnecting and Packaging Electronic Circuits, Lincolnwood, IL, September 1988.

3. Engelmaier, W., "The Use Environments of Electronic Assemblies and Their Impact on Surface Mount Solder Attachment Reliability," Proc. EIA/IPC Surface Mounting and Reflow Technology Conf.-SMART VI, Lake Buena Vista, FL, January 1990, p. 129; also in Proc. NEPCON/West '90, Anaheim, CA, February 1990, p. 1305.

4. "Round Robin Reliability Evaluation of Small Diameter Plated Through Holes in Printed Wiring Boards, " IPC Technical Report IPC-TR-579, The Institute for Interconnecting and Packaging Electronic Circuits, Lincolnwood, IL, September 1988.

5. Engelmaier, W., and T. Kessler, "Investigation of Agitation Effects on Electroplated Copper in Multilayer Board Plated-Through Holes in a Forced-Flow Plating Cell," J. Electrochemical Soc., Vol. 125, No. 1, January 1978,p. 36.

6. Engelmaier, W., "A New Ductility and Flexural Fatigue Test Method for Copper Foil and Flexible Printed Wiring," IPC Technical Paper IPC-TP-204, The Institute for Interconnecting and Packaging Electronic Circuits, Lincolnwood, IL, April 1978.

7. Engelmaier, W., "A Method for the Determination of Ductility for Thin Metallic Materials," Formability of Metallic Materials-2000 A.D., ASTM STP 753, J. R. Newby and B. A. Niemeier, eds., American Society for Testing and Materials, 1982, pp. 279-295.

8. Manson, S. S., Thermal Stress and Low-Cycle Fatigue, McGraw-Hill, New York, 1966.

9. Engelmaier, W., "Designing Flex Circuits for Improved Flex Life," Proc. 12th Electrical/ Electronics Insulation Conf., Boston, MA, November 1975.

10. Engelmaier, W., "Results of IPC Copper Foil Ductility Round Robin Study," IPC Technical Report IPC-TR-484, The Institute for Interconnecting and Packaging Electronic Circuits, Lincolnwood, IL, April 1986.

11. Iannuzzelli, R., "Predicting Plated-Through-Hole Reliability in High Temperature Manufacturing Processes," presented at IPC Annual Meeting, Boston, MA, April 1990.

12. "Flexural Fatigue and Ductility, Foil," IPC Test Method 2.4.2.1, IPC Test Methods Manual IPC-TM-650, The Institute for Interconnecting and Packaging Electronic Circuits, Lincolnwood, IL, August 1980.

13. "Standard Test Method for Ductility Testing of Metallic Foil," ASTM E 796, Annual Book of ASTM Standards, ASTM, Philadelphia, PA, 1981.

14. Miner, M. A., "Cumulative Damage in Fatigue," J. Applied Mechanics, Vol. 12, 1945.

15. Engelmaier, W., "Effects of Power Cycling on Leadless Chip Carrier Mounting Reliability and Technology," Proc. Int. Electronics Packaging Conf. (IEPS), San Diego, CA, November 1982, p. 15.

16. Engelmaier, W., "Functional Cycles and Surface Mounting Attachment Reliability," Surface Mount Technology, ISHM Technical Monograph Series 6984-002, The International Society for Microelectronics, Silver Spring, MD, 1984, p. 87

17. Engelmaier, W., and A. I. Attarwala, "Surface-Mount Attachment Reliability of Clip-Leaded Ceramic Chip Carriers on FR-4 Circuit Boards," IEEE Trans. Components, Hybrids, and Manufacturing Technology, Vol. CHMT-12, No. 2, June 1989, p. 284.

18. Clech, J-P., F. M. Langerman and J. A. Augis, "Local CTE Mismatch in SM Leaded Packages: A Potential Reliability Concern," Proc. 40th Electronic Components & Technology Conf., Las Vegas, NE, May 1990, p. 377.

19. "General Requirements for Soldering Electronic Interconnections," IPC Standard IPC-S-815B, The Institute for Interconnecting and Packaging Electronic Circuits, Lincolnwood, IL, December 1987.

20. "Acceptability of Electronic Assemblies," IPC Guidelines IPC-A-610A, The Institute for Interconnecting and Packaging Electronic Circuits, Lincolnwood, IL, February 1990.

21. Millard, D., "Performance-Related Solder Joint Inspection Results," presented at NEPCON/West '90, Anaheim, CA, February 1990.

22. Hall, P. M., "Strain Measurements During Thermal Chamber Cycling of Leadless Ceramic Chip Carriers Soldered to Printed Wiring Boards," Proc. 34th Electronic Components Conf., New Orleans, LA, May 1984, p.107.

23. Engelmaier, W., "Surface Mount Solder Joint Long-Term Reliability: Design, Testing, Prediction," Soldering & Surface Mount Technology, Vol. 1, No. 1, February 1989, pp. 14-22; also in IPC Technical Paper IPC-TP-797, The Institute for Interconnecting and Packaging Electronic Circuits, Lincolnwood, IL, January 1989.

24. Engelmaier, W., "Test Method Considerations for SMT Solder Joint Reliability," Proc. 4th Annual Int. Electronics Packaging Conf. (IEPS), Baltimore, MD, October 1984, p. 360; also in Brazing & Soldering, No. 9, Autumn 1985, p. 40.

25. Ross, R. G., "Magellan/Galileo Solder Joint Failure Analysis and Recommendations," JPL Publication 89-35 Galileo Report 1625-429, Jet Propulsion Laboratory, Pasadena, CA, September 15, 1989.

Werner Engelmaier is President, Engelmaier Associates, Inc., a firm that specializes in electronic packaging, interconnection and reliability consulting. He has almost 30 years' industrial experience in the U.S. and in Europe, including 24 years with AT&T Bell Laboratories. He has experience in reliability, manufacturing and processing aspects of electronic packaging for long service life and severe use conditions, such as telecommunications and the military; and design for reliability, accelerated reliability testing, reliability prediction, design for manufacturability and quality, processing effects, and environmental stress screening for solder joints, plated-through holes, and dynamically used flexible circuitry.

He has authored more than 80 technical publications in a variety of fields related to electronic packaging and interconnection technology, and has been awarded a number of patents in these areas. He was awarded the R&D 100 Awards in 1978 and 1981, the AT&T Bell Laboratories Distinguished Technical Staff Award in 1986, the Electronic Packaging Achievement Award in 1987, and the IPC President's Award in 1988.

Werner holds Mechanical Engineering degrees from Technologisches Gewerbe-Museum (TGM), Vienna, Austria, from the University of South Carolina, and from MIT. He chairs committees at IPC and ASTM, and is on the editorial advisory board of *Electronic Packaging & Production* magazine. He is a member of ASME, IEPS, and SMTA in addition to IPC and ASTM.

Address: Engelmaier Associates, Inc.
23 Gunther Street
Mendham, NJ 07945

CONTINUOUS QUALITY IMPROVEMENT IN ELECTRONICS MANUFACTURING: A CASE STUDY

by

Tony Christensen
Industrial Engineer
Rockwell International
Salt Lake City, Utah

ABSTRACT

This paper discusses methods and strategies used to achieve superior quality in electronics manufacturing at Collins Avionics and Communications Division (CACD) Rockwell International Division in Salt Lake City by the Automatic Direction Finder (ADF) assembly and test team. The attainment of only two defects per 148,909 possible error counts in a month's time is described. In particular, the methods used to sustain such quality performance in printed wiring board and antenna assembly applications are analyzed.

Assembly and inspection methods, aspects of the team concept, various psychological motivators, and the management approach used by the production team are discussed in detail. The paper describes methods for providing an open environment free from criticism, instilling a sense of ownership in an individual's work, and building quality into the product through self-inspection during the assembly and test process. Such practices result in sustained reliability, virtually eliminate rework, increase employee morale, reduce manufacturing cycle time, and lower operating costs in general.

Finally, the paper discusses how these concepts and guidelines can be applied universally in any electronics manufacturing industry with quality improvements similar to those experienced at CACD in Salt Lake City.

INTRODUCTION

The concept of Continuous Quality Improvement is one of continually striving to build a higher quality and more reliable product. At the same time, Continuous Quality Improvement means manufacturing the product at the least possible cost in the shortest amount of time. Both materials and processes must be uncompromising. In order to accomplish such a goal, it is essential to have the proper measurement tools, a firm management commitment, and an attitude of genuine ownership by all levels of employees.

Before launching into the strategies behind Continuous Quality Improvement utilized by Rockwell International in Salt Lake City, a brief description of the company's background is in order. Collins Avionics and Communications Division (CACD) Rockwell International Division in Salt Lake City manufactures a wide array of voice and data communication systems for ground, air, and sea applications. Radios and antennas are built from the printed wiring board stage up through the top level system. The Automatic Direction Finder (ADF) antenna built by the case study team is an airborne direction finder used by aircraft for course navigation, search and rescue operations, and relative direction to other aircraft. It receives AM signals in the VHF/UHF range and decodes the signals to provide relative bearing information.

The Automatic Direction Finder (ADF) Manufacturing Team exhibits all of the characteristics of Continuous Quality Improvement in their manufacturing efforts. The ADF Team achieved a quality rating of 0.01* against a goal of 0.80, experiencing only two defects per 148,909 possible error counts in a month's time during June of 1990. Furthermore, the team has continued to maintain a high level of quality for over a year's time.

GOAL SETTING

The first step in achieving Continuous Quality Improvement is the setting of goals by all members of the manufacturing team. It is critical that all members have the opportunity for direct input. If one person is left out of the plan, the goal cannot be achieved. An initial kickoff meeting should be held where all concerns are brought before the group and meaningful goals are set. It's not imperative

---

* Quality Rating =
(Total Workmanship Defects/Possible Error Counts) * 1000

that every person sit in on the goal setting meeting, as long as each person can provide their input to a team representative. The goals should be challenging, yet attainable. In addition, each goal should have a means whereby it can be accomplished and by whom. All team members should offer their unwaivering commitment to the goals that are established by the team. And finally, it should be emphasized that each team member will be held accountable for their specific role necessary for the achievement of the goals.

For the ADF team the key to the goal setting was the mutual agreement and commitment between the assembly, test, and inspection areas of the team. It was this commitment that led to complete team cooperation and expeditious problem solving among all team members.

TEAM SUPPORT AND CONSISTENCY

After the goals are established and agreed upon, the work can begin. Immediately key relationships among team members take effect. The assembly line lead begins interaction with the assembly line inspector to resolve workmanship problems; the assembly operators are continually trained by the assembly lead; the manufacturing electrical engineer assists the test technician in troubleshooting a test problem; the production coordinator and the assembly supervisor plan the week's manufacturing schedule. These are but a few of the many critical interactions that must take place in order for the Continual Quality Improvement process to work. Figure 1 illustrates the team players and how their efforts are directed towards the central goal of Continuous Quality Improvement. What is the role of management? Management is standing off to the side observing the workings of the team members, acting more as a cheerleader than as a coach. If a serious problem occurs, management can intercede, acting only to bring the team back on track to function as normal. Ideally, if the team performs well over an extended period of time, the team becomes self-directed and the management function can be eliminated.

In Salt Lake City this concept has come one step closer to reality with the establishment of autonomous Action Management Teams (AMT's). AMT's consist of assemblers, inspectors, test technicians, supervisors, production coordinators, and support engineers (industrial, manufacturing electrical, and quality assurance engineers). All critical manufacturing decisions are made by members of the AMT, with minimal management intervention.

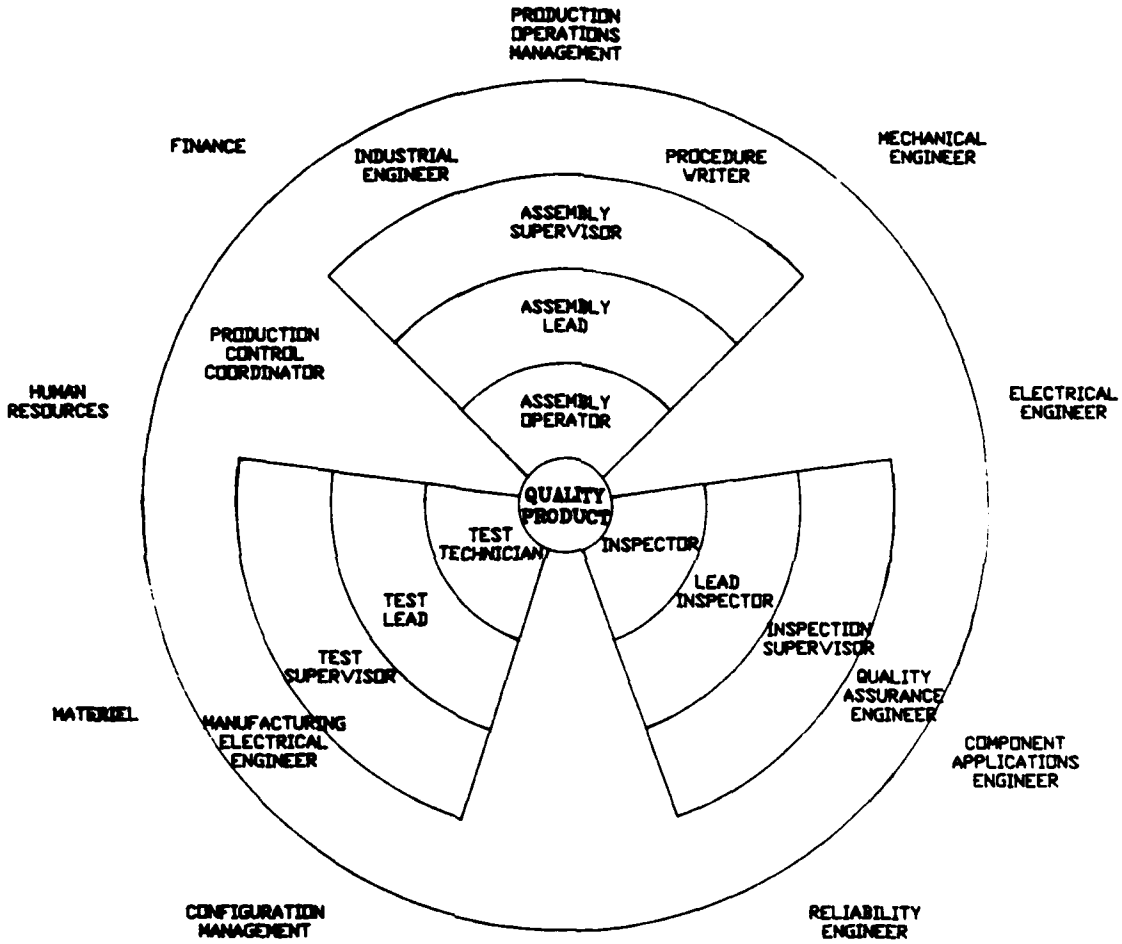

FIGURE 1. The Action Management Team Organizational Chart.

The key to proper team functioning is a commitment to fairness, consistency, and support from all team members for one another. Personal differences and individual preferences must be put aside to allow the team to completely focus on manufacturing a quality product.

TEAM RESPECT AND RECOGNITION

A comment that is continually made by each member of the ADF team is the importance of respect from other team members and respect from persons outside of the team.

First, respect among team members: Each team member understands that their work will not only be seen by the inspector, but by their fellow team members. Therefore, they take great pride in their workmanship and build quality into their work the first time around. They realize, however, if a defect they caused is discovered by another team member, it is the responsibility of the discoverer to help the person who made the defect correct it. Both persons learn from the mistake. This is the process of Continuous Quality Improvement.

Support and respect for the team leader is also important. To achieve this, the team leader should be an elected position, not an appointed one, thereby providing the team leader with the mutual support and respect he needs from the team members when making critical decisions.

Second, respect from people outside the team: Each month a quality achievement award is given to the team exhibiting the highest quality for that month. The winner receives a pizza lunch in their honor and their team's name is placed on a traveling plaque. The two teams with the next highest quality are also invited to share in the honors. Such high visibility instills a sense of pride and motivation for all team members to attain the quality award. Even more important than the award itself, is the respect received for achieving the highest quality in the plant.

ELIMINATING ADVERSARIAL RELATIONSHIPS

Along with establishing mutual trust among team members, is the need to eliminate adversarial relationships. For many who are accustomed to giving loyalty to a particular department (i.e., manufacturing, test, quality assurance, etc.), sacrificing this loyalty to the Action Management Team can be a difficult adjustment.

Most noticeable at CACD was the division between assembly and inspection. For the ADF team this division was ultimately overcome by working together and striving for complete cooperation. When the inspector discovered a negative trend or potential problem, she felt free to approach the lead assembler. The lead assembler learned to take the inspector's suggestion constructively and addressed the problem with her assemblers. Such a working relationship is not achieved overnight. First, the inspector and lead assembler must become more in tune to efficient means of reducing, correcting, and eliminating defects as opposed to the discovery of defects. The role of the assembler becomes one of assembly and self-inspection. The role of inspector becomes one of inspecting assembly processes rather than product defects.

In certain instances, incompatibilities between individual team members may be impossible to overcome. In this case it is wise for management to consider moving one or both people to another team.

OWNERSHIP

The key driver behind motivating the employee to build a quality product is to instill a sense of ownership. Every team member must have a genuine interest and concern that their job is critical to the success of the team's goal of building a quality product.

First, the worker must have increased autonomy. The workers must feel that they are in control of their job. No one works well with someone constantly looking over their shoulder. It is essential to remember that all employees, from the plant manager to a new assembly operator, feel that they are paid to think; not to merely follow instructions. Therefore, the assembly operator must be given opportunities to provide input for the improvement of their work methods. This causes the person to constantly be thinking "improvement". If they discover a better way to use a tool or a more efficient sequence to build an assembly, that idea should be incorporated. Who knows the product better than the operator who builds it or tests it? Also, employees must be given more responsibility as they become more skilled and capable. Along with responsibility comes accountability. The worker or team must account for their own work accomplished and offer corrective action for mistakes made.

The ADF manufacturing team building the F-15 Antenna provides a prime example of achieving individual and team ownership. With the start-up of a new contract, the team felt a need to properly prepare for the challenges that accompany a new contract. First, a kickoff meeting was held

involving members from each area of the manufacturing process (i.e., assembly, inspection, and test). At this meeting key issues and potential problems were identified and action items were assigned with the responsibility for follow-up. As production began, the assembly operators freely approached their industrial engineer with new ideas for improved forming tools, better methods of foam potting, and various other ideas that improved quality and reduced cycle time. The finish requirements for the antenna called for a special chem-film and painting process, necessitating that Rockwell go to an outside paint shop. As potential problems arose at the paint shop, the team would work closely with them, oftentimes sending their engineers or machinist in person to resolve the problems. Thus the concept of Continuous Quality Improvement was evidenced in the F-15 Antenna program by full team involvement.

FULL INVOLVEMENT OF TEST

In the ADF team another critical team player is the test technician. Passing or failing test usually means the difference between selling a radio or sending it back for troubleshooting and possible rework. Therefore, the insight and experience of the test technician is invaluable to the Continuous Quality Improvement process. To optimize this insight, communication lines between test and assembly must always be clear and open. The test technician may discover a component or workmanship flaw that can be corrected in assembly by simply altering an assembly technique. If communication lines are clear, this bit of valuable information can be passed along without losing valuable manufacturing time and money. Indices such as first pass rate can provide a measurement of the effectiveness of this communication line. Again, in order for effective communication, both sides must be open to constructive criticism and suggestions, realizing that constructive criticism is not directed at the individual, but for the betterment of the entire team.

STRIVING FOR CONTINUAL IMPROVEMENT

The concept of Continuous Quality Improvement is based on the idea that no matter how outstanding our quality results, we should never be satisfied. There are always ways we can improve. If we continually meet or surpass our quality goal, that goal should be continually increased.

For example, several years ago at Rockwell in Salt Lake City a significant increase in quality defects in a certain product group was noticed. The concern arose that schedule was taking priority over quality. Therefore a program was

established to help improve the quality of the product. This program consists of several flashing lights located at lead assembler and inspector stations throughout the manufacturing floor. It was decided that when an assembly passed through the line that contained three or more major defects or a "line-stopping" defect, the lead assembler or inspector was to turn on the flashing light and production would stop. This would alert the appropriate team members (engineers, supervisors, technical writers) to go to the lead or inspector, evaluate the problem, and assign corrective action items. The light was to stay on until the action items were assigned.

This system serves several purposes. One, it helps to reduce quality defects by alerting the appropriate personnel when a problem arises. Two, it reduces the time in which quality problems are solved. And three, it places ownership and control in the hands of the assemblers and inspectors. They soon realize that when they see a problem, help is readily available and the problem will be fixed. One other interesting phenomena resulted from the flashing lights. At first, the occurrence of flashing lights was quite regular, about three per week for each product group. Then the frequency decreased (in other words, quality improved). As a result, the criterion were tightened to only two major defects or a "line-stopper" warranting a light. And again in time, the frequency of lights decreased. The criterion was then tightened once more. Thus, the concept of continuous quality improvement was in action.

DAILY COMMUNICATION AND FEEDBACK

The key to a successful team is free and open communication. For communication to be effective, it must flow freely between all team members. For instance, when an assembly operator notices a parts problem, they must feel free to approach their lead, supervisor, or engineer with the problem. In the communication process the responsibility lies with both parties; the sender must feel at ease to communicate the problem, and the receiver must be willing to listen to the problem and commit to a response. This response may come in the form of an immediate solution or a reply that a solution is not immediately available, but will be provided in a reasonable period of time.

Another important ingredient to effective team communication is regular feedback. An assembler or technician cannot correct their mistakes or make improvement if they do not receive regular feedback on how they are performing. This feedback can come in many ways; verbal feedback from a supervisor or daily reports listing results from the previous

day. The key is for the feedback to be constructive and consistent. At Rockwell, each operator receives a daily efficiency report from the previous day detailing by assembly number how quickly the operator performed their task compared to a goal. A similar daily report is provided for quality indicating how many defects per possible errors were committed by each operator by assembly. These reports are to enable the operator to track their progress and positively identify any problems they are experiencing. Again, consistency is the key.

COMMITMENT TO SUPERIOR ATTENDANCE

Another ingredient to achieving superior quality on the ADF line was a commitment by each operator to superior attendance. This proves important in several ways. First, without the operator in attendance, the job will not get done. Second, in order for the operators to achieve any degree of proficiency on a learning curve, they have to continually build assemblies and learn by experience. Third, if the team is working together and practicing the system of continuous quality improvement, the employee will naturally want to go to work because they will be gaining instrinsic motivation from their work. Finally, in addition to the intrinsic motivation of the job itself, the company offers superior attendance awards and recognition to those employees who exhibit perfect attendance for a given time period.

COOPERATION AND COMMITMENT FROM THE CUSTOMER

In the Defense Electronics business we have the opportunity of working with an in-house customer. The purpose of the in-house customer is to monitor and assist us in the manufacturing process. The customer is there to help us assure that the product we build is of the highest quality. In order for this to occur, an effective working relationship must be developed between the manufacturer and the customer. At Rockwell this strong working relationship has been manifested by the openness that exists between the two parties. If the customer observes a process or product problem, they make every effort to positively approach us before it becomes a serious problem. As the manufacturer, we have the responsibility to be open and responsive to the customer's requests. For example, if a potential electrostatic discharge (ESD) problem arises, we work together with the customer until a solution is in place. Both parties benefit and a higher quality product is the result.

PRODUCT AND BUSINESS LONGEVITY

What happens when we consistently build a quality product that satisfies our customer? The ADF team knows that new business and increased contracts result. Each operator must understand that as their quality improves, they are ensuring their job security. The means to accomplish this end is by building a solid reputation of integrity with the customer. Only when the customer knows that they can rely on you, the manufacturer, for a quality product on schedule, will they return to you with their business.

CREATING A LOW STRESS ATMOSPHERE

In order for Continuous Quality Improvement to be effective at the employee level, the employees must enjoy their job. The entire system can backfire if the employee is placed under too much pressure and stress. Granted, there will be times when stress is high, but there must be a means of relieving that stress so that no one breaks. First, each team member must have a sense of humor and the ability to laugh at themselves. A light moment can go a long way in alleviating a stressful situation. Second, and most important, each team member must have respect for one another. Each person must have the understanding that the other is skilled and qualified for their job, yet is also capable of making mistakes.

If these two ingredients exist, a chemistry among the team members develops. Communication flows freely and problems are solved more easily.

CONCLUSION

Continuous Quality Improvement is a universal concept that can be applied to virtually any firm or industry. If consistently applied, the concept of Continuous Quality Improvement results in sustained product reliability, elimination of rework, increased employee morale, and customer satisfaction. The successes experienced by the ADF manufacturing team at Rockwell International Salt Lake City were achieved by applying simple practices that ensured open communication and team cohesiveness. Such practices require total team commitment and involvement. Only then can the rewards of superior quality be realized.

Anthony Christensen is an Industrial Engineer with the Collins and Avionics Communications Division of Rockwell International. His work involves the areas of quality improvement, methods improvement, and work measurement. He is a member of the group that received his company's Division Quality Award and Division Performance Award.

Tony received a BS degree in Industrial Engineering from the University of Utah and is currently pursuing studies toward a Master's degree in Business Administration at Westminister College in Salt Lake City.

Address: Rockwell International
Collins and Avionics Communications Division
5520 West Harold Gatty Rd.
Salt Lake City, UT 80000

A PROPOSED NEW TEST METHOD FOR MEASURING THE SOLDERING POWER OF STANDARD & FUTURE SOLDER PASTE FORMULATIONS

by
W. G. Kenyon, D. J. DiGuglielmo, A. Jennings & S. S. Spangler

I. INTRODUCTION:

Standard wetting balance methods adequately assess the soldering power of liquid rosin, synthetic and water soluble fluxes for soldering leaded and leadless components to plated-through hole and mixed technology surface mount boards,

In contrast, the only method available to measure solder paste soldering power

- requires multiple replications
- may not be suitable for recent solder paste formulation innovations.

A new method is needed that meets the following criteria:

- accurate indication of flux activity
  (traditional and new formulations)
- reliable, reproducible data
- very short interval between successive tests.

In this paper, a new method will be proposed and contrasted to the method presently available. In addition, a thorough description of the procedure and materials employed will be provided.

II. KEY CONCLUSIONS:

After carrying out both procedures and contrasting the data, these key conclusions can be drawn:

- *The proposed method is more accurate, since it provides a true* assessment of flux activity at the time of reflow, instead of after a prolonged heating period above the liquidus temperature.
- Minimal degradation of the flux portion occurs during the very short test time, thus the method is suitable for use with newer concepts in solder paste flux formulation.
- The method is efficient, yielding precise and reproducible results.

Although developed on one type of wetting balance, it is presumed that the method could be adapted to other types of instruments.

III. DISCUSSION:

The discussion section has been subdivided into two sub-sections,

1.) Test Program
2.) Results

The Test Program portion contains details on

a.) Test Speciment Preparation
b.) Aluminum Crown Preparation
c.) Materials
d.) Test Equipment

while the results section describes how to evaluate the data generated and how to obtain an adequate assessment of soldering power for various pastes.

Test Program

1 . Test Speciment Cleaning & Preparation: Gloves must be worn at all times when buffing and handling the 18 gauge copper wire test specimens. The wire is hand polished with "000" grade steel wool (very fine) until it becomes shiny. Following the buffing of the wire, it should be thoroughly rinsed with distilled water, then blotted dry on a paper towel. Finally, cut the wire into 25.4 mm (1") lengths with pre-cleaned wire cutters and store them in a desiccator prior to use.
Initially, two types of wire were used in this study, 18 and 24 gauge copper wire. However, it has been found that the use of the 18 gauge copper wire enables better wetting and thus more precise data.

2.) Aluminum Crown Preparation: Several layers , (approximately 8), of folded commercial aluminum foil will be needed for the construction of the aluminum crowns used to contain the solder paste during the test. A large hole punch is used to cut out a circle of foil. A smaller hole punch is used to cut out the center of the circle referred to above. The aluminum foil ring is then formed into a cup or crown that is used to contain the solder paste during the test. It must be confirmed that the crown fits tightly around the top of the post before initiating the test. In addition, only one crown is used per test.

3.) Materials: The solder pastes used in the development and evaluation of this test method are collected in Chart I. Solder pastes representative of several different flux chemistries were obtained and tested to evaluate the usefullness of the method on both present and future formulations. In addition, the tester should ensure that the melting point of the alloy in the test paste is within the operational range of the test instrument.

CHART I

REPRESENTATIVE SOLDER PASTES

NAME	CLASS	TYPE	CLEANING AGENT
WS-1	WATER SOLUBLE	Not App.	WATER
WS-2	WATER SOLUBLE	Not App.	WATER

4.) Test Equipment:

a. A Multicore Universal Solderability Tester (MUST) fitted with the Globule Test Block with an IBM AT (or equivalent) computer and Mustmate 110/210 solderability software (version 2.0) was used to develop the test.

b. Two concentric hole punches , 13/16 inch and 5/16 inch diameter, are needed to construct the aluminum crowns.

c. Spatulas, 3 cc syringes, and swabs are necessary for dispensing the solder paste onto the top of the globule block.

d. Wire cutters, two pairs of sizeable tweezers, Freon® TMS degreased steel wool and a small desiccator are needed for cleaning , handling, and storing the copper wire.
(It is anticipated that alcohol could be substituted for the CFC solvent).

C. Results

1.) Overview of Data: Graph 1. contains collected data obtained by the present method, displayed as the mean +/- one standard deviation. The complete data set for this test is collected in Table I. Each run of the present methodtakes approximately 8 min. 30 seconds. To qualify as a good paste, the time to cross the zero line must be under 2.5 seconds ; the shorter this time, the higher the ranking of the paste.

Table I

Replications of Solder Paste WS-1 Using Current Method

Test Nbr.	Ta, sec.	Tb, sec.	F at T1 mN/mm	T to 2/3 Fmax sec.	Dewetting % of Fmax
1	0.80	1.74	1.07	2.19	0
2	0.80	1.66	1.08	2.69	0
3	0.80	1.57	1.09	2.12	0
4	0.80	2.04	1.04	3.07	0
5	0.80	1.72	1.07	2.36	0
6	0.80	2.11	1.03	3.10	0

As can be seen by comparing tables I ,II and III, the present method produced ambiguous results for the ranking of the pastes from examination of the Tb values.

Table II

Replications of Solder Paste WS-2 Using Current Method

Test Nbr.	Ta, sec.	Tb, sec.	F at T1 mN/mm	T to 2/3 Fmax sec.	Dewetting % of Fmax
1	0.80	5.00	0.98	5.00	0
2	0.80	4.10	1.01	5 11	0
3	0.80	1.86	1.06	3.37	0
4	0.80	1.79	1.06	2.78	0
5	0.80	1.69	1.07	3.15	0
6	0.80	1.67	1.08	2.54	0

Table III

Replications of Solder Paste WS-2 Using Current Method

Test Nbr.	Ta, sec.	Tb, sec.	F at T1 mN/mm	T to 2/3 Fmax sec.	Dewetting % of Fmax
1	0.80	5.00	1.00	5.00	0
2	0.80	1.89	1.06	3.39	0
3	0.80	1.77	1.06	3.02	0
4	0.80	1.90	1.05	3.36	0
5	0.80	1.94	1.05	3.29	0
6	0.80	2.07	1.04	3.18	0

Additionally, in analyzing Graph 1. , there is no noticeable tracking of the effects of degradation of flux during the lengthy test procedure.

Table IV

Replications of Solder Paste WS-1 Using Proposed New Method

Test Nbr.	Ta, sec.	Tb, sec.	F at T1 mN/mm	T to 2/3 Fmax sec.	Dewetting % of Fmax
1	0.80	1.74	1.07	2.19	0
3	0.80	1.57	1.09	2.12	0
4	0.80	2.04	1.04	3.07	0
Mean	0.80	1.72	1.07	2.36	0
Std.	0.08	2.11	1.03	3.10	0

Table V

Replications of Solder Paste WS-2 Using Proposed New Method

Test Nbr.	Ta, sec.	Tb, sec.	F at T1 mN/mm	T to 2/3 Fmax sec.	Dewetting % of Fmax
6	0.40	0.60	0.25	1.70	3
8	0.40	0.69	0.24	1.03	3
9	0.40	0.73	0.27	1.68	3
Mean	0.40	0.67	0.25	1.47	3
Std.	0.00	0.05	0.01	0.31	0

Graphs 2 & 3 contains collected data obtained per new method. The results of the three separate replicate tests performed on pastes WS-1 and WS-2 are displayed in Tables IV and V, respectively. As can be seen by the precision and accuracy of the results, three separate tests done per new method engendered an identical ranking of the two pastes. The test time for each run is approximately 5 seconds. Also, by analyzing the data in Graph 4. , it is seen that the new method clearly displays the effects that a prolonged testing time has on the degradation of flux. For example, in this experiment, the same sample of paste WS-1 was tested after 10, 45, 80 and 130 seconds of heating on the globlule block (see Table VI for corresponding data).

Table VI

Effect of Heating on Solder Paste WS-2 Using Proposed New Method

Test Nbr.	Ta, sec.	Tb, sec.	F at T1 mN/mm	T to 2/3 Fmax sec.	Dewetting % of Fmax
39	0.40	0.55	0.24	1.05	2
40	0.95	2.00	0.10	4.00	4
41	0.79	2.10	0.11	4.35	2
42	4.53	5.00	-0.04	5.00	0
Mean	1.67	2.41	0.10	3.60	2
Std.	1.66	1.61	0.10	1.52	1

2.) Evaluation of Data: According to Mil. Std. 883, Method 2022[4] good wetting is established when the graphed line passes 2/3 F/max in 1 second. This standard, suited for the testing of fluxing action and wettability is not applicable for solder paste testing. The standards for evaluating the results of solder paste tests will be according to the IEC-68-2-54[3] document. The specified requirements under these standards are: time to cross zero line must be under 2.5 seconds and a suitable time to cross 2/3 Fmax must be achieved . If these criteria are met, the paste under study will be considered a good paste. The shorter the time frame for each criteria to be achieved, the better the paste.

IV. SUMMARY:

The proposed new method will offer greater flexibility to the electronics industry for evaluating present and future solder paste formulations.

- The proposed method for solder paste testing is more precise, accurate, and efficient.

- The present method uses an extremely long testing time which allows the flux to decay therefore, a true assessment of fluxing activity is not obtained.

- The proposed method uses 5 seconds as a test time, hence very little degradation occurs and a true evaluation of fluxing activity is obtained.

- The present method sometimes yields ambiguous results whereas the new method run in triplicate yielded the same conclusions.

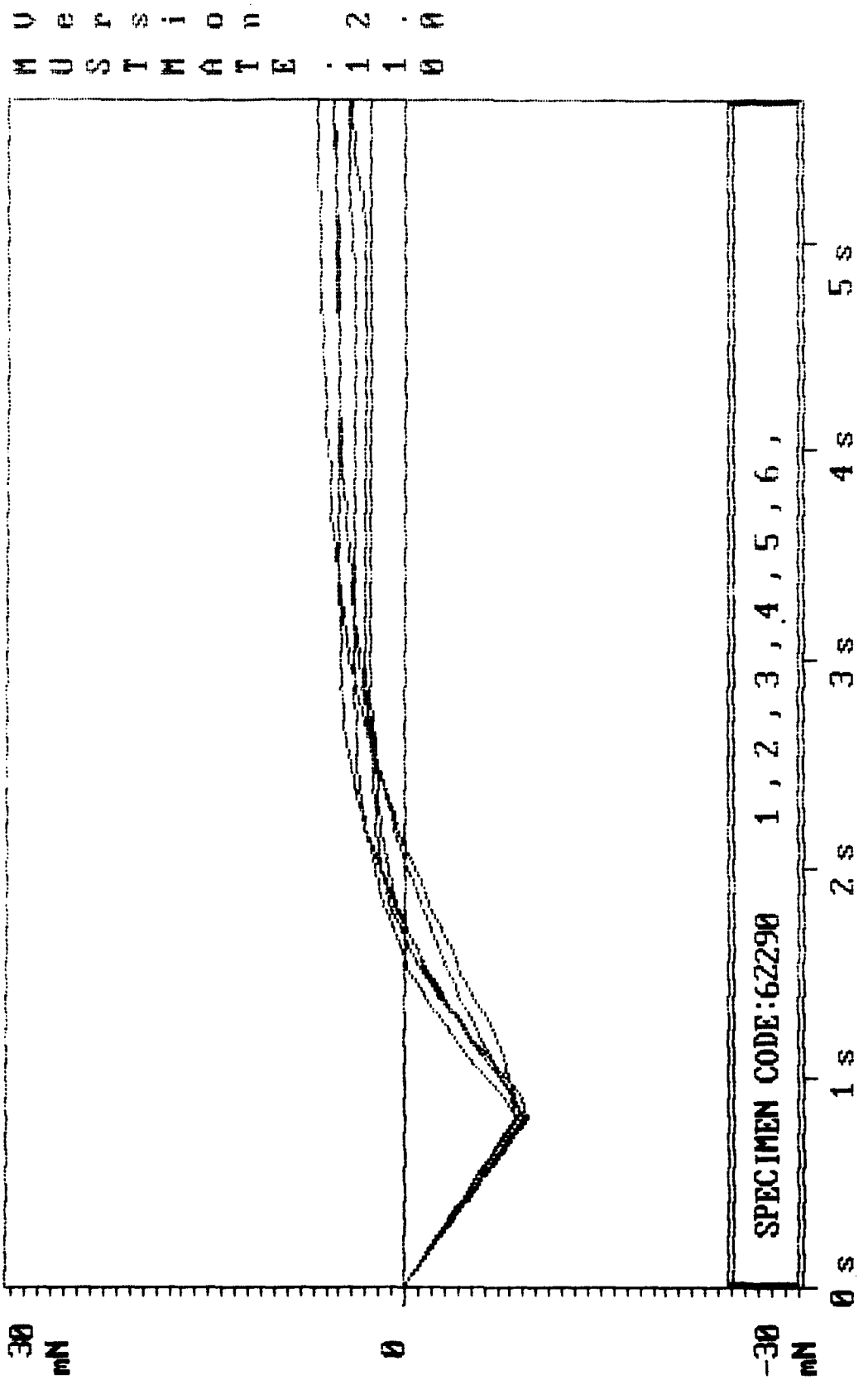
Version 1.2.1.0
30 mN
0
-30 mN
0 s
1 s
2 s
3 s
4 s
5 s
SPECIMEN CODE:62290 1 , 2 , 3 , 4 , 5 , 6 ,
1 , 2 , 3 , 4 , 5 , 6 ,

Graph 1

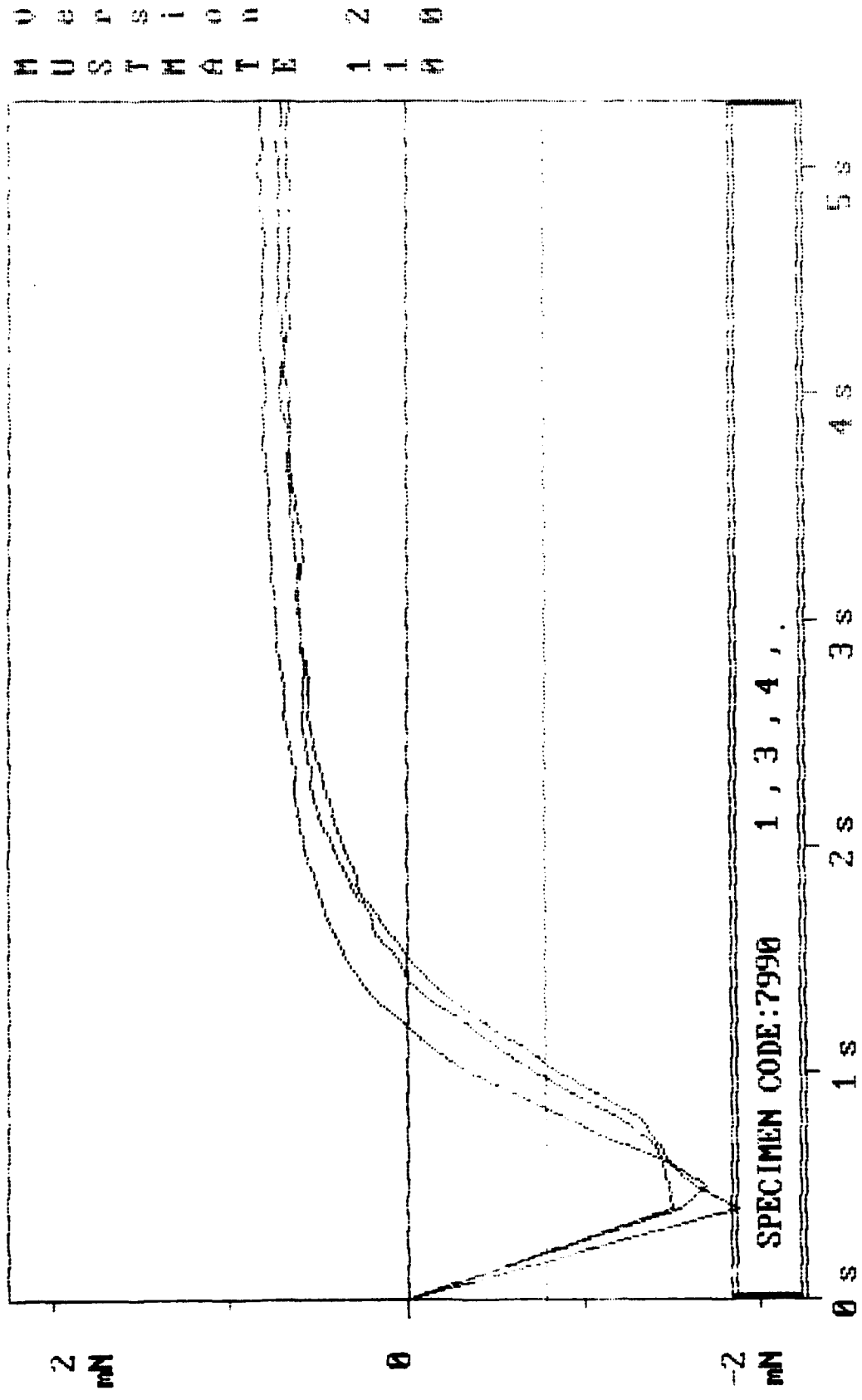
Deflection 12 in
2 mN
0
-2 mN
0 s
1 s
2 s
3 s
4 s
5 s
SPECIMEN CODE:7990 1 , 3 , 4 , ,
, 3 , 4 ,

Graph2

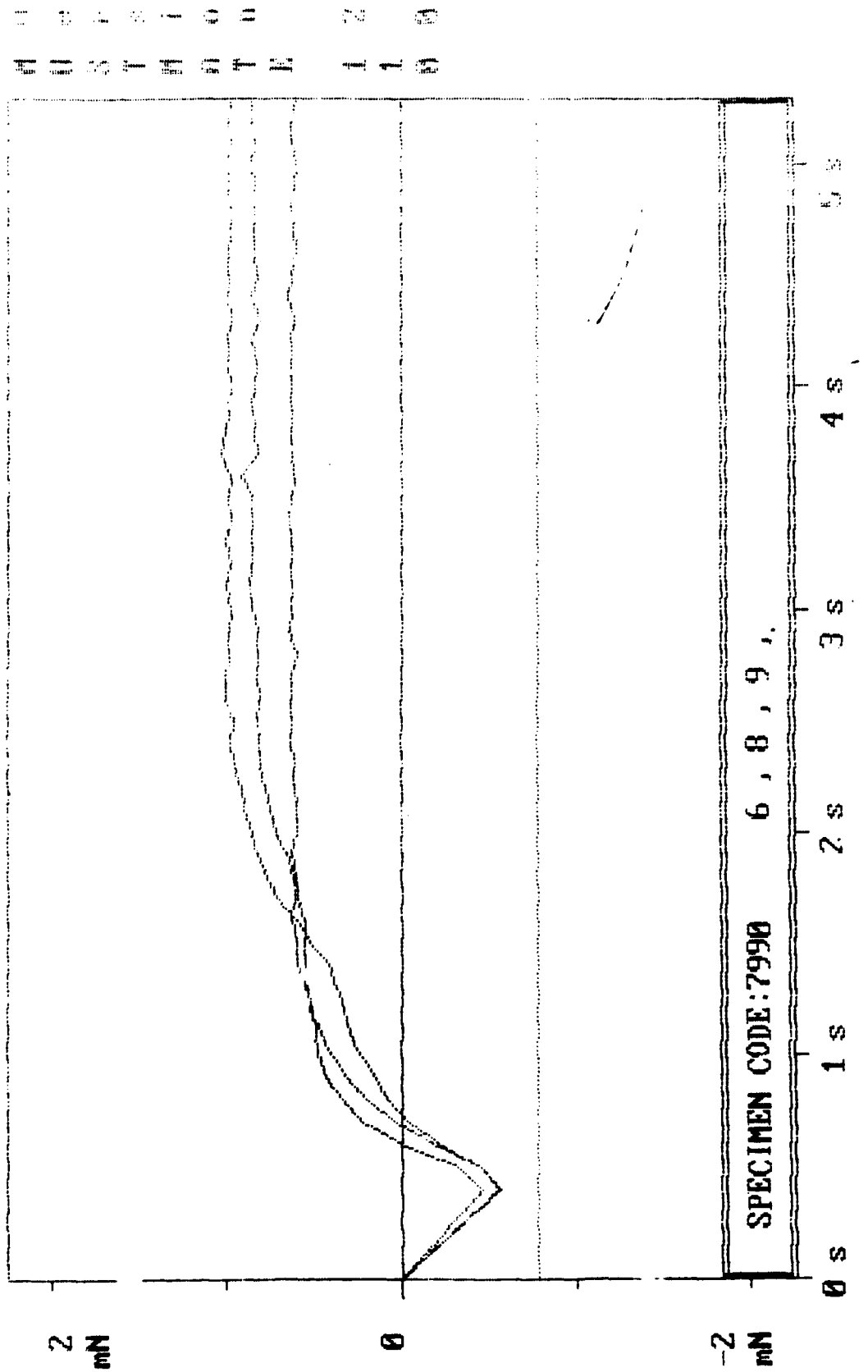

6,8,9,

Graph 3

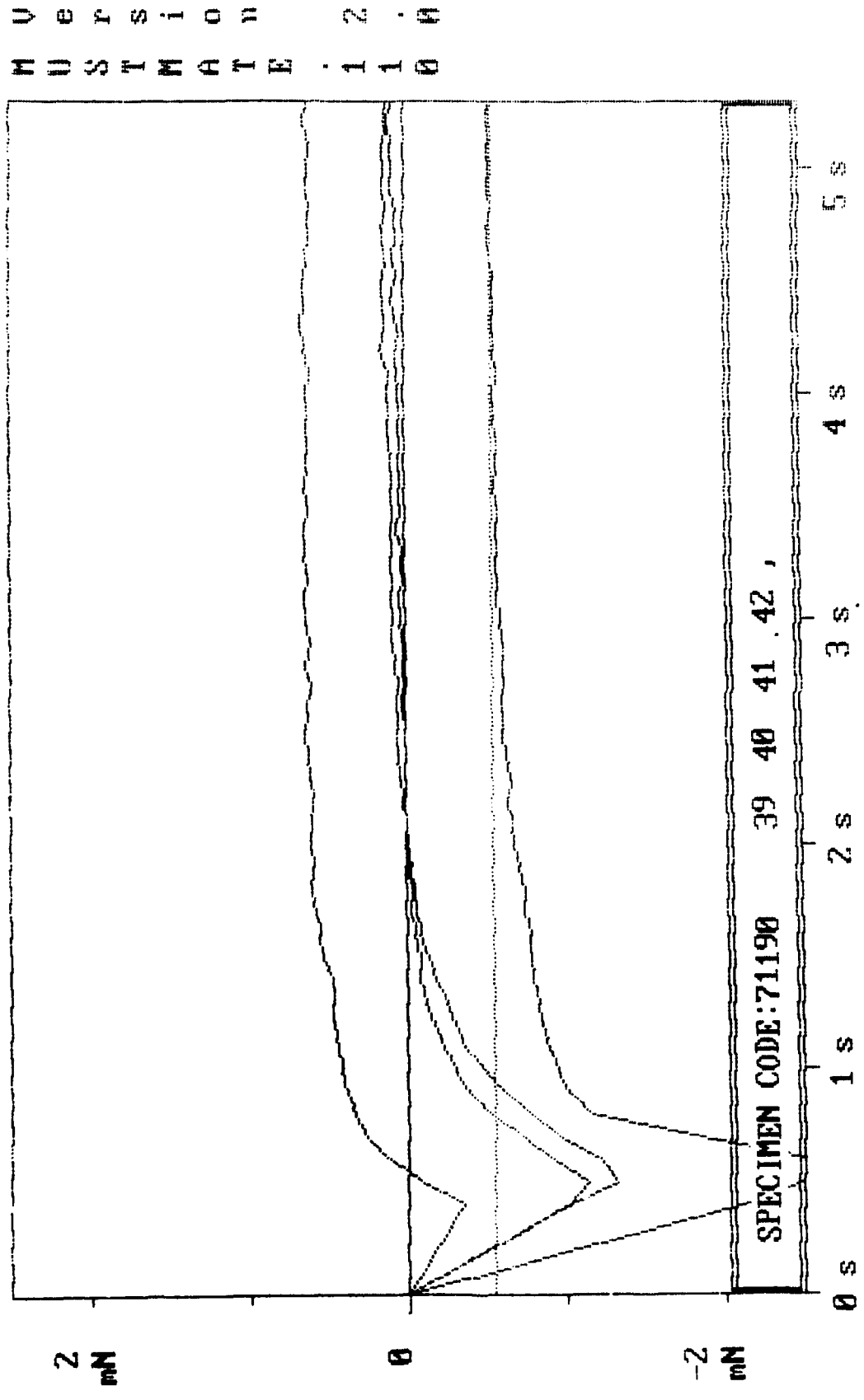
Version 2.10A
2 mN
0
-2 mN
0 s
1 s
2 s
3 s
4 s
5 s
SPECIMEN CODE:71190 39 40 41 42,
9, 40, 41, 42,

Graph 4

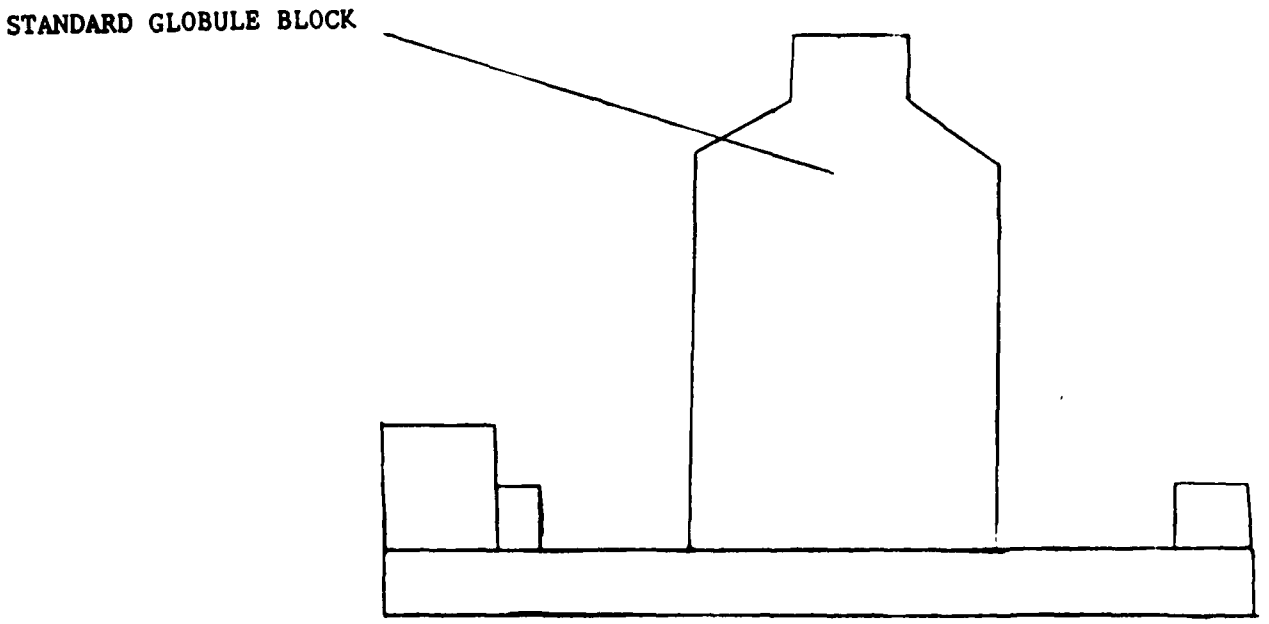

diagram a.

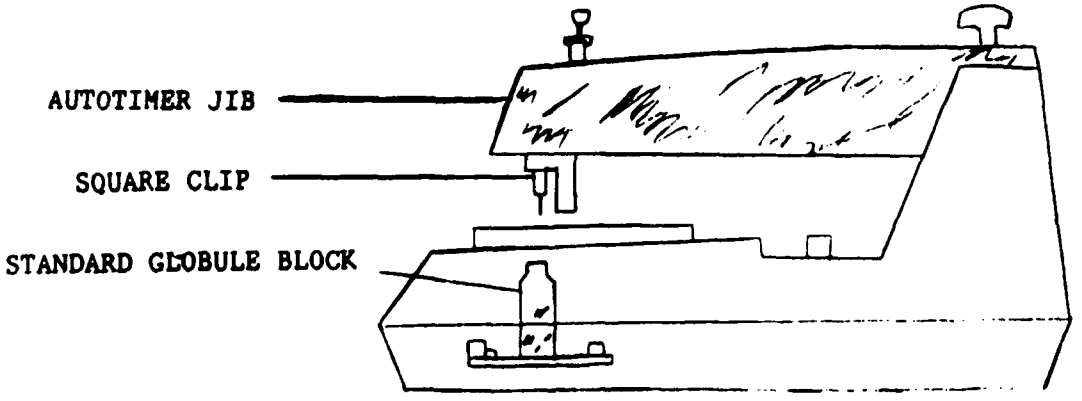

diagram b.

SIDE VIEW

diagram c.

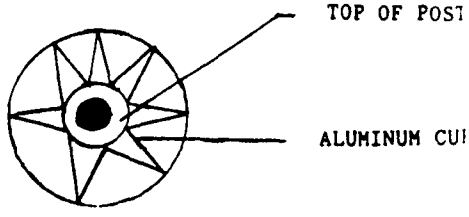

TOP VIEW

diagram d.

diagram e.

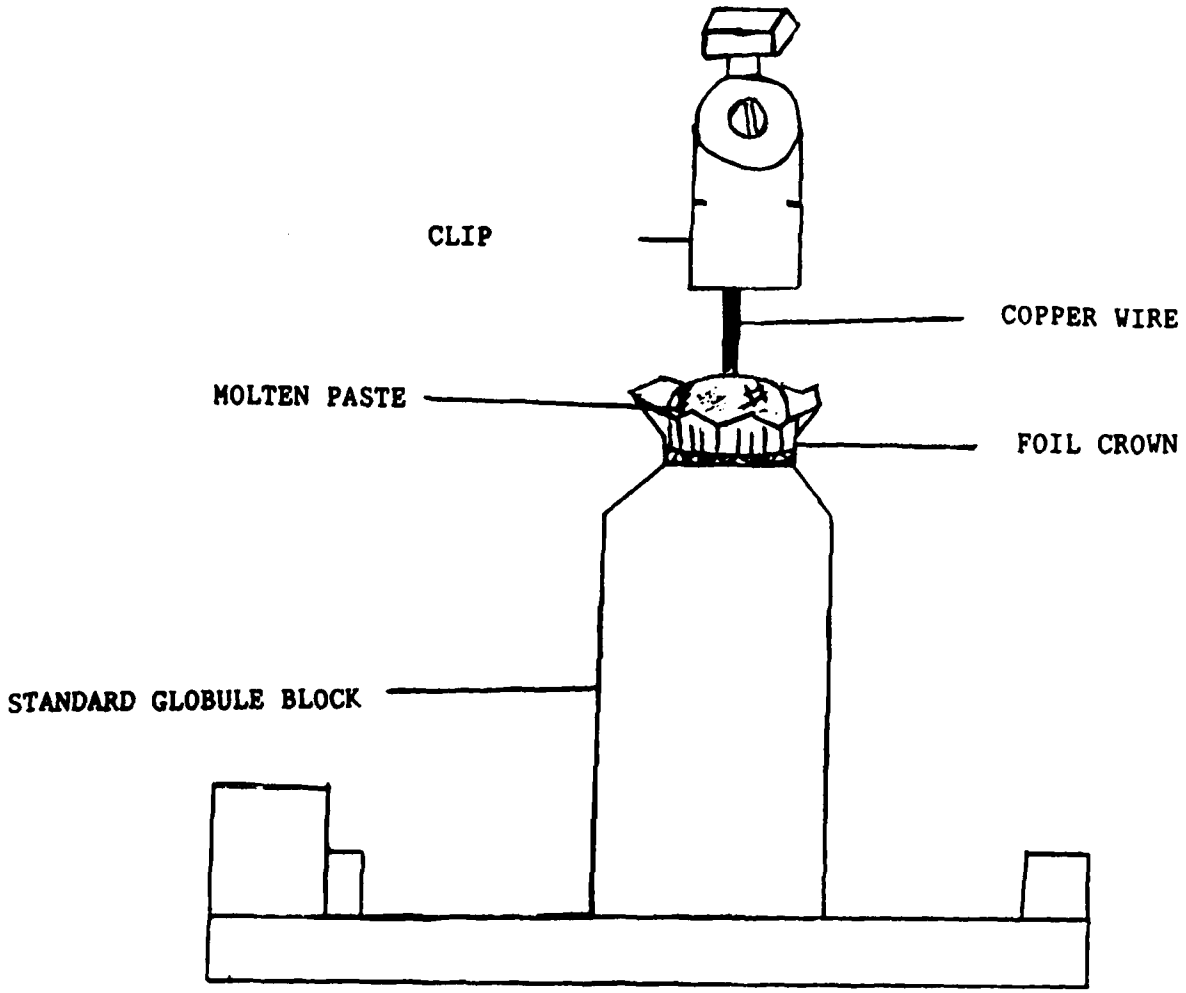
CLIP
COPPER WIRE
MOLTEN PASTE
FOIL CROWN
STANDARD GLOBULE BLOCK

diagram f.

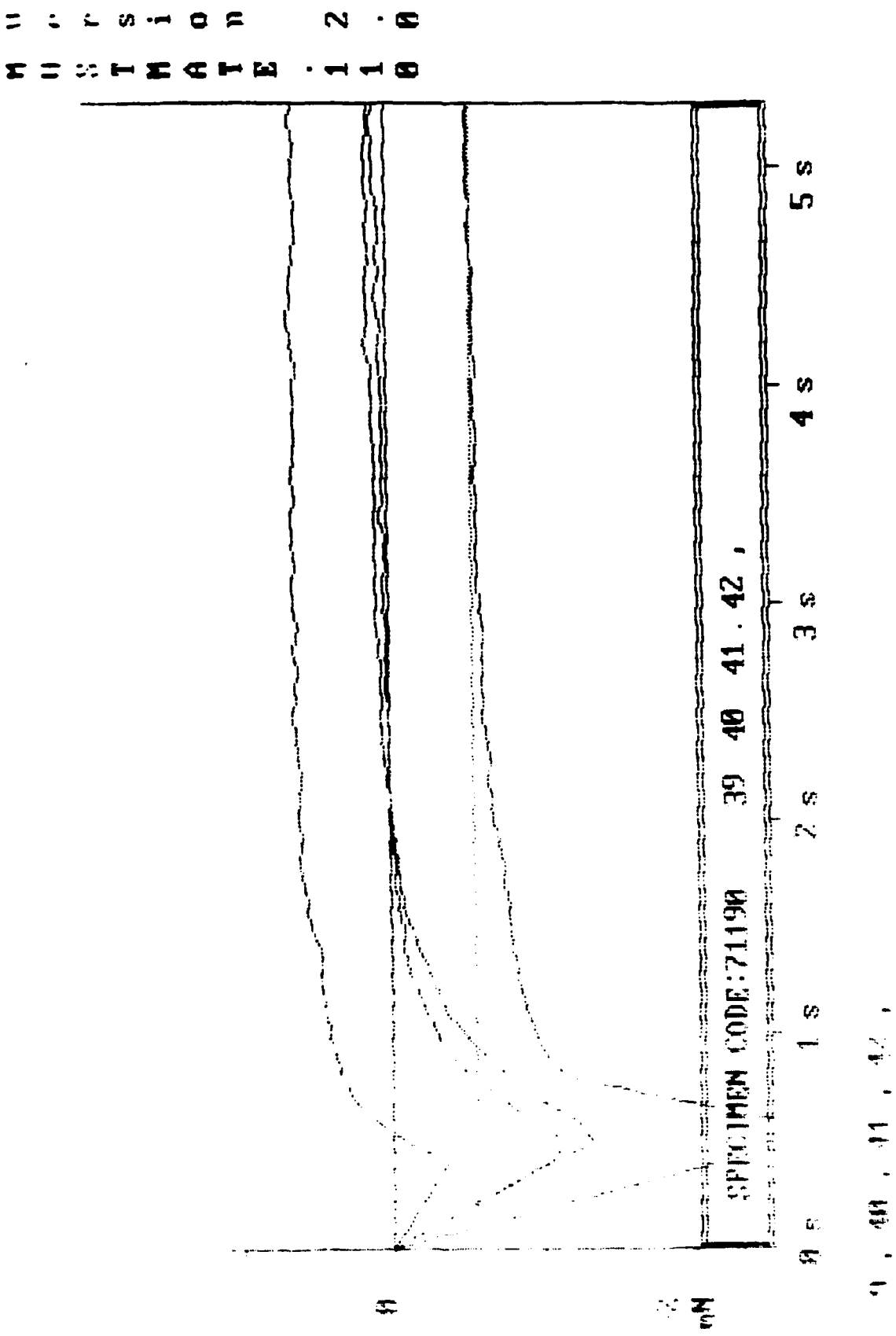
5 s
4 s
3 s
2 s
1 s
SPECIMEN CODE:71190
39 40 41.42,

REFERENCES :

1.) Standard Procedure For Candidate SA Fluxes.

2.) Military Standard for Reaching 2/3 Fmax.

3.) IEC-68-2-54[3] Document

4.) William G. Kenyon , The Evaluation of Commercial Flux/solder/Deflux Systems.

5.) William G. Kenyon , Tech Brief Abstract For '91 Program.

6.) Instruction Manual to the Multicore Universal Solderability Tester.

7.) Proceedings from W. G. Kenyon & D.J. DiGuglielmo, Electronics Department R&D Applied Technology Group.

8.) Present procedure is contained in the French Norm for soldering materials.

Bill Kenyon, Senior Scientist, DuPont Electronics, has been involved in product, process, and test development for the past 18 years. He has focused on cleaning-process studies, flux/solder/deflux evaluations, and pioneered the work responsible for modern synthetic activated (SA) flux technology. He cofounded the CFC Benchmark & Alternatives Ad Hoc Task Group and pressed for an industry semi-aqueous alternative cleaning process offering.

These contributions have led to his being awarded the 1990 Stratospheric Ozone Protection and Marketing Excellence Awards by the EPA and DuPont, respectively, who also nominated him to serve on the United Nations Environmental Program (UNEP) Technical Assessment Panel.

Bill is active in trade, professional, and industry association leadership activities, and chairs or is a member of several national and international committees. He is co-chairing the revision of QQ-S-571 with the long-range goal of harmonizing it with U.S./international standards to generate a single global standard for soldering materials. Bill is also leading a team tasked to develop new advanced assembly technologies for the '90s that will be consistent with high first-pass yields while protecting the environment.

Address: DuPont Electronics
Experimental Station
Building 336, Room 203
P.O. Box 80336
Wilmington, DE 19888-0336